In the Eye of the Swarm: Unravelling Neutrophil Swarming Dynamics in Zebrafish

Nils Ingmar Olijhoek

A thesis submitted in partial fulfilment of the requirements for the degree of Doctor of Philosophy

The University of Sheffield
Division of Clinical Medicine
School of Medicine & Population Health

11-07-2024

Acknowledgements

First, I would like to thank both Prof. Steve Renshaw and Dr. Phil Elks for providing me with this amazing opportunity and welcoming me to Sheffield, making it feel like a new place I could call home. I want to thank them for their invaluable insights and extensive knowledge that they have transferred to me over these past years, it was an absolute pleasure to work together.

I then want to thank; The lab of Prof. Simon Foster for providing the Staphylococcus aureus cell wall preparation used in some of my experiments. Milka Sarris for providing the *Tg(lyz:tRFP-5LO)* zebrafish reporter line, which I unfortunately could not work with for very long. Everyone in the Biological Services Aquarium for their excellent care of the zebrafish. Darren and Nick at the Wolfson Light Microscopy Facility for their assistance with the microscopes and advanced imaging.

I want to thank both Dr. Jochen Gherig and Dr. Laurent Thomas for hosting me at Acquifer and Prof. Georges Lutfalla and Dr. Mai Nguyen-Chi for hosting me in Montpellier during my secondments. Which were hectic, but very valuable experiences.

I also want to thank everyone in the Renshaw and Elks lab for helping me day to day, with experiments, general support, everyone's positive attitude, and infectious eagerness to learn. I will definitely remember all the great social outings we have had since transitioning back to 'regular' life after the COVID pandemic.

I also want to thank everyone within INFLANET for being so accessible, friendly, and supportive to each other. Particularly some of my fellow INFLANET students like Sankeert with whom I could make some music in the snow, Resul who was determined to turn me

into a gym bro, Liz and Maria, who celebrated possibly the hottest birthday I have ever had in Montpellier with me and all others that were an absolute joy to be around during the yearly INFLANET meetings.

Finally, I want to thank all my friends and family from overseas who came to visit over the past years and who I could show how great Sheffield can be. Especially Merit and my parents who despite the distance from home did not stop supporting me.

Abstract

Neutrophil dysfunctions are a major cause of chronic inflammatory diseases like COPD, but also infectious diseases such as COVID-19. Understanding neutrophil behaviour and pathways can lead to new therapeutic approaches aiding to relieve the burden of neutrophil-associated illnesses. Neutrophil swarming is a relatively recently described, neutrophil specific behaviour. During swarming, neutrophils are recruited in a bi-phasic manner through initial recruitment triggers followed by autocrine signalling of leukotriene B4, ultimately stabilising into a cluster of neutrophils. Although pathways driving the formation of neutrophil swarms have been increasingly understood, some initiating triggers remain undescribed and pathways resulting in arrest or resolution of swarms are largely unknown. I hypothesise that neutrophil swarming is a modulatory process that plays an essential role in the timescale of the inflammatory response. I demonstrate the use of the zebrafish model of inflammation for observing endogenous neutrophil swarm dynamics *in vivo*. Utilising a multitude of newly developed, automated analyses, neutrophil swarming observed via time-lapse imaging was, characterised, quantified and compared. Pharmacological modulation with TLR agonists via immersion did not significantly influence neutrophil swarming. However, treatment with prolyl-hydroxylase inhibitors by immersion suggested the HIF-1α pathway to play a role in the swarming response, as a significant reduction in swarms was observed. Finally, through the use of an *mfap4:mCherry/mpx:GFP* reporter line, I was able to show how interplay between macrophages and neutrophils might change swarming dynamics *in vivo.* In conclusion, this research demonstrates the use of the zebrafish model of inflammation to show innovative approaches for in depth analysis of swarming dynamics, aiming to provide a deeper understanding of neutrophil swarming, through which novel therapeutic approaches could be identified for patients affected by chronic inflammatory diseases.

Table of Contents

List of Tables

List of Figures

List of Abbreviations

In alphabetical order:

2D: Two-Dimensional

3D: Three-Dimensional

5-LO, 5-LOX, ALOX: (Arachidonate) 5-lipoxygenase

ANOVA: Analysis of Variance

ATP: Adenosine Triphosphate

APC: Antigen Presenting Cell

BCR: B-Cell Receptor

CAM: Cell Adhesion Molecule

C/EBP: CCAAT/enhancer-binding protein

CGD: Chronic Granulomatous Disease

CHT: Caudal Hematopoietic Tissue

COPD: Chronic Obstructive Pulmonary Disease:

CPLA2: cytosolic phospholipase A2

Cx43: Connexin 43

CXCL: CXC Chemokine Ligand

CXCR: CXC Chemokine Receptor

DAMP: Danger-Associated Molecular Pattern

DMOG: Dimethyloxalylglycine

DNA: Deoxyribonucleic Acid

dpf: Days Post Fertilisation

DPI: Diphenyleneiodonium

ECM: Extracellular Matrix

EGFP: Enhanced Green Fluorescent Protein

FG-4952: Roxadustat

FLAP: 5-lipoxygenase-activating-protein

fMLP: N-formylmethionyl-leucyl-phenylalanine

GFP: Green Fluorescent Protein

GRK: G protein-coupled receptor kinase

G-CSF: Granulocyte-Colony Stimulating Factor

H2O2: Hydrogen Peroxide

HIF-1α: Hypoxia-Inducible Factor-1α

HMGB1: High Mobility Group Box 1 protein

hpi: Hours Post Injury

ICAM: Intracellular Adhesion Molecule

IFN-γ: Interferon-gamma

IL: Interleukin

JAM: Junctional Adhesion Molecule

LFA1: Lymphocyte Function-associated Antigen 1

LGT: Low Gelling Temperature

LPS: Lipopolysaccharide

LTA4: Leukotriene A4

LTA4H: Leukotriene A4 Hydrolase

LTB4: Leukotriene B4

MHC: Major Histocompatibility Complex

MIP: Maximum Intensity Projection

MMP8: Matrix Metalloprotease 8

MMP9: Matrix Metalloprotease 9

MPO: Myeloperoxidase

NADPH: Nicotinamide Adenine Dinucleotide Phosphate

NE: Neutrophil Elastase

NET: Neutrophil Extracellular Trap

NLR: NOD-like Receptor

NOX: NADPH-Oxidase

PAM2CSK4: Pam2CysSerLys4

PAMP: Pathogen-Associated Molecular Pattern

PBS: Phosphate-Buffered Saline

PMA: Phorbol Myristate Acetate

Poly I:C: Polyinosinic acid

PRR: Pattern Recognition Receptor

PSGL1: P-selectin Glycoprotein Ligand 1

R837: Imiquimod

R848: Resiquimod

RBI: Rostral Blood Island

RIPK1: Receptor-interacting serine/threonine-protein kinase 1

RIPK3: Receptor-interacting serine/threonine-protein kinase 3

ROI: Region of Interest

ROS: Reactive Oxygen Species

RTM: Resident Tissue Macrophages

SD: Standard Deviation

SEM: Standard Error of the Mean

TCR: T-Cell Receptor

TLR: Toll-like Receptor

TNFα: Tumor Necrosis Factor-alpha

VAP-1: Vascular Adhesion Protein 1

VCAM: Vascular Cell Adhesion Molecule

V(D)J: Variable-Diversity-Joining

VE-cadherin: Vascular Endothelial Cadherin

VLA4: Very Late Antigen 4

Declaration

I, Nils Olijhoek, confirm that the Thesis is my own work. I am aware of the University's Guidance on the Use of Unfair Means (www.sheffield.ac.uk/ssid/unfair-means). This work has not been previously been presented for an award at this, or any other, university.

Chapter 1: Introduction

1.1 The Innate Immune System

The innate immune system is our body's first line of defence in regard to sterile inflammation and pathogenic infection and is often involved in the first stages of the inflammatory response. The innate immune system can be further divided into a cellular component and humoral component (Turvey and Broide, 2010). The humoral component of the innate immune system includes the complement system, antimicrobial peptides, Lipopolysaccharide (LPS) binding proteins, C-Reactive proteins and mannose binding lectins (Turvey and Broide, 2010). The cellular component of innate immunity consists of neutrophils, macrophages, mast cells, eosinophils, natural killer cells and dendritic cells (Turvey and Broide, 2010). Neutrophils and macrophages act on a wide variety of immunological pathways. They can sense both pathogen-associated molecular patterns (PAMPs) and danger-associated molecular patterns (DAMPs) (El-Zayat et al., 2019, Chen et al., 2009, Krysko et al., 2012). Common examples of PAMPs are LPS, found on the cell surface of gram-negative bacteria and flagellin (El-Zayat et al., 2019). Examples of DAMPs include cytokines associated with necroptosis and extracellular ATP or DNA (Krysko et al., 2012). Recognition of PAMPs and DAMPs occurs through binding with pattern recognition receptors (PRRs), including Toll-like and NOD-like receptors (TLRs, NLRs) expressed on the cell surface (El-Zayat et al., 2019, Chen et al., 2009). Macrophages can be further classified into M1 and M2 subsets *in vitro* (Galli et al., 2011). M1 macrophages are activated through Interferon-gamma (IFN-γ) signalling and elicit pro-inflammatory functions like antitumoral immunity (Galli et al., 2011). In contrast, M2 macrophages are activated by interleukin-4 and 13 (IL-4, IL-13) and are involved in anti-inflammatory pathways like wound healing and the suppression of antitumoral immunity (Galli et al., 2011). While neutrophils

can induce contrasting inflammatory functions like macrophages, clearly described subtypes have yet to be characterised. However, there are studies exploring this, illustrating distinct transcription, expression and phenotypes between neutrophil populations. (Khoyratty et al., 2021, Grassi et al., 2018, Jitka et al., 2015, Ng et al., 2019).

1.2 The Adaptive Immune System

Compared to the innate immune system, the adaptive immune responses have increased complexity, but also more specificity. In the adaptive immune system, an extra layer of immunity is built on top of the innate immune system through a process called antigen presentation (Pishesha et al., 2022). Presentation of antigens can be performed by macrophages, dendritic cells or B-cells, however atypical antigen-presenting cells have also been described (Kambayashi and Laufer, 2014). Antigens processed by the antigen presenting cell (APC) are extracellularly exposed and bound to the major histocompatibility complex (MHC) (Pishesha et al., 2022). These antigens can be subsequently recognised through binding with the T-cell receptor (TCR) or B-cell receptor (BCR) (Kambayashi and Laufer, 2014). The TCR and BCR can undergo variable-diversity-joining (V(D)J) recombination, which results in perfect recognition of the presented antigen (Christie et al., 2022). B-cells can then, through various steps, establish long-lived versions of themselves resulting in an 'immunological memory', these long-lived cells are called memory B-cells (Akkaya et al., 2020). In the scenario where the host encounters the exact same antigen again, an immune response is quickly mounted by increasing T-cell proliferation, these T-cells will then actively seek out the previously encountered pathogen or cellular threat and initiate mechanisms to dispose of them (Raskov et al., 2021, Reina-Campos et al., 2021, St John and Rathore, 2019). Ideally, this results in the inflammatory response being shorter

and being less excessive compared to the first encounter. This process is well-documented and forms the foundation of vaccination (Pollard and Bijker, 2021).

The adaptive immune system is present in all vertebrate animals including zebrafish, however in zebrafish the adaptive immune system does not fully develop in the first days after fertilisation (Miao et al., 2021). During these initial days, zebrafish will only possess an innate immune system, which makes studying innate immune cell behaviour easier due to exclusion of immunological processes introduced with adaptive immunity. This can be both a blessing and a curse, since innate immune cell behaviour is easier to contextualise, but cross-talk between the innate and adaptive immune system is missed, which could be integral to some immunological responses. This limitation will always have to be considered when using the zebrafish as a model system.

1.3 The Neutrophil

1.3.1 Origin

Neutrophils are an integral part of the innate immune system and often consist of the first cells to migrate to a site of infection or inflammation (Kolaczkowska and Kubes, 2013). Neutrophils in humans are continuously generated within the bone marrow from myeloid precursors (Grassi et al., 2018). In humans a total of $2x10^{11}$ neutrophils is generated daily and production can be influenced by granulocyte colony stimulating factor (G-CSF)(Borregaard, 2010, Lieschke et al., 1994).

During inflammation the production of neutrophils increases, resulting in an increased number of neutrophils in all tissues (Kolaczkowska and Kubes, 2013). In humans, neutrophils mature within the bone marrow via several stages, namely; myeloblast, promyelocyte,

myelocyte, metamyelocyte, band cell, and, finally, polymorphonuclear cell (Hidalgo et al., 2019). This maturation process is partially controlled by transcription factors, including PU.1 and CCAAT/enhancer-binding protein (C/EBP)α (Dahl et al., 2003, Nerlov and Graf, 1998). Once fully mature, they are released from the bone marrow. However, they are incapable of fully contributing towards innate immunity. For this to occur, a neutrophil must be primed, by for example, interacting with inflammatory cytokines within the bloodstream (Miralda et al., 2017). After a neutrophil is primed, it can fulfil its immunological role at a site of inflammation or infection.

During excessive inflammation, other extramedullary sites like the liver and the spleen can be triggered (Manz and Boettcher, 2014, Malengier-Devlies et al., 2021). This is especially relevant in the context of neutrophil swarming which is often classed as excessive inflammation (Brown and Yipp, 2023). This emergency granulopoiesis may directly interact with neutrophil swarm formation through the release of additional G-CSF, as has been shown in *ex vivo* models of neutrophil swarming (Hopke et al., 2020).

In zebrafish, several sites of haematopoiesis are present, namely the Rostral Blood Island (RBI) and the Caudal Hematopoietic Tissue (CHT) (Garcia-Lopez et al., 2023). Towards adulthood, this eventually shifts towards the pronephros (Stosik et al., 2022). In zebrafish, the pronephros functions haematopoietically similar to bone marrow in mammals (Stosik et al., 2022). In research specifically comparing neutrophils generated in the RBI to the CHT, the authors found transcriptional differences, which may indicate that neutrophil subtypes could already be present in zebrafish from as early as 34 hours post fertilisation (hpf) (Garcia-Lopez et al., 2023).

1.3.2 Neutrophil Recruitment

Whenever a tissue-resident or patrolling leukocyte binds a PAMP or a DAMP, it can secrete chemotactic cytokines, sometimes called chemokines or chemo attractants, in order to recruit additional nearby immune cells from the circulatory system (Prince et al., 2011, Metzemaekers et al., 2020). The recruitment cascade can be described in the following consecutive steps; recruitment, tethering, rolling, adhesion, crawling and, finally, transmigration (Gronloh et al., 2021).

Neutrophils have been shown to be recruited by multiple factors, including selectins expressed on tissues, extracellular ATP and chemotactic cytokines (Sadik et al., 2011, Shah et al., 2014, Petri et al., 2008). The following steps of tethering, rolling and the initial phases of adhesion, are mostly orchestrated via selectins including, P-selectin, E-selectin and L-selectin (Zarbock et al., 2011). Tissue specific selectin expression helps neutrophils to exclusively be recruited to certain tissues, for instance the endothelium (P-selectin and E-selectin) or lymph nodes (L-selectin) (Petri et al., 2008, Zarbock et al., 2011, Arbones et al., 1994). These selectins can be bound by their glycosylated ligands, including P-selectin glycoprotein ligand 1 (PSGL1), accessible on the neutrophil cell surface (Zarbock et al., 2011). Once a neutrophil is captured by selectins, full adhesion is achieved through the binding of lymphocyte function-associated antigen 1 (LFA1), an integrin expressed on the neutrophil cell surface, with intracellular adhesion molecule 1 (ICAM-1), expressed on endothelial cells (Fisher et al., 1997). The amount of ICAM-1 available for binding can be influenced by quantities of tumour necrosis factor-α (TNFα) and interleukin 1 beta (IL-1β), which are regarded as common pro-inflammatory cytokines (Myers et al., 1992, Sakurada et al., 1996, McHale et al., 1999, Bui et

al., 2020). Alternatively, ICAM-1 expression can be induced via LPS, showing that a pathogenic infection could directly alter neutrophil adhesion (Sawa et al., 2008, Myers et al., 1992).

During transmigration, neutrophils can transmigrate either between endothelial cells (paracellularly) or through an individual endothelial cell (transcellularly) (Gronloh et al., 2021, Xia et al., 2024). This process is controlled via integrins, CAMs (including ICAM-1 and vascular cell adhesion molecule 1 (VCAM-1)) and junctional adhesion molecules (JAMs) (Gronloh et al., 2021). The latter mediate cell-cell adhesion between endothelial or epithelial cells. Vascular endothelial cadherin (VE-cadherin) and neural cadherin (N-cadherin) are examples of JAMs expressed in multiple types of tissue, creating tight junctions between cells (Leckband and De Rooij, 2014). For a neutrophil to cross the endothelial barrier in paracellular fashion, it needs to disengage these cadherins. This is thought to be facilitated by small protrusions formed from the neutrophil, which nestle between endothelial cells, to mechanically disrupt the JAMs (Rabodzey et al., 2008). However, literature also describes an enzymatic component of paracellular transmigration via vascular adhesion protein 1 (VAP-1) (Koskinen et al., 2004). During transcellular transmigration, a neutrophil is entirely taken up by an endothelial cell (Carman and Springer, 2004, Barreiro et al., 2002). This is arranged via the formation of so-called transmigratory cups, formed by the endothelial cell (Jackson, 2022). These transmigratory cups have been shown to be enriched in ICAM-1 and VCAM-1 and form around the neutrophil in a LFA1 and very late antigen 4 (VLA4) dependent manner (Barreiro et al., 2002, Carman and Springer, 2004). While this process shares similarities with phagocytosis, it should not be mistaken for it, as internalised neutrophils will never enter the intracellular compartment, making transcellular uptake a fundamentally different process (Xia et al., 2024).

After a neutrophil crosses the endothelial barrier, it utilises extracellular matrix (ECM) remodelling enzymes to pave a path through the basement membrane, which consists of different laminins, collagens and proteoglycans (Dekkers et al., 2021, Gronloh et al., 2021). ECM remodelling enzymes include different proteases such as the well-described matrix metalloprotease 9 (MMP9) and serine proteases such as neutrophil elastase (NE) (Zhu et al., 2021, Chua, 2006). Once passed, neutrophils can use the same ECM remodelling to complete the final step of migration towards the site of inflammation or infection through the interstitial space.

1.3.3 Killing Mechanisms

When a neutrophil arrives at an inflammation or infection site, it can exert different immunological functions. One example is phagocytosis, a process whereby neutrophils recognize and engulf pathogens and cellular debris through PRRs on the cell surface (Lee et al., 2020, Lee et al., 2003). Once particles are taken up within the neutrophil they are encapsulated by another phospholipid bilayer, resulting in the formation of a phagosome (Bonam et al., 2019, Lee et al., 2020) This phagosome is then fuses with early endosomes, late endosomes and lysosomes respectively, in a process called phagosome maturation (Lee et al., 2020). Lysosomes, the last intracellular vesicles to fuse to the phagosome, have a very low pH of around 4,5 to 5 and contain hydrolases (Bonam et al., 2019, Lee et al., 2020). Once the phagosome is fully matured, most of the contents captured within will be degraded and consecutively transported to the Golgi apparatus for reuse or excreted through exocytosis (Bonam et al., 2019).

When phagocytosis is unable to be used, a neutrophil can employ a different immunological mechanism, called degranulation. Neutrophils use this mechanism to combat extracellular

pathogens and increase immune cell recruitment through the release of cytokines (Lacy, 2006, Naegelen et al., 2015). The degranulation process can be triggered through a various number of ways. For instance, studies have shown that neutrophil exposure to a hypoxic environment may upregulate degranulation (McGovern et al., 2011, Hoenderdos et al., 2016). Additionally, degranulation has been shown to be adhesion dependent, through binding of L-selectin and the Src family kinases Fgr and Hck (Mocsai et al., 1999, Smolen et al., 2000). When degranulation is triggered, intracellular vesicles (granules) are secreted via exocytosis. Granules can be categorised into 4 different types: primary granules (azurophilic granules); secondary granules (specific granules); tertiary granules; and secretory vesicles (Lacy, 2006). The azurophilic granules contain potent proteases, which assist in breaking down proteins into smaller polypeptides or amino acids, examples of common proteases are Myeloperoxidase (MPO), Neutrophil elastases (NE), cathepsins, and defensins (Lacy, 2006, Borregaard and Cowland, 1997). All these proteases fulfil different functions. Firstly, MPO converts hydrogen peroxide (H_2O_2) into hypochlorous acid (HOCl), which is highly microbicidal and has been shown to play a critical role in the killing of several types of bacteria, including *Mycobacterium tuberculosis* and *Streptococcus pneumoniae* (Hirche et al., 2005, Borelli et al., 1999, Xiang et al., 2017, Winterbourn et al., 2006, Aratani, 2018). NE is a serine protease which possesses ECM remodelling capabilities (Chua, 2006). Cathepsins are mostly restricted to the azurophilic granules, where they assist with recycling intracellular proteins (Turk et al., 2012). However, they have also been linked to ECM remodelling when secreted extracellularly (Wang et al., 2023). Lastly, defensins are antimicrobial peptides which have been shown to permeabilise membranes of bacteria and fungi (Fu et al., 2023).

Degranulation of neutrophils is often paired with the release of reactive oxygen species. ROS is a collective name for highly reactive molecules derived from O_2. Within neutrophils ROS are prominently produced via NADPH-Oxidase (NOX) however, more enzymes that fit into the NOX family have been identified (Panday et al., 2015). NOX-mediated respiratory burst is one of the innate immune defence mechanisms used to degrade internalised particles and bacteria (Van Acker and Coenye, 2017, Dupré-Crochet et al., 2013). Additionally, the NOX-mediated respiratory burst has been shown to play a role in several signalling pathways through crosstalk between NOX and TLRs/NLRs (Panday et al., 2015). Lastly, H_2O_2, a member of ROS, has been shown to have a direct chemotactic effect, attracting neutrophils towards a H_2O_2 gradient within the zebrafish model (Niethammer et al., 2009, Feng et al., 2010, Yoo et al., 2011).

The final killing mechanism is the secretion of neutrophil extracellular traps (NETs), which neutrophils can actively generate and secrete. This process, often referred to as NETosis, enables neutrophils to 'ensnare' and subsequently degrade extracellular pathogens (Brinkmann et al., 2004). Through experimentation with DNAse and protease using *in vitro* models of *S. flexneri* and *S. aureus* infection, NETs were found to mainly consist of extracellular DNA and chromatin (Brinkmann et al., 2004). However, many more proteins associated with NET secretion have been described (Brinkmann et al., 2004). For instance, proteins from primary, secondary and tertiary granules such as MPO, NE, lactoferrin and gelatinase have been found to associate with NETs (Brinkmann et al., 2004). The generation of NETs within neutrophils is triggered by stimulation of NOX-associated ROS production or recognition of PAMPs by PRRs on the neutrophil surface (Jorch and Kubes, 2017). This can activate protein-arginine deiminase 4 (PAD4), which converts arginine to citrulline on histones

and promotes decondensation of chromatin within the nucleus, in a NE and MPO dependent manner (Papayannopoulos et al., 2010, Jorch and Kubes, 2017). Two different forms of NETosis have been postulated, firstly, vital NETosis and secondly, suicidal NETosis (Jorch and Kubes, 2017, Yipp and Kubes, 2013). The latter results with the death of a neutrophil, while vital NETosis promotes the secretion of chromatin through exocytosis of vesicles (Jorch and Kubes, 2017, Yipp and Kubes, 2013). Current knowledge suggests that the difference lies within the way NETosis is stimulated. This could be either through phorbol myristate acetate (PMA) or bacterial components such as LPS, whereby LPS stimulates vital NETosis (Yipp and Kubes, 2013, Zhao et al., 2015, Petretto et al., 2019). In contrast, PMA might promote suicidal NETosis in a ROS dependent manner (Zhao et al., 2015, Yipp and Kubes, 2013, Berthelot et al., 2017). Furthermore, it is postulated that vital NETosis might use mitochondrial DNA, which is subsequently secreted as a NET (Yousefi et al., 2009). Vital NETosis can be beneficial since it preserves further neutrophil functions, elicits a rapid response and release of NETs and has lower toxicity compared to suicidal NETosis (Wang et al., 2022, Huang et al., 2022). Suicidal NETosis can be beneficial too as it offers enhanced pathogen trapping and killing and a stronger inflammatory response (Wang et al., 2022, Huang et al., 2022). However, both forms have to be tightly regulated as dysregulations could cause autoimmune responses, or an exacerbation of inflammation in the case of suicidal NETosis, which can be followed by tissue damage (Wang et al., 2022, Huang et al., 2022).

1.4 Neutrophil Swarming

Neutrophil swarming was originally described in 2008 by Tatyana Chtanova in the lab of Ellen Robey who saw swarming behaviour in mice lymph nodes following *Toxoplasma gondii* infection (Chtanova et al., 2008).

Subsequent elucidation was carried out by Tim Lämmermann et al. (Lämmermann et al., 2013). It is identified as a form of highly coordinated neutrophil recruitment towards a site of inflammation or infection (Lämmermann et al., 2013). An important distinction between regular neutrophil recruitment and recruitment resulting in neutrophil swarms is the bi-phasic signalling response seen in swarming. During swarming, neutrophils are recruited in two distinct steps. The first step is via classically described neutrophil recruitment, for instance, CXCL12/CXCR4 signalling, CXCL2/CXCR2 signalling, CXCL8/CXCR1/2 signalling or towards a H_2O_2 gradient (Isles et al., 2019, Niethammer et al., 2009, Kienle et al., 2021, Reátegui et al., 2017). This recruits a so-called 'pioneer' neutrophil to the injury site, which is able to start the second part of the signalling cascade (Lämmermann et al., 2013, Isles et al., 2021). In this part, release of Leukotriene B4 (LTB4), attracts more distant neutrophils in a highly coordinated fashion, resulting in a neutrophil swarm (**Fig1.**) The importance of LTB4 signalling has been illustrated via knockout neutrophil lines, lacking the high-affinity receptor of LTB4 (LTB4R1) (Lämmermann et al., 2013). These knockout lines showed that cells at more distant sites were poorly attracted, while cells nearby still performed swarm like behaviour (Lämmermann et al., 2013). These findings are corroborated by more recent findings in an *ex vivo* model of neutrophil swarming where transcellular synthesis of LTB4 was shown to be essential for swarming towards *Candida albicans* (Hopke et al., 2022). The LTB4 pathway has been shown to be conserved in humans, mouse and zebrafish, where it was shown to be dependent on calcium wave signalling via connexin 43 (Cx43) hemichannels (Poplimont et al., 2020, Isles et al., 2021, Lämmermann et al., 2013, Hopke et al., 2020).

The LTB4 molecule itself is part of the eicosanoid family of lipid mediators, which are all formed from arachidonic acid released from phospholipids in cellular membranes by cytosolic

phospholipase A2 (cPLA2) (Peters-Golden and Henderson, 2007, He et al., 2020). Arachidonic acid is then converted to leukotrienes by 5-lipoxygenase (5-LO, 5-LOX, ALOX) together with 5-lipoxygenase-activating-protein (FLAP) (Peters-Golden and Brock, 2003, Peters-Golden and Henderson, 2007). The precursor molecule of LTB4, Leukotriene A4 (LTA4) can then be hydrolysed to LTB4 by LTA4-Hydrolase (LTA4-H) (Peters-Golden and Henderson, 2007). The LTB4 synthesis process has been visualised by creating a transgenic zebrafish reporter for 5-LO which showed signal to become spatially organised close to the nuclear envelope, creating a readout for LTB4 synthesis (Poplimont et al., 2020). Additionally, LTB4 signalling and gradient propagation has been shown using a specialised receptor which is able to sense bound LTB4, resulting in a fluorescent signal (Tamás et al., 2023).

Besides the release of chemokines, other pathways have also been identified to play a role in neutrophil swarm formation. For instance, using the zebrafish model, a mechanistic link between release of NETs by pioneer neutrophils and subsequent swarming was found (Isles et al., 2021). Additionally, the pioneer neutrophil stained negative for propidium iodide, a common marker for apoptosis, suggesting it utilised a form of vital NETosis to initiate swarming (Isles et al., 2021). Furthermore, inhibition of NET-associated proteins such as gasdermin D (GSDMD), NE and myeloid-specific peroxidase (mpx), either genetically or chemically, showed a reduction in swarming events (Isles et al., 2021).

Signals triggering swarming can be divided into triggers of infection and sterile inflammation. In both cases it is believed that secondary cell death and additional LTB4 signalling, increases the size of the swarm (Kienle and Lammermann, 2016). Different types of physical injury causing sterile inflammation to trigger swarming have been described, for instance a focal laser burn, a sterile cut or a tissue puncture (Poplimont et al., 2020, Lämmermann et al., 2013,

Isles et al., 2019, Kienle and Lammermann, 2016, Ng et al., 2011). Infection with several pathogens including, *T. gondii*, *L. major*, *P. aeruginosa* and *S. aureus* have also been shown to induce swarming (Peters et al., 2008, Chtanova et al., 2008, Lämmermann et al., 2013, Yipp et al., 2012, Kamenyeva et al., 2015).

Swarming of neutrophils can be highly heterogeneous in their persistence, when swarms only last up to one hour it is referred to as 'transient swarming' (Kienle and Lammermann, 2016). Transient swarming is recognised by fast aggregation (10-15 minutes) of around 10-150 neutrophils, after which they quickly resolve (40min) (Lämmermann, 2016, Chtanova et al., 2008). Often, multiple swarms can be observed during transient swarming, which are able to fuse or compete for recruitment of neutrophils between them (Lämmermann et al., 2013, Chtanova et al., 2008). In contrast, 'persistent swarming' is characterised by a swarm which rapidly grows in size, up to multiple thousand neutrophils and persists up to several hours at the first place of recruitment (Chtanova et al., 2008, Braedon McDonald et al., 2010). The initiation of either transient or persistent swarming is thought to be associated with the type of swarming trigger. Persistent swarming is more commonly observed during sterile inflammation, while transient swarming seems to be activated by pathogens, as they are spread throughout the site of infection, creating multiple chemo-attractive gradients (Lämmermann, 2016).

Initial steps towards elucidating the physiological role of neutrophil swarming have been made. For instance, using an *in vitro* model of neutrophil swarming against fungi, it was shown that chemical inhibition of LTB4 had a detrimental effect in restricting *C. albicans* growth (Hopke et al., 2020). Additionally, NETs were found to be essential in restricting *C. albicans* growth and in promoting further accumulation of neutrophils in a swarm (Hopke et al., 2020).

Finally, it was shown that NOX-mediated ROS production was able to significantly alter neutrophil swarming dynamics (Hopke et al., 2020, Strickland et al., 2024). Inhibition of NOX resulted in dysregulated relay signalling, which corresponded to a phenotype presented in patients with Chronic Granulomatous Disease (CGD) (Strickland et al., 2024). Other research using a mouse model for neutrophil swarming has shown how G protein-coupled receptor (GPCR) desensitisation plays a role in self-limitation of neutrophil swarms. After generating multiple G protein-coupled receptor kinase (GRK) knockout lines, $Grk2^{-/-}$ mice showed distinct neutrophil behaviour *in vitro (Kienle et al., 2021)*. Further investigation concluded that GRK2 orchestrated desensitisation of GPCRs to LTB4 and CXCL2 signals, as $Grk2^{-/-}$ neutrophils were not attracted to a shift in the CXCL2/LTB4 gradient (Kienle et al., 2021). Additionally, $Grk2^{-/-}$ neutrophils were shown to have a detrimental effect in controlling bacterial infection of *P. aeruginosa* within infected lymph nodes of mice (Kienle et al., 2021).

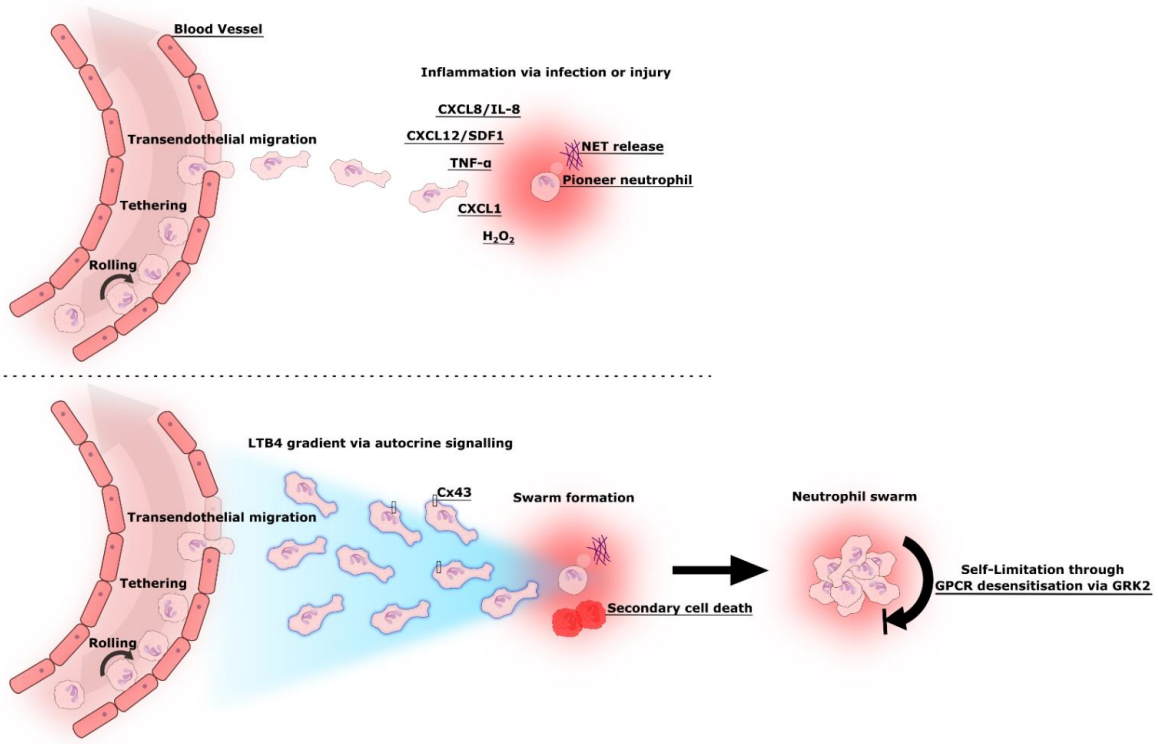

Figure 1 An overview of neutrophil swarm formation in vivo

This figure shows an overview of the current understanding of neutrophil swarming *in vivo* in mammals. In zebrafish embryos the process of tethering and rolling is less well established and may not occur until later developmental stages. The top picture illustrates the first phase of the bi-phasic signalling response where a pioneer neutrophil is recruited, gaining a circular morphology and releasing a NET via 'blebbing'. Important signalling molecules are highlighted. The bottom shows the second phase of the bi-phasic signalling response, which happens by neutrophils releasing LTB4 due to secondary cell death. Following this, an LTB4 gradient via autocrine signalling is established, recruiting more distant neutrophils. This process is driven through calcium wave signalling via connexin 43 (Cx43) hemichannels. Afterwards, a neutrophil swarm is formed which is shown to be self-limited through GPCR desensitisation via GRK2.

1.5 Resolution of Neutrophil Inflammation

Resolution of inflammation is an active process which is essential for achieving tissue homeostasis (Bernut et al., 2020, Metzemaekers et al., 2020, Loynes et al., 2010). As such, neutrophils involved in the inflammatory response have to leave the interstitial tissue. To elucidate the resolution of neutrophil inflammation one must understand the biochemical cues that; 1) cause neutrophils to stop 'forward-migration', 2) cause neutrophils to be retained at the injury site and 3) cause neutrophils to be cleared from the injury site or begin 'reverse-migration', away from the injury site (de Oliveira et al., 2016, Starnes and Huttenlocher, 2012, Huttenlocher and Poznansky, 2008).

Forward-migration can be seen as chemotactic signalling that recruits additional neutrophils towards the site of injury, whereas reverse-migration can be seen as chemotactic signalling causing neutrophils to migrate away from the site of injury (de Oliveira et al., 2016). Examples of signalling leading to forward-migration, are the CXCL12/CXCR4, CXCL2/CXCR2, CXCL8/CXCR1/2 signalling axes, as described in **1.3.2**. Since all of these exemplified signalling axes involve GPCRs, forward migration might be arrested through GPCR desensitisation by GRKs and Arrestins (Kienle et al., 2021, Gurevich and Gurevich, 2019). Another cause of reduction in forward-migration is through the release of chemorepellents, in which case cells actively migrate away from a high concentration of certain chemokines (Huttenlocher and Poznansky, 2008). After forward-migration is stopped, other chemotactic cues causing neutrophils to be retained at the injury site are still present. For instance, the CXCL12/CXCR4 signalling axis was shown retain neutrophils at inflammation sites (Isles et al., 2019). Alternatively, activation of Hypoxia-inducible factor-1α (Hif-1α), has been shown to reduce apoptosis as well as reverse-migration of neutrophils (Elks et al., 2011). A classical view of

neutrophil inflammation resolution is one where most neutrophils undergo apoptosis and are subsequently phagocytised by macrophages (Serhan and Savill, 2005, Grigg et al., 1991, Savill et al., 1989, Cox et al., 1995, Loynes et al., 2010). However, other literature describes neutrophils to be able to perform reverse-migration, a process in which neutrophils do not undergo apoptosis, but actively migrate away from the injury site (Robertson et al., 2014, Nourshargh et al., 2016, Huttenlocher and Poznansky, 2008, Starnes and Huttenlocher, 2012, Colom et al., 2015, Buckley et al., 2006, Mathias et al., 2006). This was originally shown in zebrafish and has since been confirmed in both mice and humans (Filippi, 2019, Owen-Woods et al., 2020). This migration has been shown to be orchestrated in several ways which include, competing chemoattractive or chemorepulsive gradients, receptor desensitisation, receptor internalisation and degradation, transcriptional changes and the LTB4/NE signalling axis (Starnes and Huttenlocher, 2012, Heit et al., 2002, Colom et al., 2015, Coombs et al., 2019, Buckley et al., 2006). Reverse migration can be further classified as reverse interstitial migration and reverse transmigration (Nourshargh et al., 2016). During reverse interstitial migration neutrophils will stay within the interstitial tissue, but will actively move away from foci of infection or injury (Nourshargh et al., 2016). During reverse transmigration, neutrophils will actively disrupt tight junctions of endothelial tissues, often in an effort to enter back into the bloodstream (Nourshargh et al., 2016). After swarming, neutrophils will show reverse interstitial migration, which can then be followed by transmigration.

Neutrophils have been shown to have a hierarchical response to different chemokines explaining how a new chemoattractive gradient could stimulate reverse-migration (Heit et al., 2002). In contrast, chemorepulsive gradients can be generated by excessive amounts of chemoattractants (Huttenlocher and Poznansky, 2008). Receptor desensitisation has been

shown to be essential in the self-limitation of neutrophil swarms, through desensitisation of one receptor, a contrasting chemoattractive gradient via another receptor might become more favourable, causing reverse-migration (Kienle et al., 2021). Receptor internalisation and degradation, also called receptor trafficking, often occurs rapidly after desensitisation (Coombs et al., 2019). Differential trafficking of CXCR1 and CXCR2 has been proposed as a mechanism which can cause neutrophils to switch cellular behaviour towards reverse-migration (Coombs et al., 2019). Reverse-migrating neutrophils have also been shown to undergo transcriptional changes as their phenotype and functionality differs from 'freshly' recruited neutrophils (Buckley et al., 2006). Finally, the LTB4/NE signalling axis is able to influence the cleavage of JAMs expressed by endothelial cells, eventually resulting in increased reverse transendothelial cell migration *in vivo* (Colom et al., 2015). Interestingly, LTB4 signalling is also essential for promoting neutrophil swarming, illustrating a dichotomous role (Lämmermann et al., 2013, Kienle and Lammermann, 2016, Poplimont et al., 2020). Neutrophil inflammation resolution in context of neutrophil swarming might be more complex, as swarms are formed in feedforward manner and are able to persist for up to multiple hours. While GPCR desensitisation has been shown to self-limit swarming via GRK2, exact mechanisms that cause resolution of a swarm have yet to be found, possible pathways that could be implicated are the Hif-1α pathway, the CXCL12/CXCR4 signalling axis and the LTB4/NE signalling axis (**Figure 2**).

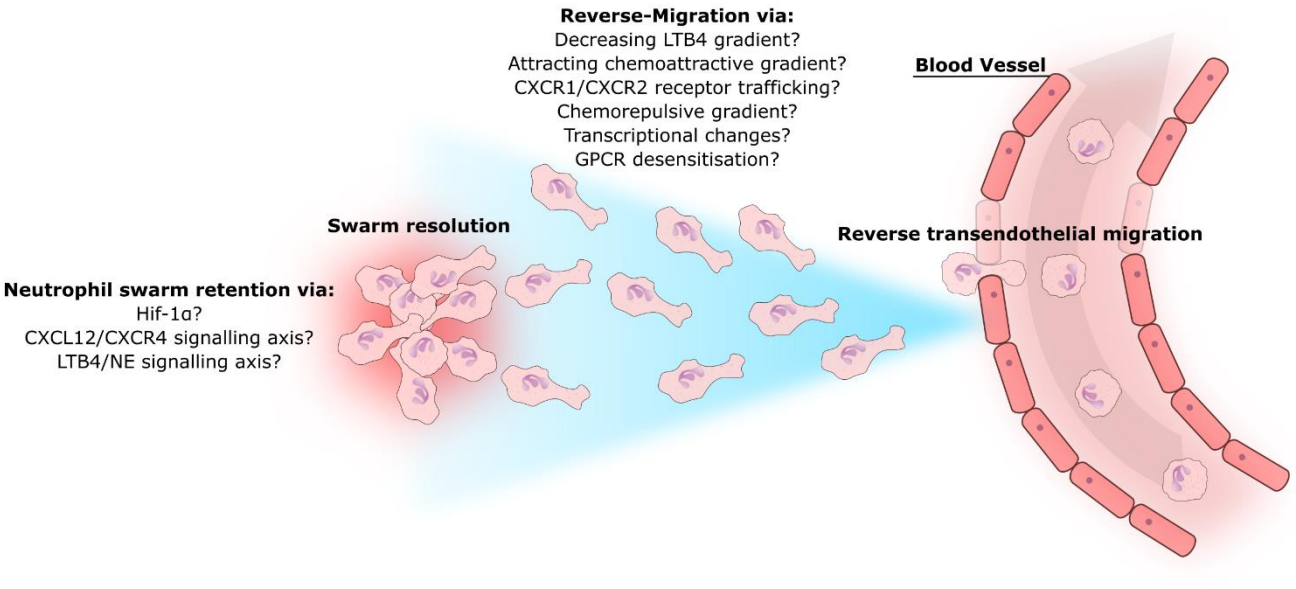

Figure 2: Potential pathways involved in neutrophil swarm resolution

This figure shows potential molecular pathways which could be involved in neutrophil swarm resolution. Potential pathways which could be interesting for inhibition are the Hif-1α and CXCL12/CXCR4 as both have been shown to retain neutrophils at sites of inflammation. Potential pathways that might be interesting to stimulate are the LTB4/NE pathway which has been shown to stimulate reverse transendothelial migration and might also be involved in swarming. Other potential drivers of reverse migration are also illustrated.

Impaired resolution of neutrophillic inflammation is thought to play a pivotal role in the onset of Chronic Obstructive Pulmonary Disease (COPD) (Hoenderdos and Condliffe, 2013). This could potentially be further dysregulated whenever neutrophil swarming occurs and fails to arrest and resolve. Besides COPD, neutrophils can play deterministic roles in COVID-19, as increased neutrophil-to-leukocyte ratios found in the blood of patients corresponded with more severe disease symptoms (McKenna et al., 2022). Finally, the cytokine storm phenomenon which occurs in these more severe cases of COVID-19 were linked to elevated neutrophil numbers as well (Vanderbeke et al., 2021, Chan et al., 2021).

1.5 Using the Zebrafish Model to Study Immunity and Neutrophil Swarming

The zebrafish was pioneered as a model system back in the 1980's by George Streisinger and has since been widely used to study both development and disease (Boueid et al., 2023, Chia et al., 2022). Due to the optical translucency of zebrafish, countless transgenic reporter lines using expression of fluorescent proteins behind promoters of target genes have been created, enabling visualisation of immune cells *in vivo* without the use of any invasive techniques (Renshaw et al., 2006, Nguyen-Chi et al., 2015, Phan et al., 2018, Poplimont et al., 2020). This opened up many possibilities to study immune responses in high detail (Speirs et al., 2024). Some findings that were first described in zebrafish, for instance, the findings that neutrophils perform reverse migration and that neutrophils are attracted to a H_2O_2 gradient after sterile tissue injury, were later confirmed in other animal models (Huttenlocher and Poznansky, 2008, Niethammer et al., 2009). The zebrafish model is also widely adopted as a model for *Mycobacterium tuberculosis* infection, using *Mycobacterium marinum* which is a natural pathogen of the zebrafish (Varela and Meijer, 2022, Meijer,

2016). This shows the wide adaptability of the zebrafish model for investigating a large range of different research topics.

Furthermore, zebrafish are exceptionally well-suited for high-throughput studies *in vivo* due to the rapid development of zebrafish embryos and the high number of samples that can be obtained when pairing adults. This has resulted in studies being able to find novel compounds that regulate immunological functions, as well as large-scale toxicology studies that have identified molecules used in everyday human life that can cause developmental dysregulations (Robertson et al., 2014, Dasgupta et al., 2020, Britton et al., 2024).

As illustrated in section **1.4 Neutrophil Swarming**, the zebrafish model has also been used to study neutrophil swarming (Coombs et al., 2019, Poplimont et al., 2020, Isles et al., 2021). The larval zebrafish model is especially well suited for more isolated study of neutrophil swarming as the adaptive immune system does not fully mature until 3 weeks post fertilisation (Miao et al., 2021). While this benefit is also preserved by the *ex vivo* models of neutrophil swarming, the *in vivo* complexity is absent (Hopke et al., 2020, Strickland et al., 2024, Hopke et al., 2022). Furthermore, neutrophil swarms are endogenously formed in zebrafish larvae compared to mice, where a large amount of fluorescently labelled, exogenous neutrophils are introduced into the system (Lämmermann et al., 2013, Kienle and Lammermann, 2016, Lämmermann, 2016). I have compiled a comprehensive comparison table of model systems for neutrophil swarming that are currently used in **Table 1**.

Table 1: Comparison of neutrophil swarming model systems

Model system	Neutrophil origin	Model type	Swarm size (cell number)	Swarm duration (timescale)	Advantages	Disadvantages
Zebrafish	Endogenous	*in vivo*	3-15[1]	Minutes-Hours[1]	*in vivo* Clear non-invasive imaging Endogenous swarms Semi high-throughput	Small scale response Genetic separation from humans Lacks fully developed adaptive immune system to capture full interactive landscape
Mouse	Exogenous	*in vivo*	50-300, 100-1000 depending on injury type[2,4]	Minutes-Hours-Days depending on injury type	*in vivo* Large scale response Exogenous swarms	Exogenous swarms Low-throughput Genetic separation from humans Invasive imaging
Cell culture	Exogenous	*ex vivo*	300-4000[3]	Minutes-Hours	Human neutrophils Large scale response Clear imaging and modelling Limited external factors High-throughput	Uses solely neutrophils, potentially missing immune interactions 2D cell culture could show different responses due to missing extracellular matrix

1 Data gathered during my thesis

2 (Ng et al., 2011)

3 (Strickland et al., 2024)

4 (Kienle and Lammermann, 2016)

1.6 Aims and Objectives

1.6.1 Background

While the events initiating neutrophil swarming have become further elucidated, the resolution of swarms have been poorly characterised. This research aims to address questions regarding neutrophil swarm resolution and more general dynamics of neutrophil swarms in the zebrafish model of inflammation, expanding upon a previously described model for neutrophil swarming in zebrafish, (Isles et al., 2021).

1.6.2 Hypothesis

I hypothesise that neutrophil swarming dynamics can determine the outcome of inflammation and that this can be manipulated therapeutically.

1.6.3 Aims and Objectives

The overarching aim of this project is to expand upon a previously described *in vivo* model of neutrophil swarming for the observation and potential manipulation of neutrophil swarming dynamics. This overarching aim can be broken down into the following specific objectives:

While many findings detail the formation of a neutrophil swarm and its associated molecular cues, swarm resolution is still not very well understood. Thus, I aim to:

1. **Define** the dynamics of neutrophil swarm resolution in the zebrafish model of inflammation.

Although neutrophil swarms have been shown to play a role in how the immune system combats infections, their purely physiological implications have not yet been described in detail (Kienle et al., 2021). Therefore, I aim to:

2. **Describe** any physiological roles neutrophil swarms might have in the zebrafish model.

As neutrophil swarming in zebrafish has not been thoroughly described and characterised, observational detection bias remains a concern. Because of this, I aim to:

3. **Reduce** observational bias when identifying neutrophil swarming in zebrafish.

To find potential therapeutic approaches for targeting neutrophil swarming, an INFLANET collaborative effort with Acquifer at Heidelberg University was established. Here, I aim to:

4. **Create** a proof of concept for a novel high-throughput screening assay to identify small molecule compounds affecting neutrophil swarming.

Neutrophil swarm formation and persistence might be influenced by a multitude of molecular factors, some of which have been described in the literature, such as pathways involving NADPH-Oxidase (Strickland et al., 2024). This led me to hypothesise that other ROS regulators, specifically HIF-1α, may also be involved. Additionally, other inflammatory pathways might not have been described yet. As such, I aim to:

5. **Identify** new molecular pathways that could affect neutrophil swarming.

Neutrophils are not the only type of innate immune cell in the zebrafish; interactions with macrophages have been illustrated by previous research (Tauzin et al., 2014, Loynes et al., 2018). Within the INFLANET network, the group of Georges Lutfalla and Mai Nguyen-Chi are experts in macrophage biology in zebrafish. Therefore, we established a collaboration to investigate whether interactions between macrophages and neutrophils might influence neutrophil swarming dynamics. Here, I aim to:

6. **Describe** the interactions of neutrophils with macrophages and how this influences swarming

Chapter 2: Methods

2.1 Zebrafish lines and husbandry

Zebrafish lines used in this research:

Table 2: Zebrafish lines used in this thesis

Line	Acronym	Reference
TgBAC (mpx:GFP)i114	*mpx:GFP*	(Renshaw et al., 2006)
Tg(mpx:GAL4-VP16)sh267;Tg (UAS:Kaede)i222	*mpx:Kaede*	(Robertson et al., 2014)
Tg (mfap4: mCherry-F)ump6Tg	*mfap4:mCherry*	(Phan et al., 2018)
Tg (fms:GFP)sh377	*fms:GFP*	(Dee et al., 2016)
Tg (lysC:EGFP)	*lysC:GFP*	(Hall et al., 2007)
Tg(mpeg1:Gal4FF) Tg(UAS-E1b:Eco.NfsB-mCherry)	mpeg1:NTR-mCherry	(Davison et al., 2007) (Ellett et al., 2011)

Zebrafish larvae were maintained in Petri dishes with approximately 60 larvae per dish, filled with E3 media supplemented with methylene blue (20µL/1L) at 28°C in light-cycling incubators (14h dark – 10h light).

Adult fish were maintained on a 14:10-hour light/dark cycle at 28°C in the UK Home Office approved, Biological Services Aquarium at the University of Sheffield. Animal work was performed conform to the Animals (Scientific Procedures) Act 1986 Amendment Regulations 2012 in any of the specified locations of this thesis.

2.2 Injuries and Neutrophil and Swarming Counts

2.2.1 Tail Fin Injuries

Tail fin injuries were performed on staged 3 days post fertilisation (dpf) zebrafish larvae. Larvae were transferred to a petri dish with fresh E3 and anaesthetised with 2ml, 4.2% tricaine. Using a surgical scalpel blade (size 10), a cut was made across the tail fin, inside of the pigment gap, taking care not to cut the circulatory loop. This would usually result with

larvae having small protrusions at the end of their tail consisting of cells from the notochord (tail amputation). Tail fin injuries without injuring the notochord (fin fold) were also performed for direct comparison (and for section **2.3 Tail Fin Regeneration Assay**). After performing tail fin injuries larvae were either used for *in vivo* time-lapse imaging or put back in a new petri dish with fresh E3 to recover from the anaesthetic, ready for manual neutrophil and swarm counts.

2.2.2 Ventral Fin Injuries

Ventral fin injuries were performed on staged 3 days post fertilisation (dpf) zebrafish larvae. Larvae were transferred to a petri dish with fresh E3 and anaesthetised with 2ml, 4.2% tricaine. Using a surgical scalpel blade (size 10), a small triangular cut was made close to the hemopoietic tissue distally from the cloaca of the fish. After performing ventral fin injuries larvae were used for *in vivo* time-lapse imaging.

2.2.3 Laser Injuries

Using a high intensity CryLaS ablation laser, injuries were made in the ventral fin or across the entire tail fin. During ventral fin injuries either point or line injuries (approximately 200µm by 20µm) were made.

Settings were as follows:

Effective injury, promoting neutrophil swarms:

- Frequency: 250Hz, Laser power: 80-100%, Dwell time: 2500µs.

Minimal injury, no neutrophil swarms:

- Frequency: 250Hz, Laser power: 20%, Dwell time: 2000µs.

Imaging was started directly after performing the laser injury. With the settings as defined in **Table 3**.

2.2.4 Counting Neutrophils and Swarms

After performing tail fin injuries (as described in **2.2.1 Tail Fin Injuries**), larvae were collected and imaged using a Leica stereomicroscope, equipped with fluorescent filters connected to an epi-fluorescent light source. Before counting, larvae were anaesthetised with 2ml, 4.2% tricaine and transferred in groups to a petri dish containing a small layer of 2% agarose (Meridian Biosciences, C# B10-41025) for easier handling and imaging. Counts of neutrophils and swarms at the wound site were performed at the following hours post injury (hpi); 0hpi, 2hpi, 4hpi, 6hpi, 8hpi, 10hpi, 24hpi. In some earlier cases the 10hpi timepoint was not recorded. Counts were done manually ±500µm around the tail fin wound. Swarms were counted alongside neutrophils whenever they were observable.

2.3 Tail Fin Regeneration Assay

For the tail fin regeneration assay, tail fins of 3dpf zebrafish larvae were cut taking care not to injury the notochord. Larvae were assessed at 4hpi for neutrophil swarms and split into respective groups. Tissue regeneration and neutrophil counts were assessed at 24 and 48hpi. For this, zebrafish larvae were anesthetised using 4.2% tricaine shortly transferred to a glass bottom imaging dish (Nunc™ Glass Bottom Dishes, Thermo Scientific™, C# 150682) filled with a minimal layer of 2% agarose gel (Meridian Biosciences, C# B10-41025).

2.4 Time-lapses

2.4.1 Mounting zebrafish larvae

To keep zebrafish larvae stable over a prolonged period of time, a set up using an agarose mould was prepared. A 2% agarose gel (Meridian Biosciences, C# B10-41025) was prepared and poured in a petri dish, in which a small, rectangular stainless-steel block was set to create a mould. The stainless-steel block was removed from the petri dish, the mould was cut out of the petri dish and moved into a smaller (dry) glass imaging dish (Nunc™ Glass Bottom Dishes, Thermo Scientific™, C# 150682) Larvae were anaesthetised with 4.2% tricaine and were taken up in a small droplet containing up to 15 zebrafish larvae which was subsequently put alongside the mould. Using a snapped off micropipette, larvae were moved into the slots of the agarose mould. Excess E3 media was removed with a P1000 pipette. A 0,8% agarose gel (low gelling temperature (LGT), SIGMA, C# A9414-25G) was slowly added on the side of the mould and larvae positions were quickly adjusted in the slots. The rest of the dish was covered in 0,8% LGT agarose gel. The dish was covered with a small layer tricaine solution (0,20mg/ml in E3) to prevent the gel from drying out and to keep larvae stable over the course of the time-lapse. For the experiments conducted on the Acquifer Imaging Machine, a 96-well plate (Corning®, Merck, CLS3925) was filled with 150µl of regular E3 media supplemented with 4.2% tricaine. No mounting was necessary as larvae would naturally fall onto their sides into a lateral orientation and the microscopy stage was in a fixed position with the objectives moving under the 96-well plate.

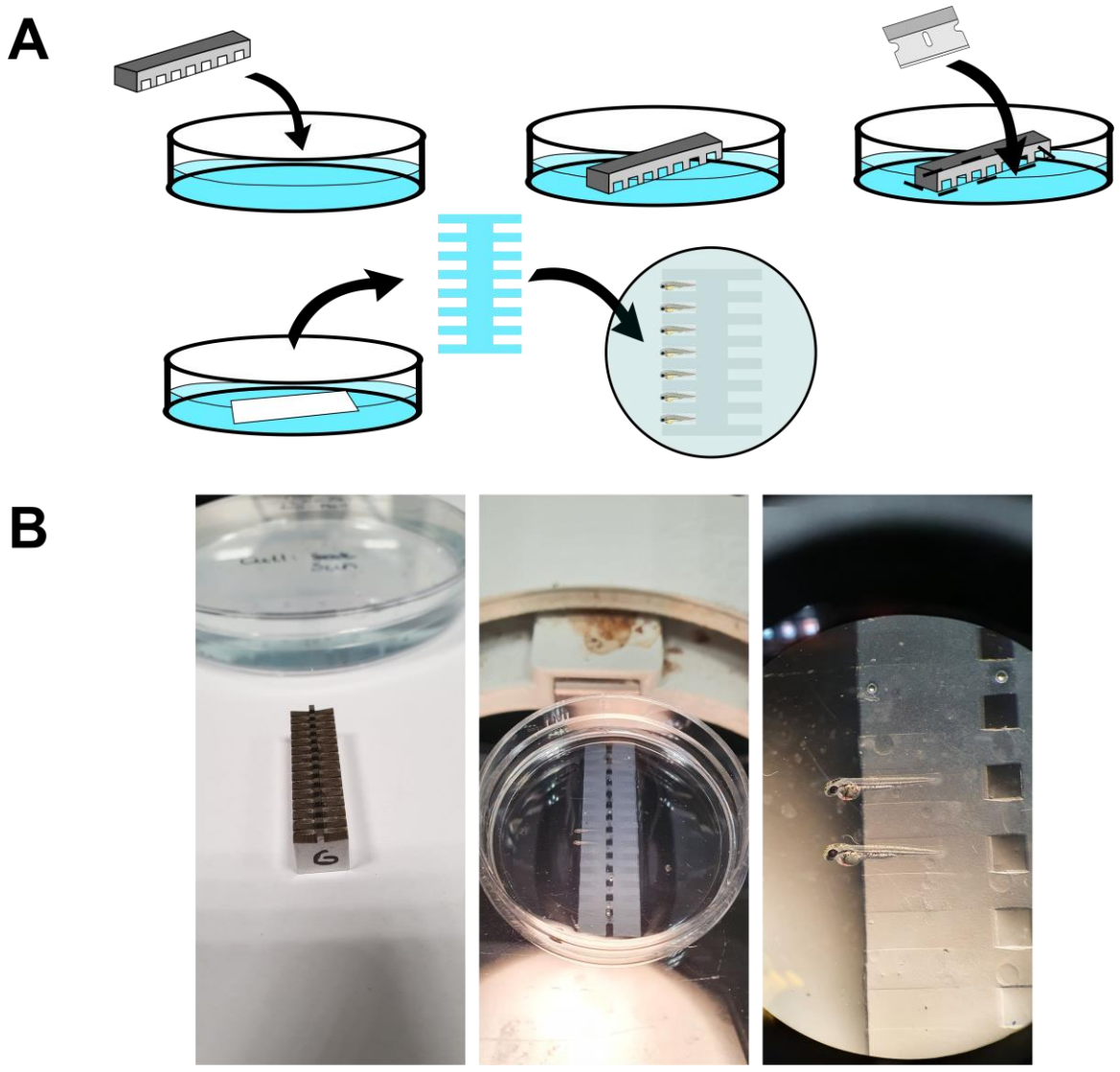

Figure 3: Mounting of zebrafish in agarose moulds for long time-lapse imaging

This figure shows the mounting process whenever an agarose mould was used for long time-lapse imaging.

A. An aluminium block with small notches was used to create the agarose mould by placing it into 2% agar, letting it solidify, cutting around the block, extracting the mould, putting it in an imaging dish, slotting in the zebrafish and securing them with 0.8% LMP agar.

B. A series of pictures illustrating how this looks in the lab. The first picture shows the block, the second picture the mould with the fish held in place using 0.8% agar and the final picture shows a x4 magnification of fish in the slots. Pictures were taken with a Samsung S10+.

2.4.2 Acquiring time-lapses

For this research multiple microscopes with different set ups were used to fulfil specific purposes. Most of the microscopes used were focused on long time lapse imaging experiments. These experiments were performed on spinning disk microscopes (**Table 3**), as these offer a lower amount of phototoxicity transferred into the sample over time, as well as a faster acquisition rate compared to traditional laser scanning confocal systems. Besides this, one of the proprietary systems used during a collaboration at Acquifer (**Table 3**), was more focused on high-throughput scalability, as this system offered compatibility with 96 well plates. Below will be given the exact microscope configuration together with objectives used and an overview of the acquisition settings.

Table 3: Comprehensive list of microscopes and image acquisition settings

Feature	Nikon Epifluorescence Microscope, Renshaw Lab, Sheffield	Nikon Spinning Disk, Wolfson Light Microscopy Facility, Sheffield	Acquifer Imaging Machine (IM), Heidelberg	Andor/Nikon Spinning Disk MRI, Montpellier
Microscope Body	Nikon Ti Eclipse TE-2000-U	Nikon Ti2 Eclipse	Custom, Acquifer	Nikon Ti Eclipse
Camera	Andor Zyla VSC-02811	Photometrics Prime 95B 22mm	Hamamatsu sCMOS 2k x 2k	Andor Zyla 4.2
Objective	Nikon Plan Fluor ELWD x20, 0.45NA	Nikon Plan Apo λ x20, 0.75NA	Nikon x20/0.75 DIC	Nikon x20/0.75 DIC
Binning	2x2	No binning	No binning	No binning
LED Intensity	50%	N/A	Omicron LED-HUB 470: 50%	N/A
Laser 488 Intensity	N/A	50%	N/A	50%
Laser 561 Intensity	N/A	75% (if used)	N/A	50% (if used)
Exposure 488	70-100ms	20-50ms	50ms	50ms
Exposure 561	N/A	100ms	N/A	300ms
Z Step	10µm	2µm	2µm	2µm
Z Stack	80µm	100µm	100µm	100µm
Experiment Duration	6-16 hours	6-16 hours	6 hours	6 hours
Time Interval	Every 15 minutes	Every 2.5 or 2 minutes	Every 5 minutes	Every 2.5 minutes
Multi-position Imaging	Depends on achieving the time interval	Depends on achieving the time interval	~20 fish imaged every 5 minutes	Depends on achieving the time interval
Region of Interest (ROI)	N/A	Cropped to the area of interest to speed up acquisition and limit data	Cropped to the area of interest to speed up acquisition and limit data	Cropped to the area of interest to speed up acquisition and limit data
Pixel size	0.325 µm	0.55 µm	0.325 µm	0.319 µm

2.5 Image processing and analysis

Images obtained after microscopy were immediately transferred to google drive after which they were downloaded locally and further processed using FIJI Image J. Pre-processing consisted of creating a maximum intensity projection (MIP) which greatly reduced data size. MIPs were chosen as I was unable to obtain high enough z-resolution during long time-lapse imaging for detailed 3D investigation of cell motility. Images were split into their respective channels, Brightfield, GFP and RFP (mCherry) when applicable. All code used for image processing and analysis can be found in an online GitHub repository (**Supplemental 5.2 Code**). A full flowchart of the analysis pipeline with steps where user input is needed is shown on the following page (**Fig 4**).

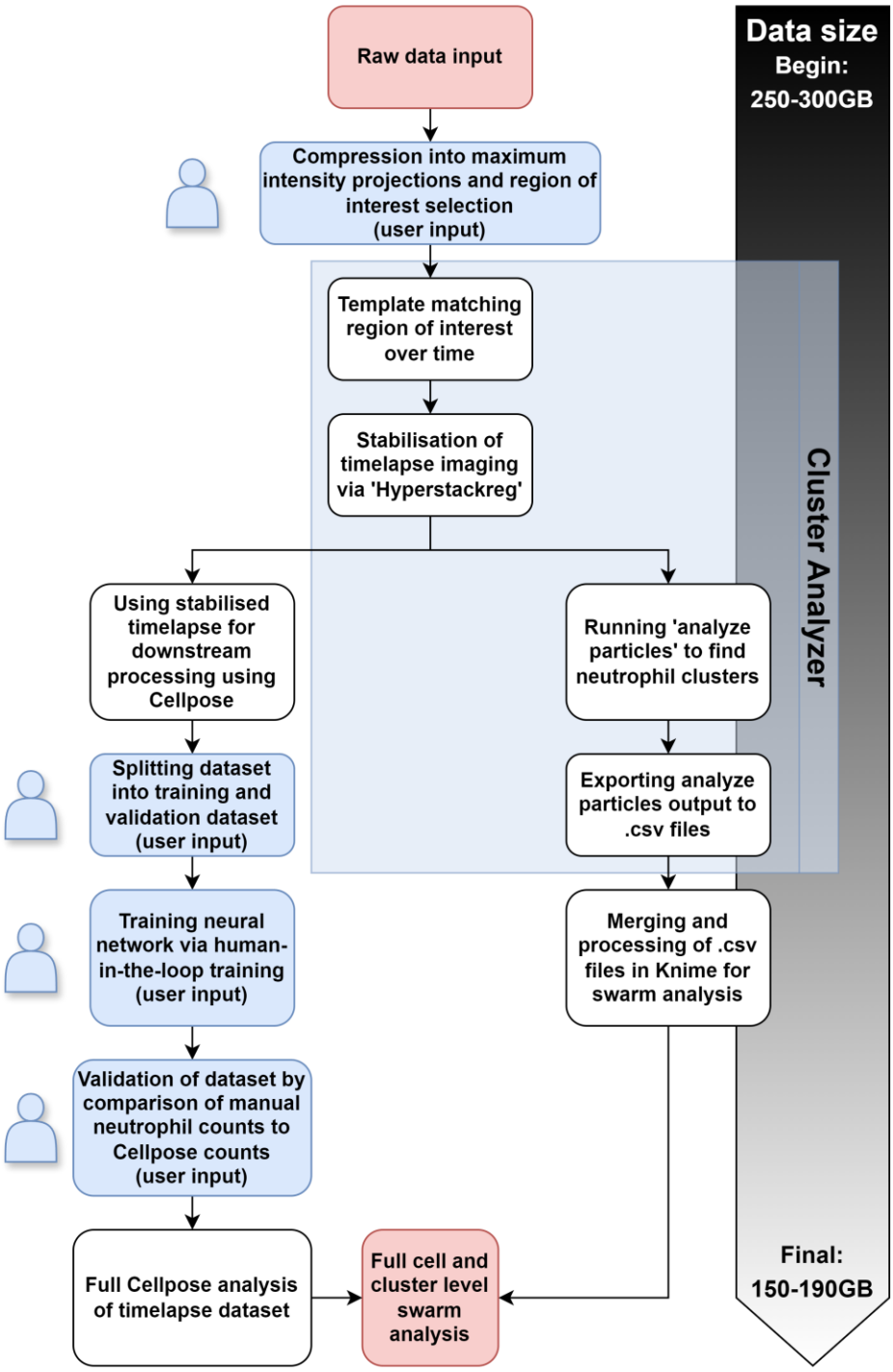

Figure 4: Flowchart of full image analysis pipeline

Data processing and full analysis resulted in a data size reduction from 250-300GB to 150-190GB after full analysis occurred. Multiple copies of some images, are still present so data-size could be pruned further, but this was disregarded in favour of dataset structure and clarity.

2.5.1 Cluster Analyser

With the use of FIJI (ImageJ) an advanced image analysis macro was developed called the 'cluster analyser' (Schindelin et al., 2012). The cluster analyser macro was developed together with Mr Sankeert Satheesan (Acquifer) and implements code that has previously been published (Thomas and Gehrig, 2020, Sharma, 2018). Template matching analysis was improved by using timepoints in the middle of time-lapses and by blurring images to improve matching accuracy. HyperStackReg was then used to further stabilise the output regions of interest (ROI). Using the cluster analyser, neutrophil clusters were extracted from user-specified regions of the zebrafish and data was saved in .csv files. Using Knime (4.6.3), a node-based workflow software, .csv files were merged and further analysed. Areas of clusters were compared using a range of metrics that could help classify swarming responses and gain insight into the data. Besides .csv files, the cluster analyser outputs ROI files and .tif files for further cell specific analyses.

2.5.2 Cellpose

Cellpose is a previously published deep learning algorithm which can be used for segmentation of fluorescent imaging data (Stringer et al., 2021). Cellpose was adapted and novel models were trained on my own imaging data for accurate segmentation. A subset of imaging data was taken for experiments that were conducted on different microscopes as illustrated in **Table 3**. Data was split into a test set and a training set, where the training set was used to train the model, and the test set was used for validation. Validation occurred through manual cell counts of the test set, which was then compared to counts obtained from the Cellpose model. Using filtering to exclude counts of smaller particles in Microsoft Excel, output of counts and tracking of objects was tuned accurately per microscope set-up **Table 3**.

2.5.3 TrackMate

The native FIJI Image J plug-in TrackMate, was used for tracking of cells (Tinevez et al., 2017). Masks created by the Cellpose segmentation step were loaded as label images and spatiotemporal settings were accurately set based on imaging interval and pixel size. Tracks were filtered according to the filter settings obtained as described in **2.4.2 Cellpose**. Tracks were critically assessed by eye and filters for track length was finetuned per sample. Tracks were coloured by their mean speed which for which the min-max range was kept consistent per experiment. All TrackMate settings were exported as .xml files for re-analysis if necessary. Data of Tracks, Edges and Spots were extracted as .csv files and used for downstream analysis of cell motility and location.

2.5.4 Python Scripts for Neutrophil-Macrophage Interaction

Python scripts were created for analysis of interactions between neutrophils and macrophages, and between neutrophils and macrophage debris. In general, this script aligns macrophage and neutrophil positions based on timepoint, calculates the Euclidean distance between them, and filters out pairs that are within 20µm of each other from the centroid of the cells, indicating interaction. It then computes the directional changes in neutrophil positions, determines the movement magnitude, and filters out movements below a minimum threshold. Next, it calculates the vector components from neutrophils to macrophages and computes the dot product between these vectors and the neutrophil movement vectors. The dot product was normalised by the movement magnitude to assess the alignment of neutrophil movement towards macrophages or macrophage debris. Finally, only the movements that show a positive alignment towards the macrophages or macrophage debris, indicating directional movement towards the target, were plotted.

2.6 TLR Agonist Treatments

The TLR agonist screen was performed by treating *Tg(mpx:GFP)*^{i114} with a range of selected compounds via immersion.

- Lipopolysaccharide (LPS) (Invivogen C# tlrl-eblps), 10µg/mL (Dissolved in E3)
- Polyinosinic:polycytidylic acid (Poly I:C) (Invivogen C# tlrl-pic), 10µg/mL (Dissolved in 100% DMSO)
- resiquimod (R848) (Invivogen C# tlrl-r848-1), 10µg/mL (Dissolved in 100% DMSO)
- imiquimod (R837) (Invivogen C# tlrl-imqs-1), 10µg/mL (Dissolved in 100% DMSO)
- high mobility group box 1 protein (HMGB1) (R&D Systems C# 1690-HMB), 2.5µg/mL (Dissolved in 100% DMSO)
- Pam2CysSerLys4 (PAM2CSK4) (Invivogen C# tlrl-pm2s-1), 10µg/mL (Dissolved in 100% DMSO)
- *N*-formylmethionyl-leucyl-phenylalanine (fMLP) (Sigma-Aldrich C# F3506), 100nM (Dissolved in E3)

Tail fin injuries were performed as described in **2.2.1 Tail Fin Injuries**. After tail fin injury, larvae were put split into groups of 3 in a 96 wells plate (Thermo Scientific™, Nunc™ MicroWell™, C# 260860), 11 wells per condition, with 1100µL end volume per well. Concentrations of each compound was x2 per well and was brought to the end concentration by pipetting 3 larvae in 550 µL of E3. E3 media was used as control. At 4hpi larvae were anaesthetised with 4.2% tricaine and assessed for neutrophil swarms using a fluorescent stereomicroscope.

Further investigation into TLR 1/2 and 2/6 agonists was performed with:

- Pam2CysSerLys4 (PAM2CSK4) (Invivogen C# tlrl-pm2s-1) (Dissolved in 100% DMSO)
- Pam3CysSerLys4 (PAM3CSK4) (Invivogen C# tlrl-pms) (Dissolved in 100% DMSO)
- CU-T12-9 (Invivogen C# tlrl-cut129) (Dissolved in 100% DMSO)
- *Staphylococcus aureus* Cell Wall Prep (CWP) (Foster Lab, Sheffield) (Dissolved in 100% DMSO)

Dilution series were as follows:

- PAM2CSK4: 0.005ng/mL, 0,05ng/mL, 0,5ng/mL, 5ng/mL, 50ng/mL
- PAM3CSK4: 0.005ng/mL, 0,05ng/mL, 0,5ng/mL, 5ng/mL, 50ng/mL
- CU-T12-9: 0.2ng/mL, 2ng/mL, 200ng/mL, 200ng/mL, 2000ng/mL
- *S.aureus* CWP: 1ng/mL, 10ng/mL, 100ng/mL, 1000ng/mL, 10000ng/mL

Tail fin injuries were performed as described in **2.2.1 Tail Fin Injuries**. After tail fin injury, larvae were put split into groups of 15 in a 6 wells plate (Thermo Scientific™, Nunc™ non-treated C# 150239), 2 wells per condition, with 3000µL end volume per well. 1% DMSO was used as control. End volume was reached by pipetting 1 embryo with 198 µL E3 clear medium using a P200 pipette with a cut off tip to ensure transfer of larvae without additional wounding. At 4hpi larvae were anaesthetised with 4.2% tricaine and assessed for neutrophil swarms using a fluorescent stereomicroscope.

2.7 Prolyl-hydroxylase Inhibitor Treatments

Tail fin injury was performed as shown in **2.2.1 Tail Fin Injuries**. Afterwards prolyl-hydroxylase (PHD) inhibitor treatments were performed via immersion. Dimethyloxalylglycine (DMOG) (Sigma-Aldrich C# D3695) and Roxadustat (FG-4952) (Selleckchem C# S1007) were used at 100µM and 5µM respectively (Elks et al., 2011, Schild et al., 2020). Zebrafish were split into groups of 15 in a 6 wells plate (Thermo Scientific™, Nunc™ non-treated C# 150239) with 3000µL end volume. Swarm counts were assessed at 6hpi. Neutrophil counts were assessed over time at 6hpi, 24hpi and 48hpi while being continuously exposed to DMOG and FG-4952, media was refreshed once at 24hpi. Treatments including 100 µM Diphenyleneiodonium (DPI) were performed precisely the same. Concentration of DPI was determined by previous work (Bernut et al., 2020).

During timelapses larvae remained continuously exposed to DMOG and FG-4592 at 100µM and 5µM respectively, supplemented into 0,8% LMP agarose gel and in E3 media on top.

2.8 CellROX Staining

To assess levels of reactive oxygen species (ROS), I used CellROX™ Deep Red (Thermo Scientific™, C# C10422). Larvae were exposed to 5µM CellROX in E3 media for 30 minutes prior to mounting for time-lapse imaging. Larvae were washed twice with E3 before mounting. CellROX concentration was based on previously established work (Bernut et al., 2019).

2.9 Macrophage depletion

2.9.1 Metronidazole treatment of *Tg(mpeg1:GAL4/UAS:NTR-mCherry)* for depletion of macrophages

Metronidazole was diluted in 0.1% DMSO (1µL/ml) and heated for 5 min at 37°C to fully dissolve. *Tg(mpeg1:GAL4/UAS:NTR-mCherry)* larvae were subsequently exposed to metronidazole at a final concentration of 10mM to ensure efficacy (Nguyen-Chi et al., 2017). Preparation of the compound as well as treatment of the zebrafish occurred in the dark by wrapping Eppendorf tubes or petri dishes with aluminium foil.

2.9.2 *Generation of irf8 crispants for macrophage depletion*

For full depletion, two guides targeting *irf8* expression were injected at a final concentration of 50 µM each by creating an injection mix of 0.5 µL of each guide at 100 µM, 1 µL of 50 µM tracer, and 1 µL Cas9 nuclease (Rutherford et al., 2024). For the control, scrambled crRNA was used at 50 µM in the place of *irf8*-targeting guides. Embryos were injected with 2 nL of

injection mix into the yolk sac at the single cell stage. At 3dpf macrophage and neutrophil numbers were assessed with a confocal fluorescent microscope.

Table 4: irf8 CRISPR guide sequences

Gene	Guide name	Sequences
irf8	irf8_crRNA_A	5' GCGGTCGCAGACTGAAACAGTGG 3'
irf8	irf8_crRNA_B	5' GTCTACAAGATGAACTCGGG 3'
n/a	scrambled_crRNA	5' GACCTGAGGGAGCAAGATCC 3'

(Rutherford et al., 2024)

2.10 Data visualisation and statistics

Data visualisation and statistical analysis were performed using GraphPad Prism 9.3.1 and using matplotlib in Python (**Supplemental 5.2 Code**). Normally distributed data were checked with a Shapiro-Wilk normality test. Nonparametric data were analysed with the respective nonparametric tests. N-numbers, statistical tests and plotting settings are communicated within graphs or in the figure description. For XY graphs obtained from time lapse imaging linear regression was performed to assess statistical differences, unless stated otherwise. Significance is shown as p-values above or beside data in graphs. Specific statistics used for datasets are outlines in figure legends.

Chapter 3: Results

3.1 Initial Investigation of Neutrophil Swarming in Zebrafish

3.1.1 Introduction

Previous research into the nature of neutrophil swarms has mainly investigated mechanisms leading to swarm formation, which is defined as highly coordinated movement of neutrophils towards a site of infection or inflammation. It has been shown that swarming exhibits a clear biphasic response where neutrophils recruited towards the wound can amplify further recruitment of more distant neutrophils (Lämmermann et al., 2013, Kienle et al., 2021, Isles et al., 2021). This second part of the response is largely regulated by the release of LTB4, as illustrated across human neutrophils *in vitro* and mouse and zebrafish neutrophils *in vivo* (Kienle et al., 2021, Isles et al., 2021, Strickland et al., 2024). Subsequent literature has shown that part of this relay mechanism is controlled by calcium fluxes, which are regulated via Cx43-hemichannels (Poplimont et al., 2020). Indications of self-regulation of the continuous accumulation of neutrophils have been shown through the use of a Grk2-/- mouse, where GRK2 significantly diminished cluster growth via GPCR desensitisation (Kienle et al., 2021).

Multiple papers have used the zebrafish model for the investigation of the swarming response, but have not thoroughly investigated the entire inflammatory time course which includes resolution of neutrophils from the site of challenge (Isles et al., 2021, Poplimont et al., 2020, Tamás et al., 2023). Here I aim to address this by performing long time-lapse imaging experiments. With these time-lapses I want to determine when neutrophil swarms take place and, more specifically, when they resolve. Further in-depth characterisation of

the neutrophil swarming response in zebrafish is essential to establish a robust framework for future research, which could help alleviate swarming related burden on patients.

Variation in immune genes has been associated with genetic differences between individual zebrafish and between strains, potentially causing differences in inflammatory responses (McConnell et al., 2023). This can be important in terms of variation in the neutrophil swarming response, as such I utilised two different transgenic zebrafish lines and assessed neutrophil swarm formation in each.

In the field of zebrafish research, there is no consensus on the optimal method for performing tail fin injuries. Some researchers avoid injuring the notochord entirely, while others include the notochord in the injury to elicit a more pronounced inflammatory response, typically resulting in a higher number of neutrophils at the wound site (Nguyen-Chi et al., 2015, Loynes et al., 2018). Thus, I determined whether the type of tail fin injury would have a significant effect on neutrophil swarm formation.

One physiological implication of neutrophil swarming has been illustrated in mono-cultures of human neutrophils. In an *ex vivo* model for chronic granulomatous disease, NADPH-Oxidase was elaborately shown as regulator for a negative feed-back loop of calcium wave propagation which corresponded with neutrophil over-recruitment found in human chronic granulomatous disease (Strickland et al., 2024). However, *in vivo* physiological effects of swarming remain relatively undescribed. As such, I used the zebrafish model of tail fin regeneration to study whether swarming would lead to differences in tissue regeneration.

3.1.2 Time Frame of neutrophil recruitment and swarming

As an approach to establish swarms within the zebrafish model, tail fin injuries were induced in *Tg(mpx:GFP)*^{i114} zebrafish larvae at 3dpf (**Figure 5A**). Manual counts were performed for neutrophils and swarms in close vicinity to the wound area. Within zebrafish, I defined neutrophil swarms as 3 neutrophils or more in close contact over more than 15 minutes. Neutrophillic inflammation showed a bell-shaped curve resembling a Gaussian distribution, with a pronounced peak at the central value and symmetrically decreasing values on either side (**Fig 5B**). This illustrates both the recruitment and resolution phase of neutrophils taking place from 0-4 hours and 8-24 hours respectively, with peak inflammation occurring around 6hpi. In this initial experiment, a lack in swarming responses was observed (**Figure 5C**). Taken together, these results confirm that the neutrophil response in zebrafish is quantifiable and capable of generating neutrophil swarms, albeit with potentially low frequency of occurrence.

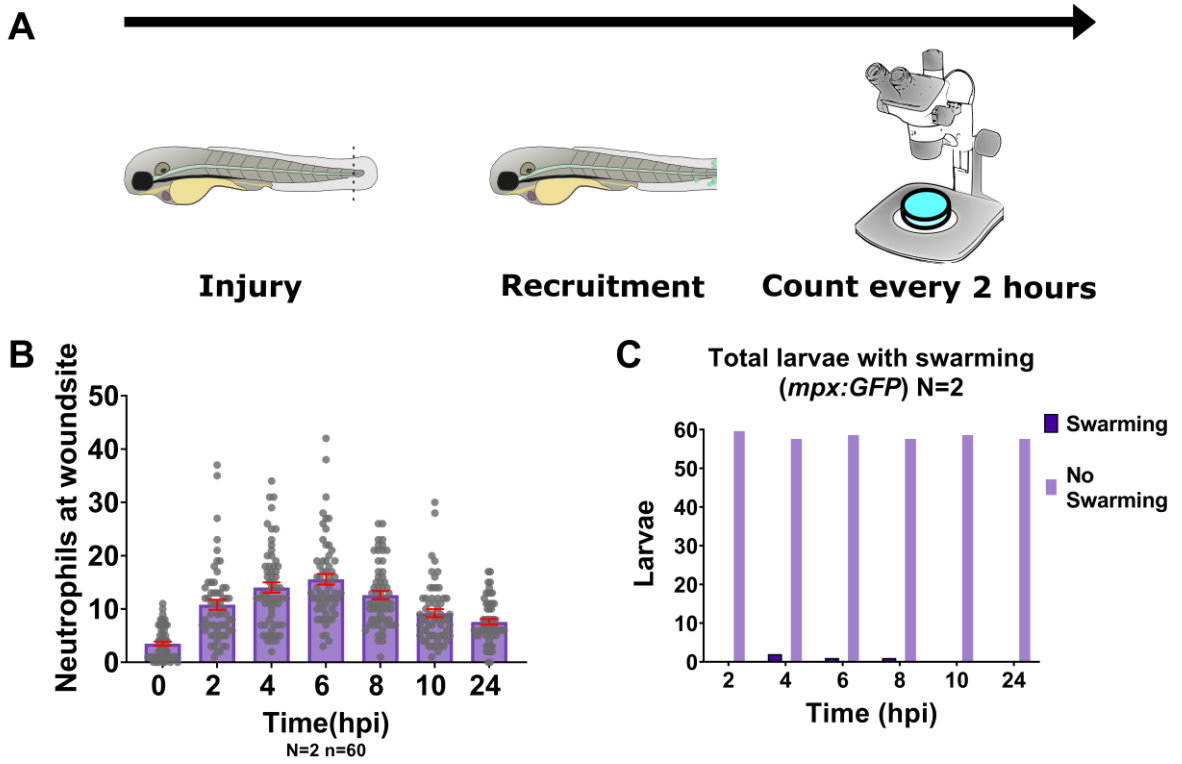

Figure 5: Identifying the peak of neutrophil presence and swarming in Tg(mpx:GFP)i114 larvae

A. Illustration of the experimental approach utilized for this study. Injury was performed on 3dpf zebrafish larvae.

B. Graph depicting the total neutrophil count at the wound site across various time points. Counts were performed using a stereoscope, neutrophils were visualised by using the *Tg(mpx:GFP)i114* reporter line.

C. Graph showing the number of swarms formed in the examined zebrafish larvae at different time points

3.1.3 Genetic background unlikely to alter the neutrophil swarming response

To address whether any genomic variability causes considerable differences in neutrophil swarming, I utilised *Tg(mpx:GFP)*^{i114} and *Tg(mpx:GAL4)*^{sh267}*; Tg(UAS:Kaede)*^{i222} zebrafish larvae (**Figure 6**). These data were obtained from two independent experiments and as such cannot be directly compared. However, based on the data, we can infer that the genetic background does not significantly impact the neutrophil swarming response, as the neutrophil recruitment, resolution and the number of swarms observed over time did not differ meaningfully. This assertion is supported by data presented later in this thesis (**Figure 21-22**), which illustrates swarming responses in the *Tg(LysC:EGFP)* line. This demonstrates that, despite the use of several genetic backgrounds, neutrophil swarming remains a robust and observable process across different genetic lines.

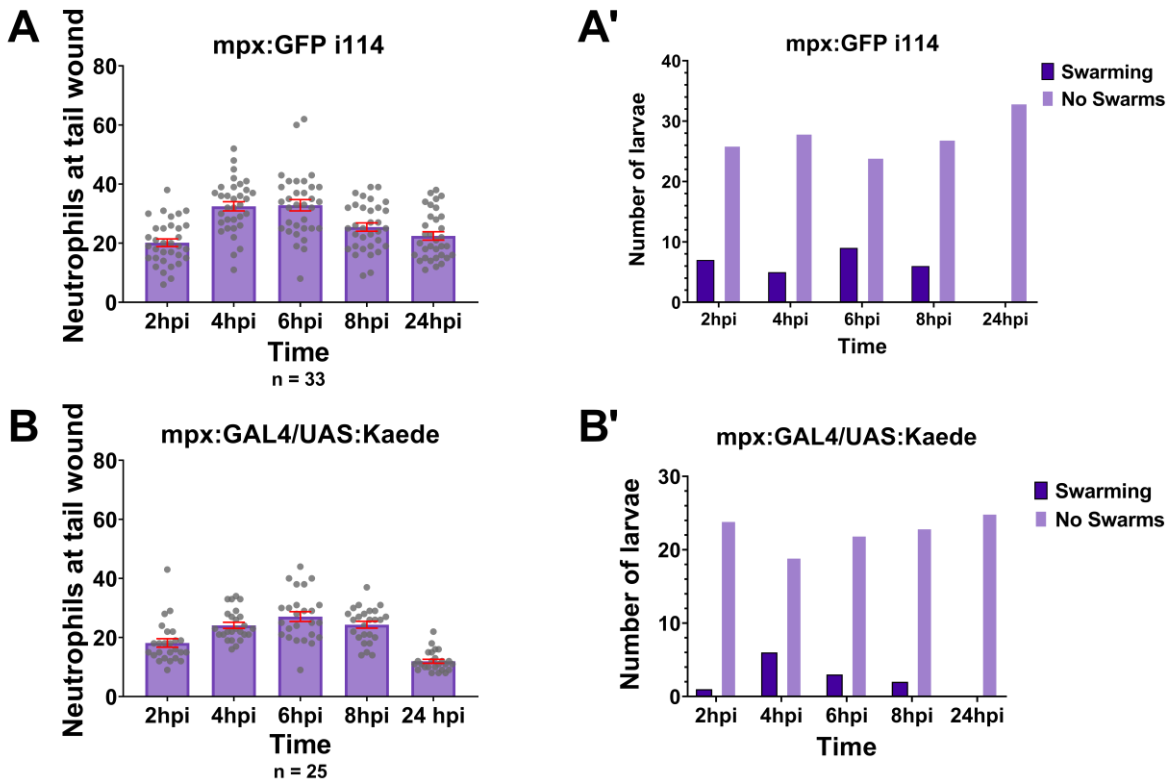

Figure 6: Neutrophil recruitment and swarming in *Tg (mpx:GFP)i114* and *Tg (mpx:GAL4/UAS:Kaede)* zebrafish larvae

A. Total neutrophil count at the wound site over 24 hours for 3dpf *Tg(mpx:GFP)^{i114}* zebrafish larvae.

A'. Corresponding swarming events at different time points across 24 hours for *Tg(mpx:GFP)^{i114}* zebrafish larvae.

B. Total neutrophil count at the wound site over 24 hours for 3dpf *Tg(mpx:GAL4/UAS:Kaede)^{i222}* zebrafish larvae.

B'. Corresponding swarming events at different time points across 24 hours for *Tg(mpx:GAL4/UAS:Kaede)^{i222}* zebrafish larvae.

3.1.4 Tail fin injury type does not affect swarm formation

To compare two canonically used tail fin injury methods, I created two groups: one group had tail fin injuries sparing the notochord (fin fold) and the other group had injuries that included the notochord (tail amputation). I then assessed the number of neutrophil swarms at 4hpi using a fluorescence stereomicroscope. There was no significant difference in swarm formation between the two groups (**Figure 7**). This suggests that the swarming process is more robustly dependent on the underlying signalling mechanisms rather than the severity of tissue injury.

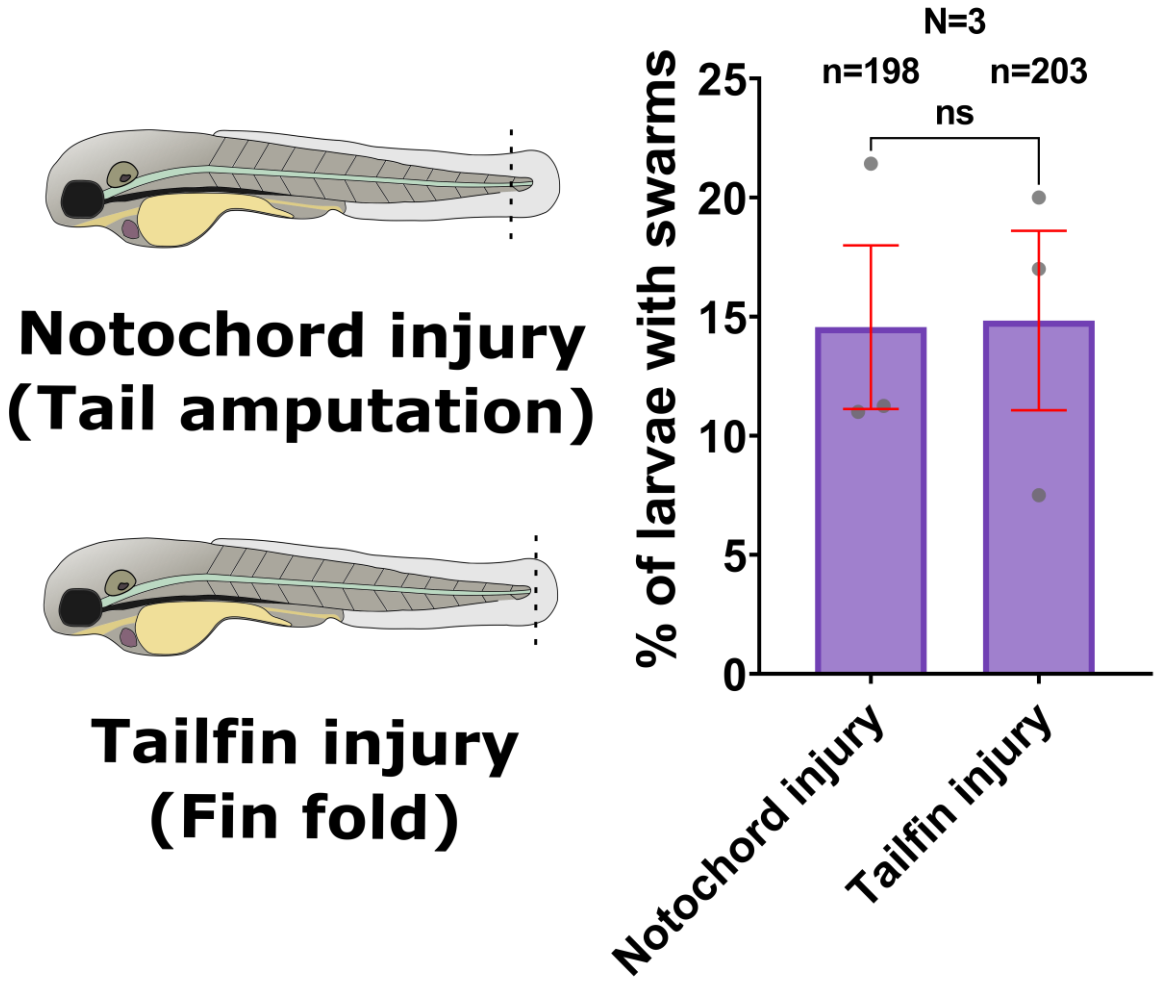

Figure 7: Tail fin injury type does not affect swarm formation

This figure shows the % of larvae that developed a neutrophil swarm after either a tail fin injury cutting the notochord (tail amputation) or tail fin injury sparing the notochord (fin fold). Swarm formation was examined using a fluorescence stereomicroscope at 4hpi. Out of 3 experimental repeats consisting of a total of 198 and 203 zebrafish larvae for both groups respectively, there was no significant difference in the number of swarms that formed. Data was analysed by Wilcoxon matched-pairs signed rank test, P>0.9999.

3.1.5 Peak swarming occurs between 2 and 8 hours after a tail fin injury

To investigate in further detail when swarms form and resolve I set out to do time-lapse imaging. For successful *in vivo* imaging, existing protocols were optimised to keep zebrafish larvae stable over long periods of time, in some cases up to 15 hours. After the time-lapse was acquired, a FIJI ImageJ macro was used to generate binary masks of the fluorescent data, subsequential extraction of the maximum area per timepoint was performed, as a general measurement of neutrophil swarms that occurred. When this is plotted against time, it shows that the biggest areas are found between 2 and 8hpi of the tail fin, which is in line with the peak of inflammation observed in earlier experiments (**Figure 8**).

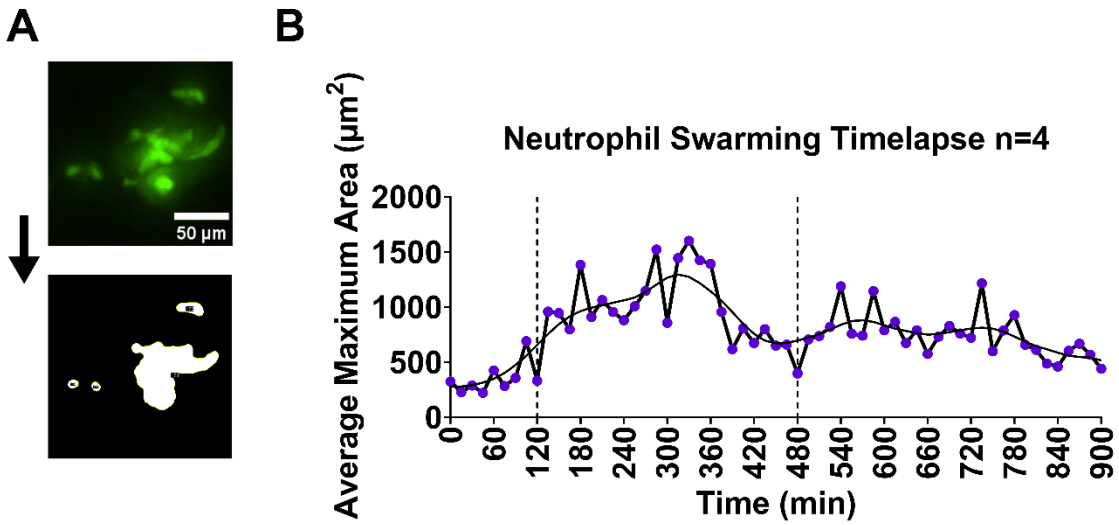

Figure 8: Swarm size peaks from 2 to 8 hours post-injury

A. Binary mask created from fluorescent data using an ImageJ macro, default automatic thresholding with analyse particles recognizing any object above 20µm.

B. Graph showing the maximum swarm area extracted per time point, plotted over 15 hours, indicating the largest swarm size occurs between 2- and 8hpi. Data is averaged from four different 3dpf *Tg(mpx:GFP)*^{i114} larvae.

3.1.6 Elevated neutrophil numbers correlate with swarming

To further understand how neutrophil swarming influences the progression of inflammation in the zebrafish model, I conducted two separate time-lapse experiments focusing on the recruitment and resolution phases of inflammation. Larvae were categorised into groups with and without swarms based on careful observation of the time-lapses in FIJI ImageJ post-experimentation. In the first time-lapse, I observed the period from 1 to 7 hours post-tail fin injury at 15-minute intervals. Larvae at 3dpf were injured, mounted in low-melting agarose promptly, and imaging commenced at 1hpi (**Figure 9B**). Linear regression analysis revealed a significant increase in neutrophil numbers in larvae with swarms compared to those without, though the recruitment rate of neutrophils was not significantly different. In the second time-lapse, I examined the resolution phase of 3dpf old larvae from 6 to 12hpi (**Figure 9C**). Larvae were kept in a petri dish with E3 media and mounted later, with imaging starting 6hpi. Linear regression analysis again showed a significant elevation in neutrophil numbers in larvae with swarms. However, the rate of resolution, indicated by neutrophil clearance from the injury site, did not differ significantly. These results indicate that, although the rates of recruitment and resolution of neutrophils towards and away from the wound site do not differ significantly, there is a significant elevation in neutrophil numbers in larvae exhibiting neutrophil swarming events compared to those without.

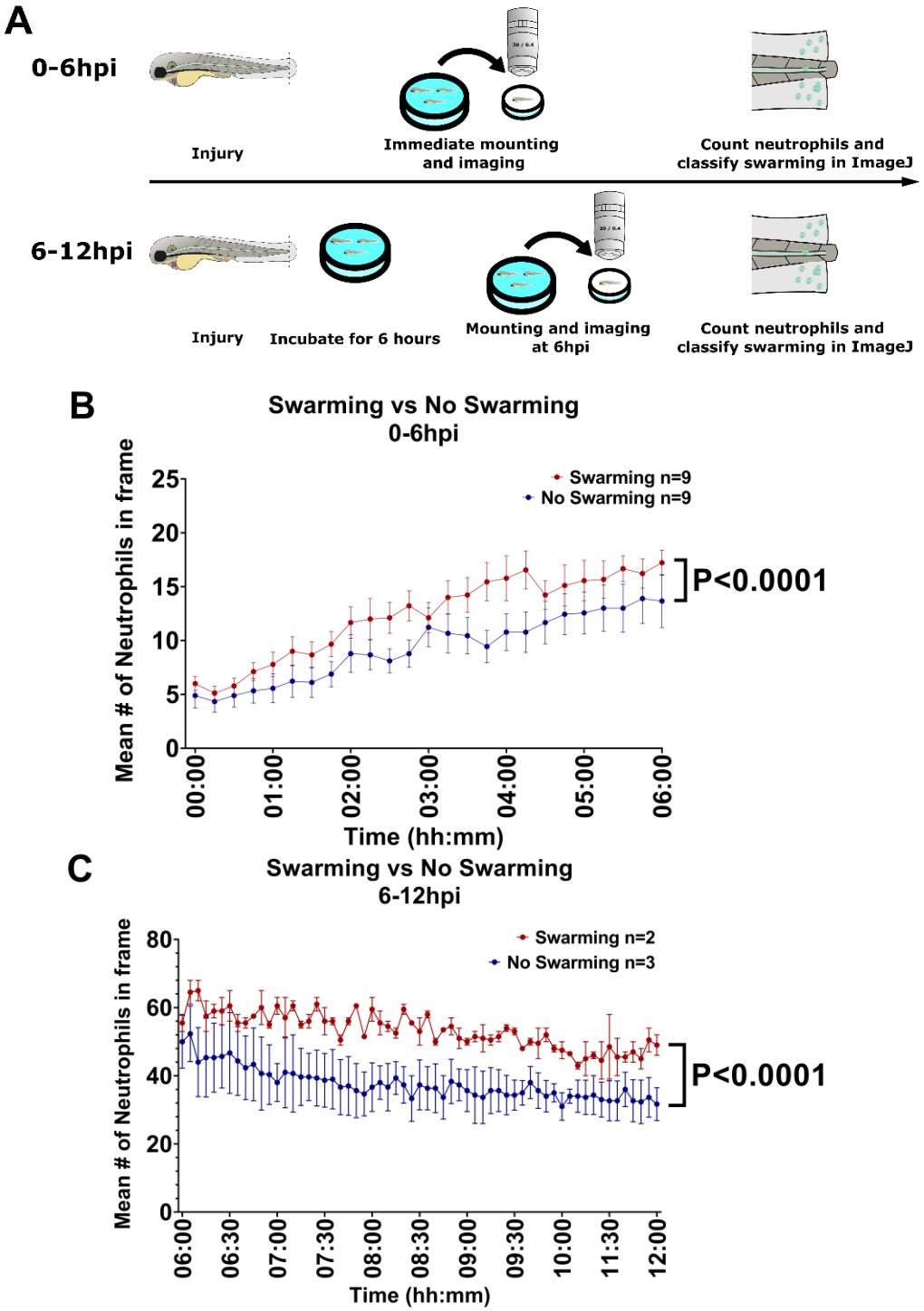

Figure 9: Neutrophil recruitment and inflammation resolution in larvae with and without swarms

A. Experimental timeline: Tail fin transection performed on 3dpf larvae followed by mounting in 0.4% agarose for time-lapse imaging of the initial 6 hours of the inflammatory response. In a separate experiment, tail fin transection was performed, and larvae were put back in E3 media for 6 hours before mounting to assess the resolution phase.
B. Number of neutrophils at the wound over 6 hours (1 to 7hpi) with 15-minute intervals, showing mean and SEM from 9 samples in both groups. Significant elevation difference ($P<0.0001$, $F=48.84$, $DFn=1$, $DFd=447$) but no significant slope difference ($P=0.1278$, $F=2.328$, $DFn=1$, $DFd=446$) analysed by linear regression.
C. Number of neutrophils at the wound over 6 hours (6 to 12hpi) with 5-minute intervals, showing mean and SEM from 2 samples in the swarming group and 3 in the non-swarming group. Significant elevation difference ($P<0.0001$, $F=315.9$, $DFn=1$, $DFd=357$) but no significant slope difference ($P=0.9616$, $F=0.002327$, $DFn=1$, $DFd=356$) analysed by linear regression.

3.1.7 Time-lapse imaging reveals distinct phenotypic differences in the swarming response

After acquiring the time-lapses in **Figure 9**, there were challenges in distinguishing a clear swarming response from a more general inflammatory response due to individual detection bias. I hypothesised that generating an average intensity projection of the entire time-lapse would highlight differences by showing whether neutrophils are localised to specific regions in the tail fin, indicative of potential swarming, or exhibit more motility, characteristic of a general inflammatory response.

When the time-lapses from 6 to 12hpi (**Supplemental Movie 1**) were converted into average intensity projections, a striking difference in neutrophil localisation and motility was revealed, providing a visual representation of neutrophil swarming not previously visualised in this manner (**Figure 10**). This method facilitated the creation of a parameter to easily assess whether a zebrafish larva initiated a swarming response using time-lapse imaging. However, it was necessary to double-check positive, high-intensity samples to confirm the presence of a neutrophil swarm. As high-intensity signal would not always indicate swarms, but could also indicate single, sessile neutrophils. This approach was a significant step towards reducing individual detection bias in following experiments.

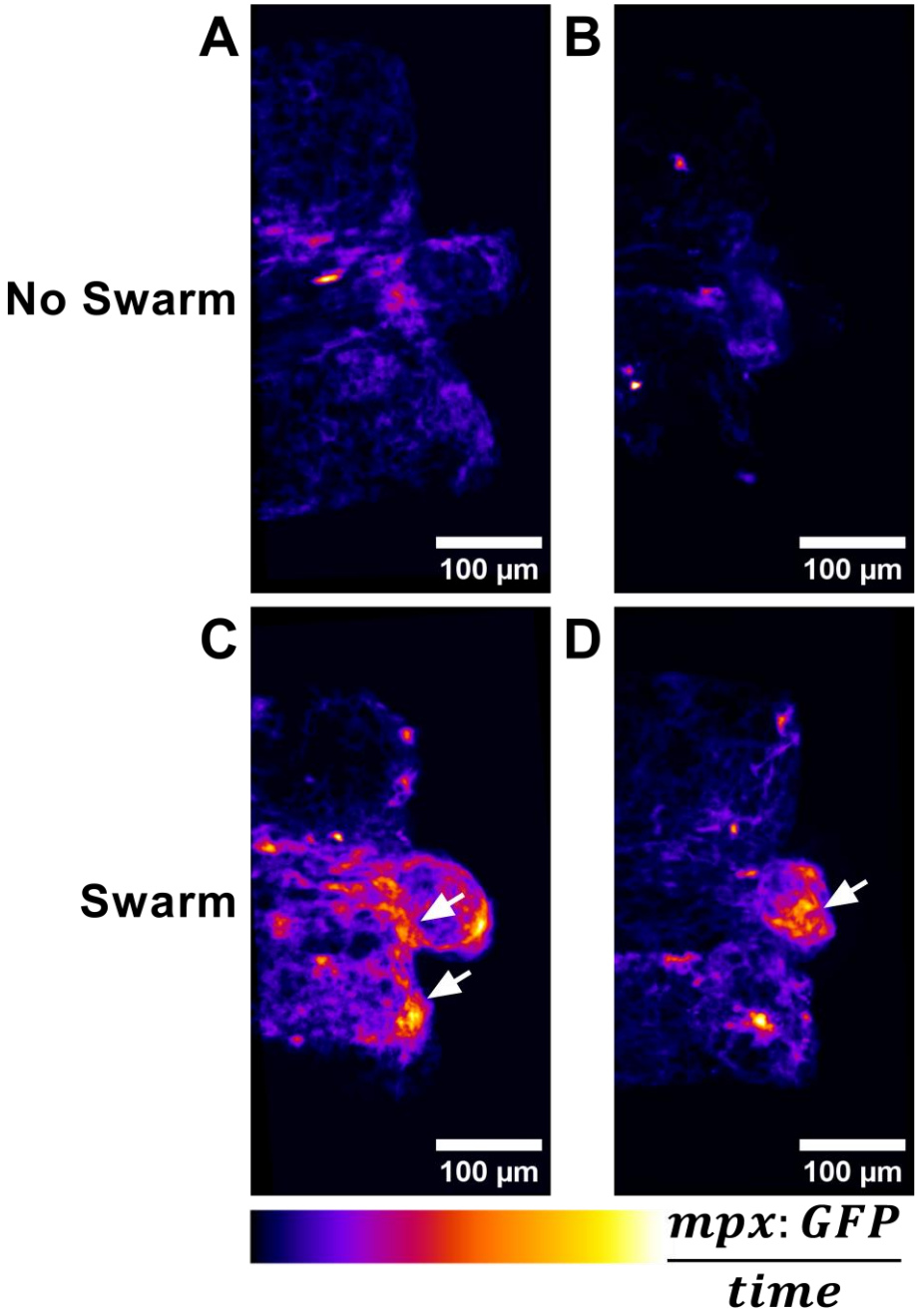

Figure 10: Phenotypic differences in the swarming response in *Tg(mpx:GFP)^{i114}* larvae

A-B. Comparison of larvae with and without a neutrophil swarming response, showing significantly lower signal in non-swarming larvae.

C-D. Images indicating swarm locations with white arrows. Where activity is seen low signal indicates motile neutrophils, while high signal indicates sessile neutrophils. Signal obtained from average intensity projections of all time points (6-12hpi), with the "Fire" LUT in ImageJ applied for visualisation.

3.1.8 Neutrophil swarming correlates with significant impairment in tissue regeneration

As I previously observed significantly elevated levels of neutrophils during both the recruitment and resolution phases when swarming was initiated, I aimed to investigate whether this finding had a measurable physiological effect on the zebrafish larvae. To do this, I performed an experiment where I anaesthetised and consecutively injured the tail fin of 3dpf zebrafish larvae, ensuring not to injure the notochord as this would severely slow down tissue regeneration. These larvae were then allowed to recover from the anaesthetic in a new petri dish filled with E3 media. At 4hpi, I examined the larvae for swarms and separated them into groups with or without swarming. Subsequently, these groups were assessed for tail fin regeneration at 24- and 48hpi (**Figure 11**). I also evaluated neutrophil numbers to confirm the previously described elevated levels.

At 24 hours, there was no significant difference in the tail fin area regenerated between larvae with and without swarms (**Figure 11B**). However, there was a significant increase in neutrophil numbers at the tail fin wound, corroborating earlier results (**Figure 11D**). At the 48-hour timepoint, the inverse was observed: the number of neutrophils present at the wound was not significantly different (**Figure 11E**), but the amount of tail fin regeneration was significantly greater in larvae without swarms (**Figure 11C**). These data suggest an interesting correlation between delayed inflammation resolution after neutrophil swarming at 24hpi, which could explain the impairment in tissue regeneration.

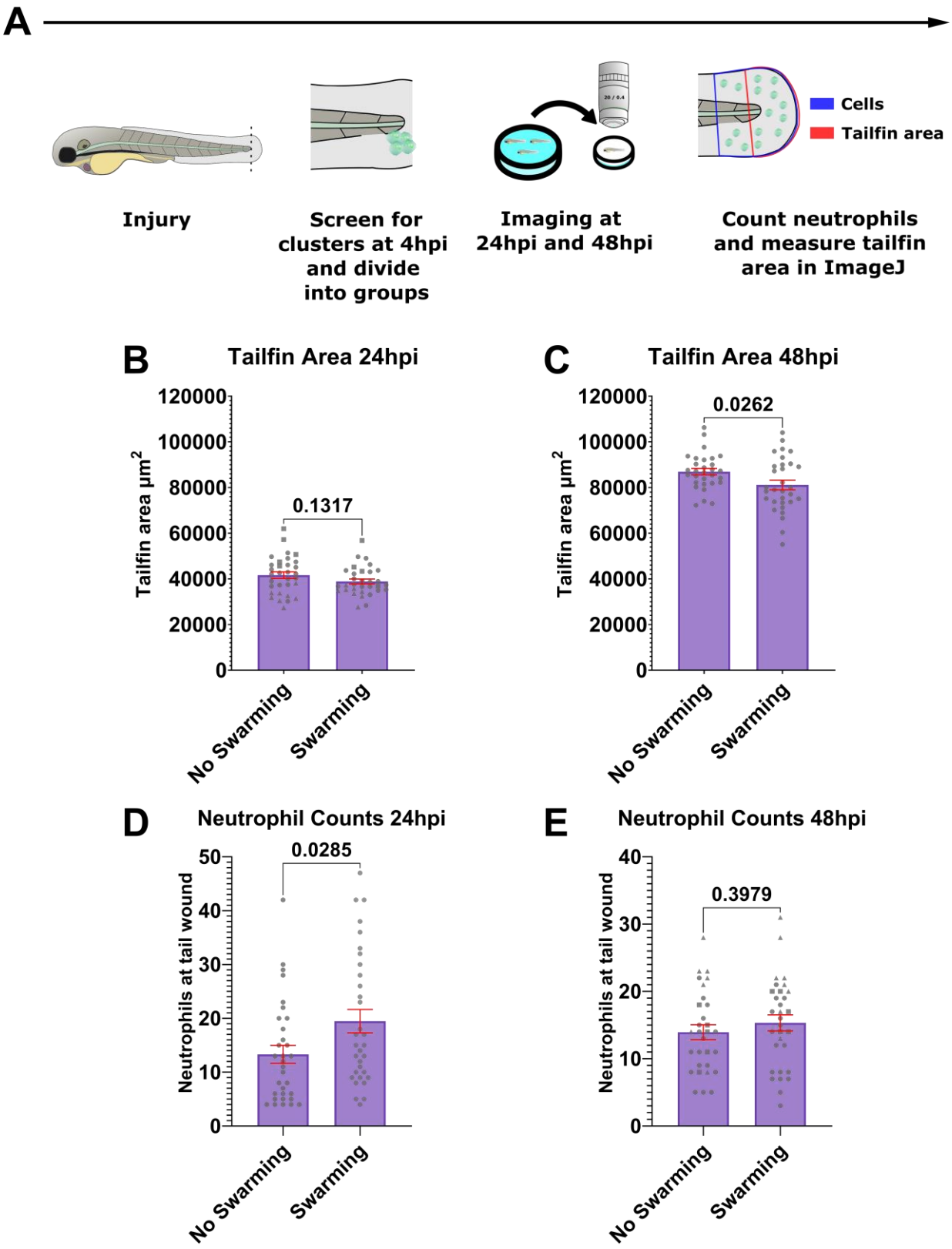

Figure 11: Swarming is associated with reduced tissue regeneration

A. Experimental timeline: Larvae were injured, screened at 4hpi, and sorted into swarming or non-swarming groups. At 24 and 48hpi, larvae were anesthetised briefly and transferred onto a glass imaging dish with a thin agarose layer for a single image. Images were used to count neutrophils at the tail fin wound and measure tail fin regeneration using ImageJ. Images were obtained on a Nikon eclipse TE-2000U (Plan Fluor ELWD x20/0.45NA objective, Andor Zyla VSC-02811 camera).

B. Measurement of tail fin area at 24hpi.

C. Measurement of tail fin area at 48hpi, showing significant impairment in larvae that previously exhibited a swarming response.

D. Neutrophil count at 24hpi, indicating a significant increase in larvae with a swarming response, suggesting impaired inflammation resolution.

E. Neutrophil count at 48hpi, showing no significant difference in neutrophil numbers between larvae with or without a swarming response.

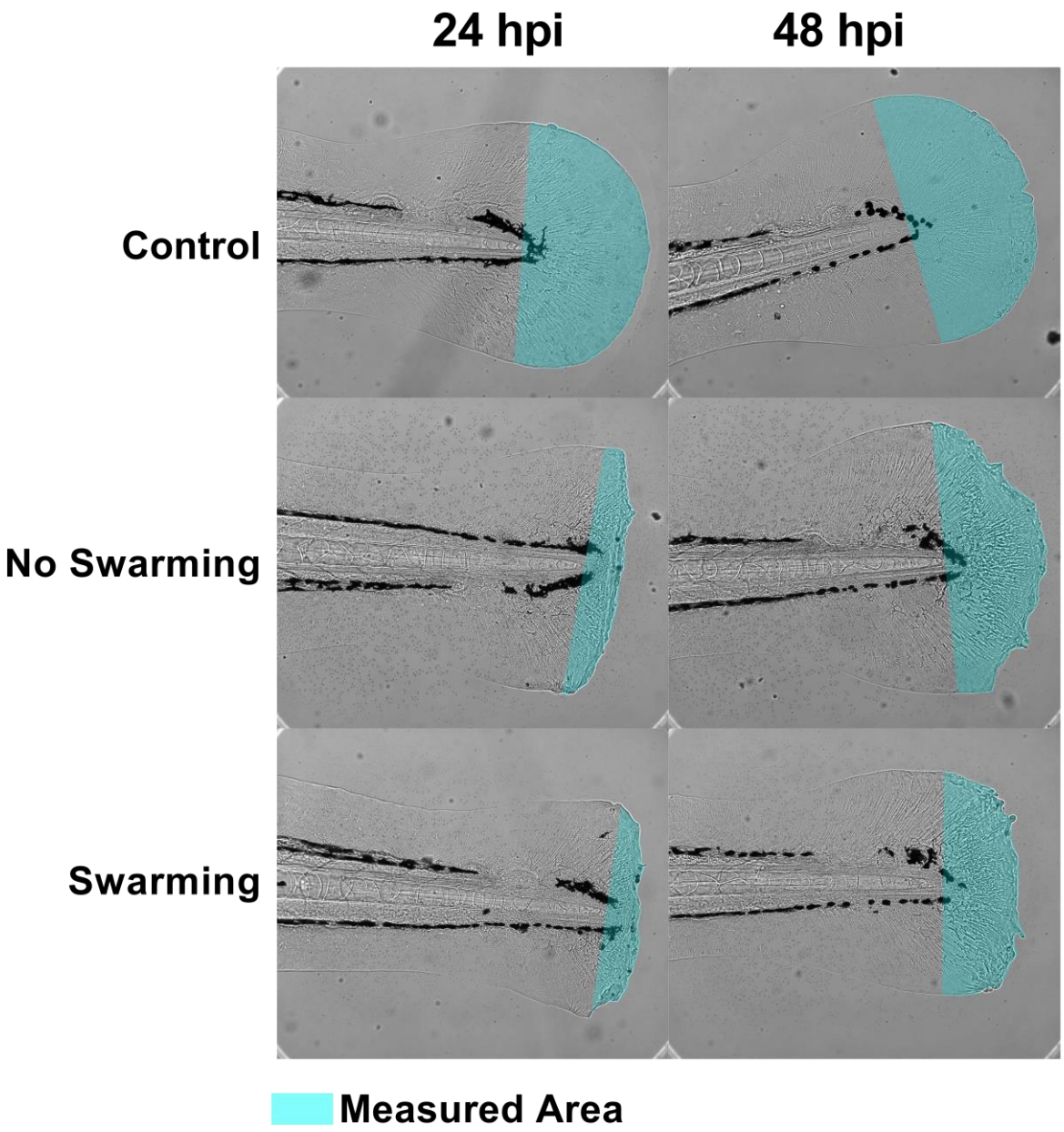

Figure 12: Swarming is associated with reduced tissue regeneration

This figure shows the representative images of **Figure 11**, and the areas that were used for measurements. Full regeneration of the tail fold injury after 48 hours has not occurred, compared to what the tailfin should look like indicated by the control.

3.1.9 Conclusion & Discussion

While previous studies have shown the use of the zebrafish model for researching initiation of neutrophil swarming *in vivo*, resolution of inflammation remained unaddressed (Poplimont et al., 2020, Isles et al., 2021). To determine when neutrophil swarms resolve, I performed long time-lapse imaging experiments, where I observed swarms most often form between 2 and 8hpi. Suggesting most swarms resolve around 8hpi. However, neutrophil swarms can form at later timepoints if autocrine LTB4 signalling and amplification are initiated, although the likelihood of this occurring in a more resolutive state is expected to be low.

In general, I found considerable variability in individual swarming responses. While this allowed me to easily classify a swarming from a non-swarming response using average intensity projections of a time-lapse, it also caused issues for statistical analyses as statistical power was diminished. A possible source of this variability could be genetic differences, which have been implicated in many inflammatory genes, including those in the NLR family, part of the innate immune system (McConnell et al., 2023).

This led me to question whether variability in the swarming response is stochastically connected to the required signalling pathways or potentially due to genetic differences. I used *Tg(mpx:GFP)i114* and *Tg(mpx:GAL4)^{sh267}; Tg(UAS:Kaede)^{i222}* zebrafish larvae to test whether different genetic compositions would affect neutrophil swarm formation. I found no significant difference in the occurrence of neutrophil swarms between these two lines. Although one might argue it is only a single gene difference, due to inbreeding and outcrossing against different wildtype zebrafish backgrounds, these two lines should have considerable genetic differences. Moreover, this finding is corroborated by results presented later in this thesis where *Tg(LysC:EGFP)* larvae also showed formation of neutrophil swarms.

Within zebrafish research, two types of tail fin injury are often used: one sparing the notochord and one including injury to the notochord (Nguyen-Chi et al., 2015, Loynes et al., 2018). To determine whether the type of injury affects the neutrophil swarming response, larvae with injuries sparing the notochord were compared to those including it. I found no significant difference in the number of neutrophil swarms formed. This may suggest the reliance of swarming on the LTB4 pathway, which is essential, rather than on the severity of the injury (Lämmermann et al., 2013). Furthermore, it suggests that even though notochord injuries generally lead to higher numbers of neutrophils moving towards the injury, this does not necessarily correlate with increased swarming.

To explore whether neutrophil swarms have a measurable impact on the overarching neutrophil response in zebrafish, I employed two different time-lapse approaches to monitor neutrophil numbers during the recruitment and resolution phases at the tail fin wound. The findings revealed that although the rate of neutrophil recruitment and resolution did not significantly differ between larvae with or without swarms, there was a significant increase in the number of neutrophils remaining at the wound site following swarming. This observation was further supported by results from a tail fin regeneration assay. However, this raises a complex question: do neutrophil swarms arise due to a higher number of neutrophils, or do the swarms themselves trigger additional neutrophil recruitment and retention? This limitation will have to be considered when interpreting future results and should be addressed in future research, requiring a carefully designed approach, by for instance using positive controls for swarming which have not yet been identified.

Previous literature investigating neutrophil swarming rely on time-lapse imaging paired with highly detailed cell tracking for conveying differences between swarming responses (Lämmermann et al., 2013, Kienle et al., 2021, Isles et al., 2021). While this has been considered and will remain the gold standard for communicating results, I have found an alternative to illustrate differences between swarming responses. Using the visual clarity of the zebrafish compared to other *in vivo* models such as the mice, I was able generate high quality, average intensity projections which show easily interpretable differences between a swarming and non-swarming response. This approach revealed distinct phenotypic differences in neutrophil movement and localisation, providing a valuable and less biased readout of the swarming response. This method, proved crucial for subsequent analyses, discussed in the following results chapter.

As of today, neutrophil swarms have been directly implicated in context of disease in two ways. First, swarming is shown to help contain bacterial infections in lymph nodes of mice infected with *Pseudomonas aeruginosa* (Kienle et al., 2021). Second, neutrophil swarms have been shown to occur more frequently in an *ex vivo* mono-culture model of neutrophils, using samples from CGD donors (Strickland et al., 2024). Thus, I wanted to explore whether undescribed physiological effects of neutrophil swarms existed in the zebrafish model. Using the tail fin regeneration assay, I illustrated that swarms caused a delay in inflammation resolution, correlating with a decrease in the regenerated tail fin area following injury. These findings are in accordance with earlier described results where elevated numbers of neutrophils were observed after swarming, and is further corroborated by published literature, which describes excessive neutrophil responses to be detrimental to tissue regeneration (Bernut et al., 2020).

Furthermore, other research has also presented distinct roles for neutrophils and macrophages in tissue regeneration (Li et al., 2012). Neutrophils have been described to be early responders that can hamper tissue regeneration, while macrophages arrive during later stages of the inflammatory response and are essential for proper tissue regeneration (Li et al., 2012). In the case of swarming, excessive neutrophilic inflammation and retention could cause a hampered macrophage response, which could be interesting to investigate experimentally. Further experiments into the correlation between tissue regeneration and neutrophil swarming could further elucidate the point at which neutrophil swarming can become a detrimental process. The *cftr* -/- mutant, described in previous research, could be used to potentially link this to relevant disease phenotypes (Bernut et al., 2020). However, to accurately assess how neutrophil swarming impacts this, positive or negative controls for neutrophil swarming have to be designed. This could be done by pharmacologically promoting or inhibiting neutrophil swarming, but at the time of writing this thesis, no clear controls have been identified yet. I will further explore the idea of pharmacologically manipulating neutrophil swarming in **Chapter 3.3**.

In conclusion, I presented an overview of basic methods employed for studying neutrophil swarming in zebrafish. Using these methods, I determined a range when swarms typically occur and resolve. I found that the genetic background of zebrafish larvae does not significantly impact their ability to form neutrophil swarms. Additionally, different tail fin injury types were assessed for their effect on swarming with similar outcomes. I described how swarms might lead to impaired inflammation resolution from the wound site and introduced a new method for showing differences in swarming and non-swarming responses using average intensity projections of time-lapse imaging. Finally, I demonstrated that the

occurrence of neutrophil swarms correlated with a small, yet significant decrease in tissue regeneration using the tail fin regeneration model.

3.2 Establishing a Proof of Concept for a High-Throughput Neutrophil Swarming Assay

3.2.1 Introduction

As illustrated by results in **Figure 9** and **Figure 11**, neutrophil swarming might play a significant role in the impairment of inflammation resolution and possibly further inflammation resolution during chronic inflammatory diseases. Chronic inflammatory diseases in which neutrophils play a role, such as arthritis or Chronic Obstructive Pulmonary Disease (COPD) could be influenced by the regulation of the swarming response within an individual. If this is the case, understanding how the neutrophil swarming response is regulated could give rise to new therapeutical approaches. However, these regulatory pathways remain largely undescribed especially during resolution of neutrophil swarms. As such, the use of a high-throughput assay for swarming might aid in finding new regulatory pathways by performing small molecule screens. While neutrophil mono-culture assays have been developed for screening neutrophil swarming responses, as of today, no large-scale *in vivo* screening assays for neutrophil swarming are available (Strickland et al., 2024). This is where the use of the zebrafish model might offer a solution, as zebrafish have been successfully used for *in vivo* high-content screens in the past (Dasgupta et al., 2020).

As part of the INFLANET network, one of our objectives was to utilise Acquifer's expertise, to conduct large-scale compound screens on various inflammatory processes, including neutrophil swarming. Since there had not been any previous attempts to scale up the investigation of the swarming response in zebrafish, we needed to carefully consider which parameters to include and how to measure them. As mentioned in **Chapter 3.1.7**, swarming is a process still subject to individual detection bias; some observers might classify a response

as a swarm while others might not. This detection bias can be influenced by several factors, including the temporal resolution of the time-lapses and the exposure settings, which can alter the perception of a cluster or individual cells. Thus, in a collaboration with Acquifer at the University of Heidelberg, I set out to develop a proof of concept for a high-throughput screening assay for neutrophil swarms with minimised detection bias.

One of the challenges was identifying the appropriate tools to enable accurate readouts from imaging. Widely available solutions were required to address a multitude of anticipated issues for successfully establishing a high-throughput assay. Some of the anticipated issues were the following; firstly, stabilising the time-lapse to correct for sample movement during imaging; secondly, identifying the cells within the image; thirdly, tracking the cells within the image; and finally, classifying a swarming versus a non-swarming response. For this, open access software tools were preferred to align with the overall grant goal of open-access science.

In addition to computational and analytical challenges, other biological parameters needed to be determined. In assay development it is essential to control variability as much as possible to avoid false positives or false negatives. In terms of creating injuries, manual injuries are susceptible to variability from individual technique as well as how controlled one is to create small injuries. In comparison, laser injuries using a high-powered laser can be controlled with micrometre precision and will use the same degree of laser power for each injury, ensuring reproducible injuries. Thus, I hypothesised that laser injuries would be more suitable than mechanical injuries performed by a researcher when developing the assay for swarming. Acquifer's Imaging Machine (IM) supports laser injuries, which have previously been used to initiate swarming (Poplimont et al., 2020, Lämmermann et al., 2013). Moreover, we aimed to shorten the entire inflammatory response, if possible. Tail fin injuries sometimes

take a long time to stabilise neutrophil recruitment and further inflammation resolution, adding unwanted variability to a robust assay. This will be further illustrated by **Chapter 3.2.6**. Therefore, I hypothesised that creating smaller injuries would produce shorter responses, enabling the visualisation of both initiation and resolution of inflammation within a reasonable time frame. Thus, we had to test different laser injury settings and locations to find the optimal location to elicit a significant inflammatory response which will be explored in **Chapter 3.2.5-3.2.6**.

Once all computational and biological decisions were made, proof of principle had to be shown, illustrating the assay would be able to pick up differences in neutrophil swarming. To this extent, treatments with immunomodulatory compounds were planned, however due to unforeseen problems with cross-border transport of selected compounds, proof of principle was demonstrated by comparing two previously described methods of generating neutrophil swarms, namely sterile mechanical injury and laser injury (Poplimont et al., 2020, Isles et al., 2021).

3.2.2 Optimising methods for recognition and stabilisation of image regions

When the development of the macro commenced, the primary objective was to minimise data size to create datasets that would be easier to manipulate and navigate. To achieve this, a template matching approach for region recognition was employed (Thomas and Gehrig, 2020). In template matching, a template image of the desired object or region is extracted from the time-lapse and used to correlate with other images in the sequence. This method facilitated both the reduction of data size, by selecting only specific regions of an image, and the tracking of these regions throughout the sequence, serving as an initial stabilisation step.

Since the original size of the template area is saved, regions of interest can be created around the recognised area, allowing for cropping across different channels within an image. The brightfield image was chosen as it contains the most information about any sample movement that may have occurred. However, for time-lapse imaging of tail fin injuries, template matching occasionally mismatched, resulting in inaccurate images for downstream analysis (**Supplemental Movie 2**). To address this, various approaches were tested, ultimately identifying two key parameters to optimise the template matching algorithm. The first parameter involved selecting the middle of a time-lapse for template creation. I hypothesised that creating the template image in the middle of the time-lapse would enhance matching accuracy, as the beginning and end states of tail fin injuries often differ significantly, leading to template matching failures towards the end. The second parameter was image blurring; given the large input region for an entire tail fin and the pixel-based nature of template matching, blurring was hypothesised to help recognise more variable structures by generalising the image.

Indeed, combining these methods reduced template mismatching from an initial 12.5-37.5% to 0% (**Figure 12B**). This improvement is corroborated by measurements of the centroid point of the matched region on the X-axis, which showed significantly more movement without blurring or timepoint selection (**Figure 12C**). Additionally, smaller movements of the template-matched region were slightly reduced (**Supplemental Movie 2**). After template matching, template ROIs were extracted and used to crop other channels accordingly. However, as illustrated in **Supplemental Movie 2**, template matching still produced movement artefacts. To eliminate these artefacts and further stabilise the image, HyperStackReg was utilised with 'Rigid Body' transformation. Rigid body transformation was

chosen as this preserves the image properties, by not introducing sheer or changing its size. After HyperStackReg was applied to the brightfield image, the transformations were extended to other channels within the time-lapse. This fully stabilised the image, but introduced slight background noise in the fluorescent channel, which was removed by background subtraction (**Supplemental Movie 3**). These results collectively demonstrate that the combination of template matching and HyperStackReg can reduce data size, effectively recognise areas within a larger sample, and stabilise the time-lapse for more accurate downstream analysis. A full overview of the analysis pipeline can be found in **Chapter 2: Methods, Figure 4**.

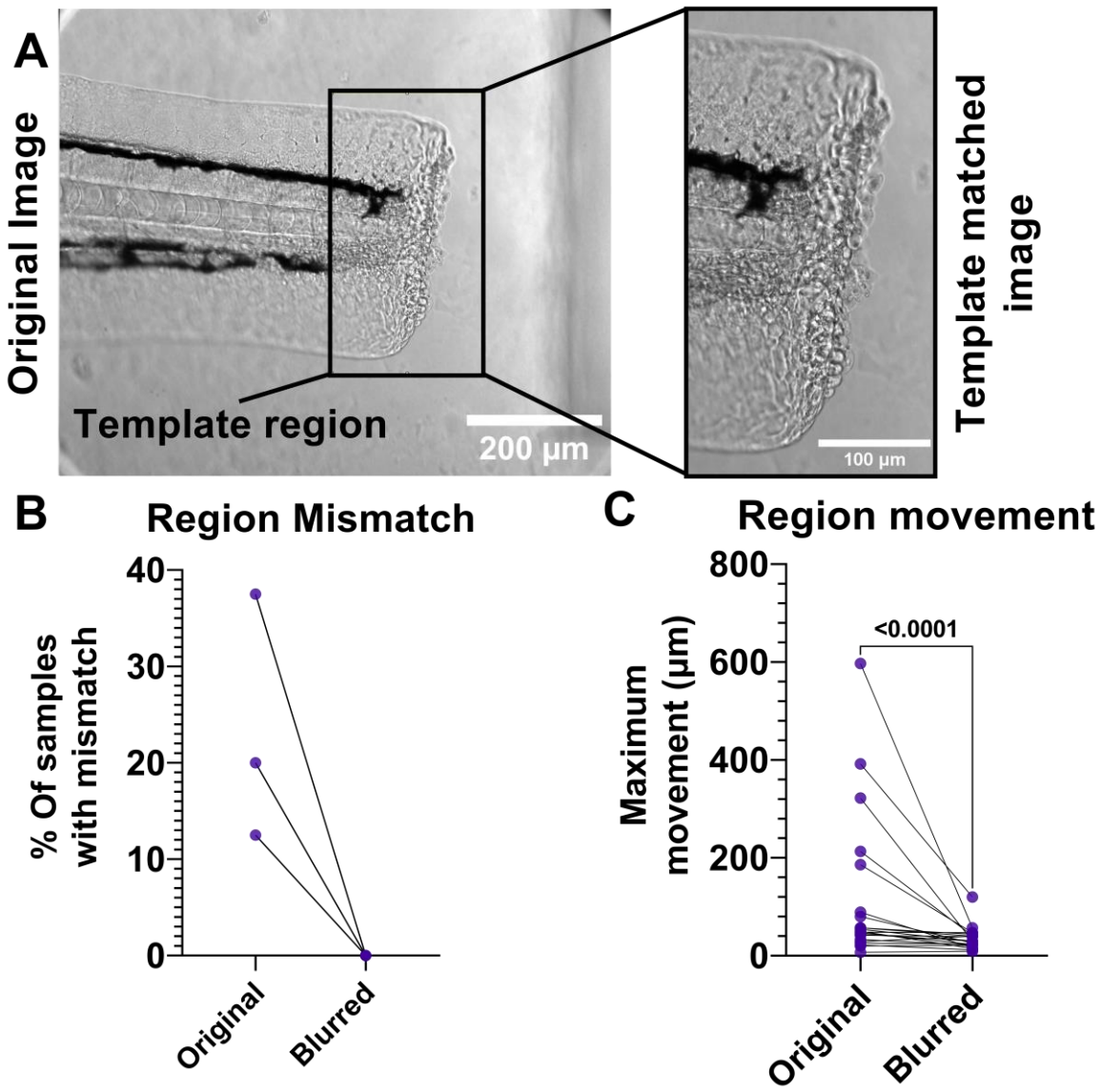

Figure 12: Template matching can be optimised by using blurred images and selecting time points

A. The template matching region demonstrates how data can be significantly reduced by retroactively selecting regions of interest within the original image or time-lapse.

B. This graph illustrates the frequency of mismatches in the dataset, which ranges from 12.5% to 37.5% initially, reducing to 0%. N=21 larvae from 3 experimental repeats (5, 8, 8).

C. This graph depicts the movement of the centre of the template-matched region across the image. Maximum movement is defined as the difference between the maximum and minimum X-axis locations. Switching from the original template matching method to using blurred images resulted in a significant reduction in this movement. $P<0.0001$, Wilcoxon matched-pairs signed rank test, N=21 larvae from 3 experimental repeats (5, 8, 8).

3.2.3 Creating data readouts to help minimise individual detection bias.

To track the development of neutrophil swarms after the time-lapse was cropped and stabilised, the 'analyze particles' function in ImageJ was utilised. Small pre-processing steps were introduced to reduce background noise from the stabilisation step and to make neutrophils easier to detect. These steps included background subtraction followed by a light Gaussian blur. Subsequently, a threshold was applied to create binary images for the analyze particles function. Settings were optimised to discard small objects or background signals. After running analyze particles, outlines were created and saved as regions of interest (ROIs). ROIs were measured, after which both measurements and ROIs were saved in the user-determined output destination.

For high-throughput data analysis, data pruning can be beneficial. Thus, an automatic classifier for the swarming response was tested. Multiple parameters were selected based on the area of the measured objects. Together with Sankeert I observed that the frequency distribution of the area differed between zebrafish with a swarming response and those without (**Figure 13A-B**). Due to this difference, various parameters were identified for automatic classification. The following parameters were explored and tested: skewness, indicating the asymmetry of a distribution; outliers, based on the number of large areas detected; range, defined as the maximum area minus the minimum area measured in the timelapse; and kurtosis, a measure of the 'tailedness' of the distribution which indicates an increased number of measurements towards the extremities of a distribution (**Figure 13A**).

Using these parameters individually or in combination, K-means clustering into two groups was performed. After clustering, true positive and true negative ratios (TPR, TNR) were assessed. For obtaining the TPR and TNR, original timelapses were blinded, shuffled and

assessed for swarming responses. The TPR ranged from 50% to 87.5% accuracy, while the TNR ranged from 78.57% to 92.86% (**Table 5**). The TPR indicated accurate classification of a swarming response, and the TNR indicated accurate classification of a non-swarming response. Although the TPR was variable and less accurate, the TNR, with an accuracy of 92.86% when clustering based on skewness, could be used for automatic classification of non-responders. This helps manage data size and provides an automated way of data filtering. However, the automatic approach was abandoned as the prediction accuracy was not up to the expected standard.

Consequently, other possibilities were explored, leading to the creation of an overview sheet where data were visually represented for quick assessment by researchers (**Figure 14**). Here, average intensity projections were used as a visual aid. Additionally, varying parameters are plotted to further assist in classification. By performing simple filtering and formatting steps, samples can be sorted by the best predictor of true negatives, in this case, skewness.

In conclusion, these data readouts fulfil different tasks, ranging from data pruning and accessibility, to helping researchers classify inflammatory responses in regards to neutrophil swarming, minimising individual detection biases that can be present. Furthermore, these readouts include other parameters aside from the area measurement which can be used for swarm tracking and counting as will be illustrated in following results.

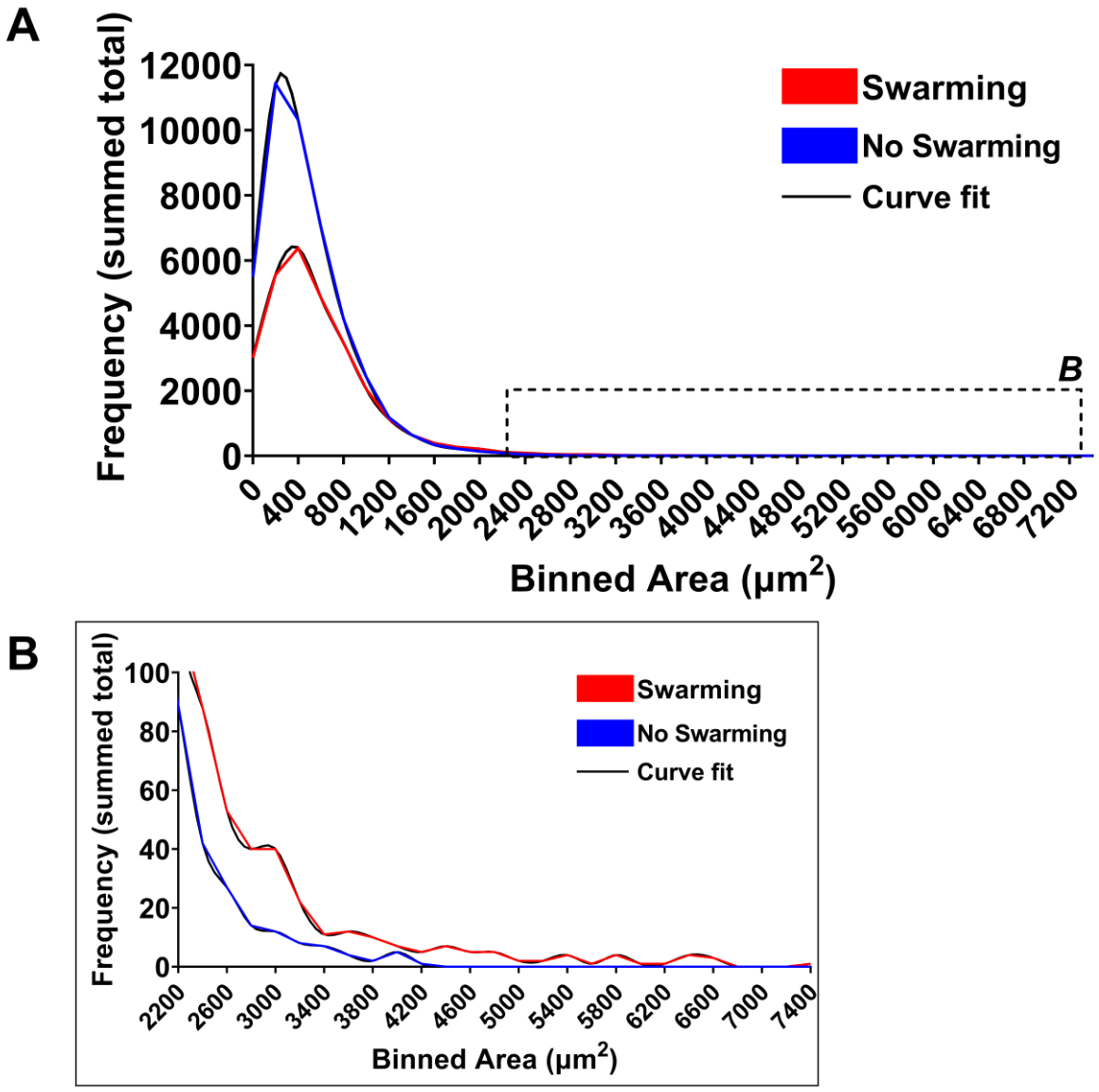

Figure 13: Frequency distributions of object areas reveal differences in swarming and no swarming

A. This graph shows the distribution of frequencies relating to specific area sizes of detected objects. Objects were obtained via analyse particles in ImageJ and areas were binned. A small shift towards the right can be seen in larvae that mounted a swarming response. Indicating varying skewness in the frequency distributions between responses. Furthermore, a difference in Kurtosis might be present, indicating an increased number of measurements towards one of the extremities of the distribution (n=22, N=3, all frequencies totalled).

B. This graph is a magnification of the tail from the distribution plotted in **A**. Here the difference in frequencies of large areas, likely swarms is observed, with more large areas present in larvae with a swarming response (n=22 N=3, all frequencies totalled).

Swarm Classification with K-means clustering based on:	TNR (Specificity)	TNR (Sensitivity)
Skewness	92.86%	75.00%
Outlier count	85.71%	75.00%
Range	85.71%	50.00%
Skewness + Outlier count	85.71%	87.50%
Skewness + Range	78.57%	75.00%
Kurtosis	85.71%	75.00%
Kurtosis + Skewness	85.71%	75.00%

Table 5: Parameters extracted from imaging data can be used to classify swarming responses automatically

To obtain the True Negative Rate (TNR) and True Positive Rate (TPR), previously acquired time-lapses were blinded, shuffled and examined for their swarming response. Based on area measurements from the 'analyse particles' function in ImageJ, various parameters, as listed in the first column, were extracted using a Knime Workflow. These parameters, either singular or in chosen combinations, were then used to perform K-means clustering into two clusters. Skewness was the most effective for identifying non-swarming responses, while a combination of skewness and outlier count was the best for identifying swarming responses. The highest combined TNR and TPR were also achieved using the latter parameter combination. The parameters are defined as follows: skewness, the symmetry of the distribution; outlier count, the number of outliers identified based on Z-score; range, the difference between the maximum and minimum area measured; kurtosis, the 'tailedness' of the distribution.

A

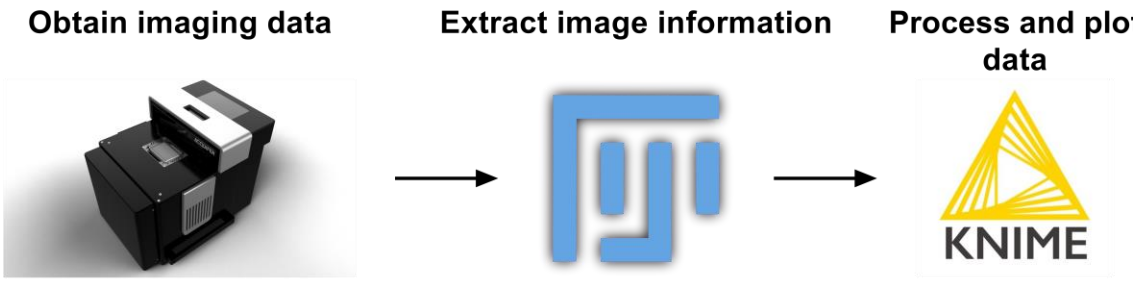

B

	Label	Skewness(Area)	Mean(Area)	Range(Area)	Standard deviation(Area)	Count*(Area)	Max*(Area)	Member count	Outlier count	Mean_max_distance	Image
2	1 MAX_C001_1	1.502537563	578.1978417	3207	417.91518	834	3208	834	4	2629.802158	
3	2 MAX_C002_1	0.427919271	716.5748219	2667	392.9000991	421	2668	421	0	1951.425178	
4	3 MAX_C004_1	0.08211586385	652.3214286	1674	307.5596853	252	1680	252	0	1027.678571	
5	3 MAX_C005_1	0.7948625817	630.2258065	2338	394.1039208	372	2342	372	0	1711.774194	
6	1 MAX_C006_1	2.389792517	678.8898305	3740	476.1239162	472	3742	472	6	3063.110169	

Figure 14: Overview sheet produced through image analysis pipeline to help reduce detection bias

A. A visual representation of the image analysis pipeline. Images were obtained using the Acquifer Imaging Machine (IM), then image information was extracted using Fiji ImageJ. Finally, relevant extracted data was plotted using Knime.

B. The final output sheet produced with Knime aids researchers in correctly identifying swarming responses, allowing quick access to and correlation of data with the original samples and timelapses. Multiple parameters are included to highlight potential swarming responses. (**1**) Examples of a clear swarming response indicated by green coloration of parameters and a clear spot of neutrophil accumulation in the average intensity projection. (**2**) Example of a response which could be a swarm indicated by green coloration of the Mean(Area) as well as a clear spot of neutrophil accumulation in the average intensity projection. (**3**) Examples of an inflammatory response without neutrophil swarming indicated by yellow/orange/red coloration of parameters and a lack of neutrophil accumulation indicated in the average intensity projection.

3.2.4 Using a specially trained neural network for cell recognition and counting.

The image pipeline discussed in **Chapter 3.2.3** was primarily designed for recognising neutrophil clusters, which could indicate swarms. However, when these clusters formed, the number of cells within the cluster was lost due to overlapping signal which traditional thresholding methods could not discern into singular neutrophils. Since neutrophil counts are often used as indicator of inflammation resolution, a new method had to be identified for accurate neutrophil counts to detect changes in swarm resolution (Bernut et al., 2020, Loynes et al., 2018, Mathias et al., 2006). Moreover, obtaining accurate tracking and cell movement information became nearly impossible when cells clustered.

To address this, a neural network based on Cellpose was trained to detect individual neutrophils within clusters. Training followed a 'human-in-the-loop' approach, where manual segmentation optimised cell detection, the model then 'learned' from manual corrections, until the desired result was achieved (Wu et al., 2022). Input images for the Cellpose algorithm were obtained using methods described in **Chapter 3.2.2** to stabilise timelapse data. These stabilised timelapses were split into individual images using a FIJI macro, then processed through Cellpose for segmentation. Cellpose tended to over-segment and thus overcount cells compared to manually counted validation data (**Figure 14A**). This was corrected by filtering out smaller objects using the measured area, as these are unlikely to be cells, resulting in counts nearly identical to manual counts (**Figure 14A-B**). Filters were optimised for the validation set data and consequently applied for the entire dataset. Changes in cell numbers were accurately tracked over time, indicating that automated counting could replace manual counting, which is highly beneficial for high-throughput workflows (**Figure**

14C). Additionally, this increased the assay's robustness, as cell counts became deterministic using an algorithm. Using Cellpose for segmentation also allowed cells within clusters to be extracted, enabling the number of cells within specific clusters to be identified (**Figure 15, Supplemental Movie 4**). This also provided the opportunity for more accurate cell tracking with Trackmate, where label images could be loaded and tracked using a Linear Assignment Problem (LAP) tracker (Jaqaman et al., 2008).

In summary, these results demonstrate how novel neural networks can be specifically trained on specialised data, providing accurate cell counts comparable to manual analysis while retaining the deterministic benefits of automated analysis. This enables in-depth investigation of cellular behaviour within complex inflammatory responses such as neutrophil swarming, as individual cells can be identified even within clusters.

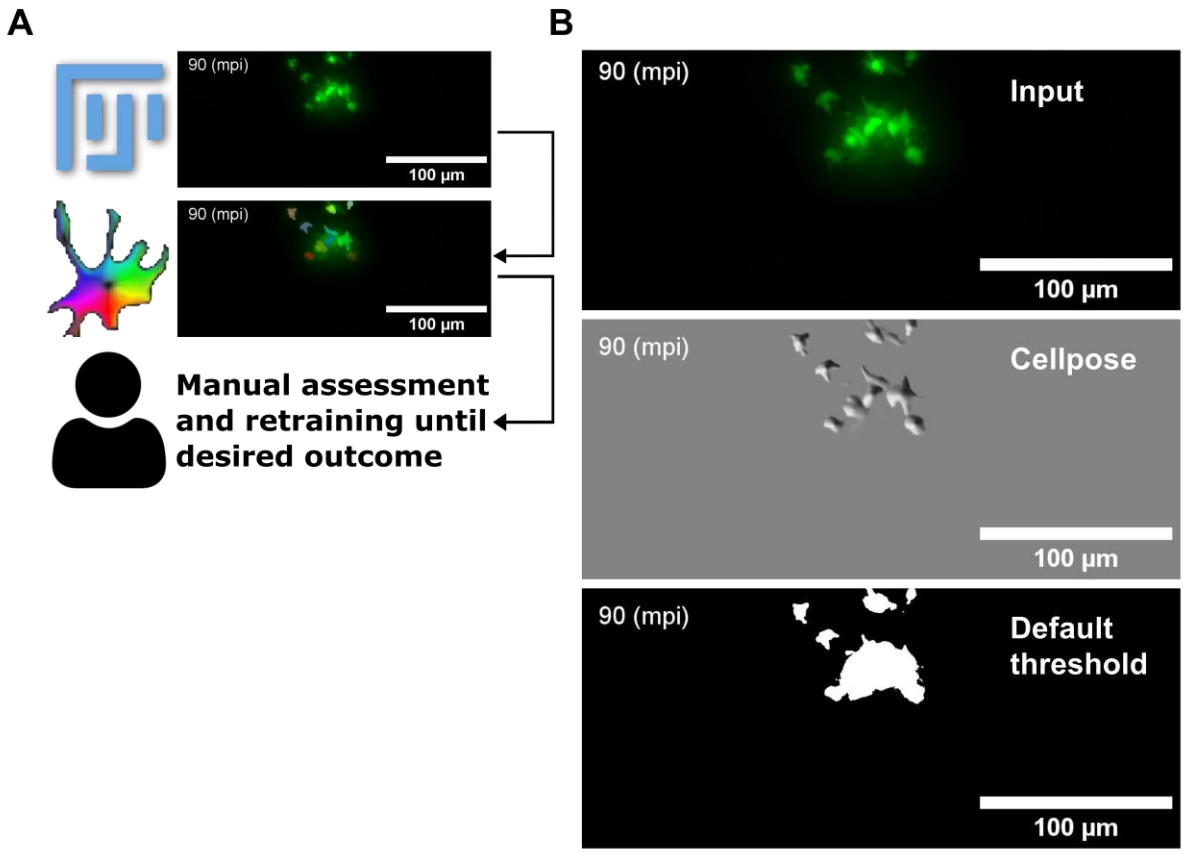

Figure 15: Cellpose is able to segment neutrophils within clusters

A. A 'test set' was extracted from the full dataset to train a novel Cellpose network. Output data from the previously described ImageJ analysis macro was used for generation of initial Cellpose segmentation. During subsequential training, manual input was provided each cycle to optimise cell segmentation.

B. The fully optimised Cellpose neural network was able to segment cells within clusters automatically and accurately. Output was compared to a default thresholding approach which significantly underperformed in the same task. This is further illustrated in **Figure 16**.

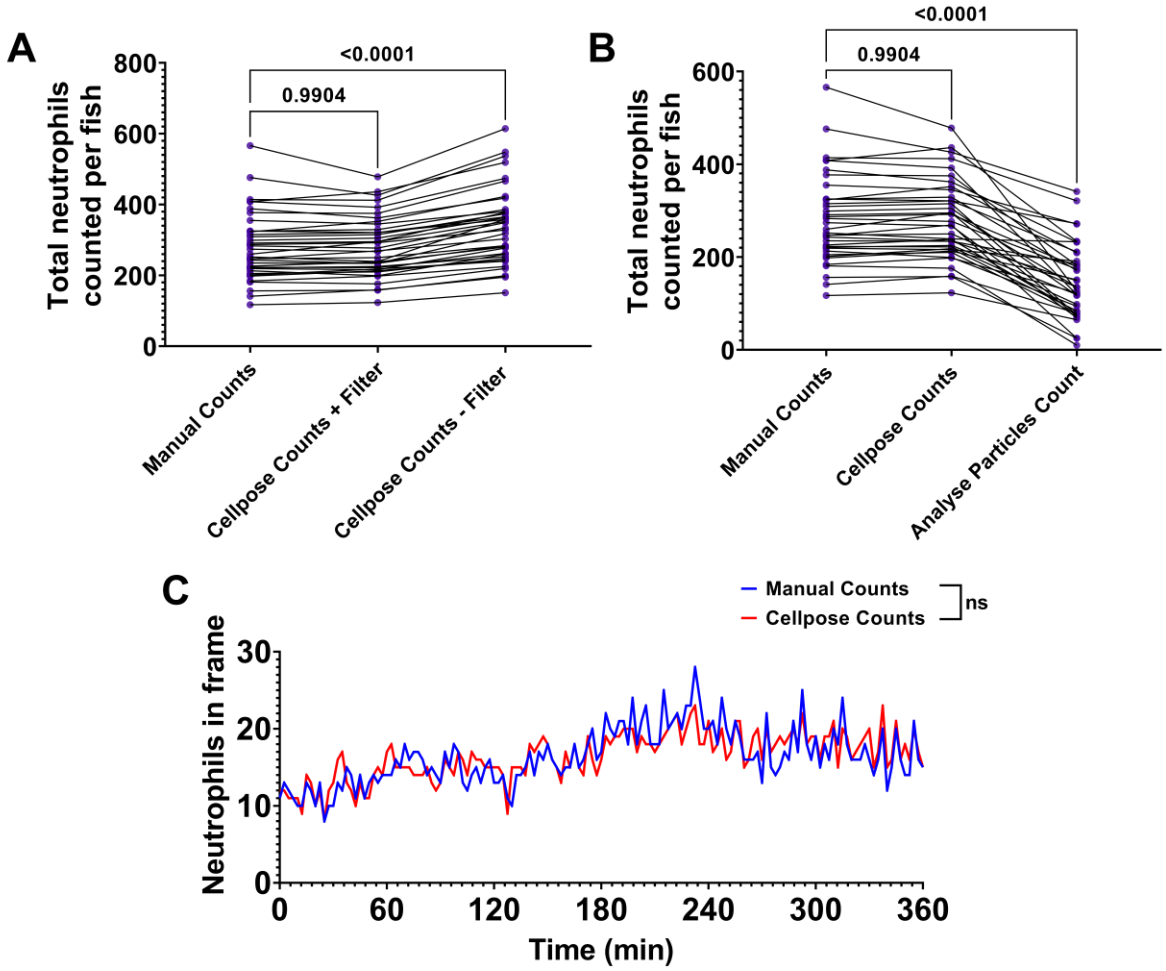

Figure 16: Cellpose enables accurate cell counts with a specially trained neural network

A. Within an isolated validation dataset, manual neutrophil counts were compared to those obtained using a specially trained Cellpose neural network. This graph shows how Cellpose over-segmented and thus overcounted cells when no filters for object size were applied, as seen in the third column of datapoints. However, when a filter for the area (325pxl^2) was applied, counts became indistinguishable from manual assessment (Repeated measures one-way ANOVA with Geissner-Greenhouse correction, Dunett's multiple comparison test, N=5 n=37 (9,5,8,8,7)).

B. Manual counts and Cellpose counts (with filter) were also compared to cell counts obtained from Analyse Particles in ImageJ, using the previously explained analysis macro (Repeated measures one-way ANOVA with Geissner-Greenhouse correction, Dunett's multiple comparison test, N=5 n=37 (9,5,8,8,7)).

C. Cellpose counts accurately followed the inflammatory response, showing the same curve in cell counts over time as manual assessment. This graph represents the entire response of a single zebrafish larva, tested with linear regression; Slope: F = 0.2019, DFn = 1, DFd = 286, P=0.6536; Intercept: F = 0.004179, DFn = 1, DFd = 287, P=0.9485.

3.2.5 Location of laser injuries is essential for measurable inflammatory responses

To increase sensitivity in high-throughput assays, it is essential to reduce variance as much as possible. Therefore, I investigated the use of laser injuries to elicit swarming responses in zebrafish larvae. Laser injuries can be performed more deterministically and with less individual bias compared to manual injuries. As the tail fin injury model of inflammation is extensively used in zebrafish research, I assessed whether a sufficient response could be initiated by performing a laser injury across the tail fin. I used a high-intensity ablation laser to burn the tail fin tissue, resulting in a relatively small burn line (**Figure 17**). A clear retraction of the tail fin tissue was also observed (**Supplemental Movie 5**).

While the wound creation was successful, a neutrophil response was not triggered (**Figure 17**). Only occasionally did a small number of neutrophils interact with the linear burn wound (**Figure 17, Supplemental Movie 5**). I hypothesised that this could be due to the wound not being severe enough to elicit a proper response or the wound's location being too far from the hemopoietic tissue where neutrophils usually reside, resulting in the chemotactic gradient not being able to reach far enough to recruit distant neutrophils. Burning the entire tail fin with a laser was incredibly time-inefficient, taking up to a maximum of 2 minutes per larvae, and unsuitable for high-throughput; thus, one parameter which could be changed was injury location, as previous research has illustrated that laser injuries near the hemopoietic tissue can cause neutrophil swarming (Poplimont et al., 2020).

The fin tissue around the cloaca of the zebrafish larva has previously been used to produce neutrophil swarming responses with laser injuries (Poplimont et al., 2020). Therefore, I investigated creating injuries in a similar area, more distally from the cloaca, in the thin

transparent tissue on the ventral side of the larva. When laser injuries were induced with enough power in this location, measurable inflammatory responses were triggered, some of which included neutrophil swarms (**Figure 18B**). This aligns with previously published literature which demonstrated that laser injuries in zebrafish can produce neutrophil swarms and provided enough confidence for taking laser injuries forward in the assay (Poplimont et al., 2020).

The aforementioned laser injuries used in literature were point wound injuries (Poplimont et al., 2020). As such I determined whether a point wound injury would perform differently from a more linear injury where more tissue was damaged by the laser. Point injuries seemed to attract less neutrophils (**Supplemental Movie 6**), after which I decided to go forward with the larger linear laser injuries (**Figure 18A, Supplemental Movie 7**).

Taken together, these results illustrate that laser injury can be used for the generation of neutrophil swarms, albeit dependent on the location of the inflicted wound as well as requiring high laser power to elicit a measurable response.

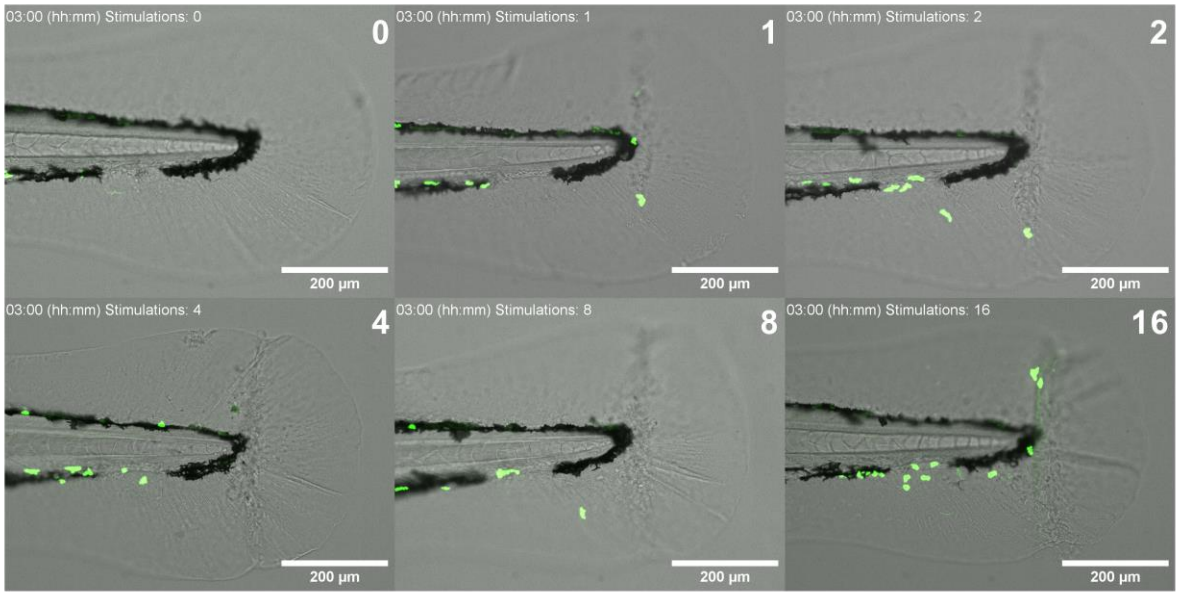

Figure 17: Tail fin laser injuries show low neutrophil recruitment

This figure shows laser injuries made in the tail fin of 3dpf zebrafish larvae, 3 hours post-injury. The top right indicates the number of stimulations with a high-intensity CryLaS ablation laser across the tail fin. Settings were: 250Hz, 20% power, 500µs dwell time. An increasing amount of tissue damage corresponding to the number of stimulations is visible. However, even at 16 stimulations, only a very small number of neutrophils were recruited to the wound when compared to traditional tailfin injuries, where on average an estimated 15 neutrophils would have arrived to the wound site (**Figure 5**). This suggests the injury was not severe enough to trigger a proper response or that the wound was too far from the hemopoietic tissue where neutrophils reside during homeostasis.

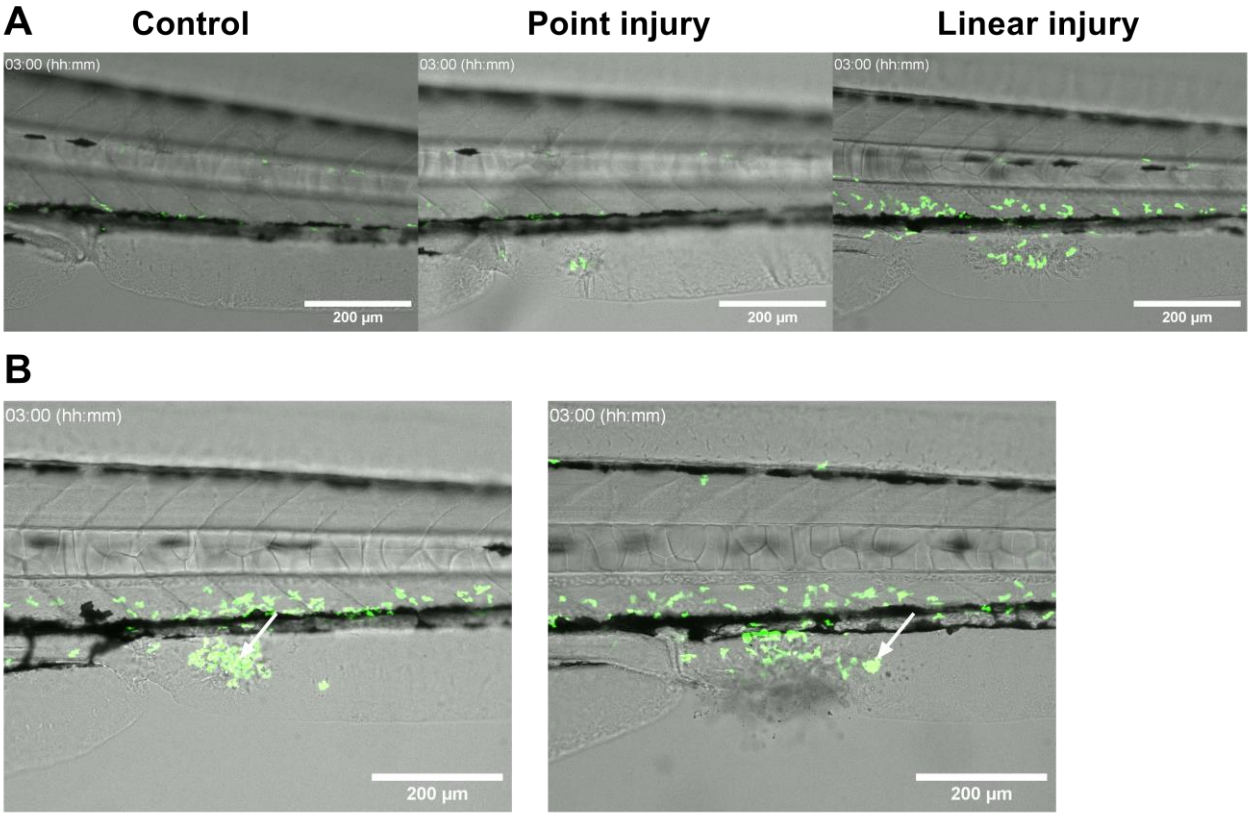

Figure 18: Ventral laser injuries recruit neutrophils and generate neutrophil swarms

A. A comparison of 3dpf zebrafish larvae without laser injury, point injury or linear injury 3 hours post-injury. It was observed that point injuries did not recruit a relevant number of neutrophils compared to the larger and more severe linear laser injuries. Laser settings were: 250Hz, 20% laser power, 2000µs dwell time.

B. Two 3dpf zebrafish larvae displaying a swarming response 3 hours post-laser injury. For this experiment, laser power was increased to create more severe wounds. This illustrates that with sufficient laser power and in a location close to the hemopoietic tissue, swarming responses can be triggered via laser injury. Laser settings were: 250Hz, 80% laser power (left) 100% laser power (right), 2500µs dwell time.

3.2.6 Location of an injury affects the time course of a neutrophil response

To further investigate how changing the injury location affects the inflammatory response, I compared sterile cuts in the ventral fin tissue to regular tail fin transection. I performed smaller 'notch' cuts in the ventral tissue of the larva, approximately in the same location as the laser wounds illustrated previously (**Figure 18**). I hypothesised that having the location closer to the hemopoietic tissue of the zebrafish would cause more rapid recruitment of neutrophils compared to tail fin injuries, potentially missing the opportunity to capture the initial recruitment phases. However, since the wound is smaller and recruitment is faster, it should also reduce the total time for inflammation resolution. This allows studying inflammation resolution within a more practical time frame for time-lapse imaging compared to tail fin injuries, where previous data suggested inflammation could still be present 24 hours after injury in some cases (**Figure 11D-E**).

When comparing notch cuts in the ventral fin tissue to tail fin injuries, rapid recruitment is apparent, resulting in neutrophils being present when imaging started approximately 1 hour after injury (**Supplemental Movie 8**) (**Figure 19**). Comparing neutrophil counts over time between both injury locations reveals a significant difference in cell numbers (**Figure 19-21**). While neutrophil recruitment towards the tail fin injury increased until the end of the timelapse, ventral fin injuries showed neutrophil recruitment saturating around 3.5 hours, after which the average number began to slowly decrease (**Figure 21A**).

To assess the speed of resolution, the delta displacement of cells was measured. Cells were tracked using a combination of Cellpose and Trackmate as previously explained. After obtaining tracks, the distance of cells to the wound was measured for both tail fin and ventral fin injuries (**Figure 22A**). This allowed calculation of the change (delta) in distance from one

time frame to another, resulting in a measurement of active movement towards the injury (negative value) or away from the injury site (positive value) suggesting resolution. Plotting these values and performing linear regression provides an estimate of when a switch from recruitment to resolution occurs (**Figure 22B, E**). However, neutrophils can also undergo apoptosis or be cleared via efferocytosis, so cell counts need to be correlated. Changes in cell counts were assessed similarly, taking counts from one time frame to another. A significant switch in reduction of cells was not found (**Figure 22C**), suggesting neutrophils to exhibit partial reverse migration and not total clearance away from the wounded area in which cells were counted.

Overall, ventral fin injuries initiated inflammation resolution, measured as active migration away from the wound, significantly earlier than tail fin injuries (**Figure 22E**). Initial recruitment rate, measured as positive movement towards the wound, was significantly higher in tail fin injuries due to the severity of the injury and the longer chemotactic distance compared to the ventral fin injuries (**Figure 22F**). This went paired with a higher rate at which neutrophils would decrease their acceleration towards the wound site (**Figure 22D**).

In summary, ventral fin injuries have a significantly earlier switch towards inflammation resolution compared to tail fin injuries. This is paired with a significantly lower number of total neutrophils recruited and a different recruitment rate. For a high-throughput assay, faster inflammation resolution is preferred as it increases the throughput and reduces data volume. This facilitates investigating differences in resolution timepoints of samples treated with immunomodulatory compounds, in an accessible way.

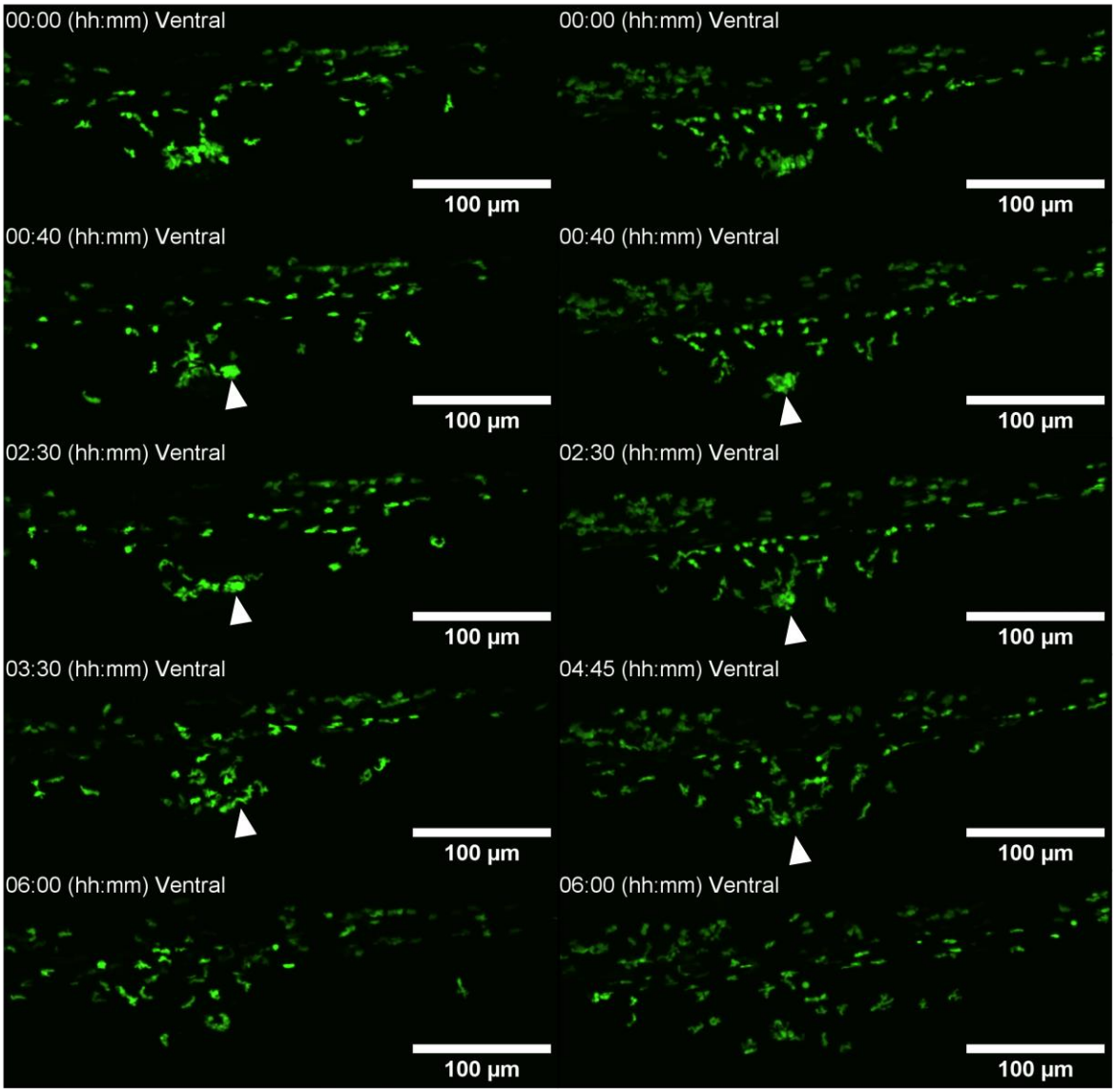

Figure 19: Ventral fin notch cut injuries show neutrophil swarms and subsequent resolution

This figure shows 2 ventral fin 'notch' cut injuries in 3dpf *Tg(mpx:GFP)*^{i114} zebrafish larvae. A large number of neutrophils are already present at the start of the timelapse which quickly aggregate into neutrophil swarms around 40 minutes later. After neutrophil swarms resolve, further inflammation resolution is initiated, illustrated by dispersed neutrophils at the wound site at 6 hours, this is further analysed in (**Figure 19-20**).

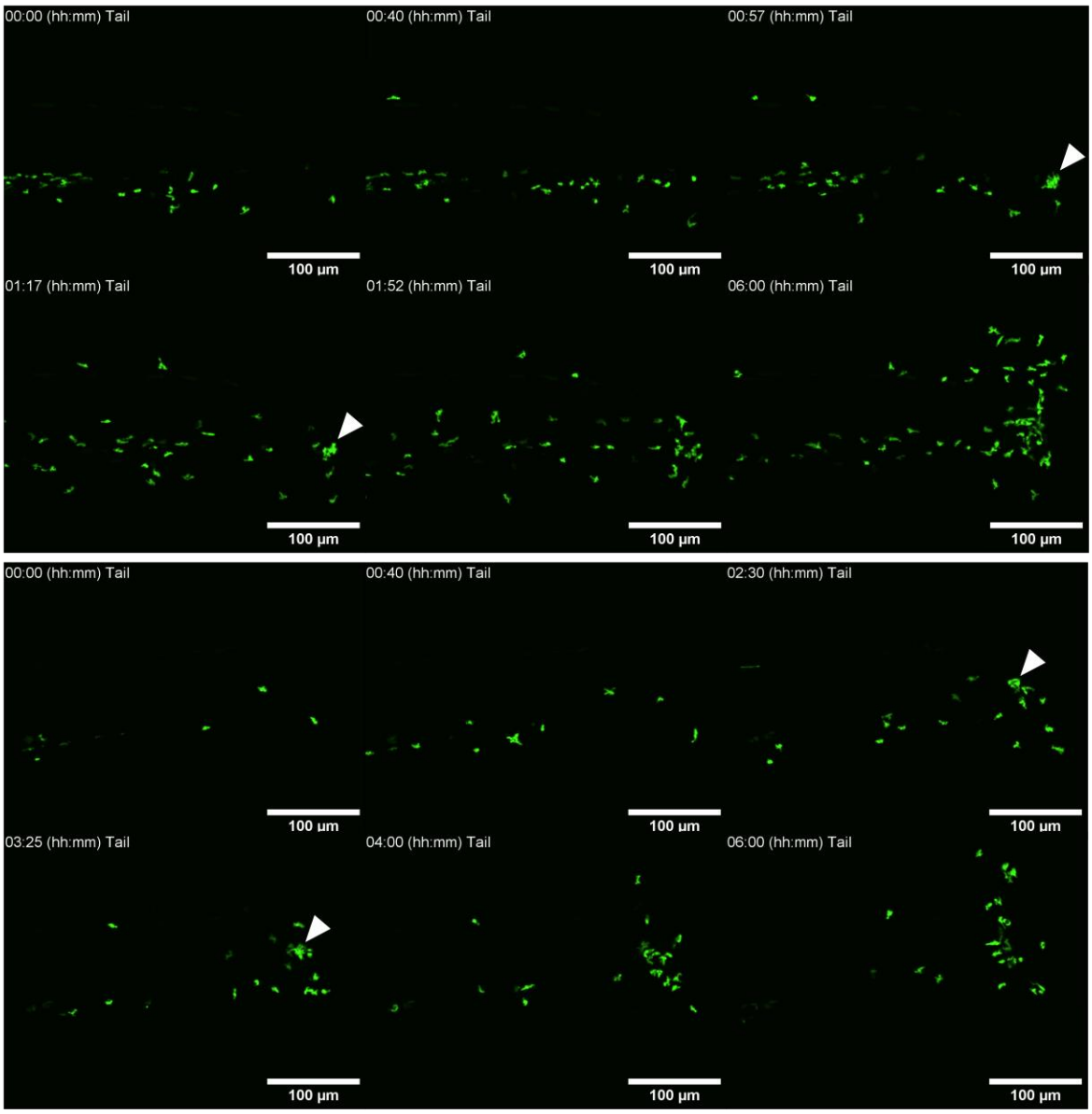

Figure 20: Tail fin injuries show neutrophil swarms and suggest continued neutrophil recruitment at 6 hours post injury

This figure shows 2 tail fin injuries in 3dpf *Tg(mpx:GFP)*^{i114} zebrafish larvae. Cells slowly aggregate into small neutrophil swarms either early on at 57 minutes (top) or later at 2 hours and 30 minutes (bottom). After neutrophil swarms resolve, further inflammation resolution is seemingly delayed compared to ventral fin injuries, illustrated by the increase in neutrophils at 6 hours, this is further analysed in (**Figure 19-20**).

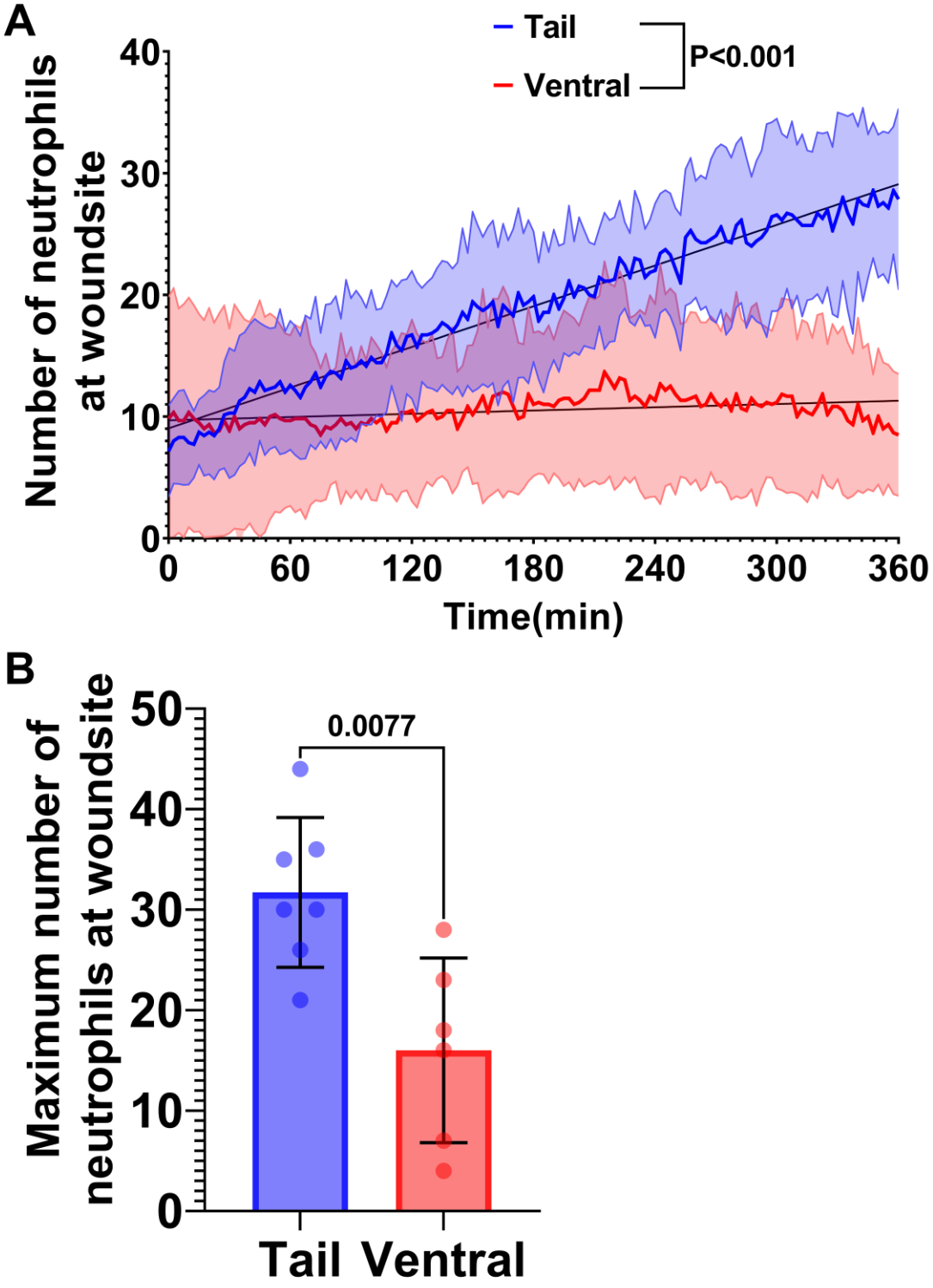

Figure 21: Neutrophil numbers are significantly different depending on injury location

A. The average number of neutrophils present at the wound site over time. Neutrophils were automatically counted using the image analysis macro and Cellpose as previously described. A significant difference in neutrophil recruitment to tail fin or ventral fin injuries is shown. Tail fin injuries exhibit a continuous increase in neutrophil recruitment until the end of the time-lapse at 6 hours, while ventral fin injuries show a small increase in cell numbers until 4 hours, after which neutrophil numbers slowly decline. Linear regression, Tail fin n = 7, ventral fin n = 6, $F = 374.8$, $DFn = 1$, $DFd = 1881$, $P < 0.0001$.

B. The maximum number of neutrophils at the wound site throughout the entire timelapse. Tail fin injuries show a significant increase in neutrophil recruitment compared to ventral fin injuries, due to the severity of the wound. Unpaired t-test with Welch's correction, Tail fin n = 7, ventral fin n = 6, SEM 15.71 ± 4.610.

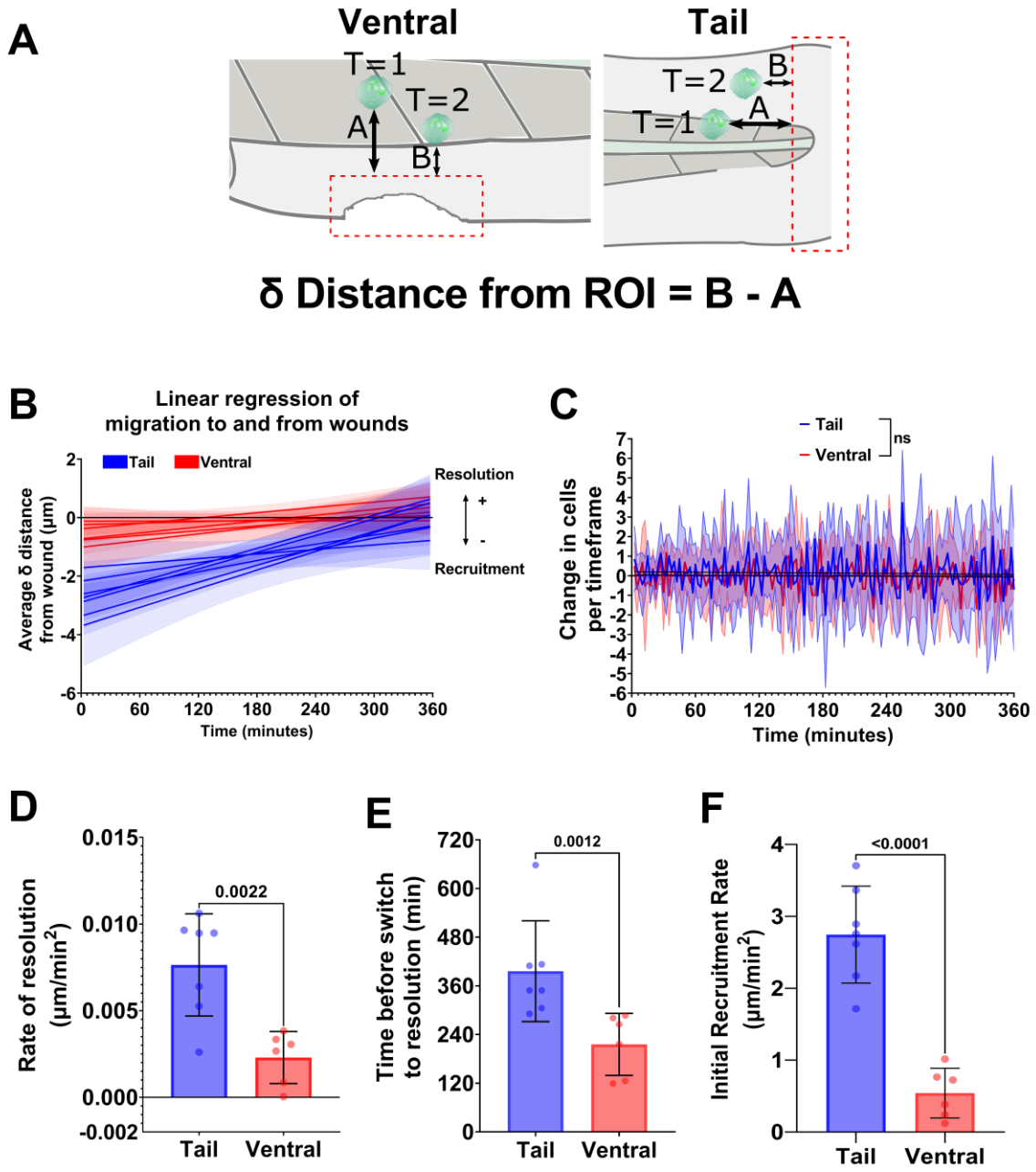

Figure 22: The neutrophil response changes between tail fin and ventral fin injuries

A. The change in distance from the region of interest (ROI), or delta distance, was obtained by subtracting the distance of a single tracked neutrophil at time point 2 (T=2) from time point 1 (T=1). When this is done for all tracked neutrophils, an overall vector of movement towards or away from the wound can be generated. This is indicated by either a negative value, where cells collectively accelerate towards the wound, or a positive value, where cells collectively accelerate away from the wound.

B. A plot of linear regression on the delta distance values, showing an approximation of the rate of inflammation resolution via reverse migration of neutrophils. A difference can be observed between both injury locations, further detailed in 20D-F. Tail fin n = 7, ventral fin n = 6.

C. The average change in cell numbers over time for both injury locations. There was no significant difference found in the rate at which the number of neutrophils changed during the response. Linear regression, slope; F = 0.003619, DFn = 1, DFd = 1868 P=0.9520, intercept; F = 2.595, DFn = 1, DFd = 1869, P=0.1074

D. The rate of resolution (slope) was significantly different depending on the injury location. Unpaired t-test with Welch's correction, tail fin n = 7, ventral fin n = 6, SEM -0.005344 ± 0.001273.

E. The estimated time before a switch towards active resolution (X-intercept) was significantly different between both injury locations, with ventral fin injuries showing collective acceleration away from the wound earlier than tail fin injuries. Unpaired Mann-Whitney test, tail fin n = 7 median 348.8, ventral fin n = 6 median 240.7.

F. The initial recruitment rate (Y-intercept) was significantly higher in tail fin injuries, indicating higher collective acceleration of neutrophils towards the wound compared to ventral fin injuries. Recruitment rate was obtained by transformation of the resolution rate (Y=Y*-1). Unpaired t-test with Welch's correction, tail fin n = 7, ventral fin n = 6, SEM -2.205 ± 0.2916.

3.2.7 Validation of a high-throughput assay for neutrophil swarming by comparison of injury types

Once all previously described tools were developed and decisions were made, it was time to validate whether a high-throughput assay would be feasible for investigating neutrophil swarming. Due to unforeseen complications with shipping between the UK and Germany, I was unable to obtain immunomodulatory compounds for investigating neutrophil swarm resolution. However, while performing laser injuries alongside mechanical injuries (where tissue was cut using a blade or needle), I anecdotally observed an increased number of neutrophils and seemingly higher inflammatory responses for mechanical injuries. Therefore, I decided to determine whether the semi-automated assay could detect this observational difference, validating whether the approach and tools were functioning as intended.

To do this, automatic laser and manual mechanical injuries were made in the ventral fin of 3dpf zebrafish larvae as previously described. Due to limitations in the availability of zebrafish lines in Heidelberg, some results were obtained from a *Tg(lysC:GFP)* transgenic neutrophil line in addition to the *Tg(mpx:GFP)*^{i114} transgenic neutrophil line I have used elsewhere in this thesis . Timelapses always started 1 hour after the first mechanical injury was performed, with laser injuries made 30 minutes before the timelapse started. This meant the response was tracked from 60 minutes post-injury (mpi) to 420mpi for mechanical injuries and 30mpi to 390mpi for laser injuries. To increase the number of samples, a 5-minute imaging interval was chosen, though this meant accurate cell tracking could not be performed due to the low temporal resolution.

When laser injuries were compared to mechanical injuries, there was a significant difference in the number of neutrophils recruited, which agreed with my hypothesis (**Figure 23A**). For

mechanical injuries, there was a significant positive correlation between wound size and the total number of neutrophils recruited over time; however, this was not the case for larvae that underwent laser injury (**Figure 23C**). Moreover, wounds created mechanically were significantly larger than those created by laser injury on average (**Figure 24D**). Further investigation into neutrophil swarming showed a significant increase in the number of neutrophil clusters detected in the timelapses (**Figure 24A**). Additionally, the maximum size of these clusters was significantly larger, indicating a higher inflammatory response (**Figure 24B**).

Classification of swarming responses was performed post-experimentation. Neutrophil swarms formed significantly more often in mechanically injured larvae, as indicated by the percentage of larvae developing a swarming response (**Figure 24C**). Besides swarms occurring more frequently in mechanically injured larvae, swarm dynamics, measured as the duration of a swarm, showed a small but significant increase (**Figure 24E**).

Further analysis of swarming responses evaluated neutrophil numbers between larvae with and without a swarming response to reassess whether earlier results could be replicated under different conditions. Indeed, in this new experimental setup, inflammation resolution was significantly delayed in larvae that initiated a swarming response (**Figure 25**). This delay in inflammation resolution, indicated by heightened neutrophil levels at the wound site, was found in both mechanically and laser-injured larvae (**Figure 25**).

In summary, these data illustrate that the developed analysis tools and initial assay could successfully detect an expected difference based on earlier observations, highlighting the feasibility of a high-throughput swarming assay. Furthermore, in-depth analysis for different injury types was conducted on swarm locations, swarm size, swarm duration and the impact of swarms on inflammation resolution, measured by neutrophil numbers.

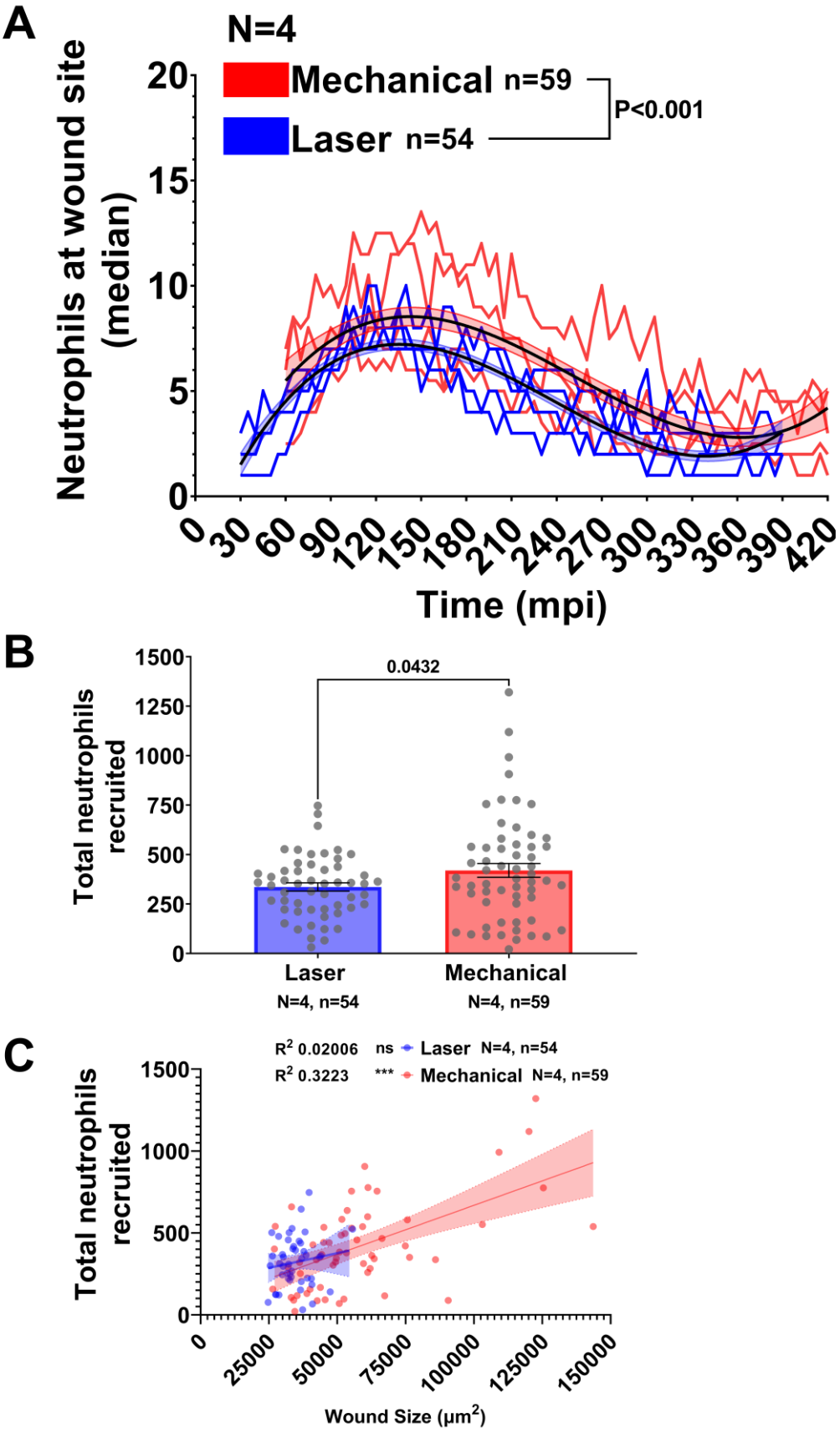

Figure 23: Laser injuries recruit less neutrophils in total compared to mechanical injuries

A. The median number of neutrophils present at the wound site over time. A significant increase in neutrophils over time is observed when larvae were mechanically injured compared to laser injury. Data was compared using non-linear regression of a third-order polynomial fit, $P < 0.001$. Laser injury, $R^2 = 0.7278$; Mechanical injury, $R^2 = 0.4894$.

B. The total number of neutrophils recruited to the wound site over an entire timelapse. Mechanical injuries recruited a significantly higher number of cells compared to laser injuries. Unpaired t-test with Welch's correction, SEM 83.81 ± 40.89. Variance was significantly different $P<0.001$, F-test; F, DFn, Dfd; 3.013, 58, 53.

C. Correlation between wound size and the total number of neutrophils recruited. No significant correlation between wound size and neutrophil recruitment was found for laser injuries. However, for mechanical injuries, a significant correlation was determined. Data was fit via linear regression. Laser injury, $P = 0.3534$, slope = 0.003598, 95% CI = -0.004136 to 0.01133, Y-intercept = 196.5, 95% CI = -74.97 to 467.9. Mechanical injury, $P < 0.001$, slope = 0.005966, 95% CI = 0.003671 to 0.008261, Y-intercept = 71.78, 95% CI = -74.15 to 217.7.

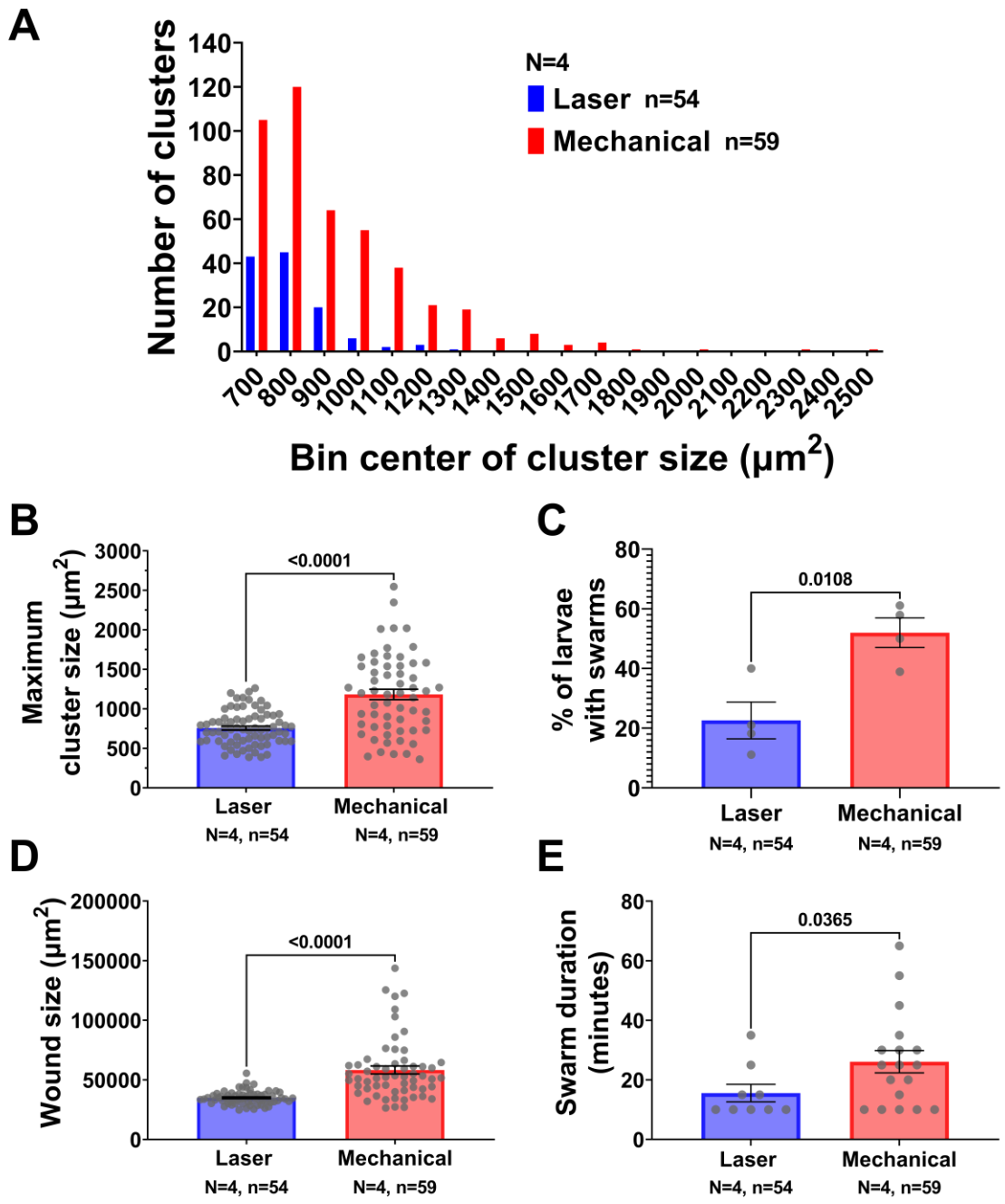

Figure 24: Laser injuries produce significantly less swarms compared to mechanical injuries

A. Frequency distribution of the number of clusters according to binned cluster size. Clusters were extracted by filtering for objects with an area greater than or equal to 735 µm². Differences are suggested in the number and size of neutrophil clusters formed between laser and mechanical injuries.

B. Maximum cluster size was significantly different between injury types, with mechanical injuries resulting in larger neutrophil clusters compared to laser injuries. Unpaired t-test with Welch's correction, SEM 393.1 ± 72.56. Variance was significantly different P<0.001, F-test; F, DFn, Dfd; 4.952, 58, 53.

C. The percentage of larvae that developed swarms across 4 experimental repeats. A significantly higher percentage of larvae initiated neutrophil swarming post-mechanical injury compared to laser injury. Unpaired t-test with Welch's correction, SEM 29.39 ± 7.907. Variance was not significantly different, P=0.7253, F-test; F, DFn, Dfd; 1.556, 3, 3.

D. The size of wounds created post-mechanical or laser injury. Mechanical injury resulted in significantly larger wounds compared to laser injury. Unpaired t-test with Welch's correction, SEM 23033 ± 3433. Variance was significantly different P<0.001, F-test; F, DFn, Dfd; 17.88, 58, 53.

E. Duration of neutrophil swarms post-laser or mechanical injury. When swarming was initiated, the type of injury had a small but significant effect on swarm duration. Swarm duration was measured by implementation of a python script which would recognise clusters between frames within close proximity, after which these were linked to indicate whether a swarm was occurring and for how long. Unpaired t-test with Welch's correction, SEM 10.56 ± 4.773. Variance was not significantly different, P=0.0928, F-test; F, DFn, Dfd; 3.273, 17, 8.

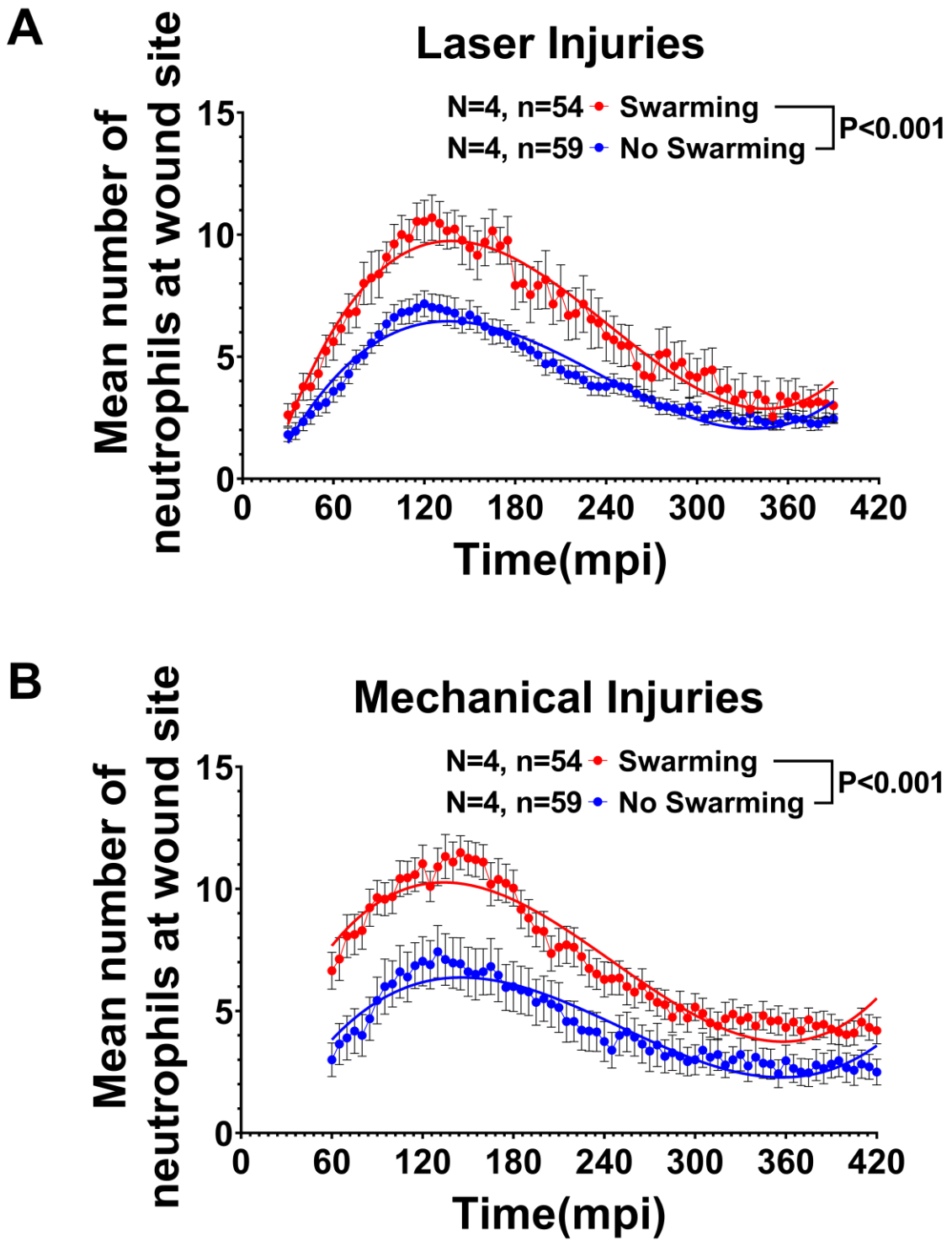

Figure 25: Swarming delays inflammation resolution in both mechanical and laser injuries

A. The mean number of neutrophils measured over time post-laser injury. Larvae that developed neutrophil swarms exhibited a significant elevation in the neutrophil response, resulting in delayed resolution. This is indicated by neutrophils being retained at the wound site longer compared to larvae without swarms. Data was compared using non-linear regression of a third-order polynomial fit, $P < 0.001$, Swarming, $R^2 = 0.4090$; No swarming, $R^2 = 0.2813$.

B. The mean number of neutrophils measured over time post-mechanical injury. Consistent with the data shown in A, larvae that developed neutrophil swarms exhibited a significant elevation in the neutrophil response, resulting in delayed resolution. This is indicated by neutrophils being retained at the wound site longer compared to larvae without swarms. Data was compared using non-linear regression of a third-order polynomial fit, $P < 0.001$, Swarming, $R^2 = 0.2889$; No swarming, $R^2 = 0.1036$.

3.2.8 Conclusion & Discussion

I aimed to establish a novel high-throughput assay for performing small molecule screens related to the neutrophil swarming response. To achieve this, a collaboration with Acquifer, a member of INFLANET, was established. They provided both expertise and the necessary equipment for this part of the project. Together with Sankeert Satheesan, a PhD student at Acquifer, we used Acquifer's Imaging Machine (IM) to develop the new high-throughput assay.

Before fully utilising the IM, a plan was drafted to reliably characterise neutrophil swarming responses and process data robustly. A new ImageJ macro was developed to streamline data processing, combining older methods like template matching and HyperStackReg to ensure reliable data output (Thomas and Gehrig, 2020; Sharma, 2018). These methods stabilised time-lapse imaging and cropped data to specific regions of interest (ROI). Modifying the template matching program to use Gaussian blurred images greatly increased accuracy across various time-lapse data.

A major issue in classifying swarming responses is individual detection bias, caused by differences in experimental approaches, imaging settings and background knowledge. The macro was partially designed to circumvent this issue by creating a more deterministic classification approach. Various parameters were assessed using K-means clustering, grouping data into swarming or non-swarming categories. Skewness, a measure of distribution symmetry, was one of the best predictors for automatic classification. However, I considered the accuracy of automated classification at 92,86% specificity and 75% sensitivity to be too low, as I was looking for both specificity and sensitivity to be above 95%. Thus, instead of relying solely on automatic classification, the choice was made to provide a solution

combining deterministic and visual approaches. In the current solution researchers receive an Excel sheet outputting various parameters based on neutrophil area measurements, along with average intensity projections showing overall neutrophil motility. This visual output, combined with the parameters, should assist researchers in accurately defining and understanding the neutrophil swarming response. However, as of yet a blinded comparison between classifications with and without the tool is not made and is recommended for future assessment.

After choosing computational tools, biological parameters were determined, including injury location, timelapse duration and the use of automatic laser injuries by the IM. Laser injuries in the tailfin did not promote sufficient neutrophil recruitment to initiate swarms. This could be due to the chemotactic signal not reaching the hemopoietic tissue or the lack of continuous need for inflammatory cells, unlike in tailfin amputation. Neutrophils are known for matrix remodelling through NE secretion alongside neutrophil derived MMP-8 and MMP-9 (Zhu et al., 2021). Matrix remodelling can create Proline-Glycine-Proline (PGP), a potent neutrophil chemotaxis regulator similar to CXCL8, causing neutrophil recruitment (Weathington et al., 2006, Gaggar et al., 2008).

Ultimately, performing a laser wound on the entire tailfin was too time-intensive for the high-throughput setup we envisioned. Instead, laser injuries were made in ventral fin tissue with a varying range of laser intensities as illustrated in previous research (Poplimont et al., 2020). This change resulted in the desired response for a high-throughput setup using the IM. Furthermore, ventral fin injuries spatiotemporally differed from tailfin injuries, initiating inflammation resolution significantly earlier. Previously described methods of high-throughput screening for inflammation resolution using zebrafish, performed tail fin injuries

and chose only one timepoint at 12hpi to assess inflammation resolution (Robertson et al., 2014). To investigate the more intricate dynamics at play during neutrophil swarming this was not an option for the assay presented in this chapter. Ventral fin injuries allowed for shorter timelapses, capturing all aspects of the inflammatory response which was more suitable for investigating neutrophil swarming in a high-throughput setting.

However, smaller injuries in the ventral fin lacked the linear structure of a tailfin injury, which theoretically allows swarms to form anywhere. Nonetheless, non-swarming responses in the ventral fin model suggested that underlying signalling mechanisms were still required for swarming. This is likely to be LTB4 as LTB4 has been shown to be essential for the relay phase of the bi-phasic swarming response where more distant neutrophils are attracted and subsequent accumulation occurs (Strickland et al., 2024, Philippe et al., 2012, Lämmermann et al., 2013, Isles et al., 2021, Poplimont et al., 2020). After making all computational and biological considerations, implementation into the IM followed. A planned treatment with immunomodulatory compounds was cancelled due to customs issues, leading to another experiment to be designed for validation of the assay.

Anecdotal observations suggested a difference between laser and mechanical wounds. Using the novel swarming assay, an experiment was conducted to verify this observation, with 4 experimental repeats involving over 100 zebrafish larvae comparing mechanically induced and laser-induced injuries. Data supported the observational difference, showing significant differences in swarming responses between laser and mechanical injuries. Laser injuries resulted in fewer and smaller swarms, with lower variances in neutrophil recruitment, maximum cluster area and wound size compared to mechanical injuries. This is likely due to increased wound size from mechanical injuries as well as the previously mentioned matrix

remodelling that was triggered compared to laser injuries, which would stay relatively contained and would evidently shrink in size after the initial swelling ceased.

In assay development, the Z-score is used for validation and optimisation (Zhang et al., 1999). Z-score is defined as follows; $Z' = 1 - \frac{3(\sigma p + \sigma n)}{|\mu p - \mu n|}$, where σ p,n = standard deviation of the positive or negative control and μ p,n = mean of positive or negative control. The Z-score formula suggests that low variance in controls and a large difference between means result in the best assay. Ideally, a Z-score would be calculated for the swarming assay, but due to time constraints this could not be performed. While a negative control for swarming could be provided in the form of an LTB4 inhibitor, positive controls for swarming have not yet been clearly identified as of writing this thesis (Isles et al., 2021). One option could be localised injection of LTB4, however LTB4 is the linchpin of the swarming response and identifying pathways upstream of autocrine LTB4 production are exactly where I would hypothesise therapeutic approaches to be found (Poplimont et al., 2020, Kienle et al., 2021, Isles et al., 2021, Strickland et al., 2024). Performing no injury could be another control, but this would compare inflammatory responses rather than swarm formation after inflammation and recruitment of neutrophils is triggered.

Ultimately, using the Z-score suggests that automatic laser injuries are preferred for generating swarms, as variances are smaller and more controllable than manual mechanical injuries. However, laser injuries rarely generated clear swarming events. A higher intensity laser could create more severe wounds, which may lead to increased neutrophil swarms to be formed.

In terms of the high-throughput nature of the assay, 20 zebrafish could be imaged per experiment. This is relatively limited considering the system is built for screening 96-well plates, but time-lapse data from 20 zebrafish would quickly grow into several hundred gigabytes of data. This illustrates that even with more samples, data storage and processing would become a rapidly growing problem.

Neutrophil swarming is a dynamic event requiring high temporal resolution to avoid missing any occurrences. In this case, temporal resolution was set at 5-minute intervals, allowing detection of swarming events, but insufficient for investigating cell motility or cell-cell interaction. For this, an interval of 2.5 minutes would be needed, reducing the sample size to 10 zebrafish. Since neutrophil swarming is relatively stochastic when occurring endogenously, this could result in insufficient statistical power. As such, if this assay and workflow are used for future investigation of neutrophil swarming, considerations will need to be made regarding experimental design and which measurements are essential for concluding differences in swarm formation and resolution. Improvements could include creating a new baseline where swarming is initiated using a positive control, increasing statistical power. This idea will be further described in **Chapter 3.3**.

In future iterations of high-throughput neutrophil swarming I would recommend attempting to increase the sample throughput. One way this could be achieved is by increasing the number of larvae within a single well. With further development of image recognition and stabilisation software one could image a single well with possibly up to 3 different larvae, which can be recognised and stabilised during image analysis. This would increase sample size while maintaining similar imaging times. In this case one would have to switch to a 10x objective which will result in a loss of image quality. This would result in the loss of cell-specific

movements, but it would allow for a faster screening process to determine whether neutrophil swarming has downstream phenotypic implications.

In summary, these data show the successful development of a novel proof-of-concept high-throughput screening assay for investigating neutrophil swarming dynamics, including formation and resolution. A tailored image analysis pipeline was created for detailed analysis of large time-lapse data. This pipeline was then used to create a proof of principle by exploring differences between laser and mechanical injuries, where a clear observational difference was confirmed by detailed data after acquiring time-lapse imaging with Acquifer's IM.

3.3 Determining Avenues for Pharmacological Manipulation of Neutrophil Swarming

3.3.1 Introduction

Neutrophils commence chemotaxis after extracellular molecules bind to cell surface receptors (Metzemaekers et al., 2020). These molecules often consist of either PAMPs or DAMPs that bind to PRRs, or smaller chemotactic molecules such as the CXCL family that bind to the CXCR family of GPCRs (Li and Wu, 2021, Isles et al., 2019, Kienle et al., 2021, van der Vaart et al., 2012). Previous literature indicates that TLRs play a role in activation of neutrophils (Prince et al., 2011). Furthermore, a recent study found that zebrafish lacking the TLR2 receptor showed decreased recruitment of neutrophils after wounding, illustrating potential for modulation (Hu et al., 2021). As described in **Chapter 3.2**, variability in zebrafish larvae exhibiting a neutrophil swarming response after injury remained a challenging aspect of my experiments. I hypothesised that promoting a pro-inflammatory phenotype could potentially reduce this variability and aid in increasing statistical power in experiments by providing a higher baseline of samples with neutrophil swarms. Because of the relationship between TLR signalling and neutrophil migration and activation, I selected a range of TLR agonists, with the idea that treatment could upregulate neutrophil recruitment and activation in an effort to increase the occurrence of neutrophil swarms.

Literature suggests a role for NOX in the relay signalling mechanism of neutrophil swarms, which correlates to a disease phenotype found in samples from donors with CGD (Strickland et al., 2024). NOX is known as a main regulator of ROS in neutrophils, which has been previously shown to augment neutrophil swarming and help delay germination of *Candida albicans* in an *ex vivo* model (Hopke et al., 2020, Panday et al., 2015). Another pathway that

is directly interacting with ROS is the HIF-1α pathway (Taylor and Scholz, 2022, Willson et al., 2022, Movafagh et al., 2015, Zheng et al., 2022). During hypoxia HIF-1α and HIF-1β subunits dimerise to form a complex which then functions as a transcription factor, driving downstream expression of target genes (Taylor and Scholz, 2022). Under normoxic conditions, prolyl-hydroxylases (PHDs), hydroxylate proline residues located at P402 and P564 within the oxygen-dependent degradation domain (Masson et al., 2001). The hydroxylated HIF-1α subunit is recognised by the von Hippel-Lindau (VHL) protein, which is an E3 ubiquitin ligase (Hon et al., 2002, Min et al., 2002, Kubaichuk and Kietzmann, 2019). Following ubiquitination, HIF-1α is targeted for proteasomal degradation, eliminating downstream effector function (Kubaichuk and Kietzmann, 2019).

HIF-1α accumulation within neutrophils has been shown to occur after an increase in mitochondrial ROS (Willson et al., 2022). I hypothesised that HIF-1α activation via ROS production, could activate downstream signalling that changes neutrophil swarming responses. Previous research has illustrated that HIF-1α activation can lead to increased neutrophil retention at wound sites in the zebrafish model, which could affect the dynamics of neutrophil swarming (Elks et al., 2011). Within mice, Hif-1α has been shown to be implicated in neutrophil recruitment during fungal-elicited granulomatous inflammation, as a knockout line of Hif-1α showed impaired neutrophil recruitment to agarose beads containing Aspergillus conidia (da Silva-Ferreira et al., 2022).

To test whether HIF-1α could be implicated in the onset of neutrophil swarming, experiments utilising prolyl-hydroxylase (PHD) inhibitors were designed. PHD inhibitors prevent HIF-1α from becoming hydroxylated, stabilising it within the cell and enabling dimerisation with HIF-1β for nuclear localisation and expression of target genes (Zheng et al., 2022). DPI functions as an inhibitor of NOX and mitochondrial ROS, effectively reducing the levels of intracellular

ROS available for HIF-1α stabilisation (Prajsnar et al., 2021, Lodge et al., 2020). In this chapter I discuss experiments using these inhibitors, which provided preliminary results regarding the effect of HIF-1α and ROS on neutrophil swarming *in vivo*.

3.3.2 Screening TLR agonists for effects on neutrophil swarming

To determine whether the neutrophil swarming response could be upregulated via pharmacological treatment, a selection of TLR agonists was chosen for their pro-inflammatory effects (Cen et al., 2018, Kircheis and Planz, 2023). This included lipopolysaccharide (LPS), a cell wall component of Gram-negative bacteria that binds to the TLR4 receptor; polyinosinic acid (Poly I:C), structurally similar to double-stranded RNA, which initiates an antiviral response via binding to TLR3; resiquimod (R848), a TLR7/TLR8 agonist that also initiates an antiviral response; imiquimod (R837), which causes the same response as R848 but only binds to TLR7; high mobility group box 1 protein (HMGB1), which binds to TLR2/4; Pam2CysSerLys4 (PAM2CSK4), a synthetic diacylated lipopeptide binding to TLR2/6; and N-formylmethionyl-leucyl-phenylalanine (fMLP), a peptide that binds to formyl peptide receptor 1 (FPR1) (Bao et al., 1992).

Treatment of these compounds occurred in immersion to find potential candidates upregulating neutrophil swarming, concentrations were chosen based on previous experiments performed in Sheffield (KAMUYANGO, 2017). Tailfin injury was performed on 3dpf zebrafish larvae and neutrophil swarming was assessed at 4hpi. Out of all the compounds chosen, only PAM2CSK4 seemed to elicit a response (**Figure 26**). However, the finding in question was in contrast to my initial hypothesis, as I expected an increase in neutrophil swarms rather than a reduction.

In conclusion, these data show that immersion treatment with a range of TLR agonists as well as fMLP, ultimately had no effect on the percentage of larvae that would develop a neutrophil swarm, except for PAM2CSK4 which suggests a non-significant reduction in the number of swarms that formed at 4 hours post tail fin injury. While this finding was not statistically significant, due to high variability in this screen, it could still be biologically relevant and was thus further investigated.

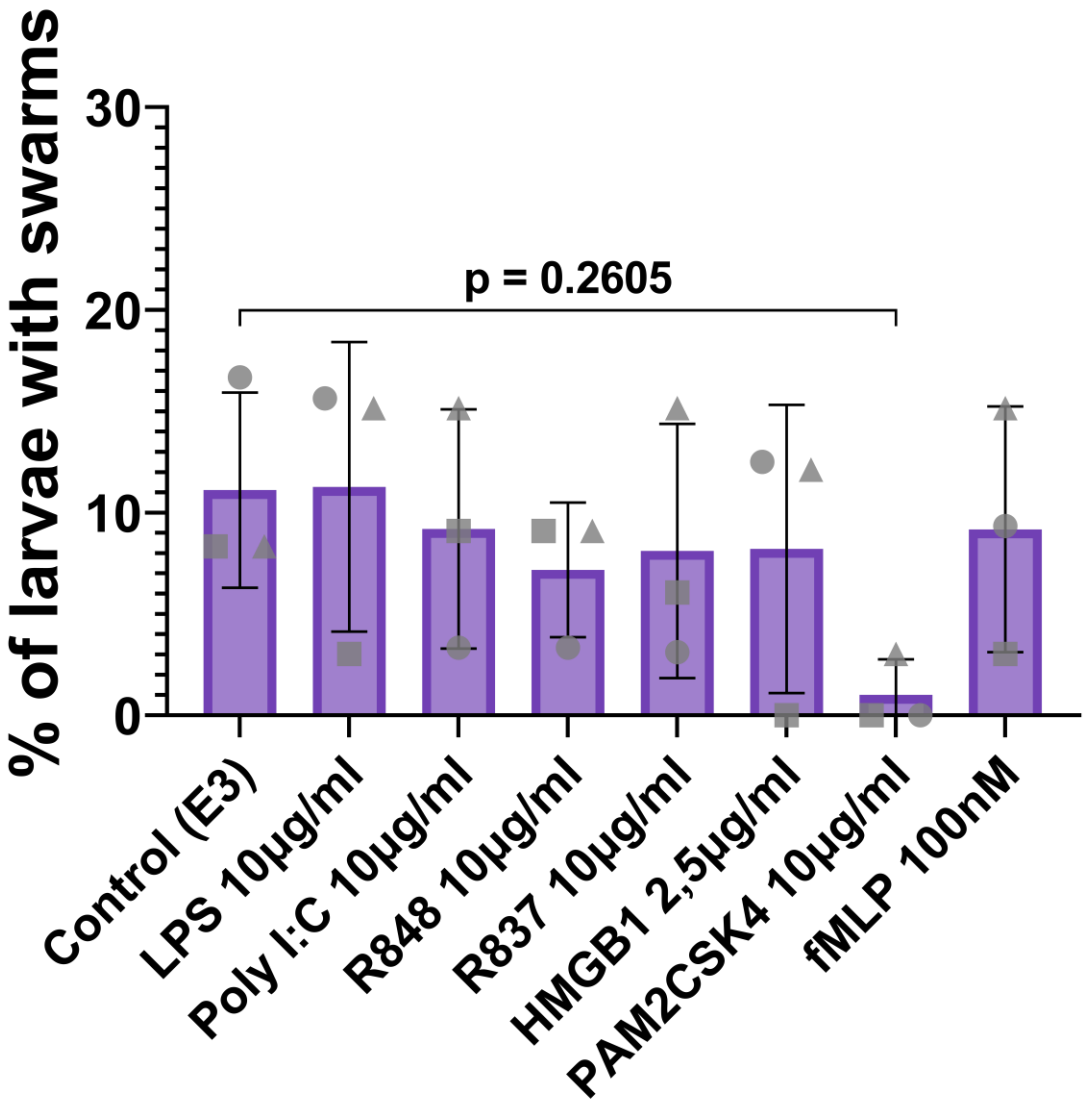

Figure 26: PAM2CSK4 suggests a reduction in neutrophil swarming at 4hpi

This figure shows a curated selection of compounds, chosen for their pro-inflammatory effects to upregulate the neutrophil swarming response. From left to right, the name of the compound, abbreviation and respective receptor; Lipopolysaccharide (LPS) TLR4; Polyinosinic:polycytidylic acid (Poly I:C) TLR3; resiquimod (R848) TLR7/TLR8; imiquimod (R837) TLR7; high mobility group box 1 protein (HMGB1) TLR2/4; Pam2CysSerLys4 (PAM2CSK4) TLR2/6; *N*-formylmethionyl-leucyl-phenylalanine (fMLP) formyl peptide receptor 1 (FPR1). Out of all compounds, PAM2CSK4 suggests a decrease in neutrophil swarms at 4hpi. N=3 control; n=24,12,12 treatments; n=32,33,33. Data was analysed using a Friedman-test with Dunn's correction for multiple hypothesis testing. P values of all other compounds except PAM2CSK4 were P>0.9999. Data is shown as mean ± SD.

3.3.3 TLR agonist treatment does not affect the neutrophil swarming response

As PAM2CSK4 might have an inhibitory effect on the formation of neutrophil swarms (**Figure 26**), I aimed to further elucidate the mechanism through which this might occur. Therefore, I expanded the selection of TLR agonists to include compounds binding to TLR1/2 and TLR2/6, as PAM2CSK4 binds to TLR2 and dimerises with TLR6 at the cell membrane. I hypothesised this would help discern whether this effect was dependent on TLR2/6 or TLR1/2.

The expanded selection of TLR agonists included *Staphylococcus aureus* cell wall preparate which contains cell wall components of Staphylococcus such as peptidoglycan, which is able to function as a PAMP (CWP), which binds to TLR2/6, PAM3CSK4, which is similar to PAM2CSK4 but binds to TLR1/2, and CU-T12-9, a small molecule identified in previous literature to bind to TLR1/2 (Guan et al., 2010, Cheng et al., 2015, Fournier, 2012, Parra-Izquierdo et al., 2021, Chen et al., 2019, Sutton et al., 2021). All TLR agonist treatments aimed to upregulate the inflammatory response by increasing the downstream Nfκb expression levels which can lead to increased release of cytokines REF. This was then hypothesised to lead to increased recruitment of neutrophils and a higher probability of swarms to occur.

Tail fin injury was performed on 3dpf zebrafish larvae and neutrophil swarms were assessed at 4hpi. For each compound, a dilution series was made to test for potential toxicity and to find an EC50 at which an effect would occur. However, none of the selected TLR1/2 and TLR2/6 agonists showed a significant response in either the number of neutrophils recruited to the wound site or the percentage of larvae developing a neutrophil swarm at 4hpi (**Figure 27, 28**). This suggests that the finding in (**Figure 26**), which indicated a reduction in the

number of neutrophil swarms, was likely due to other parameters and not the agonist treatment as this finding could not be replicated.

In summary, these data illustrate that the reduction in neutrophil swarming initially caused by PAM2CSK4 (**Figure 26**) was unlikely related to the agonist treatment, as experiments using an expanded selection of TLR1/2 and TLR2/6 agonists were unable to reproduce the result. Ultimately, this shows that immersion treatment of zebrafish larvae with TLR agonists is insufficient to elicit a repeatable effect on the formation of neutrophil swarms.

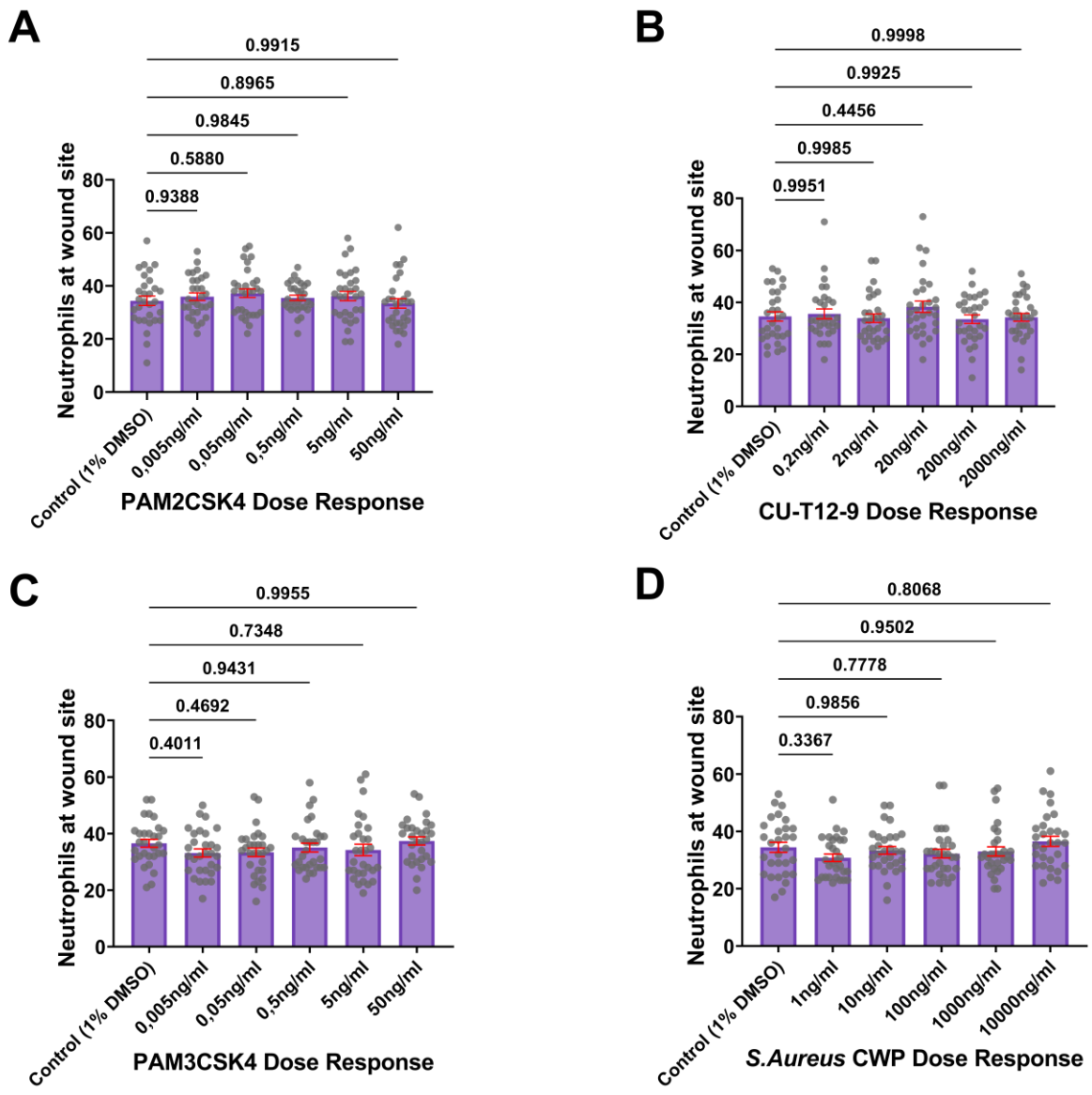

Figure 27: TLR 1/2 and TLR 2/6 agonists did not modulate neutrophil recruitment via immersion

Tail fin injury was performed on 3dpf zebrafish larvae and neutrophil recruitment was assessed at 4hpi. A dilution series was made and administered via immersion including 1% DMSO to help with penetration of the compound into the larva. Data is plotted as mean ± SEM. All data was analysed using an Ordinary One-Way ANOVA with Dunnett's correction for multiple hypothesis testing. P values are shown in bold.

A. Neutrophil counts after treatment with PAM2CSK4 did not result in a measurable difference in neutrophil recruitment across any of the administered dosages. N=3 n=10,10,10

B. Neutrophil counts after treatment with CU-T12-9 did not result in a measurable difference in neutrophil recruitment across any of the administered dosages. N=3 n=10,10,10

C. Neutrophil counts after treatment with PAM3CSK4 did not result in a measurable difference in neutrophil recruitment across any of the administered dosages. N=3 n=10,10,10

D. Neutrophil counts after treatment with *Staphylococcus Aureus* cell wall preparate (CWP) did not result in a measurable difference in neutrophil recruitment across any of the administered dosages. N=3 n=10,10,10

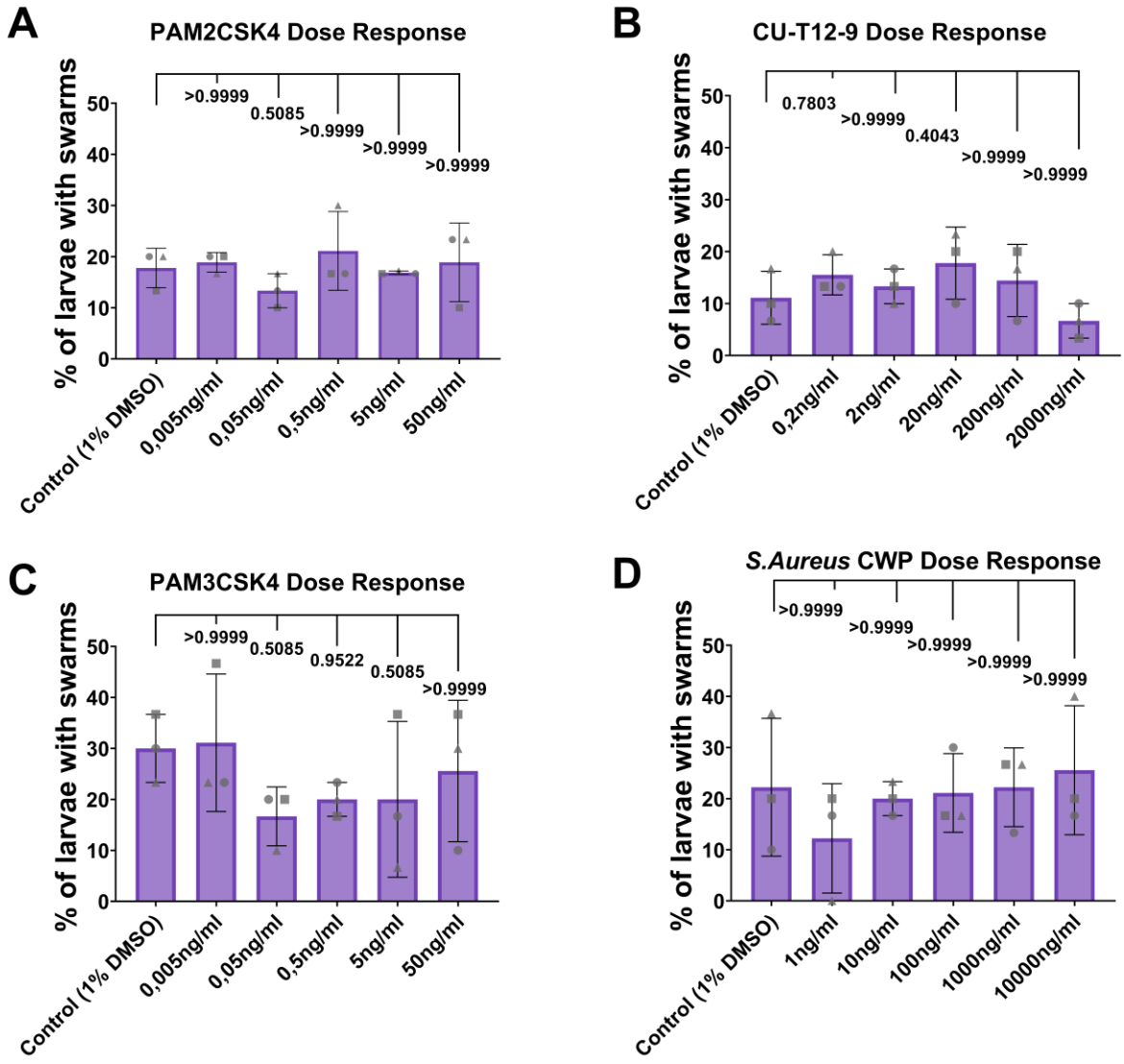

Figure 28: TLR 1/2 and TLR 2/6 agonists did not modulate neutrophil swarming via immersion

Tail fin injury was performed on 3dpf zebrafish larvae and neutrophil swarming was assessed at 4hpi. A dilution series was made and administered via immersion including 1% DMSO to help with penetration of the compound into the larva. Data is plotted as mean ± SEM. All data was analysed using a Friedman-test with Dunn's correction for multiple hypothesis testing. P values are shown in bold.

A. Neutrophil counts after treatment with PAM2CSK4 did not result in a measurable difference in neutrophil swarming across any of the administered dosages. N=3 n=30,30,30

B. Neutrophil counts after treatment with CU-T12-9 did not result in a measurable difference in neutrophil swarming across any of the administered dosages. N=3 n=30,30,30

C. Neutrophil counts after treatment with PAM3CSK4 did not result in a measurable difference in neutrophil swarming across any of the administered dosages. N=3 n=30,30,30

D. Neutrophil counts after treatment with *Staphylococcus Aureus* cell wall preparate (CWP) did not result in a measurable difference in neutrophil swarming across any of the administered dosages. N=3 n=30,30,30

3.3.4 Treatment with prolyl-hydroxylase inhibitors suggests a role for HIF-1α in neutrophil swarm formation

To test whether HIF-1α might be implicated in the neutrophil swarming response, HIF-1α was stabilised with the prolyl-hydroxylase inhibitors Dimethyloxalylglycine (DMOG) and Roxadustat (FG-4592). Zebrafish larvae were injured via tail fin injury at 3dpf and immersed in E3 media with DMOG or FG-4592. After 6 hours, larvae were assessed for swarm formation using a fluorescent stereomicroscope. Additional experiments to determine neutrophil recruitment and resolution were performed separately, counting neutrophils at the tail fin at 6hpi, 24hpi, and 48hpi, replacing the treatment solution once at 24hpi.

For neutrophil recruitment and resolution, a small but significant difference was found at 6hpi (**Figure 29**). Larvae treated with DMOG showed a significantly lower number of neutrophils at the wound site compared to the control. In these experiments, DMOG did not affect neutrophil numbers at 24hpi and 48hpi. Treatment with the other PHD inhibitor FG-4592, did not have any significant effect on neutrophil recruitment or resolution to a tail fin wound (**Figure 29**).

Treatment with DMOG and FG-4952 resulted in a significant reduction in the number of neutrophil swarms, suggesting that stabilisation of HIF-1α during normoxia through PHD inhibition can decrease the swarming response (**Figure 30**).

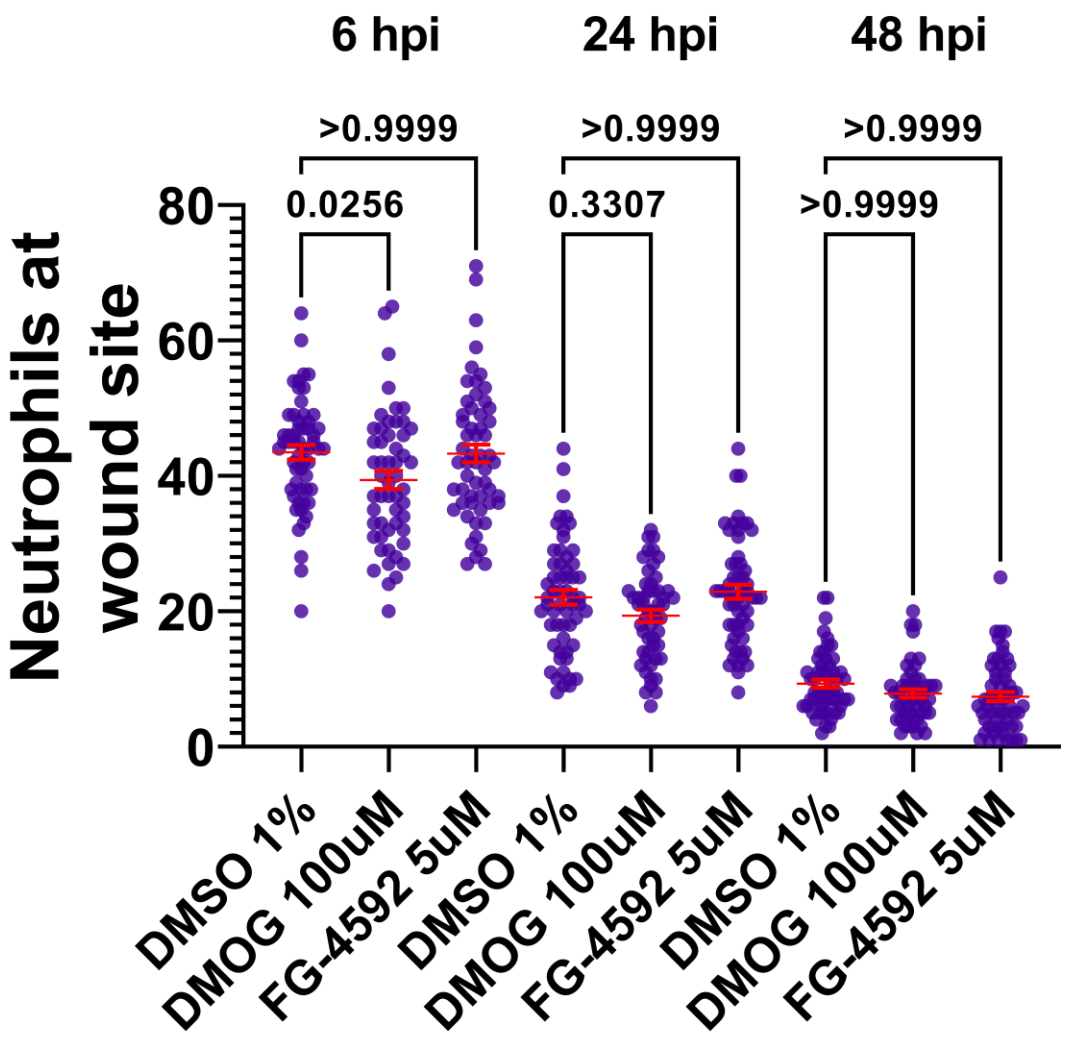

Figure 29: PHD inhibitors had no effect on neutrophil retention

This figure shows neutrophil counts of 3dpf zebrafish larvae post tail fin injury. Treatment with the prolyl-hydroxylase inhibitors DMOG and FG-42592 were performed to stabilise HIF-1α in normoxic conditions, 1% DMSO was used as control. Results show a significant reduction in the number of neutrophils present at the wound site at 6hpi post DMOG treatment. However, this decrease is recovered at later timepoints. FG-4592 treatment suggests no effect on neutrophil recruitment at 6hpi. Neither DMOG or FG-4592 treatment affected neutrophil numbers at the 24hpi and 48hpi time points. Data was analysed per timepoint using an Ordinary One-Way ANOVA with Bonferroni correction for multiple hypothesis testing. N=2, DMSO 1%; 6,24,48hpi n=58,58,57 DMOG; 6,24,48hpi n=53,53,49 FG-4592; 6,24,48hpi n=56,57,57 Data is plotted as mean ± SEM

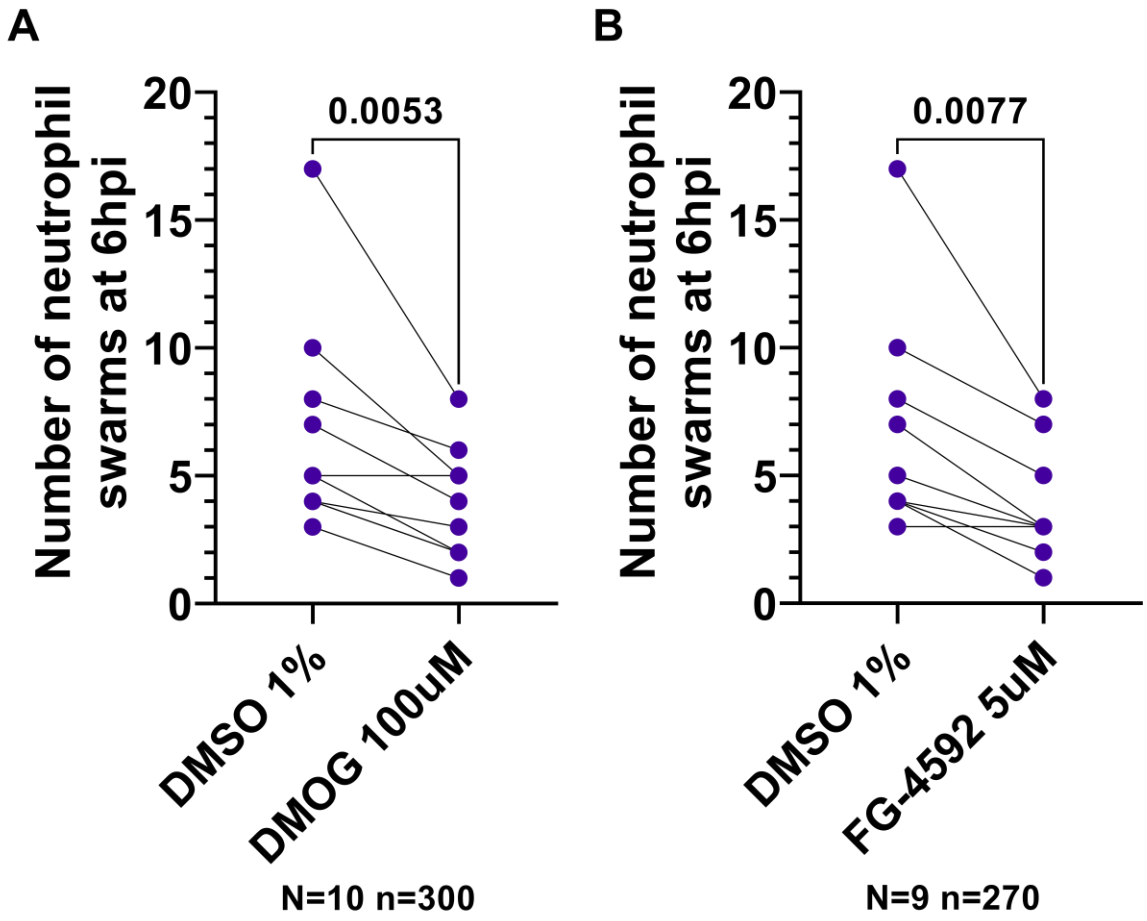

Figure 30: PHD inhibitors decreased the number of swarms at 6hpi

This figure shows the number of neutrophil swarms in 3dpf zebrafish larvae post tail fin injury. Treatment with the prolyl-hydroxylase inhibitors DMOG(**A**) and FG-42592(**B**) were performed to stabilise HIF-1α in normoxic conditions, 1% DMSO was used as control. Results show a significant reduction in the number of neutrophils swarms at the wound site at 6hpi post PHD inhibitor treatment. Data was analysed per timepoint using a Paired T-test. N=10 and 9 for DMOG and FG-4592 treatment respectively, n=30 per experiment.

3.3.5 DPI treatment shows partial increase in neutrophil swarming after HIF-1α stabilisation

Previous literature has shown that NOX is involved in the orchestration of the relay signalling present in neutrophil swarming, which is tied to production of ROS (Strickland et al., 2024). To determine whether the reduction in neutrophil swarms from HIF-1α stabilisation was related to ROS, I used Diphenyleneiodonium chloride (DPI) to inhibit NOX and reduce intracellular ROS. After DPI treatment, I found a statistically significant increase in the number of swarms in larvae treated with DMOG but not with FG-4592. Furthermore, I observed a small, but statistically insignificant, reduction in the number of swarms in the control condition (**Figure 31**). This partially corroborates findings from literature, but I was unable to find an increase in swarming in the control condition after DPI treatment, which I would have expected based on said literature (Hopke et al., 2020, Strickland et al., 2024).

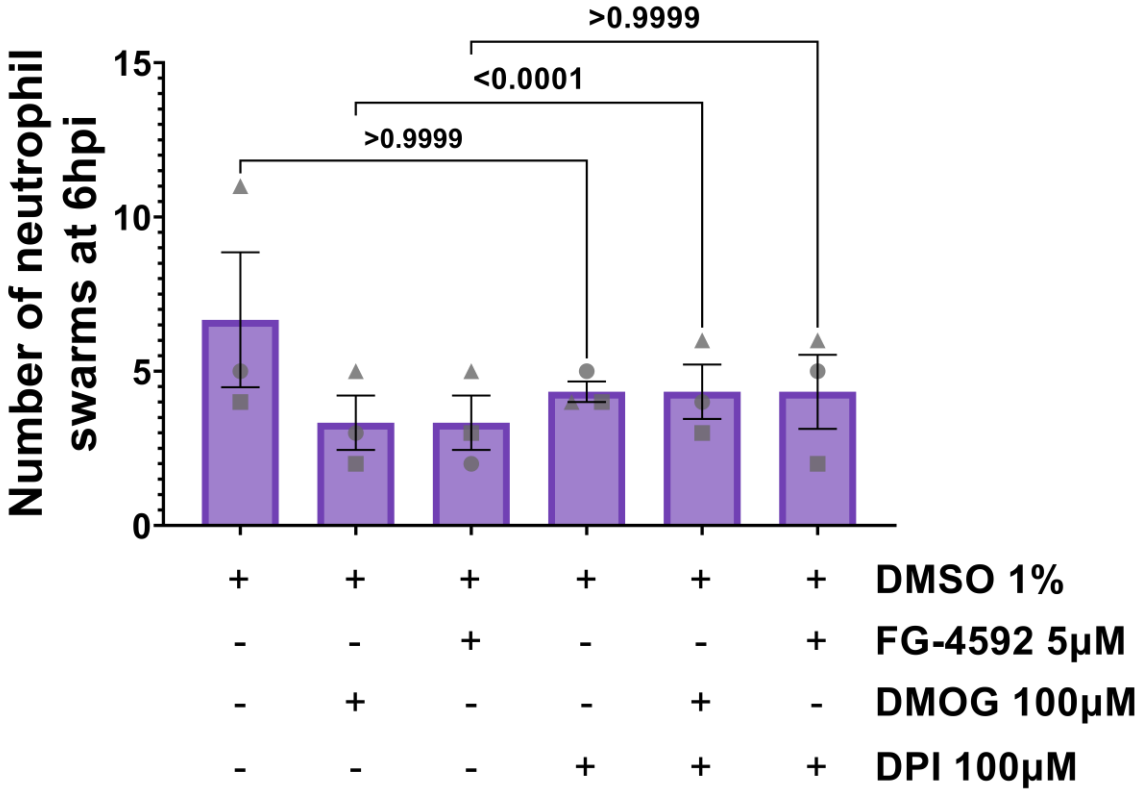

Figure 31: DPI partially recovers reduction in neutrophil swarms post PHD inhibitor treatment

This figure shows the number of neutrophil swarms in 3dpf zebrafish larvae post tail fin injury. Treatment with the prolyl-hydroxylase inhibitors DMOG and FG-42592 were performed to stabilise HIF-1α in normoxic conditions, 1% DMSO was used as control. Results show a significant increase in the number of neutrophils swarms at the wound site post DPI treatment combined with DMOG. Data was analysed per timepoint using a RM one-way ANOVA using Bonferroni correction for multiple hypothesis testing. N=3 n=30,30,30 per condition.

3.3.6 Determining the relation between HIF-1α, ROS and neutrophil swarming in further detail

To determine the relationship between ROS and HIF-1α in more detail, I performed time-lapse imaging using CellROX™ Deep Red. This dye is non-fluorescent in its reduced state and exhibits bright fluorescence following oxidation by ROS. In an initial experiment using ventral fin injuries, data suggested a potential decrease in ROS levels post-PHD inhibitor treatment (**Figure 32**), indicating interaction between the HIF-1α pathway and ROS generated at injury sites. Interestingly, one of the larvae with the highest measured ROS also had a neutrophil swarm (**Figure 33, Supplemental Movie 9**). However, the CellROX signal was not as pronounced as expected (Bernut et al., 2020). I hypothesised that tail fin injuries could provide a better readout, as these injuries encompass a larger area and possibly yield better visualisation. However, the signal remained relatively weak and the previous finding could not be replicated (**Figure 34**). Furthermore, DPI, which should have functioned as a negative control by reducing the CellROX signal, showed no difference from the control (**Figure 34**). Due to potential inaccuracies, CellROX was excluded from further experiments.

I further investigated how PHD inhibitor treatment impacts neutrophil recruitment and motility. I found that PHD inhibitor treatment did not have a significant effect on the motility of neutrophils towards the site of injury, suggesting that the previously observed reduction in swarming is more likely part of a process that does not impact chemotactic migration (**Figure 35, Supplemental Movie 10**). However, I also found that treatment with DPI suggested impaired recruitment of neutrophils and possibly reduced motility, which

aligns with previously published research (**Figure 35, Supplemental Movie 10**) (Niethammer et al., 2009).

In conclusion, these results suggest that HIF-1α could be implicated as an effector of the neutrophil swarming response, possibly through the regulation of ROS. However, future experiments are needed to further elucidate this intricate and complex process.

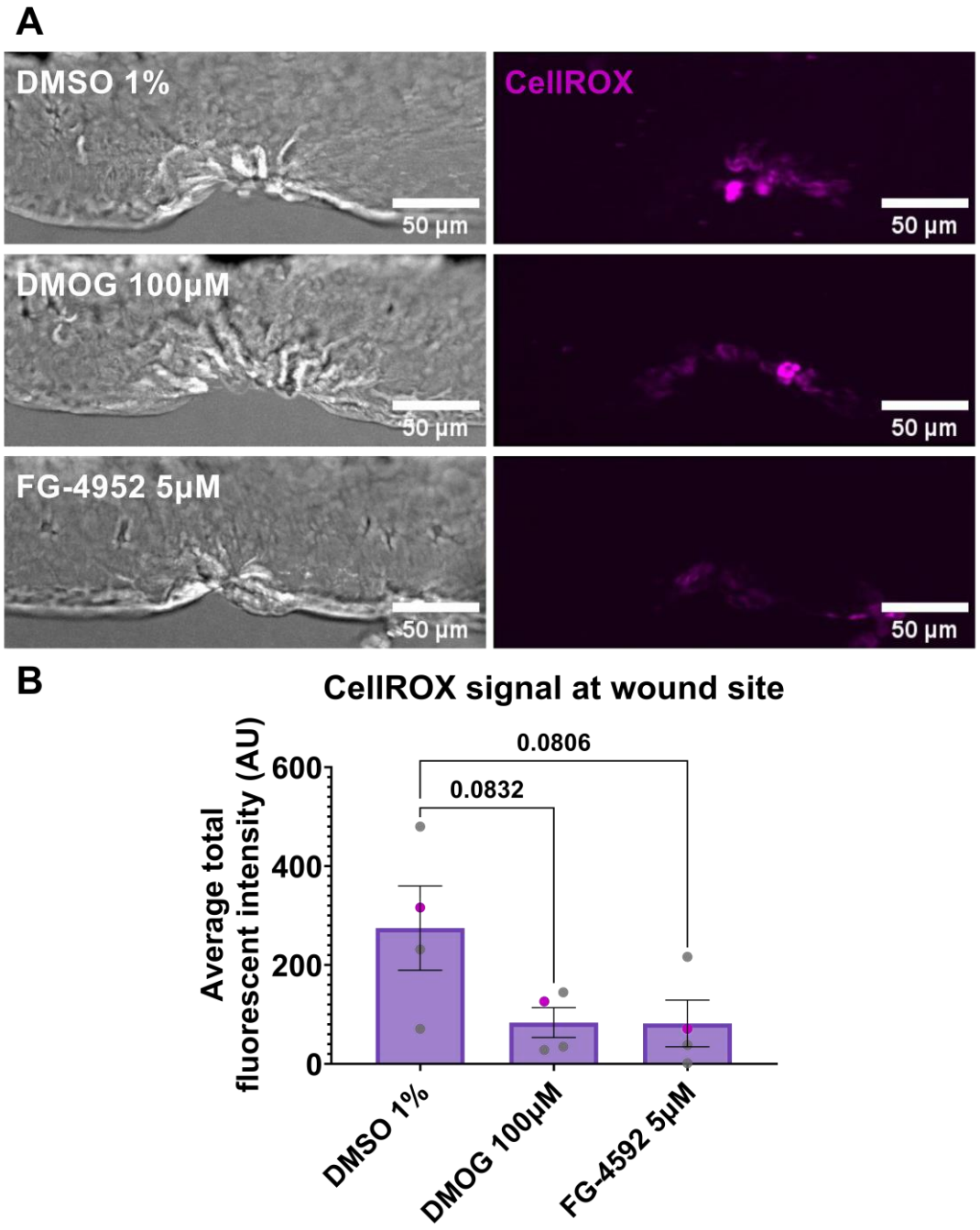

Figure 32: CellROX staining indicates a potential reduction in ROS at the injury site post HIF-1α stabilisation

Larvae were pre-treated with CellROX™ Deep Red for 30 minutes pre-injury, transferred to a clean petri-dish for injury and quickly mounted for time-lapse imaging. PHD inhibitors were added 2 hours pre-injury and larvae remained continuously exposed during the entire experiment.

A. Maximum intensity projections of the brightfield channel and sum projections of the CellROX signal. Images were gathered with a 2-minute interval over the course of a 2-hour timelapse after ventral fin wounding.

B. The CellROX signal was analysed using a macro in FIJI Image J. Background was measured and subtracted from the measured CellROX signal. CellROX signal was averaged per larvae and plotted as Average total fluorescent intensity (Arbitrary Units). Purple data points represent the images shown in **A**. Data suggest a potential decrease in CellROX signal post PHD inhibitor treatment. Data plotted as mean ± SEM and analysed with an Ordinary one-way ANOVA with Dunnett's correction for multiple hypothesis testing. N=1 n=4 per group.

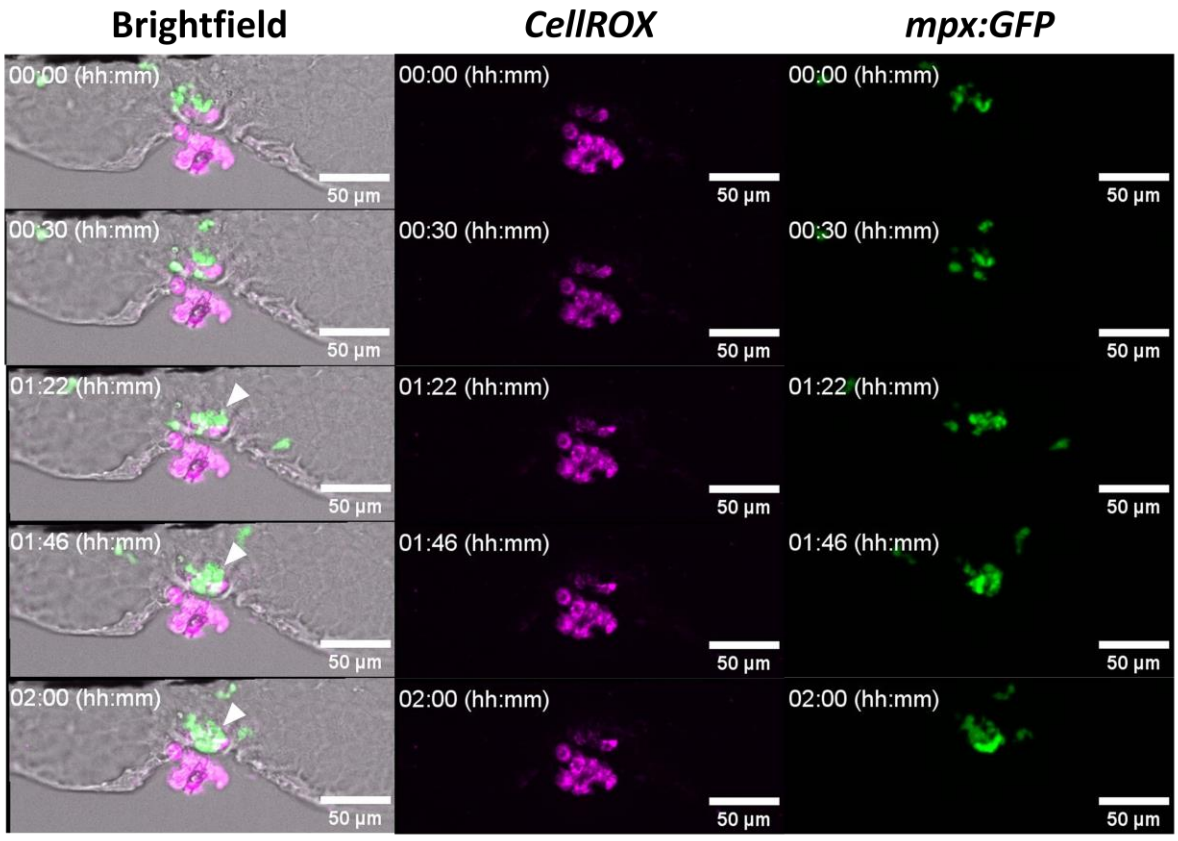

Figure 33: One example of swarming co-localising with CellROX signal

This figure shows a panel of the time-lapse made to quantify cell ROX signal post PHD inhibitor treatment (**Figure 32**). The panel shown above was 1% DMSO control with the highest CellROX signal as quantified in **Figure 32B**. A swarm was observed to localise with CellROX signal, furthermore this was the only swarm that was observed in this experiment.

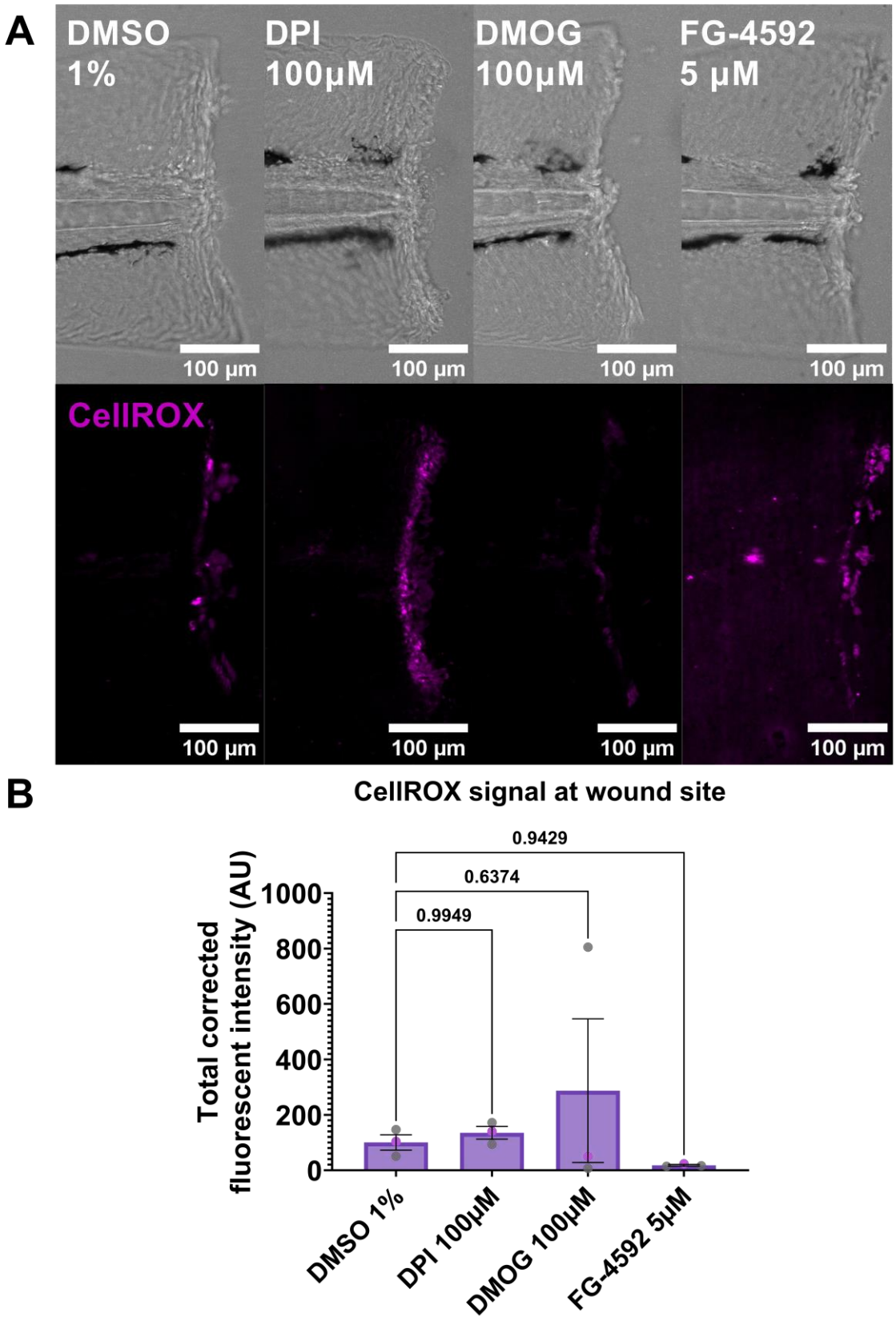

Figure 34: CellROX staining post tail fin injury was unable to recapitulate a reduction in ROS post PHD inhibitor treatment

Larvae were pre-treated with CellROX™ Deep Red for 30 minutes pre-injury, transferred to a clean petri-dish for injury and quickly mounted for time-lapse imaging. PHD inhibitors were added 2 hours pre-injury and larvae remained continuously exposed during the entire experiment.

A. Maximum intensity projections of the brightfield channel and average projections of the CellROX signal. Images were gathered with a 2-minute interval over the course of a 2-hour timelapse after tail fin wounding. DPI was used as a negative control, however, staining for ROS still occurred.

B. The CellROX signal was analysed using a macro in FIJI Image J. Background was measured and subtracted from the measured CellROX signal. CellROX signal was averaged per larvae and plotted as Average total fluorescent intensity (Arbitrary Units). Purple data points represent the images shown in **A**. Data suggests a potential decrease in CellROX signal post PHD inhibitor treatment. Data plotted as mean ± SEM and analysed with an Ordinary one-way ANOVA with Dunnett's correction for multiple hypothesis testing. N=1 n=3 per group.

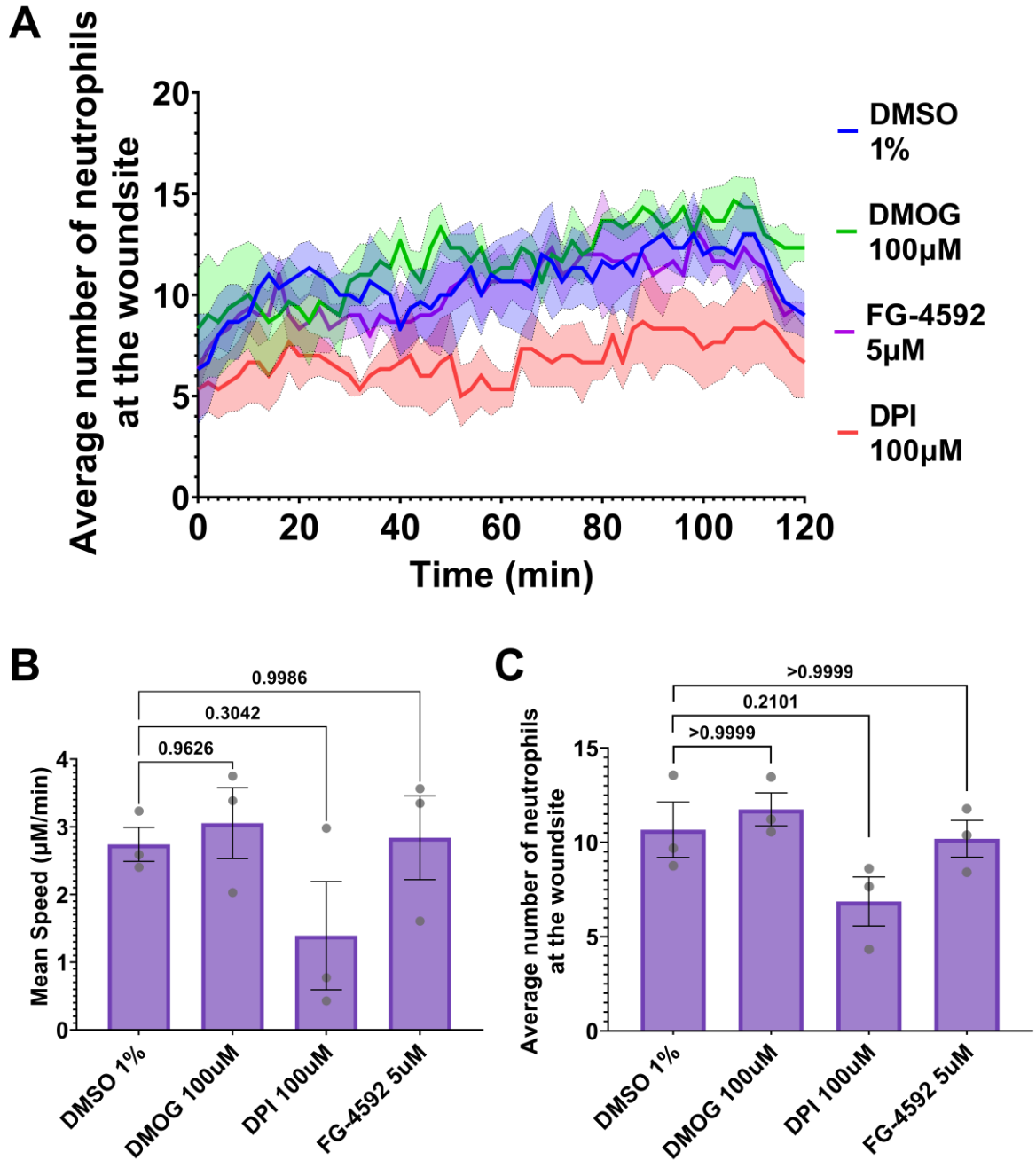

Figure 35: HIF-1α stabilisation via PHD inhibitors suggests no effect on neutrophil recruitment or motility

A. Neutrophil counts obtained via Cellpose segmentation over the course of a 2-hour timelapse suggests no difference in neutrophil recruitment post PHD inhibitor treatment, however data do suggest potentially lower recruitment following DPI administration. Full timelapses can be seen in **Supplemental Movie 10**

B. The mean speed of all neutrophils within single larvae was extracted and compared to determine any effects of PHD inhibitor and DPI treatment on neutrophil motility. Data suggest

no difference post PHD inhibitor treatment, but do suggest potentially impaired motility following DPI administration. Data is shown as mean ± SEM. Data was analysed using an Ordinary one-way ANOVA with Dunnett's correction for multiple hypothesis testing. N=1 n=3 per group.

C. The average number of neutrophils at the wound site was evaluated over the course of the full time-lapse as shown in **A**. Data indicates no difference in the average number of neutrophils following administration PHD inhibitors, but does suggest a potentially lower number of neutrophils after treatment with DPI. Data is shown as mean ± SEM. Data was analysed using an Ordinary one-way ANOVA with Dunnett's correction for multiple hypothesis testing. N=1 n=3 per group

3.3.7 Conclusion & Discussion

Previously published research found that TLR2 regulates neutrophil recruitment in zebrafish in a MyD88-dependent manner (Hu et al., 2021). Furthermore, TLR signalling has been shown to activate neutrophils (Prince et al., 2011). Due to the large variability in swarming responses as indicated in **Chapter 3.1** and **3.2**, I aimed to upregulate neutrophil swarming via immersion treatment of larvae with a range of TLR agonists. From the initial screen, PAM2CSK4 was identified as a promising target, but unexpectedly reduced the number of neutrophil swarms after treatment. However, further experiments could not replicate this finding, and it was ultimately disregarded as a pharmacological approach for manipulating swarms. This suggests that the experimental approach might have been inappropriate, as TLR signalling is widely implicated in the regulation of innate immune responses in zebrafish (van der Vaart et al., 2012). Possibly, immersion treatment with agonists had limited penetration into deeper tissues due to low permeability in fish. DMSO, added at a relatively high concentration of 1%, can enhance permeability, but might have been insufficient in this case (Jacob and Herschler, 1986).

Another approach could have been the localised injection of TLR agonists into the tail fin tissue of the fish (KAMUYANGO, 2017). However, this procedure is complicated due to the extremely thin tail fin tissue. Moreover, this would result in a localised chemoattractive point to which neutrophils could potentially perform continuous migration, accumulating without a swarming response. This could have been resolved by injection in multiple locations, giving the opportunity to see clear swarming towards one of the points, but it would have unnecessarily complicated the experimental approach.

Besides TLR agonists, other compounds could be considered. Previously published work has shown that granulocyte colony-stimulating factors (G-CSF and GM-CSF) enhance swarming in

an *ex vivo* model of neutrophil swarming (Hopke et al., 2020). Both G-CSF and GM-CSF have been approved by the FDA for treatment of neutropenia in patients and could offer a potential therapeutic approach for regulation of neutrophil swarming in patients, but further research needs to elucidate the exact effects on neutrophil swarming *in vivo* (Mehta et al., 2015).

Recent research indicated that inhibition of NOX causes dysregulation in the relay phase of the bi-phasic swarming response (Strickland et al., 2024). This, along with other previously published work, suggests a role for ROS in the swarming response, where an increase in ROS correlates with controlled swarming, and the absence of ROS correlates with unregulated swarming (Hopke et al., 2020, Strickland et al., 2024). Other research suggests that ROS, specifically mitochondrial ROS in neutrophils is needed for generation of LTB4, which drives subsequent neutrophil swarming (Golenkina et al., 2024, Lämmermann et al., 2013). However, the same research also suggests an increase of LTB4 after inhibition of NOX dependent ROS production, which corroborates the finding in *ex vivo* models (Strickland et al., 2024, Golenkina et al., 2024). This is because an increase in LTB4 could explain how relay signalling has a significantly larger range after NOX inhibition (Strickland et al., 2024).

HIF-1α is an important regulator of gene expression during hypoxia, which is often present at sites of prolonged injury or for instance in granulomas formed after mycobacterial infection (Darby and Hewitson, 2016, Oehlers et al., 2015). During normoxia, HIF-1α is continuously targeted for proteasomal degradation, however during hypoxia HIF-1α levels stabilise leading to its activation as a transcription factor, driving downstream expression of target genes (Taylor and Scholz, 2022, Hon et al., 2002). Besides hypoxia, HIF-1α accumulation can also

occur through the production of ROS (Movafagh et al., 2015). Within neutrophils specifically, accumulation has been shown to occur after an increase in mitochondrial ROS (Willson et al., 2022). The interactions of ROS with swarming as well as HIF-1α led me to investigate HIF-1α as a potential regulator of the swarming response, downstream of ROS. Furthermore, activation of HIF-1α has been shown to retain neutrophils at wound sites, which could influence neutrophil swarming (Elks et al., 2011).

To determine whether HIF-1α affects the swarming response, I used PHD inhibitors to ubiquitously stabilise HIF-1α during normoxia (Elks et al., 2011, Schild et al., 2020). Surprisingly, I was unable to replicate previously established results indicating increased neutrophil retention after PHD inhibitor treatment (Elks et al., 2011). Exactly why this happened remains unclear. It may suggest a potential error in the experimental setup whereby pipetting during the media refresh step interfered with the inflammatory response by damaging the larvae, which should be considered for future repeats. In another experimental set up where no media refreshes were performed, ubiquitous HIF-1α stabilisation via PHD inhibitor treatment significantly reduced neutrophil swarms at 6hpi, indicating that HIF-1α is able to modulate the swarming response in a currently undescribed manner. In further experiments using CellROX, I attempted to visualise how ROS and ubiquitous HIF-1α activation may interact to drive this reduction in swarming (Bernut et al., 2020). Initial results were encouraging, but further experiments suggested that the visualisation of ROS might be inaccurate, meaning no conclusive results were found. If I were to repeat this experiment, I would use another transgenic reporter line to enable the use of CellROX green instead of CellROX deep red, which should provide a more pronounced signal.

Using *in vivo* time-lapse data to elucidate the effect of PHD inhibitor treatment on individual neutrophil motility, I found no effect on motility or recruitment of neutrophils towards the wound site. However, treatment with DPI suggested impaired motility and recruitment towards the wound site, which agrees with published literature (Niethammer et al., 2009). To gain a conclusive view of these results, further repeats will be necessary.

One of the limitations in the pharmacological treatments I have performed is the lack of clear positive and negative controls for neutrophil swarming. Ideally, positive and negative controls would be present to correctly assess how the swarming dynamics change post-treatment of my chosen TLR agonists or PHD inhibitors, however at the time of writing this thesis no known positive or negative control for neutrophil swarming has been discovered. In essence, these experiments aimed to gain more insights into precisely this issue and potentially identify novel controls for neutrophil swarming, though none were identified.

Another potential limitation was the lack of pre-treatment with the PHD inhibitors DMOG and FG-4592. If I were to repeat these experiments, I would include a 2-hour pre-incubation step to ensure that the compound has sufficient time to exert its biological effect before performing the tailfin injuries. This may have affected the experimental outcomes and should be considered in future research.

Future experiments could incorporate G-CSF and DPI, as these have been shown to significantly impact neutrophil swarming in *ex vivo* models (Hopke et al., 2020, Strickland et al., 2024, Hopke et al., 2022). This aligns with data presented in this thesis where the use of DPI resulted in an apparent albeit non-significant reduction in neutrophil movement and

neutrophil accumulation at the tailfin injury. It would be interesting to determine whether the effects of G-CSF can be recapitulated in an *in vivo* model.

In summary, TLR agonist treatment via immersion did not affect the formation of neutrophil swarms following tail fin injury. However, I generated preliminary results suggesting a potential role of HIF-1α in the swarming response via PHD inhibition. The intricate and complex signalling orchestration between ROS, HIF-1α, and swarming needs further exploration in future experiments to solidify current data. Other methods, including the use of dominant negative HIF-1α, could help further elucidate the precise regulation of HIF-1α that contributes to the reduction in neutrophil swarms (Elks et al., 2011).

3.4 Interactions Between Macrophages and Neutrophils During Neutrophil Swarming

3.4.1 Introduction

Neutrophils are not the sole innate immune cells regulating inflammatory responses. Various cell types collaborate, performing specialised tasks to control inflammation progression without adverse effects (Théry and Amigorena, 2001, Raskov et al., 2021, Speirs et al., 2024). In zebrafish, initial development of the adaptive immune system starts from 5dpf onwards with arising pre-cursor T-cells (Dee et al., 2016). However, the adaptive immune system only fully matures around 3 weeks post-fertilisation (Miao et al., 2021). Most research using the zebrafish model occurs before day 5 post-fertilisation. Therefore, responses measured and observed after injuries or infections are mainly governed by the innate immune system, which includes neutrophils and macrophages (Li et al., 2012, Meijer, 2016, Nguyen-Chi et al., 2017, Bernut et al., 2020).

Using the zebrafish model, macrophages have been shown to be involved in tissue regeneration and play a major role in the onset of mycobacterial dissemination within the zebrafish model of tuberculosis (Meijer, 2016, Nguyen-Chi et al., 2017).

Previous research showed how lyses and release of NETs occurred after a pioneer neutrophils arrived at sites of injury (Isles et al., 2021). This process played a role in subsequent swarm formation (Isles et al., 2021). However, what exactly drives the pioneer neutrophil to arrive and start this process has remained undescribed.

Previous research has suggested that interactions between macrophages and neutrophils partially shape the resolution of inflammation (Tauzin et al., 2014, Loynes et al., 2018, Loynes et al., 2010). These studies describe how macrophage recruitment correlates with

inflammation resolution from the wound site via reverse migration of neutrophils and how the clearance of apoptotic cells is necessary for resolving neutrophilic inflammation (Loynes et al., 2010, Tauzin et al., 2014). Based on these findings, I hypothesised that macrophages may somehow play a role in directing the pioneer neutrophil and subsequent swarming.

Within the INFLANET network, I have access to the Laboratory of Host Pathogen Interactions (LPHI) at Université de Montpellier. Colleagues Professor Georges Lutfalla and Dr Mai Nguyen-Chi, experts in macrophage biology, agreed to a collaborative project where I aimed to obtain preliminary results on how neutrophil-macrophage interactions may shape the neutrophil swarming response.

I designed experiments where I crossed the *Tg(mfap4:mCherry)*^{ump6Tg} reporter line visualising macrophages, with the *Tg(mpx:GFP)*^{i114} line visualising neutrophils (Renshaw et al., 2006, Phan et al., 2018). I investigated both ventral fin and tail fin injuries as described in **Chapter 3.1-3.2** to determine which model would provide the best visualisation of neutrophil-macrophage interaction.

3.4.2 Macrophages coordinate themselves around neutrophils after ventral fin injury

To observe the extent to which neutrophils and macrophages react during an inflammatory response in zebrafish, I compared two methods of injury to asses which would provide the best visualisation of any neutrophil-macrophage interactions. First, I performed an experiment involving a ventral fin injury, as described in **Chapter 3.2.6**. The ventral fin injury successfully induced a significant inflammatory response, evidenced by the recruitment of numerous neutrophils before the time-lapse even started, at approximately 1hpi. Interestingly, as time progressed, macrophages localised around neutrophils which remained close to the wound edge, after which neutrophils performed reverse migration from the wound (**Figure 36A-B, Supplemental Movie 11**). This finding aligns with previous observations in mice, where myeloid cells are hypothesised to stabilise swarms *in vivo* and research suggesting macrophage interactions drive inflammation resolution (Tauzin et al., 2014, Kienle and Lammermann, 2016).

In conclusion, these data recapitulate that myeloid cell recruitment, particularly macrophages in the zebrafish model, may occur around neutrophil swarms as previously suggested by studies in mice (Kienle and Lammermann, 2016).

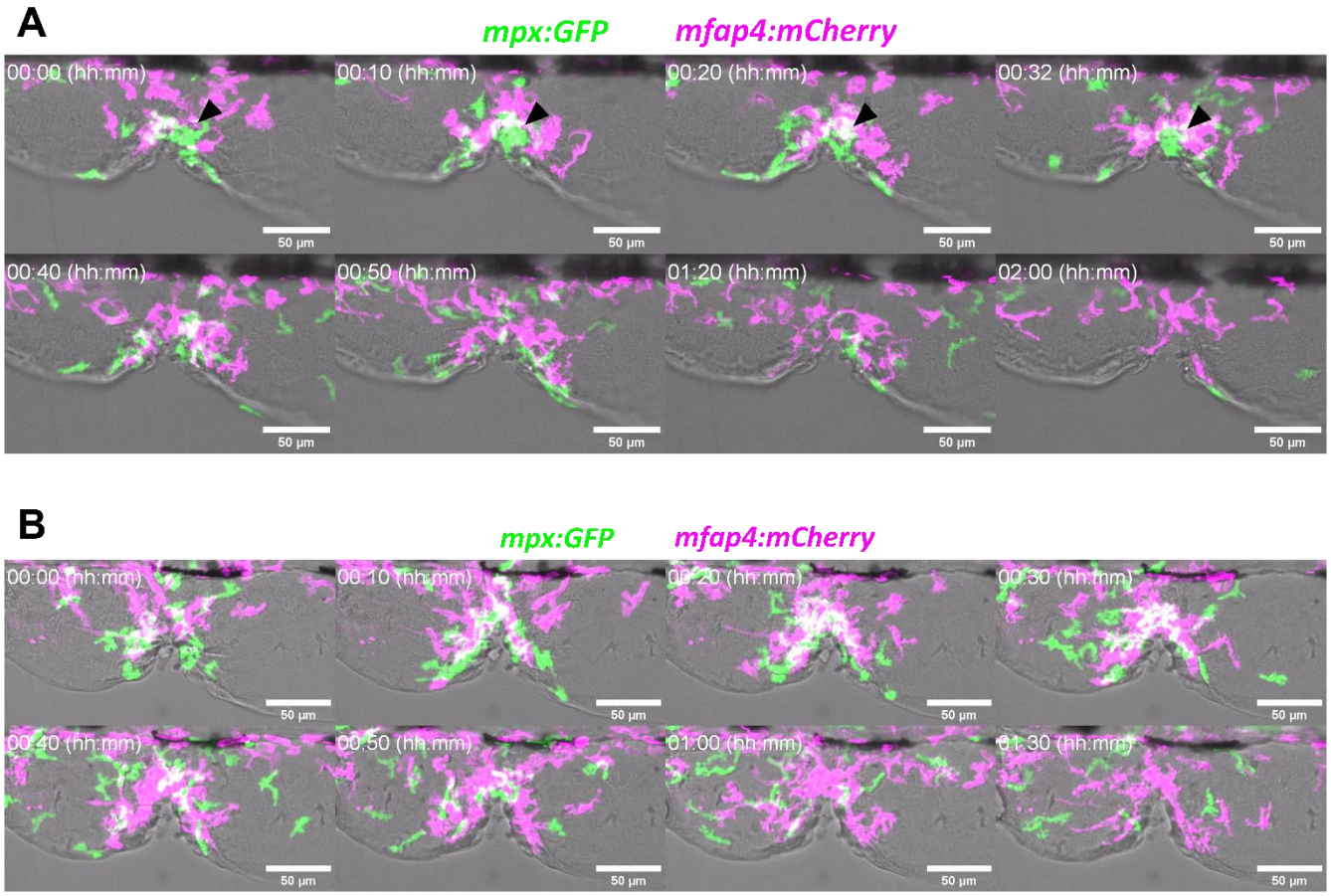

Figure 36: Macrophages organise around a neutrophil swarm preceding neutrophil swarm resolution

Notch cut injuries were made in the ventral fin of 3dpf zebrafish. An outcross between the *Tg(mpx:GFP)*^{i114} and *Tg(mfap4:mCherry)*^{ump6Tg} lines was made to visualise both neutrophils and macrophages.

A. Shows how macrophages configure themselves around a neutrophil swarm which is occurring at the wound edge (black arrowhead). Shortly macrophages stabilise their position around the neutrophils. At 50 min (~2hpi) neutrophil begin to leave the wound site. After 2 hours only macrophages remain at the wound site, however some neutrophils would still approach the wound for short moments (**Supplemental Movie 11**).

B. Shows another example of macrophages arriving and stabilising their own positions after which neutrophils begin leaving the wound site at 50min. After 1 hour and 30 minutes most neutrophils have left the wound site. The full timelapse can be seen in **Supplemental Movie 11**.

3.4.3 Neutrophil-macrophage interactions may spatially direct neutrophil swarms

Besides the experiments involving ventral fin injury, as shown in **Figure 36**, I also performed tail fin injuries to visualise neutrophil-macrophage interactions. Previous findings suggested these injury types to trigger different inflammatory dynamics (**Figure 22**). Interestingly, an unexpected dynamic was displayed. Fluorescent debris, likely from a cell death event as later observed in other examples (**Supplemental Movie 12**), was the main point to which neutrophils responded and swarmed (**Figure 37, Supplemental Movie 12**). Detailed analysis of tracking data obtained from Cellpose and Trackmate, combined with a python script, revealed that neutrophil swarming, indicated by cluster formation throughout the time-lapse, visually colocalised with sites where neutrophil movement towards macrophages was displayed, suggesting interactions (**Figure 38, Supplemental Figure 1-3**). Struck by the finding that this swarm was apparently directed towards a site of potential macrophage cell death (**Figure 37**), I further investigated whether neutrophil swarms preferentially form after macrophage cell death. In total 50% of swarms were observed in close proximity of cellular debris potentially generated from a cell death event (**Figure 39**). Using a python script, I analysed neutrophil movement and interactions towards macrophage 'debris' specifically. While visual overlap was found for macrophage debris and neutrophil clusters (**Figure 40, Supplemental Figure 4-6**), quantification showed no significant difference between interactions with living macrophages, macrophage debris, nor any difference in subsequent neutrophil swarming (**Figure 41**). This could implicate that macrophage cell death may not be a driver of neutrophil swarms. Further investigation suggested increased neutrophil interactions with macrophage debris after macrophage cell death (**Figure 42**), indicating that

neutrophils may be drawn to locations of macrophage cell death. From all swarms that formed in these experiments, only a single swarm formed far from any detectable macrophages (**Figure 43, Supplemental Movie 12**).

In summary, examples of neutrophil swarming, clustering, and interactions with macrophages after tail fin injury indicate that macrophages potentially play a role in shaping neutrophil responses, including swarming. However, it remains unclear whether this response is mainly driven by macrophage cell death, interactions and signalling provided by active macrophages at the wound site or from cell death events of other non-immune cells at the wound.

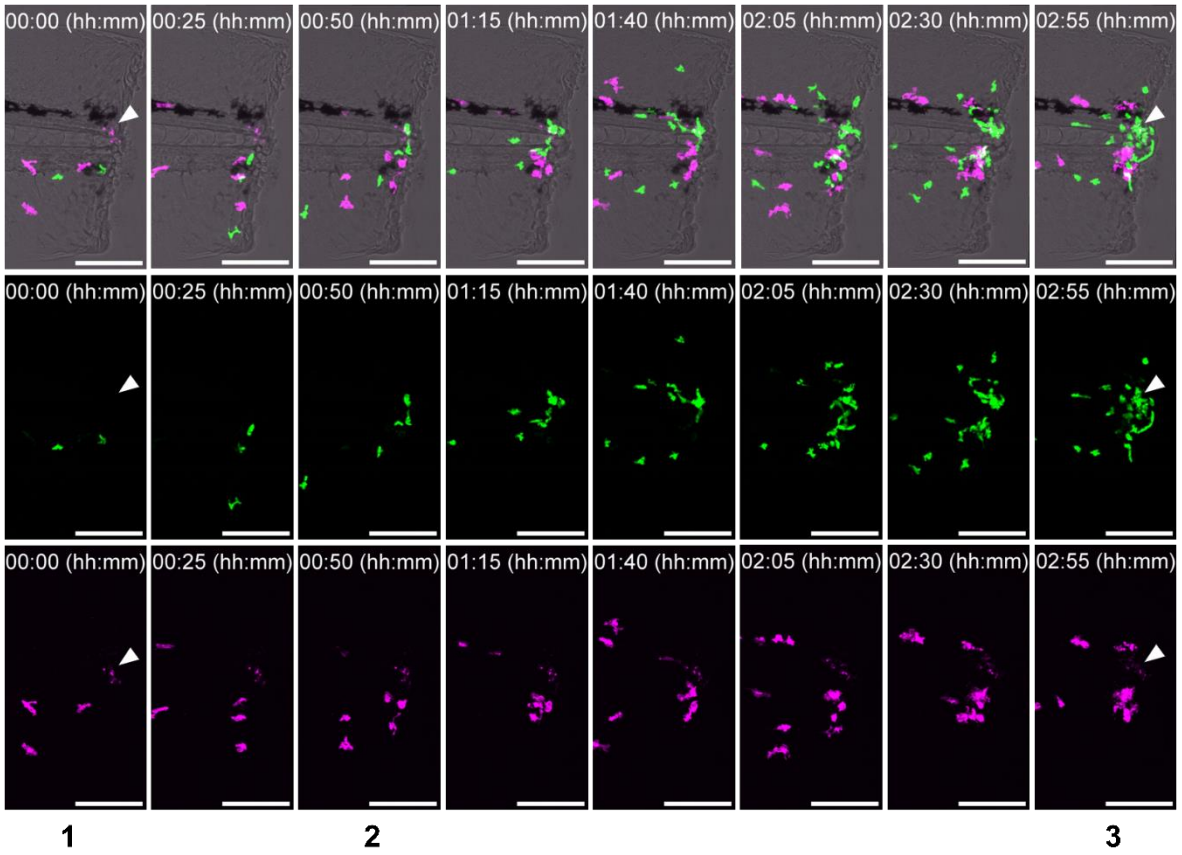

Figure 37: A neutrophil swarm forms in proximity to macrophage debris

Tail fin injury was performed on 3dpf old zebrafish larvae. An outcross between the *Tg(mpx:GFP)*^{i114} and *Tg(mfap4:mCherry)*^{ump6Tg} lines was made to visualise both neutrophils

and macrophages. A more detailed overview is provided in **Supplemental Movie 12.** Scalebar = 100µm

1. Shows the location of cellular debris from a macrophage at the white arrowhead.

2. Shows the first neutrophil arriving at the cellular debris.

3. Shows the full neutrophil swarm that persists at this location.

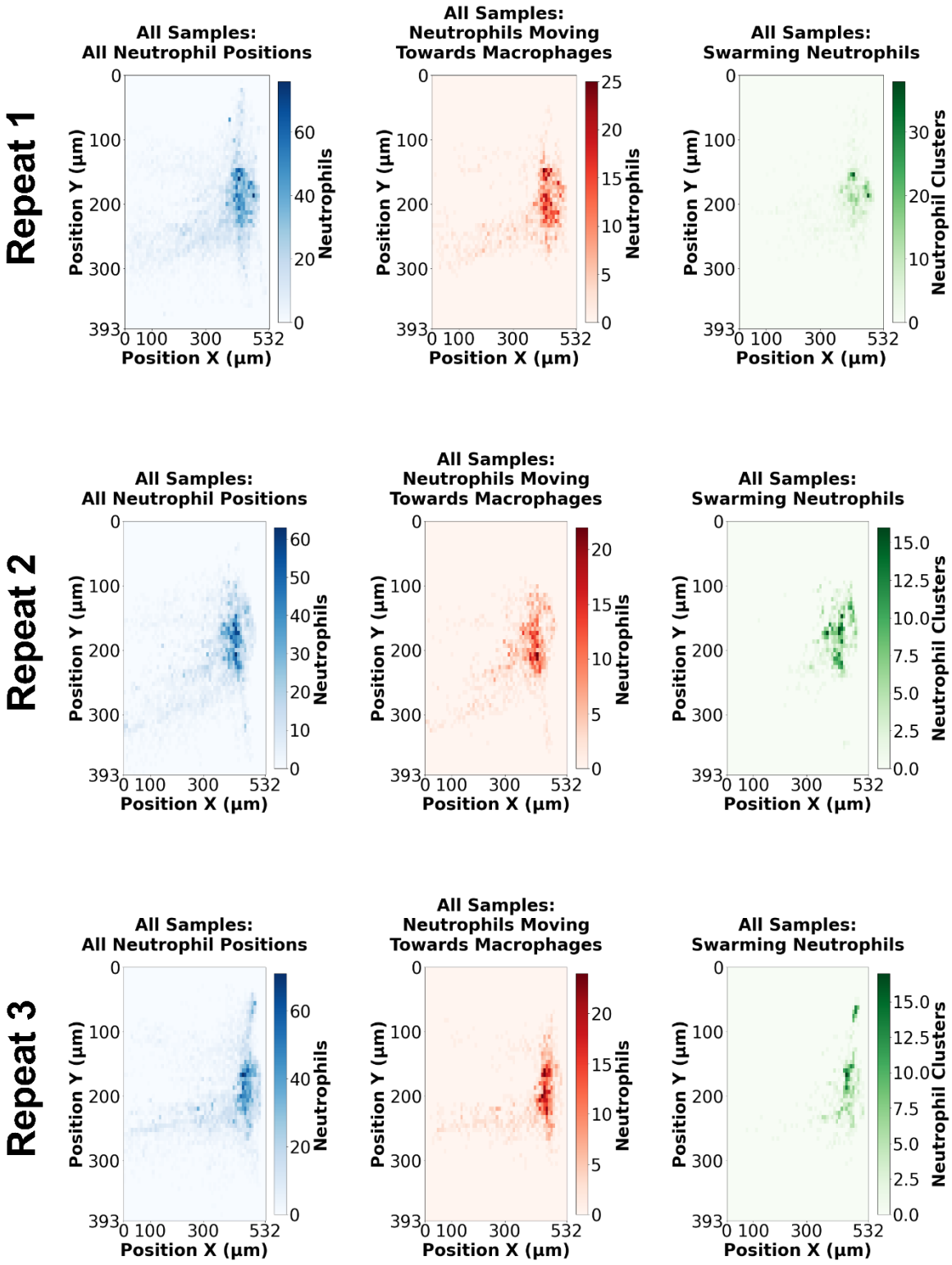

Figure 38: Heatmaps suggest overlap between neutrophil-macrophage interactions and locations of swarms

A python script was used to analyse tracking data obtained from Cellpose and Trackmate as described in Chapter 3.2. Blue heatmaps show the location of all neutrophils. Red heatmaps show neutrophils moving towards macrophages which were obtained by filtering for movement towards macrophages present within a 20µm radius of a neutrophil centroid. Green heatmaps show the locations of neutrophil clusters filtered for areas bigger than 3x the average area of a single neutrophil, as an indication of neutrophil swarms. Repeat 1-3, indicate individual experimental repeats, samples indicate larvae. Only in the last experimental repeat one can see that a swarm occurred away from neutrophil-macrophage interactions towards the top of the tail fin. Heatmaps were created from all larvae within one experimental repeat, n=5, 4, 5 for each respective repeat. Heatmaps of individual larvae can be found in **Supplemental Figure 1-3**.

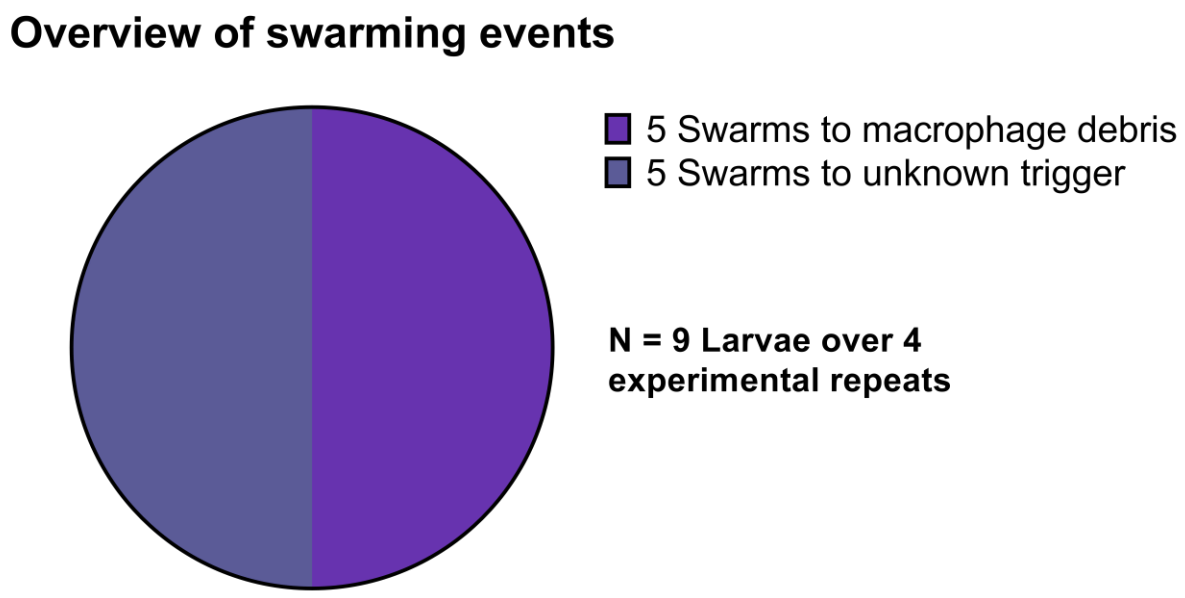

Figure 39: 50% of swarms formed in proximity of macrophage debris

This figure illustrates the distribution of swarms that would form towards macrophage cell debris and of swarms that would form to an unknown trigger which could not be discerned in this particular experiment. This data was manually analysed through careful visual inspection of each time-lapse.

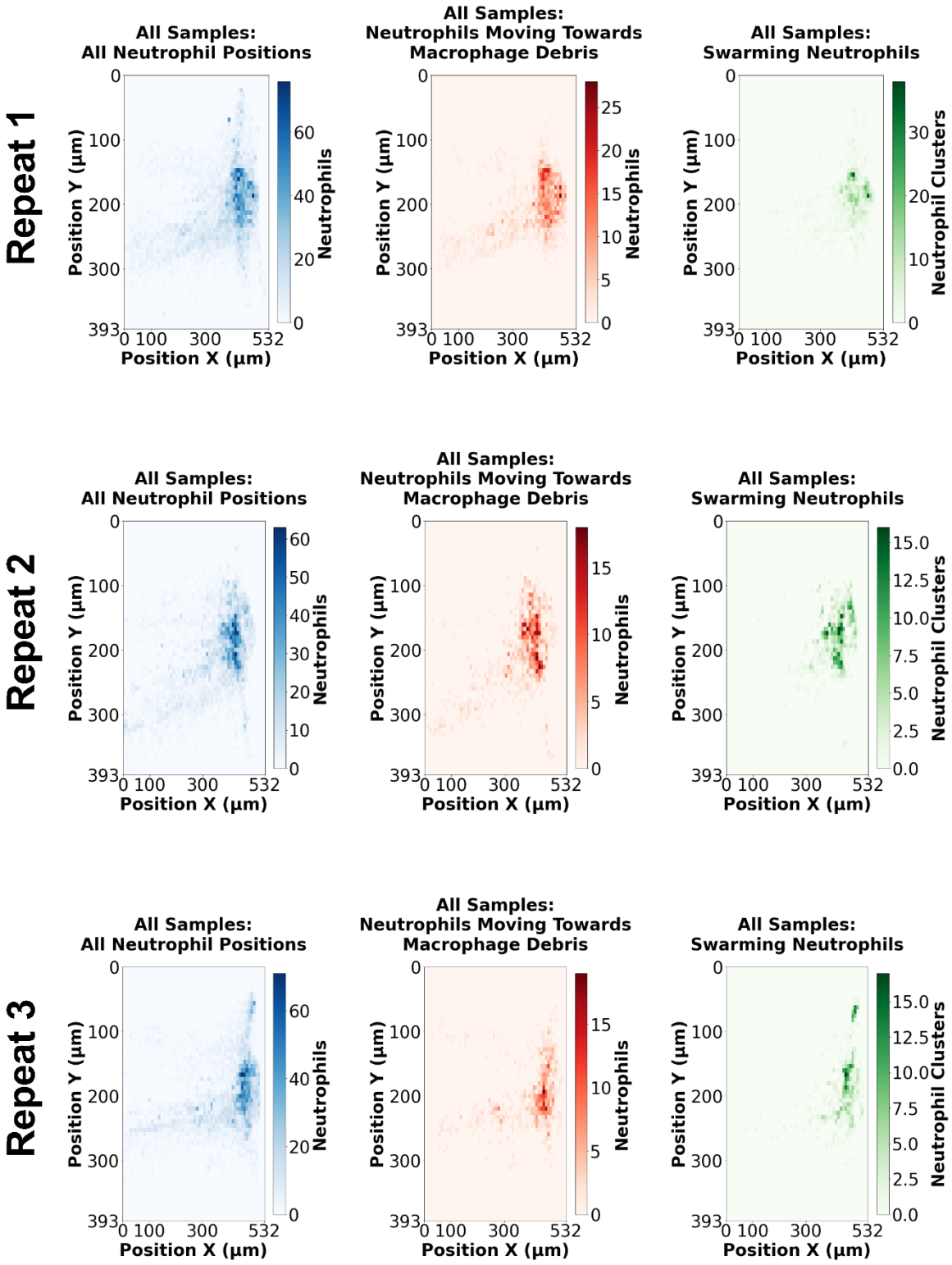

Figure 40: Heatmaps suggest interactions of neutrophils with macrophage debris and locations of swarms

A python script was used to analyse tracking data obtained from Cellpose and Trackmate as described in Chapter 3.2. Blue heatmaps show the location of all neutrophils. Red heatmaps show neutrophils moving towards macrophage debris which were obtained by filtering for movement towards macrophage debris present within a 20µm radius of a neutrophil centroid. Macrophage debris was obtained by creating a threshold and mask for small particles and excluding large objects, in this case macrophages. Green heatmaps show the locations of neutrophil clusters filtered for areas bigger than 3x the average area of a single neutrophil, as an indication of neutrophil swarms. Repeat 1-3, indicate individual experimental repeats, samples indicate larvae. Heatmaps were created from all larvae within one experimental repeat, n=5, 4, 5 for each respective repeat. Heatmaps of individual larvae can be found in **Supplemental Figure 4-6**.

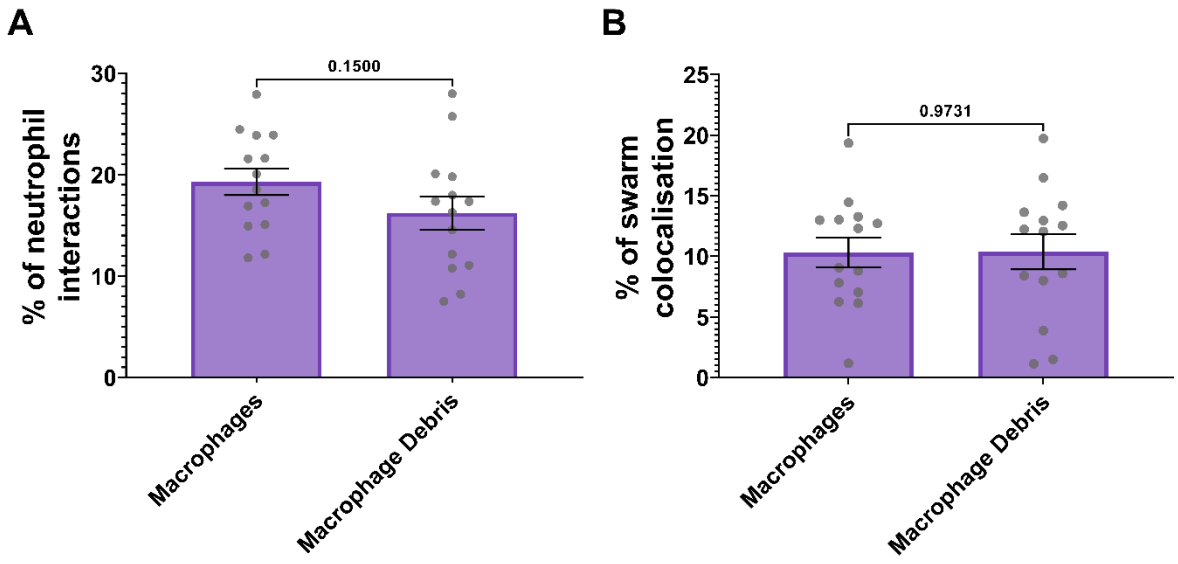

Figure 41: Quantification of interactions cannot conclude whether swarming responses are driven by macrophage cell death

A. Shows the % of neutrophils that interacted either with macrophages that were alive or with macrophage debris. No significant difference was found between these two types of interactions. Data was analysed with an unpaired, two-tailed t-test. Data is visualised as mean ± SEM.

B. Shows the % of neutrophils interacting with macrophages or macrophage debris colocalising with the locations of swarms, indicated by the location at which clusters formed throughout the time-lapse. No significant difference was found between these two types of interactions and their colocalisation with neutrophil swarms. Data was analysed with an unpaired, two-tailed t-test. Data is visualised as mean ± SEM.

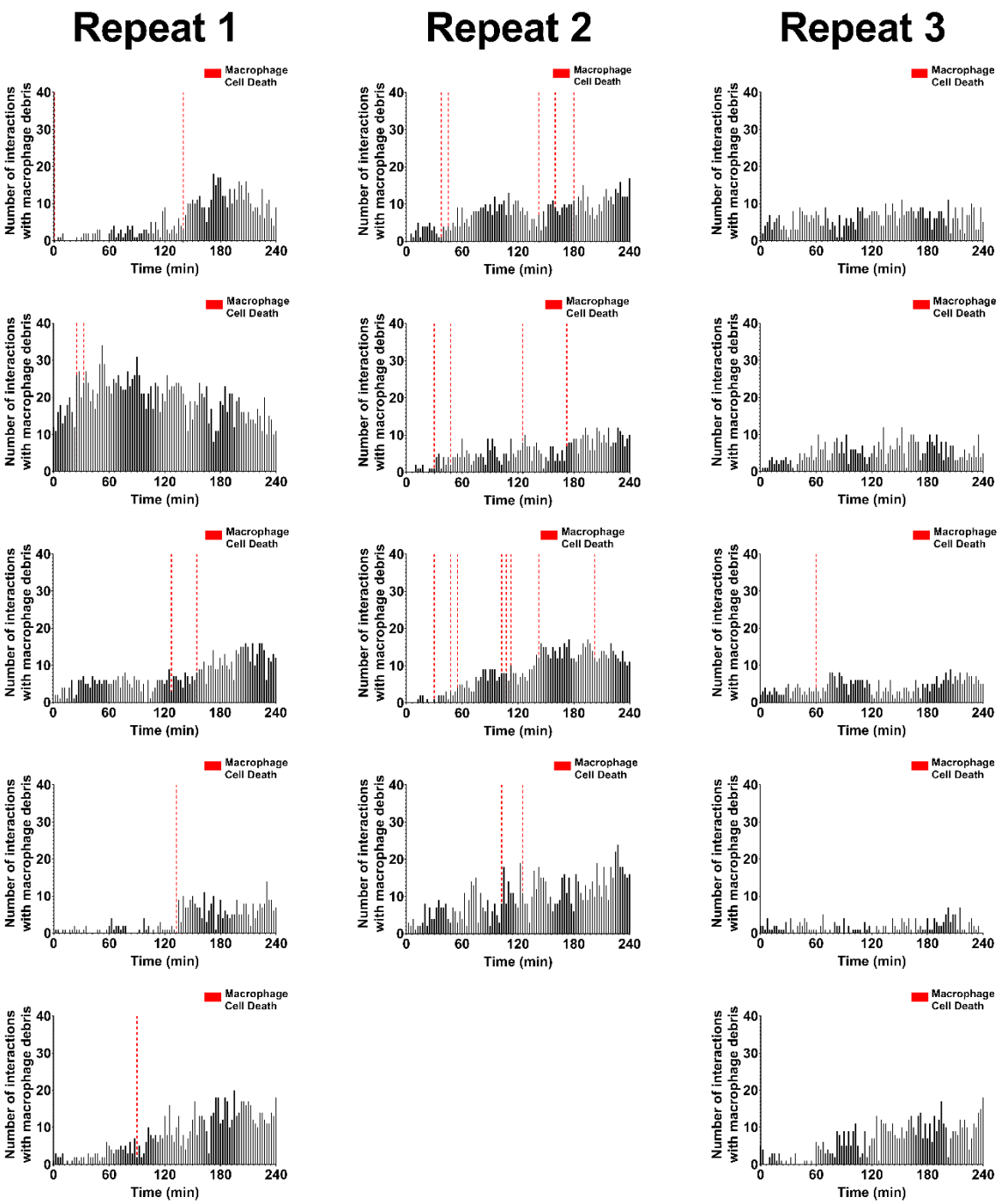

Figure 42: Neutrophil interactions with macrophage debris increase after macrophage cell death

This figure visualises the number of neutrophil interactions with macrophage debris that occurs over time. Red lines indicate moments of macrophage cell death, determined by careful observation of each time-lapse. This indicates a spatiotemporal response of neutrophils to macrophage cell death.

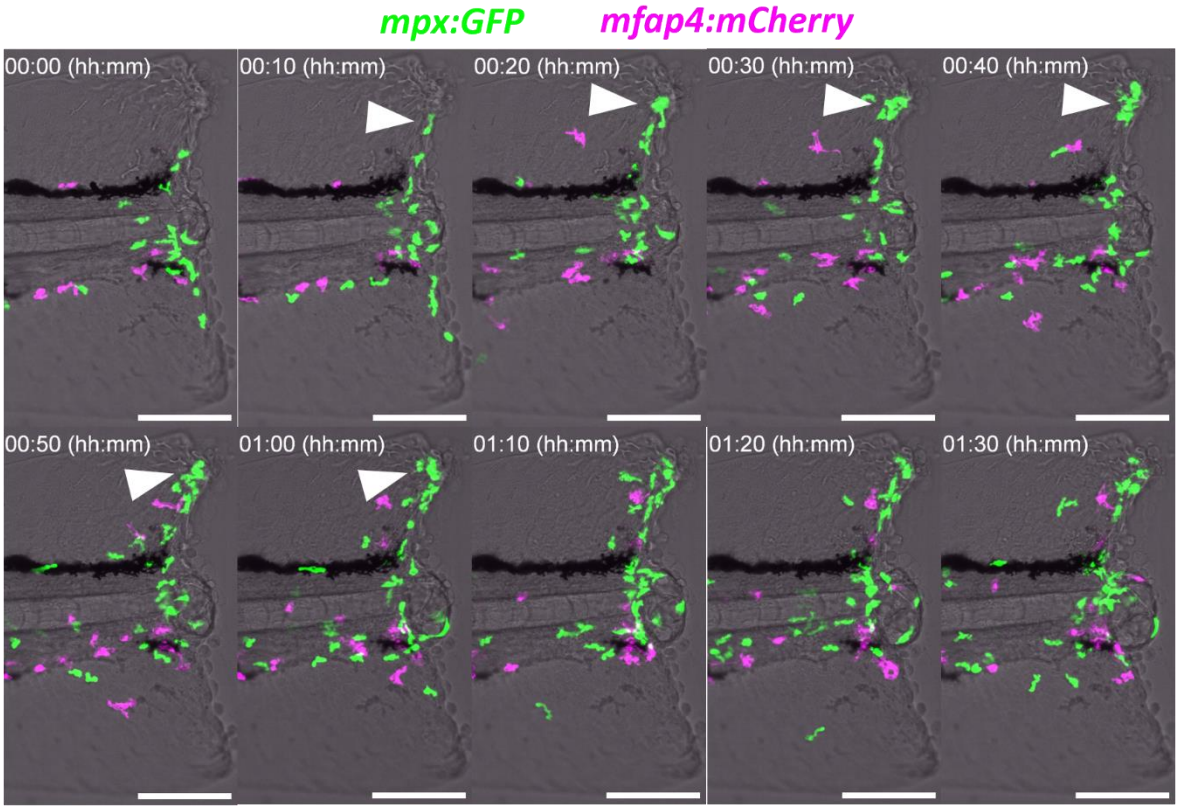

Figure 43: Neutrophil swarm outside the vicinity of macrophages

This figure shows the only example of a neutrophil swarm that occurred at considerable distance from any macrophages in these datasets (white arrowhead). This illustrates that while neutrophils and macrophages often got recruited to approximately the same area of the tail fin (**Figure 38, 40**), swarms can still occur outside the range of neutrophil-macrophage interactions.

3.4.4 Metronidazole treatment of *Tg(mpeg1:NTR-mCherry)* significantly reduced macrophage numbers

From the imaging data in **Chapter 3.4.3**, I hypothesised that swarming could be directed towards sites of macrophage cell death. As quantification of imaging data proved challenging, I explored techniques for biological intervention to test my hypothesis. One such intervention involved significantly reducing or fully depleting macrophages from zebrafish larvae to determine if neutrophil swarming differed in the absence of macrophages. A previously described method for chemical ablation of cell types has been extensively used in zebrafish research (Davison et al., 2007, Ellett et al., 2011, Nguyen-Chi et al., 2015). I applied this technique to chemically ablate macrophages in 3dpf zebrafish larvae.

Chemical ablation resulted in a significant reduction of macrophages in the larvae (**Figure 44**), but also rendered them vulnerable during long time-lapse imaging, with many larvae dying during imaging (data not shown). Depletion was not entirely efficient as the negative control remained significantly lower than the treated samples. This, along with potential side effects of chemical treatment on the neutrophil response, led me to explore other techniques for macrophage depletion.

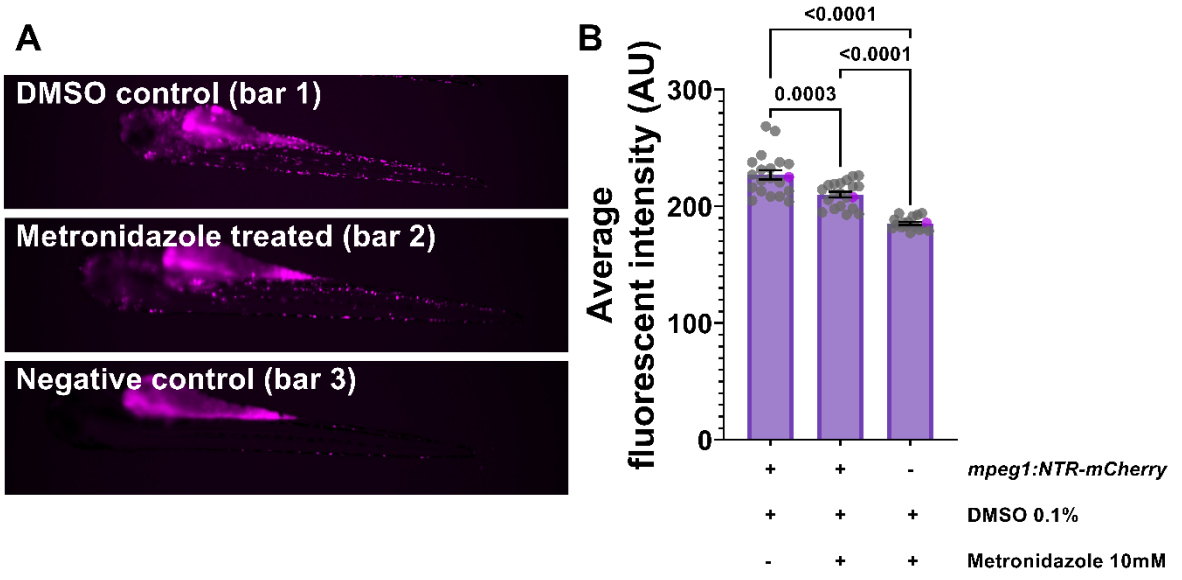

Figure 44: Significant reduction of macrophages following metronidazole treatment in a chemical ablation system

This figure shows the use of the metronidazole-nitroreductase system for chemical ablation of cell types. In this case the *Tg(mpeg1:Gal4FF) Tg(UAS-E1b:Eco.NfsB-mCherry)* lines were crossed for macrophage specific ablation following metronidazole treatment at 10mM. Treatment was started at 2dpf for 24 hours and larvae were assessed for ablation at 3dpf.

A. Representative images of the quantified signal in **B** indicated by the coloured data points.

B. Quantification of the images shown in **A**, a significant reduction in fluorescent intensity can be seen between the control and the treated group, however the negative control suggests that ablation was not nearly 100% efficient. Metronidazole was added to the negative control to check for additional signs of toxicity, but in this experiment, none was found. Later time-lapse experiments of which data got corrupted, showed early death occurring compared to experiments shown in Chapter 3.4.2. Data was analysed with an Ordinary one-way ANOVA with Dunnett's correction for multiple hypothesis testing. Data shown as mean ± SEM.

3.4.5 CRISPR-Cas9 knockdown of irf8 significantly reduced macrophage numbers and increased neutrophil numbers

Besides the chemical ablation techniques described in Chapter 3.4.3.a, genetic techniques for cell population depletion can be considered. These often result in a cleaner reduction of cell population by fully inhibiting development, unlike the metronidazole nitroreductase system where cell death occurs after cell development and maturation, resulting in accumulation of cell debris (Nguyen-Chi et al., 2017). I used a recently published approach for macrophage depletion through knockdown of *irf8* via CRISPR-Cas9 in *Tg(fms:GFP)*^{sh377} zebrafish (Rutherford et al., 2024). Because previous studies have reported that morpholino knockdown of *irf8* leads to an increase in neutrophil populations, *irf8* knockdown was also performed in *Tg(mpx:GFP)*^{i114} zebrafish to confirm these findings (Prajsnar et al., 2021, Li et al., 2011). A striking reduction of macrophages was seen in *Tg(fms:GFP)*^{sh377} larvae at 3dpf and 4dpf, confirming the efficacy of this approach; however, at the 4dpf timepoint, macrophages slowly began to reappear (**Figure 44-45**) (Rutherford et al., 2024). In terms of neutrophils, a small but significant increase in neutrophil numbers following *irf8* knockdown was observed, confirming published data (**Figure 46-47**).

In summary, using a genetic knockdown of *irf8* via CRISPR-Cas9 was a successful approach for full depletion of macrophages, in agreement with published literature(Rutherford et al., 2024). This knockdown was less variable and had fewer side effects that could potentially influence the neutrophil response. However, the observed increase in neutrophils must be considered for future experiments, which were not performed as of writing this thesis due to time constraint.

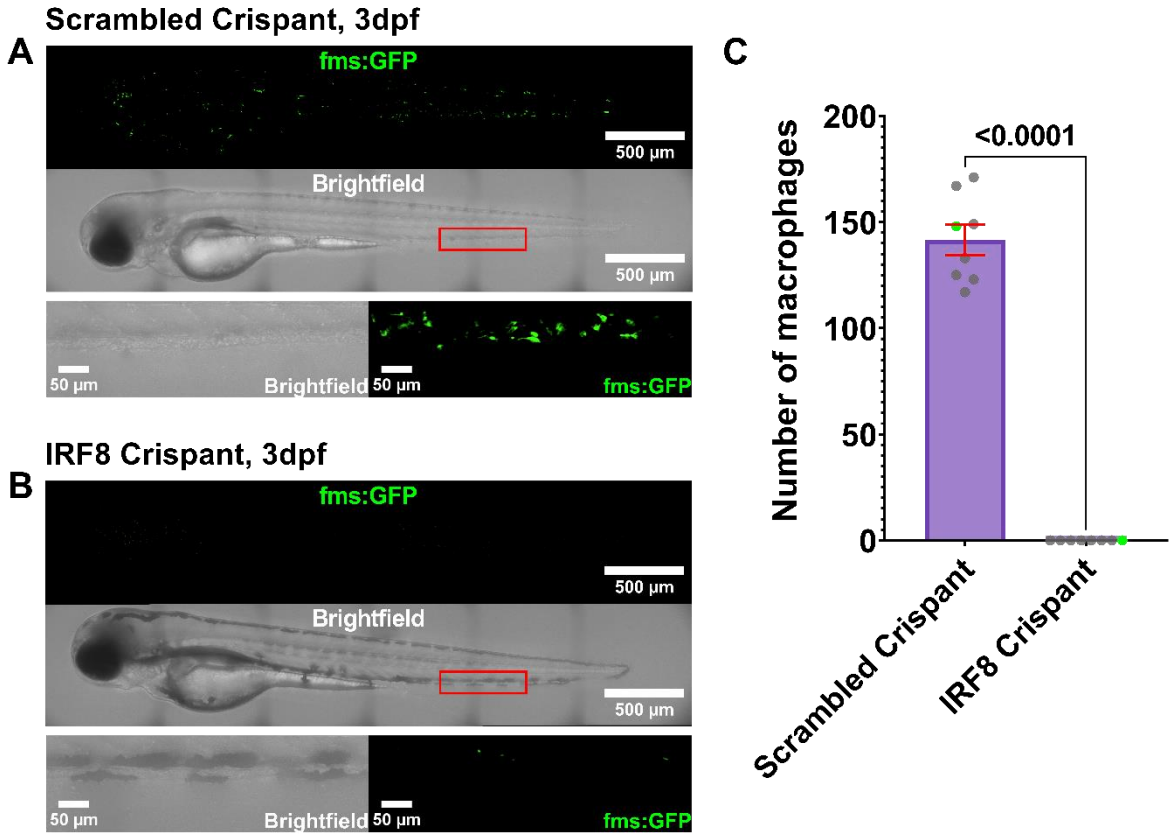

Figure 45: Significant reduction of macrophages following knockdown of *irf8* via CRISPR-Cas9

A. Representative images of the data quantified in **C** indicated by the coloured data point. Scrambled control refers to the injection of randomised non-targeting guide RNA.

B. Representative images of the data quantified in **C** indicated by the coloured data point. A combination of 2 RNA guide sequences against *irf8* was used for effective, whole-body depletion of macrophages.

C. Quantification of the number of macrophages in whole larvae. A complete depletion of macrophage population can be observed at 3dpf. N=1 n=8 per group.

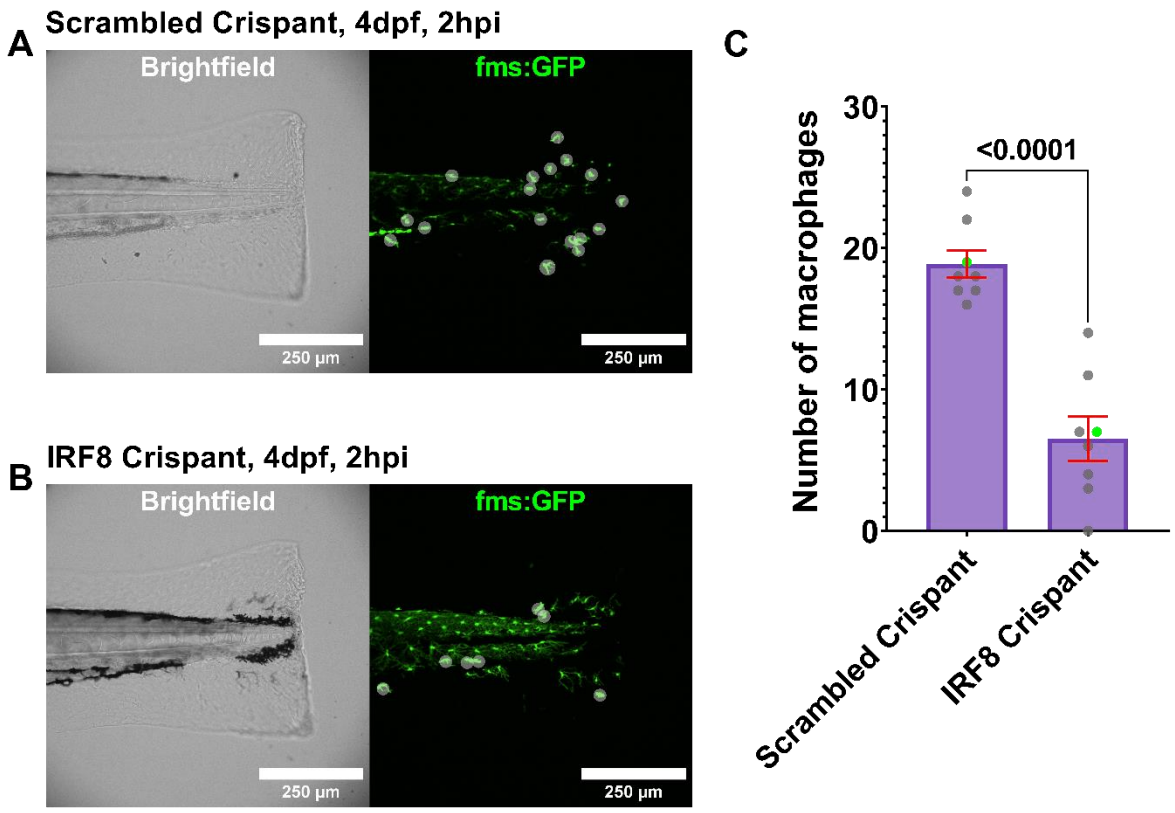

Figure 46: Significant reduction in macrophages in *irf8* crispants following tail fin injury

Larvae from **Figure 45** were further assessed for macrophage numbers and response at 4dpf at 2hpi. The number of macrophages that were recruited to the wound was significantly higher in the scrambled crispant as macrophages were not depleted in these samples, however compared to the total depletion seen at 3dpf in **Figure 45** a small number of macrophages was seen to migrate towards the wound site at 4dpf, indicating that macrophages mature in another *irf8* independent manner. Background labelling of xanthophores in the *fms:GFP* line can be observed, but these were excluded from macrophage counts.

A. Representative images of the data quantified in **C** indicated by the coloured data point. Scrambled control refers to the injection of randomised non-targeting guide RNA. Macrophages indicated by highlighted circles.

B. Representative images of the data quantified in **C** indicated by the coloured data point. A combination of 2 RNA guide sequences against *irf8* was used for effective, whole-body depletion of macrophages. However, at 4dpf macrophages slowly appeared to generate in an *irf8* independent manner. Macrophages indicated by highlighted circles.

C. Quantification of the number of macrophages responding to the tail fin wound at 2hpi. Still a significant reduction in macrophage numbers can be observed at 4dpf. N=1 n=8 per group.

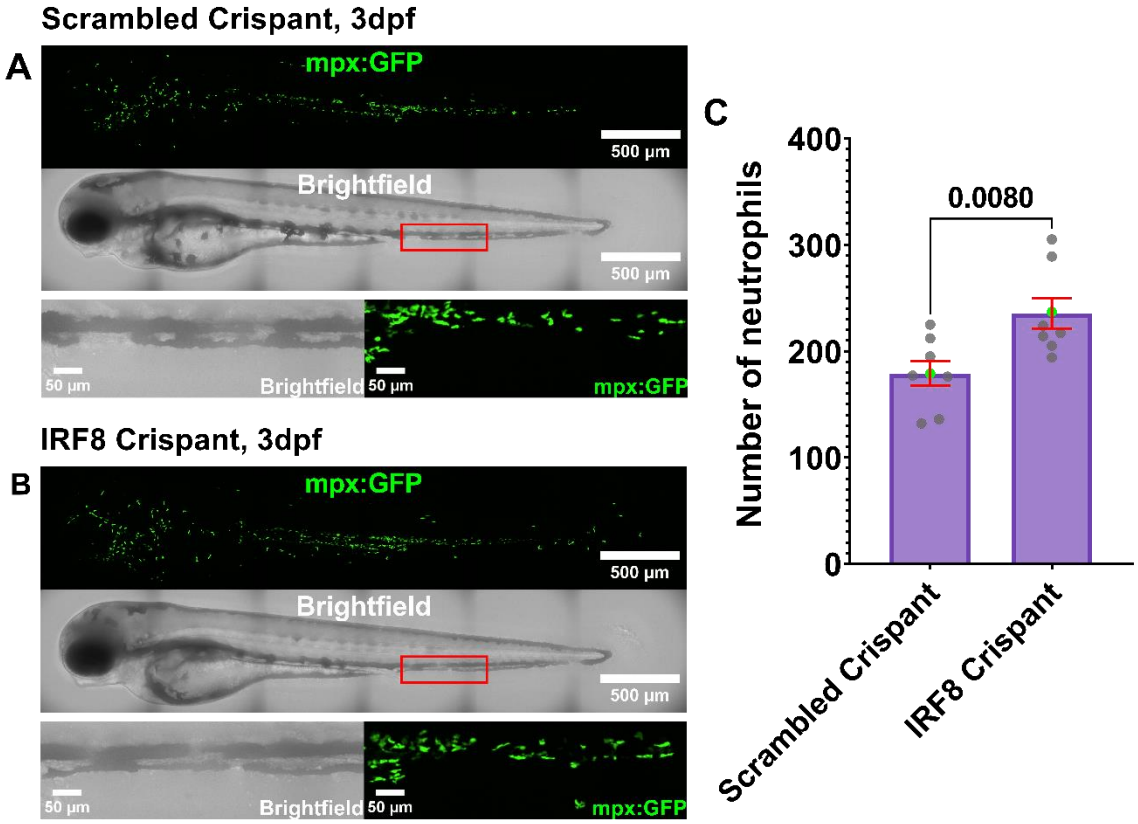

Figure 47: Significant increase in neutrophils after knockdown of *irf8* via CRISPR-Cas9

A. Representative images of the data quantified in **C** indicated by the coloured data point. Scrambled control refers to the injection of randomised non-targeting guide RNA.

B. Representative images of the data quantified in **C** indicated by the coloured data point. A combination of 2 RNA guide sequences against *irf8* was used for effective, whole-body depletion of macrophages.

C. Quantification of the number of neutrophils in whole larvae. In contrast to **Figure 45-46** where a decrease in macrophages was found, I find that *irf8* knockdown leads to a significant increase in neutrophils throughout the entire larva. This recapitulates previously published studies using a morpholino approach (Prajsnar et al., 2021, Li et al., 2011). N=1 n=10 per group. Data was analysed with an unpaired two-tailed t-test. Data was plotted as mean ± SEM

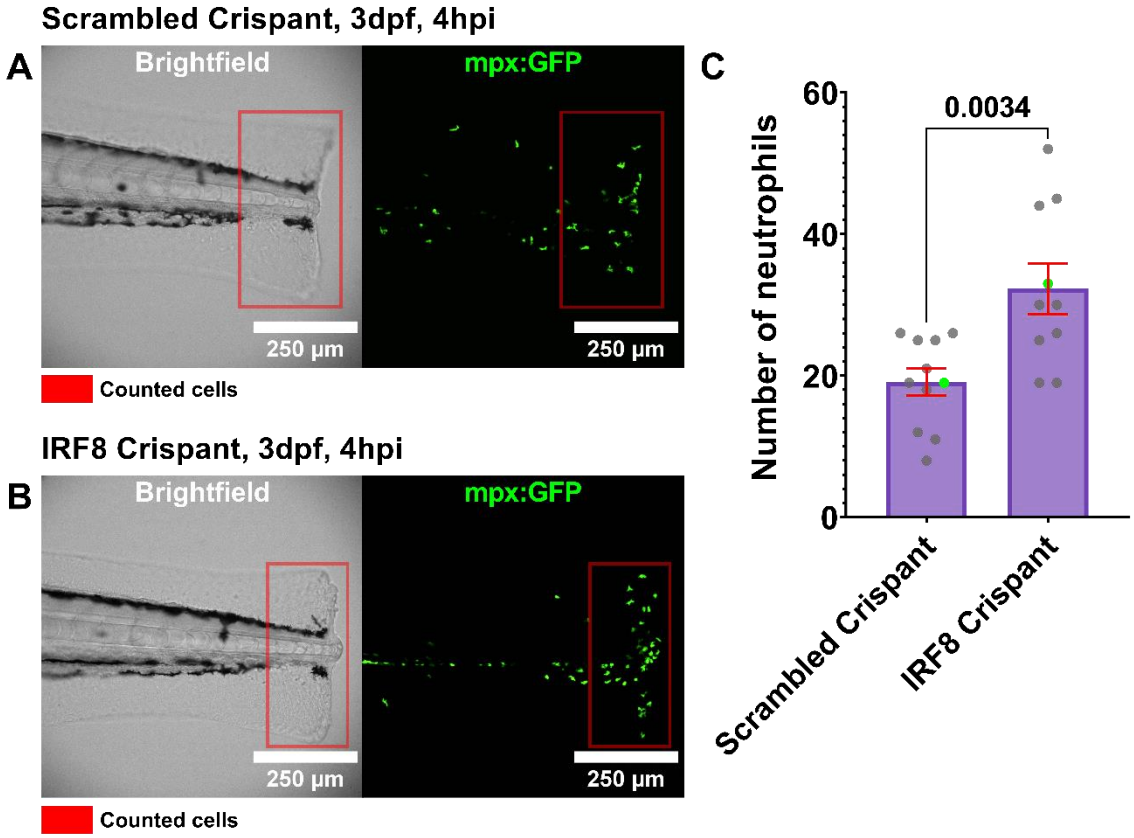

Figure 48: Significant increase in neutrophils in *irf8* crispants following tail fin injury

Larvae from **Figure 47** were further assessed for neutrophils numbers and response at 3dpf at 4hpi. The number of neutrophils that were recruited to the wound was significantly higher in *irf8* crispant.

A. Representative images of the data quantified in **C** indicated by the coloured data point. Scrambled control refers to the injection of randomised non-targeting guide RNA. Macrophages indicated by highlighted circles.

B. Representative images of the data quantified in **C** indicated by the coloured data point. A combination of 2 RNA guide sequences against *irf8* was used for effective, whole-body depletion of macrophages. However, at 4dpf macrophages slowly appeared to generate in an *irf8* independent manner. Macrophages indicated by highlighted circles.

C. Quantification of the number of macrophages responding to the tail fin wound at 2hpi. Still a significant reduction in macrophage numbers can be observed at 4dpf. N=1 n=10 per group. Data analysed with an unpaired two-tailed t-test. Data was plotted as mean ± SEM

3.4.6 Conclusion & Discussion

As neutrophils are not the only type of innate immune cell regulating inflammatory responses in zebrafish, I aimed to explore the potential role of macrophages in neutrophil swarming. In collaboration with the Laboratory of Host Pathogen Interactions (LPHI) at Université de Montpellier, I sought to obtain preliminary results on how neutrophil-macrophage interactions may shape the neutrophil swarming response.

Experiments using an outcross of reporter lines visualising macrophages (*Tg(mfap4:mCherry)*^{ump6Tg}) and neutrophils (*Tg(mpx:GFP)*^{i114}) resulted in multiple findings.

First, I observed macrophages to localise to a ventral fin injury around neutrophils, these data recapitulate that myeloid cell recruitment, particularly macrophages in the zebrafish model, may occur around neutrophil swarms as previously suggested by studies in mice (Kienle and Lammermann, 2016). I also observed that neutrophils may perform revere migration after macrophage arrival, which agrees with previous research, however more experiments and detailed quantification will have to be performed to fully conclude this (Tauzin et al., 2014). The finding of macrophages seemingly shielding off the wound, aligns with previous research, which found that resident tissue macrophages (RTMs) cloak microlesions, resulting in shorter and less pronounced neutrophil responses in the mouse model (Uderhardt et al., 2019). This could explain why the laser injuries illustrated in Chapters **3.2.5** and **3.2.6** were, in most cases, unable to induce pronounced neutrophil swarming events. The threshold between what is considered a microlesion and a macrolesion in zebrafish could influence macrophage cloaking and alter neutrophil swarming dynamics.

I showed that 50% of the swarms I observed were spatiotemporally colocalised with locations of macrophages and macrophage cell death, which contrasts previously published literature

suggesting that macrophage and neutrophil interactions mainly drive neutrophil reverse migration (Tauzin et al., 2014). However, there are indications that macrophages could stimulate neutrophil recruitment, for instance during bacterial skin infection by perivascular macrophages or by alveolar macrophages after nanoparticle stimulation of murine lungs (Abtin et al., 2014, Liu, 2023).

Examples of macrophage cell death and swarming of neutrophils in close proximity were striking, though further quantification could not determine any causative effect. Future experiments using localised injection of clodronate liposomes, which can trigger macrophage apoptosis, could shed more light on this (Nguyen-Chi et al., 2017, Moreno, 2018). Neutrophil responses to clodronate injections could then be compared to control injections to see if the number of neutrophil swarms change. However, I have not been able to discern whether swarming of neutrophils following macrophage cell death is specific to certain types of cell death.

Multiple types of cell death have been described in literature, including apoptosis, necroptosis, and pyroptosis, each with distinct pathways (Bertheloot et al., 2021). Pyroptosis is often described as the most pro-inflammatory type of cell death, caused by pore formation via gasdermins and subsequent leakage of pro-inflammatory cytokines such as IL-1β and IL-6 (Liu et al., 2020, Yu et al., 2021). Necroptosis should also be considered, as both types of cell death disrupt the cell membrane, facilitating the release of pro-inflammatory cytokines and DAMPs such as extracellular ATP (Frank and Vince, 2019, Ye et al., 2023). The imaging data I have obtained may suggest some form of lytic cell death rather than controlled cell death such as apoptosis, but to definitively say this further research is required.

Because of their pro-inflammatory nature, pyroptosis or necroptosis of macrophages are likely candidates for triggering neutrophil swarming. However, to conclusively determine this, future experiments will need to inhibit key molecules or knock out key genes associated with each type of cell death: caspase-8 and caspase-9 for apoptosis; RIP1K for necroptosis, and GSDMD for pyroptosis (Tummers and Green, 2017, Li et al., 2017, Mifflin et al., 2020, Burdette et al., 2021). Additionally, approaches outside of the zebrafish model, such as a co-culture cell model using the transwell system, could be considered (Patel et al., 2018).

Another interesting finding is that the locations of both macrophages and neutrophils, as well as the subsequent neutrophil clusters, were mostly around the area of highest tissue damage, the notochord. This made extracting cell-cell interactions difficult due to the high aggregation of both cell types in a small spatial distance. Injuries sparing the notochord might allow macrophages and neutrophils to respond in a more dispersed pattern, increasing the ability to visualise close cell contact and potential swarm-implicated effects.

While my data suggest that neutrophil swarming can occur at sites of neutrophil-macrophage interactions and macrophage cell death, this does not mean that the swarming process itself depends on macrophages. It merely illustrates that macrophages may potentially act as a potential trigger for neutrophil swarming, as neutrophil swarms have been extensively studied in *ex vivo* models containing solely neutrophils (Hopke et al., 2020, Strickland et al., 2024).

Depletion of macrophages might help in answering whether macrophages may potentially influence neutrophil swarming. I tested two approaches for macrophage depletion within the zebrafish model. The first approach was chemical depletion via the metronidazole-nitroreductase system; the second approach was a recently described method of *irf8*

knockdown via CRISPR-Cas9 (Davison et al., 2007, Rutherford et al., 2024). The *irf8* gene determines macrophage maturation during the transitory primitive wave in embryonic development (Li et al., 2011). Researchers showed that influencing irf8 through knock-out or overexpression could steer and attenuate the number of macrophages developing in zebrafish (Li et al., 2011). While both methods significantly decreased macrophages, *irf8* knockdown led to cleaner depletion and would thus be my suggestion for further experimentation.

Chapter 4: Conclusion

For this study I hypothesised that dynamics of neutrophil swarms could significantly impact inflammation resolution. To determine whether this was the case, I aimed to identify novel mechanisms and effects of neutrophil swarming in the zebrafish model, expanding our understanding of neutrophil responses and providing a foundation for further research and development of potential therapeutic approaches.

4.1 Neutrophil Swarming Time Frame

Compared to earlier research of neutrophil swarms in the zebrafish model that mainly investigated initiating events, I aimed to observe and determine the entire swarming response (Poplimont et al., 2020, Isles et al., 2021). Using long time-lapse imaging I was able to discern that most neutrophil swarms would form between 2 and 8 hours and that there were unique visual differences between swarming and non-swarming responses.

4.2 Injury Type and Swarming Response

I compared two methods of tail fin injury, one sparing the notochord and one injuring it, as both methods have been used in zebrafish research (Loynes et al., 2018, Nguyen-Chi et al., 2017). I found that both methods would result in the same number of neutrophil swarms being formed, indicating that even though notochord injuries often coincide with increased recruitment of neutrophils, it did not necessarily result in more swarms to be formed. This suggests dependency on the underlying signalling mechanisms that cause neutrophil swarms, rather than the degree of tissue damage.

In **Chapter 3.2** I discuss how temporal dynamics of neutrophil swarms and the overall neutrophil response is different between two locations of injury, namely ventral fin and tail

fin injuries. I found that tail fin injuries would form swarms at later timepoints and that overall inflammation resolution was significantly slower than the smaller ventral fin wounds.

4.3 Impact of Swarming on Neutrophil Recruitment, Resolution and Tissue Regeneration

Using time-lapse imaging I could classify swarming from non-swarming responses and I observed significant differences in neutrophil recruitment, as well as resolution. I found that larvae with neutrophil swarms have impaired inflammation resolution, in part due to elevated levels of neutrophils being recruited initially. To further investigate the impact of this impaired resolution, I used a tail fin regeneration assay (Bernut et al., 2020). I was able to recapitulate the impaired inflammation resolution after swarming, which I could then correlate to a small, but significant decrease in tail fin regeneration at 48 hours after the injury. This suggests that neutrophil swarms might play a detrimental role in tissue regeneration via impaired inflammation resolution.

4.4 Novel Methodologies and High-Throughput Assay Development

In a collaborative effort with INFLANET partner Acquifer at the University of Heidelberg, we developed novel image analysis pipelines for detailed quantification of neutrophil swarming. Image analysis tools were developed to assist in classification of neutrophil swarms with reduced individual detection bias. Ultimately, these tools were utilised to create a high-throughput assay of neutrophil swarming *in vivo*. While high-throughput assays for swarming have already been created, these assays are based on *ex vivo* techniques which cannot fully recapitulate an *in vivo* setting. By using the zebrafish model these *in vivo* mechanisms and interactions are retained.

From earlier observations I hypothesised that there could be a big difference in performing laser injuries or sterile, mechanical injuries to trigger the neutrophil swarming response. As

such, we decided to use these two different techniques to validate our assay. We were indeed able to pick up a difference in swarming intensity and the general occurrence of neutrophil swarms when larvae were injured in one of these ways. Data suggested smaller and less swarming events post laser injury compared to mechanical injury, which agreed with my initial observations. With this successful validation, we provided a novel approach to test for new pharmacological compounds that could potentially alter neutrophil swarming responses and be adapted into new therapeutic strategies.

4.5 Role of TLR Signalling, HIF-1α and ROS

With the tools designed in **Chapter 3.2**, I became interested in identifying potentially novel pathways that play a role in neutrophil swarming as well as identifying ways to pharmacologically modulate swarming responses.

Due to continuous challenges posed by the variability and stochasticity of neutrophil swarms, I aimed to explore an approach to upregulate neutrophil swarming, reducing the overall variability in my data. Previous literature illustrated that TLRs function to alter neutrophil responses and migration (Prince et al., 2011, van der Vaart et al., 2012, Hu et al., 2021). I hypothesised that immersion treatment of TLR agonists could lead to an increased pro-inflammatory response which might result in the upregulation of neutrophil swarms, however after screening a selection of TLR agonists and performing a multitude of experiments, I did not discover any significant effect of TLR agonist treatment via immersion on neutrophil swarming.

During this time a publication performed a detailed and elegant investigation into the role of NOX in neutrophil swarming. They found that inhibition of NOX would lead to a severe defect

in relay signalling during neutrophil swarming, causing a phenotype that could be directly related to patients with CGD (Strickland et al., 2024).

NOX is one of the main sources of ROS within cells, which can be deterministic in neutrophil migration and activation (Yan et al., 2014, de Oliveira et al., 2016). Because of this striking finding I wanted to explore other pathways that closely interact with ROS and determine whether these could have an effect on neutrophil swarming. Ultimately, I chose to investigate the HIF-1α pathway which can be regulated by ROS (Willson et al., 2022, Movafagh et al., 2015). Furthermore, the HIF-1α pathway has been implicated in neutrophil retention at wound sites in zebrafish, which could affect swarming dynamics (Elks et al., 2011).

In experiments where I activated HIF-1α through the use of PHD inhibitors, I found a significant decrease in the number of neutrophil swarms formed at 6hpi. However, further experiments suggested that neutrophil migration and recruitment was not significantly impacted. This potentially means that HIF-1α plays a direct role, likely downstream from ROS, on neutrophil swarm formation, but not neutrophil recruitment. However, further experimentation with for instance dominant negative HIF-1α should be undertaken to further elucidate the precise mechanisms at play.

4.6 Interactions Between Neutrophils and Macrophages

In zebrafish larvae, there are multiple cell types that respond to inflammatory triggers. While full adaptive immunity does not develop before 2 weeks post fertilisation, innate immune cells are fully developed and present within the fish as soon as 2 days post fertilisation (Dee et al., 2016, Speirs et al., 2024). To study whether other innate immune cells, specifically macrophages, would have any effect on the dynamics of neutrophil swarming I collaborated with Georges Lutfalla and Mai Nguyen-Chi in the Laboratory of Pathogen Host Interactions at

Université de Montpellier. Using an outcross of Tg(*mfap4:mCherry*)^{ump6Tg} with Tg(*mpx:GFP*)^{i114} I was able to visualise both macrophages and neutrophils during neutrophil swarming.

I found that macrophages and macrophage cell death often localised in close proximity to subsequential neutrophil swarming events. This finding may indicate a more pro-inflammatory role of macrophages compared to what literature, specifically in the zebrafish model, has described so far (Loynes et al., 2010, Tauzin et al., 2014, Loynes et al., 2018). However, it has been suggested that macrophages can play a direct role in the recruitment of neutrophils to tissues. For instance, alveolar macrophages after nanoparticle treatment of the murine lung and perivascular macrophages during bacterial skin infection (Abtin et al., 2014, Liu, 2023). I found that apparent macrophage cell death may be a trigger for neutrophils to migrate, interact, and even form a swarm. However, I have so far been unable to demonstrate a mechanistic link between macrophage cell death and swarming, and I have been unable to define whether this phenomenon is tied to a specific type of cell death. This could be explored in future experimentation by targeting key molecules of apoptosis, necroptosis and pyroptosis, respectively.

Besides this, I was able to observe a similar phenomenon of macrophage recruitment towards neutrophils described previously in mice, where neutrophil swarms are hypothesised to be stabilised by myeloid cells arriving at a later timepoint (Kienle and Lammermann, 2016). In zebrafish, I saw macrophages localise around areas of high neutrophilic inflammation post ventral fin injury, however this phenotype did not last for long as neutrophils migrated away from the wound site relatively rapidly at approximately 1-2 hours after the injury was made. Macrophage arrival was associated with neutrophils leaving the wound site which may be in agreement with literature (Tauzin et al., 2014). Interestingly, this is opposite from what may

be occurring in tail fin injuries, which exemplifies that injury type should be considered when investigating the neutrophil response. Furthermore, macrophages seemingly shielding off ventral fin injuries, shared a lot of similarities with previously published research showing RTMs to exhibit a cloaking mechanic to microlesions using the mouse model (Uderhardt et al., 2019).

4.7 Macrophage Depletion Methods for Future Study

In an effort to further elucidate the effect of macrophages on neutrophil swarming I wanted to explore methods for depletion of macrophages from the zebrafish model. Previously a chemical system using metronidazole and nitroreductase has been successfully employed to this extent (Davison et al., 2007). However, this method could have side effects due to the metronidazole treatment and does not stop macrophages from developing entirely, instead, once a macrophage fully matures, nitroreductase build up within the cell will cause cell death (Davison et al., 2007). This creates a relatively messy system in which cellular debris could be an issue in activating consistent neutrophil responses. As such, I pivoted to a recently described CRIPSR-Cas9 technique, effective in reducing microglial population within the zebrafish brain at 5dpf (Rutherford et al., 2024). This technique targets genetic knockdown of *irf8* which has previously been shown to regulate macrophage development during the first transitional wave (Li et al., 2011). However, modulating *irf8* has also been shown to cause a change in neutrophil populations (Prajsnar et al., 2021, Li et al., 2011).

I found that *irf8* knockdown via CRISPR-Cas9 was the most effective method of depleting macrophages from the zebrafish model, however I was able to recapitulate an increase in neutrophils, which has to be considered when contextualising future results. Nonetheless, I

would suggest the *irf8* CRISPR-Cas9 approach for future experimentation and elucidation of the role of macrophages in the neutrophil swarming response.

4.8 Future Prospects

To build upon the research presented in this thesis, I will discuss some potential next steps to consider. The first step is the implementation of image analysis with reduced individual bias and higher reproducibility as presented in **Chapter 3.2.3**. The analysis methods developed in this thesis will be condensed into a dedicated methods publication for researchers to use in the future. Expanding these tools will help create a library of objective measures for assessing neutrophil swarming responses in zebrafish, with potential applicability to other models.

Additionally, one of the most striking findings of this thesis is the potential role of macrophages and neutrophils in regulating the neutrophil swarming response *in vivo*. While the underlying LTB4 signalling will remain the lead cause of amplified swarming signals, other immune cells may upregulate or downregulate the LTB4 signalling response. My data suggest that secondary cell death, particularly of macrophages, could play a role in shaping a subset of neutrophil swarming responses, however several questions remain. For instance, is this potential response dependent on the type of cell death that the macrophage undergoes? It is also unclear whether this response is specific to macrophages or generally influenced by the type of cell death. If this response is indeed dependent on the type of cell death, it could be tested through visualisation or inhibition of key enzymatic drivers, such as Caspase-3 for apoptosis or Receptor-interacting serine/threonine-protein kinases 1 and 3 (RIPK1 and RIPK3) for necroptosis. Alternatively, to investigate how macrophages shape the

neutrophil swarming response, they could be ablated from the model system altogether. This can be achieved through various techniques, as discussed in **Chapter 4.7**.

4.9 Conclusion

Neutrophils are implicated in many different diseases, ranging from chronic inflammatory diseases such as COPD to infectious diseases such as COVID-19. Enriching our knowledge of neutrophil specific behaviours is essential in shaping our understanding of neutrophils in disease. One of these behaviours is neutrophil swarming. In this thesis I have shown how neutrophil swarming dynamics in zebrafish may change due to a multitude of factors including; injury type; injury location; pharmacological manipulation; and interactions of neutrophils with macrophages. Furthermore, I developed and used novel image analysis tools for in depth analysis of swarming which can be used more broadly on any type of fluorescent imaging data, from any type of model system and has been validated in a high-throughput assay of *in vivo* swarming. Taken together, this thesis provides a deeper understanding of neutrophil swarming and enables further research to potentially find novel targets for development of therapeutic approaches for patients affected by neutrophil related illnesses.

Chapter 5: Supplementary

5.1 Movies

All movies can be found as a .zip file on Zenodo: https://doi.org/10.5281/zenodo.14853069

5.2 Code

All of the code used in this thesis can be found in the following online GitHub repository: https://github.com/NilsOlijhoek/In-the-Eye-of-the-Swarm-Thesis-2024

5.3 Figures

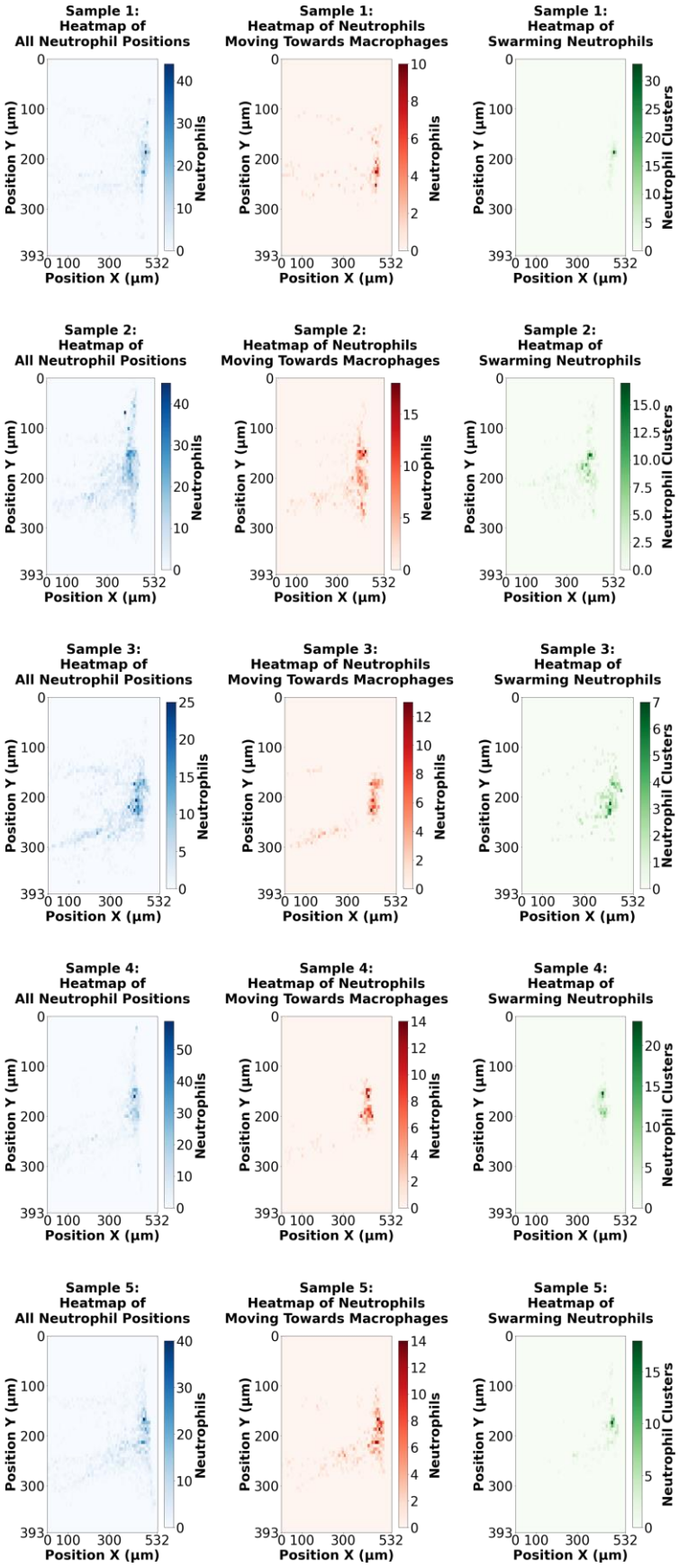

Supplemental Figure 1: Individual samples that made up Figure 36 Repeat 1.

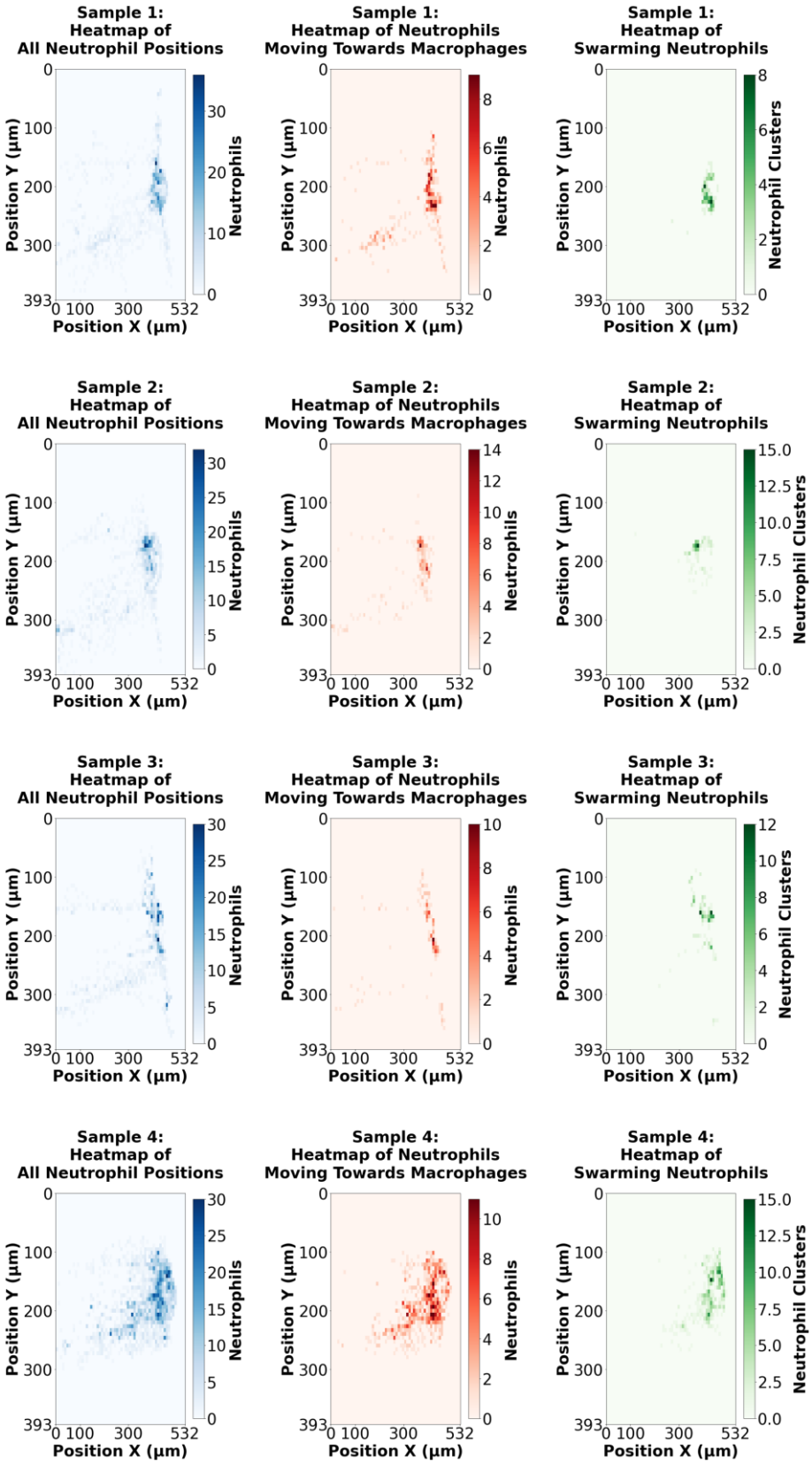

Supplemental Figure 2: Individual samples that made up Figure 36 Repeat 2.

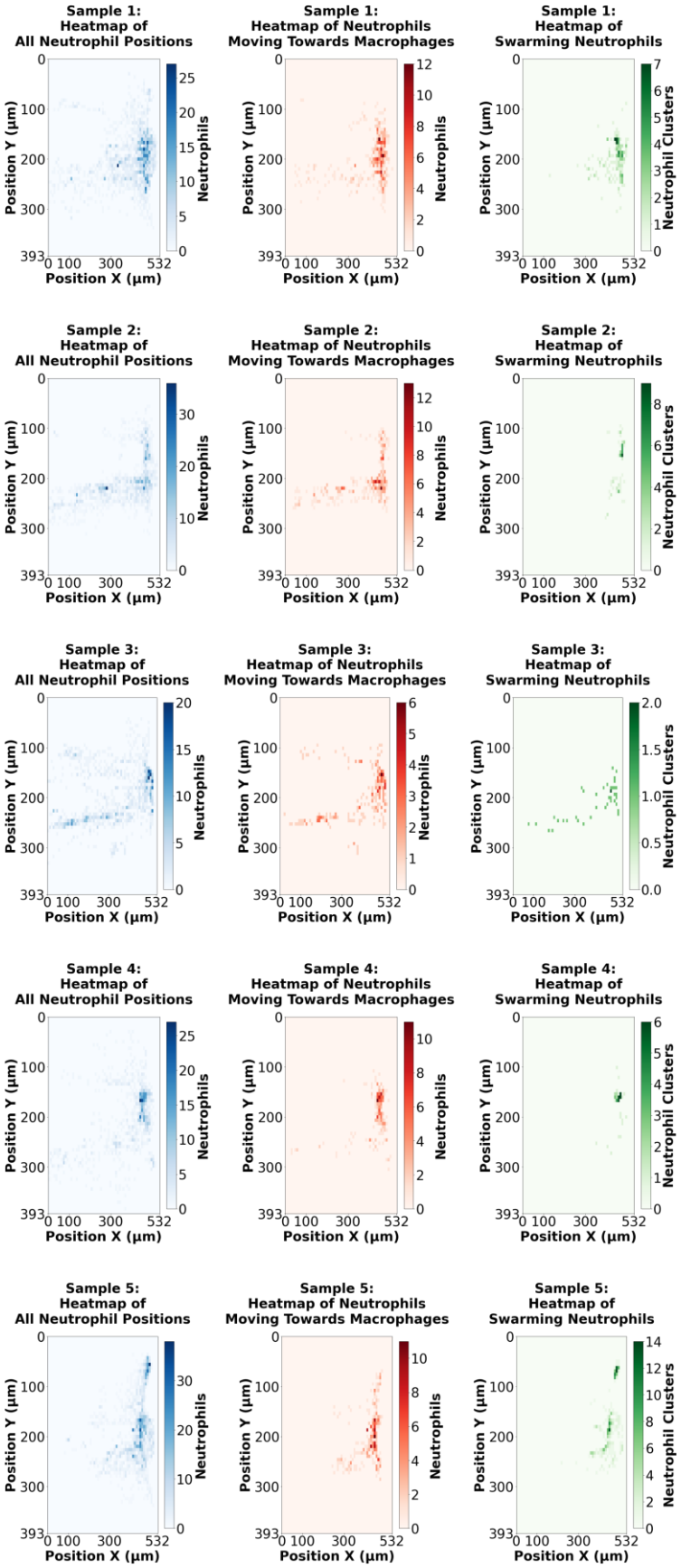

Supplemental Figure 3: Individual samples that made up Figure 36 Repeat 3.

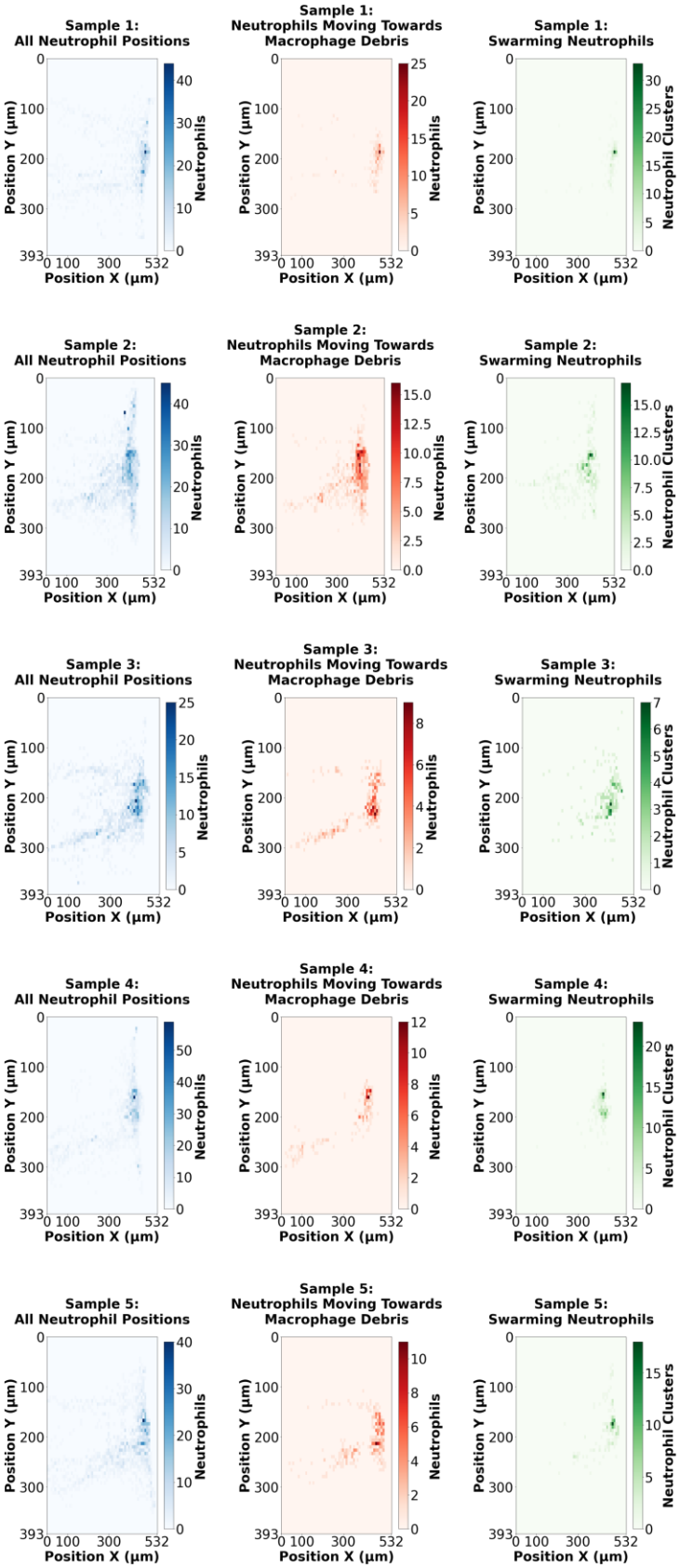

Supplemental Figure 4: Individual samples that made up Figure 37 Repeat 1.

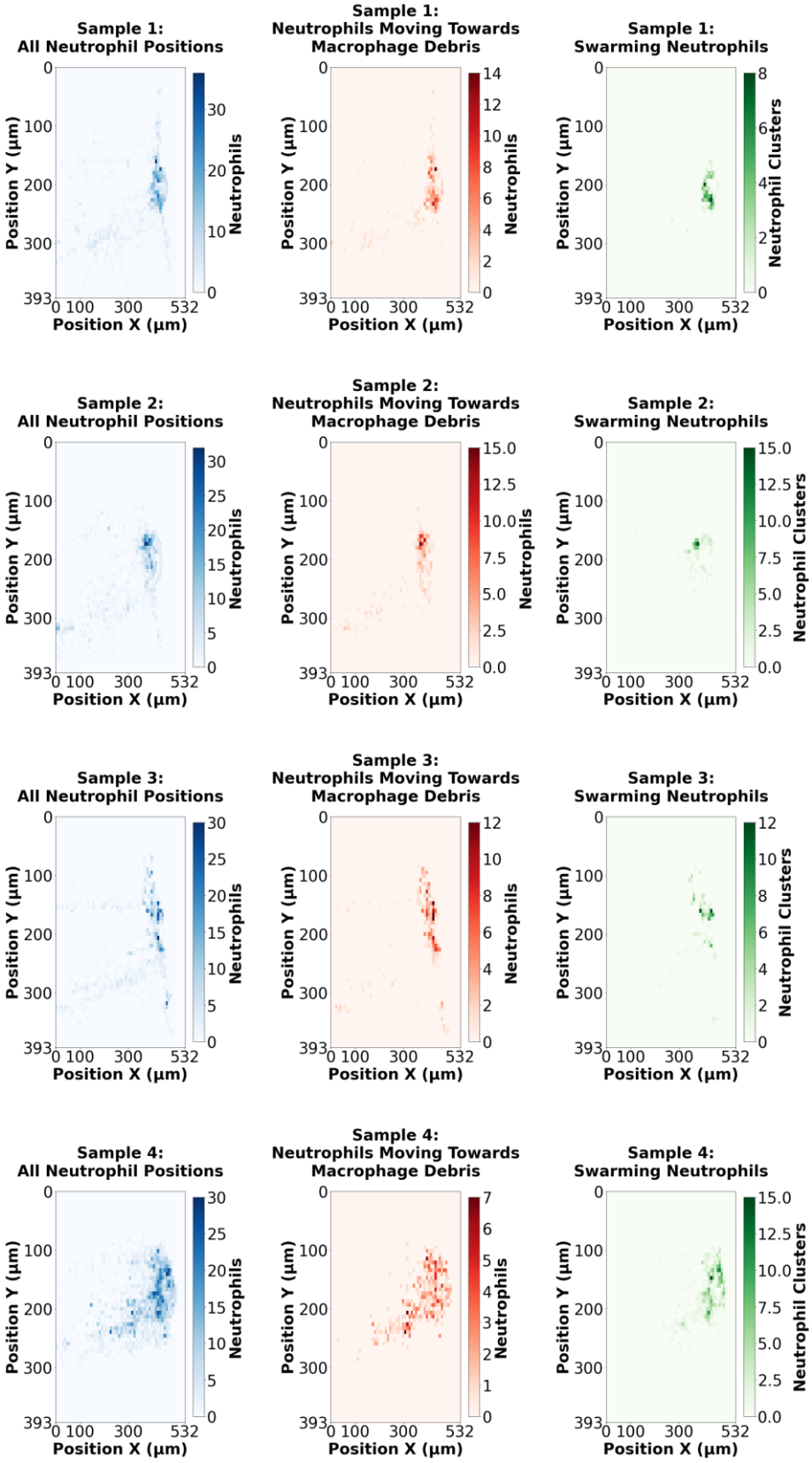

Supplemental Figure 5: Individual samples that made up Figure 37 Repeat 2.

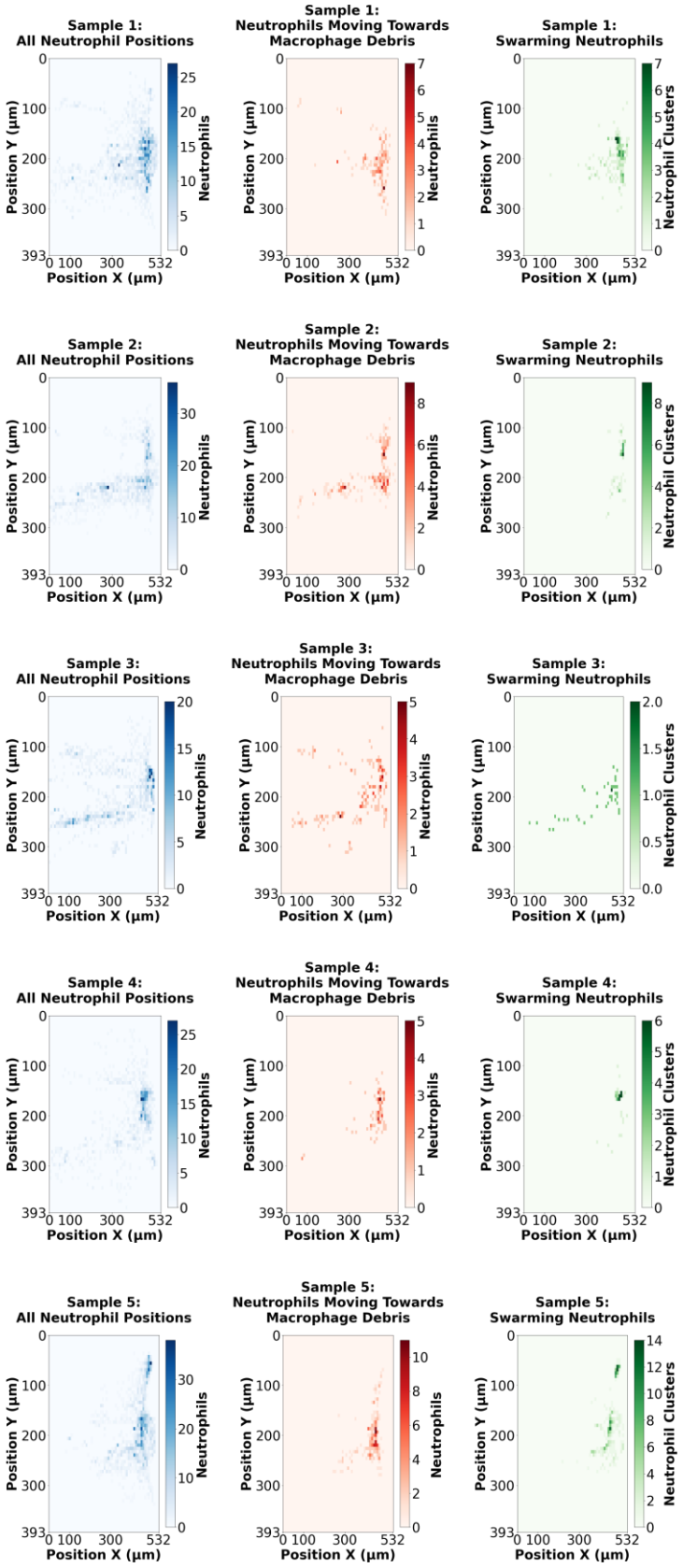

Supplemental Figure 6: Individual samples that made up Figure 37 Repeat 3.

5.3 Annex

To validate the code used for generation of neutrophil heat plots in **Chapter 3.4.3** I generated synthetic data for 3 different scenarios using a new python script included in the GitHub repository found in **Chapter 5.2**. This script generated a macrophage on a fixed spot in location x=200 and y=200. Neutrophils were then randomly populated in a range from x=50-450 and y=50-350. In the first scenario, neutrophils actively move away from the centred macrophage by using these formulas:

x = x_start - (200 – (x_start) * (frame / frames)

y = y_start - (200 – (y_start) * (frame / frames)

In the second scenario, neutrophils remain fully static. Finally, in the third scenario neutrophils actively move and converge towards the macrophage using these formulas:

x = x_start + (200 – (x_start) * (frame / frames)

y = y_start + (200 – (y_start) * (frame / frames)

In these formulas x and y are the current x and y coordinated of a neutrophil at a certain timepoint (frame), x_start and y_start are the x and y coordinates of these neutrophils at t=0 (frame=1).

In total 10 neutrophils are generated that travel over 10 time points (frames). Using this set-up the code should output 2 heatmaps that are one uniform colour, one for neutrophils moving away from the centre macrophage and one for neutrophils remaining static over time. Instead, the final scenario, where neutrophils are moving towards the macrophage, should result in a distinct heatmap with neutrophils showing up.

For the sake of handling of the data by the previously made heatmaps for swarms were also synthetically generated, however these were not taken into consideration for the plotting of the validation, as these are not representative swarming events. Looking at the plots generated in **Annex Figure 1**. We can see that the aforementioned expectations for the heatmaps are indeed met, indicating proper functioning of the analysis used for the heat plots in **Chapter 3.4.3**.

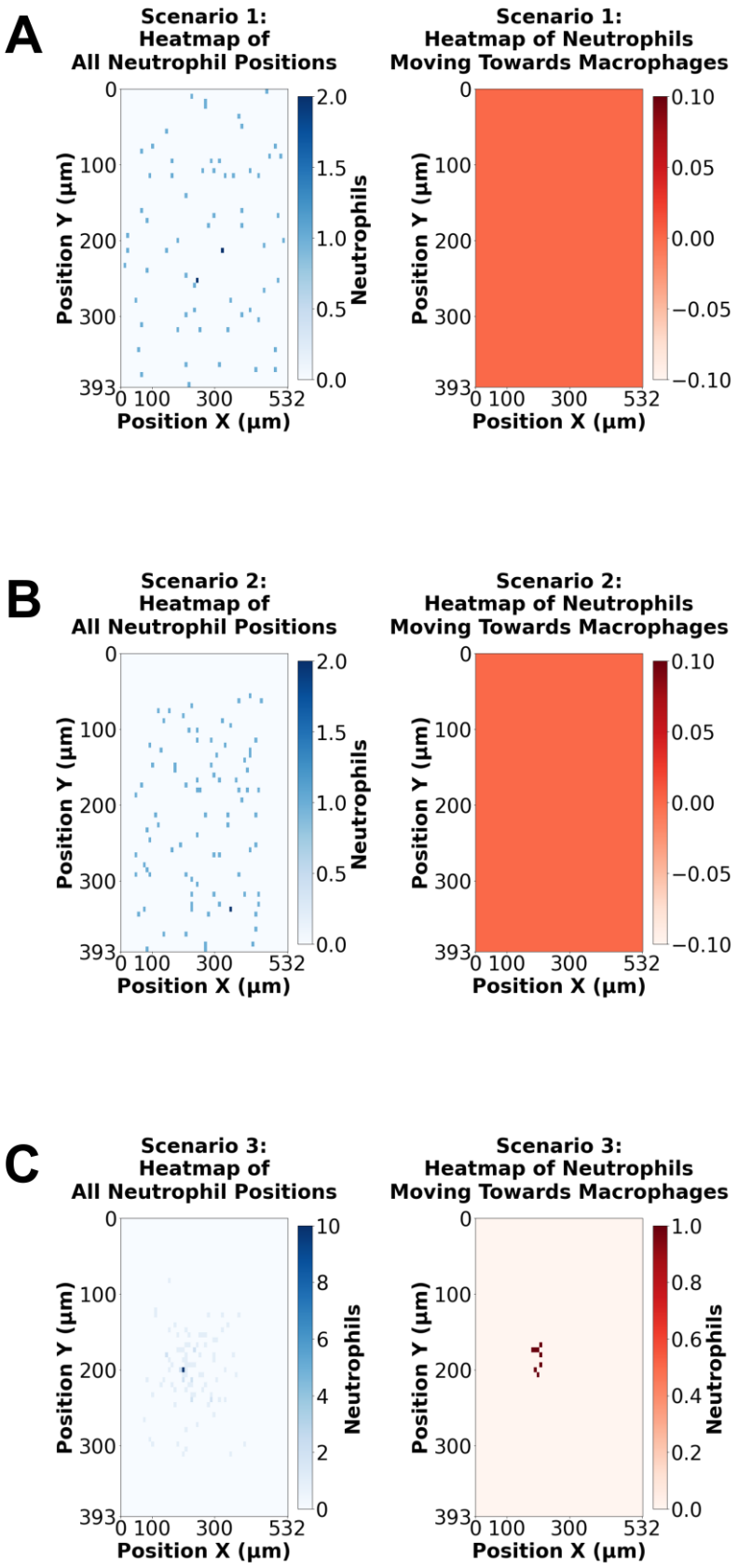

Annex Figure 1: Different scenarios for validation of code used to create heat plots.

This figure shows different scenarios of synthetically generated data, where neutrophils either move actively away from a single centred macrophage at x=200 and y=200, are static or move actively towards this macrophage. This is plotted as scenario 1, 2 and 3 respectively. And shows that only neutrophils moving towards the macrophage show up on the heatmap, validating code used in **Chapter 3.4.3**.

Chapter 6: Bibliography

ABTIN, A., JAIN, R., MITCHELL, A. J., ROEDIGER, B., BRZOSKA, A. J., TIKOO, S., CHENG, Q., NG, L. G., CAVANAGH, L. L., VON ANDRIAN, U. H., HICKEY, M. J., FIRTH, N. & WENINGER, W. 2014. Perivascular macrophages mediate neutrophil recruitment during bacterial skin infection. *Nat Immunol,* 15**,** 45-53.

AKKAYA, M., KWAK, K. & PIERCE, S. K. 2020. B cell memory: building two walls of protection against pathogens. *Nat Rev Immunol,* 20**,** 229-238.

ARATANI, Y. 2018. Myeloperoxidase: Its role for host defense, inflammation, and neutrophil function. *Arch Biochem Biophys,* 640**,** 47-52.

ARBONES, M. L., ORD, D. C., LEY, K., RATECH, H., MAYNARD-CURRY, C., OTTEN, G., CAPON, D. J. & TEDDER, T. F. 1994. Lymphocyte homing and leukocyte rolling and migration are impaired in L-selectin-deficient mice. *Immunity,* 1**,** 247-60.

BAO, L., GERARD, N. P., EDDY, R. L., JR., SHOWS, T. B. & GERARD, C. 1992. Mapping of genes for the human C5a receptor (C5AR), human FMLP receptor (FPR), and two FMLP receptor homologue orphan receptors (FPRH1, FPRH2) to chromosome 19. *Genomics,* 13**,** 437-40.

BARREIRO, O., YÁÑEZ-MÓ, M. A., SERRADOR, J. M., MONTOYA, M. A. C., VICENTE-MANZANARES, M., TEJEDOR, R., FURTHMAYR, H. & SÁNCHEZ-MADRID, F. 2002. Dynamic interaction of VCAM-1 and ICAM-1 with moesin and ezrin in a novel endothelial docking structure for adherent leukocytes. *Journal of Cell Biology,* 157**,** 1233-1245.

BERNUT, A., DUPONT, C., OGRYZKO, N. V., NEYRET, A., HERRMANN, J. L., FLOTO, R. A., RENSHAW, S. A. & KREMER, L. 2019. CFTR Protects against Mycobacterium abscessus Infection by Fine-Tuning Host Oxidative Defenses. *Cell Rep,* 26**,** 1828-1840 e4.

BERNUT, A., LOYNES, C. A., FLOTO, R. A. & RENSHAW, S. A. 2020. Deletion of cftr Leads to an Excessive Neutrophilic Response and Defective Tissue Repair in a Zebrafish Model of Sterile Inflammation. *Front Immunol,* 11**,** 1733.

BERTHELOOT, D., LATZ, E. & FRANKLIN, B. S. 2021. Necroptosis, pyroptosis and apoptosis: an intricate game of cell death. *Cell Mol Immunol,* 18**,** 1106-1121.

BERTHELOT, J.-M., LE GOFF, B., NEEL, A., MAUGARS, Y. & HAMIDOU, M. 2017. NETosis: At the crossroads of rheumatoid arthritis, lupus, and vasculitis. *Joint Bone Spine,* 84**,** 255-262.

BONAM, S. R., WANG, F. & MULLER, S. 2019. Lysosomes as a therapeutic target. *Nature Reviews Drug Discovery,* 18**,** 923-948.

BORELLI, V., BANFI, E., PERROTTA, M. G. & ZABUCCHI, G. 1999. Myeloperoxidase exerts microbicidal activity against Mycobacterium tuberculosis. *Infect Immun,* 67**,** 4149-52.

BORREGAARD, N. 2010. Neutrophils, from Marrow to Microbes. *Immunity,* 33**,** 657-670.

BORREGAARD, N. & COWLAND, J. B. 1997. Granules of the Human Neutrophilic Polymorphonuclear Leukocyte. *Blood,* 89**,** 3503-3521.

BOUEID, M. J., EL-HAGE, O., SCHUMACHER, M., DEGERNY, C. & TAWK, M. 2023. Zebrafish as an emerging model to study estrogen receptors in neural development. *Front Endocrinol (Lausanne),* 14**,** 1240018.

BRAEDON MCDONALD, K. P., 1 GUSTAVO B. MENEZES,1, * SIMON A. HIROTA, I. S., 1, CHRISTOPHER C. M. WATERHOUSE, 3 PAUL L. BECK,2,4 DANIEL A. MURUVE,1,4 PAUL KUBES1 & † 2010. Intravascular Danger Signals Guide Neutrophils to Sites of Sterile Inflammation. *Science,* Science. , 2010, Vol.330(6002), p.362-366.

BRINKMANN, V., REICHARD, U., GOOSMANN, C., FAULER, B., UHLEMANN, Y., WEISS, D. S., WEINRAUCH, Y. & ZYCHLINSKY, A. 2004. Neutrophil Extracellular Traps Kill Bacteria. *Science,* 303**,** 1532-1535.

BRITTON, K. N., JUDSON, R. S., HILL, B. N., JAREMA, K. A., OLIN, J. K., KNAPP, B. R., LOWERY, M., FESHUK, M., BROWN, J. & PADILLA, S. 2024. Using Zebrafish to Screen Developmental Toxicity of Per- and Polyfluoroalkyl Substances (PFAS). *Toxics,* 12.

BROWN, L. & YIPP, B. G. 2023. Neutrophil swarming: Is a good offense the best defense? *iScience,* 26**,** 107655.

BUCKLEY, C. D., ROSS, E. A., MCGETTRICK, H. M., OSBORNE, C. E., HAWORTH, O., SCHMUTZ, C., STONE, P. C. W., SALMON, M., MATHARU, N. M., VOHRA, R. K., NASH, G. B. & RAINGER, G. E. 2006. Identification of a phenotypically and functionally distinct population of long-lived neutrophils in a model of reverse endothelial migration. *Journal of Leukocyte Biology,* 79**,** 303-311.

BUI, T. M., WIESOLEK, H. L. & SUMAGIN, R. 2020. ICAM-1: A master regulator of cellular responses in inflammation, injury resolution, and tumorigenesis. *J Leukoc Biol,* 108**,** 787-799.

BURDETTE, B. E., ESPARZA, A. N., ZHU, H. & WANG, S. 2021. Gasdermin D in pyroptosis. *Acta Pharmaceutica Sinica B,* 11**,** 2768-2782.

CARMAN, C. V. & SPRINGER, T. A. 2004. A transmigratory cup in leukocyte diapedesis both through individual vascular endothelial cells and between them. *Journal of Cell Biology,* 167**,** 377-388.

CEN, X., LIU, S. & CHENG, K. 2018. The Role of Toll-Like Receptor in Inflammation and Tumor Immunity. *Front Pharmacol,* 9**,** 878.

CHAN, L., KARIMI, N., MOROVATI, S., ALIZADEH, K., KAKISH, J. E., VANDERKAMP, S., FAZEL, F., NAPOLEONI, C., ALIZADEH, K., MEHRANI, Y., MINOTT, J. A., BRIDLE, B. W. & KARIMI, K. 2021. The Roles of Neutrophils in Cytokine Storms. *Viruses,* 13**,** 2318.

CHEN, G., SHAW, M. H., KIM, Y.-G. & NUÑEZ, G. 2009. NOD-Like Receptors: Role in Innate Immunity and Inflammatory Disease. *Annual Review of Pathology: Mechanisms of Disease,* 4**,** 365-398.

CHEN, Y., LU, S., ZHANG, Y., YU, J., DENG, L., CHEN, H., ZHANG, Y., ZHOU, N., YUAN, K., YU, L., XIONG, Z., GUI, X., YU, Y. & MIN, W. 2019. TLR2 agonist Pam3CSK4 enhances the antibacterial functions of GM-CSF induced neutrophils to methicillin-resistant Staphylococcus aureus. *Microb Pathog,* 130**,** 204-212.

CHENG, K., GAO, M., GODFROY, J. I., BROWN, P. N., KASTELOWITZ, N. & YIN, H. 2015. Specific activation of the TLR1-TLR2 heterodimer by small-molecule agonists. *Sci Adv,* 1.

CHIA, K., KLINGSEISEN, A., SIEGER, D. & PRILLER, J. 2022. Zebrafish as a model organism for neurodegenerative disease. *Front Mol Neurosci,* 15**,** 940484.

CHRISTIE, S. M., FIJEN, C. & ROTHENBERG, E. 2022. V(D)J Recombination: Recent Insights in Formation of the Recombinase Complex and Recruitment of DNA Repair Machinery. *Front Cell Dev Biol,* 10**,** 886718.

CHTANOVA, T., SCHAEFFER, M., HAN, S.-J., VAN DOOREN, G. G., NOLLMANN, M., HERZMARK, P., CHAN, S. W., SATIJA, H., CAMFIELD, K., AARON, H., STRIEPEN, B. & ROBEY, E. A. 2008. Dynamics of Neutrophil Migration in Lymph Nodes during Infection. *Immunity,* 29**,** 487-496.

CHUA, F. 2006. Neutrophil Elastase: Mediator of Extracellular Matrix Destruction and Accumulation. *Proceedings of the American Thoracic Society,* 3**,** 424-427.

COLOM, B., JENNIFER, BEYRAU, M., WOODFIN, A., ODY, C., ROURKE, C., CHAVAKIS, T., BROHI, K., BEAT & NOURSHARGH, S. 2015. Leukotriene B4-Neutrophil Elastase Axis Drives Neutrophil Reverse Transendothelial Cell Migration In Vivo. *Immunity,* 42**,** 1075-1086.

COOMBS, C., GEORGANTZOGLOU, A., WALKER, H. A., PATT, J., MERTEN, N., POPLIMONT, H., BUSCH-NENTWICH, E. M., WILLIAMS, S., KOTSI, C., KOSTENIS, E. & SARRIS, M. 2019. Chemokine receptor trafficking coordinates neutrophil clustering and dispersal at wounds in zebrafish. *Nature Communications,* 10.

COX, G., CROSSLEY, J. & XING, Z. 1995. Macrophage engulfment of apoptotic neutrophils contributes to the resolution of acute pulmonary inflammation in vivo. *Am J Respir Cell Mol Biol,* 12**,** 232-7.

DA SILVA-FERREIRA, S., DUARTE-OLIVEIRA, C., ANTUNES, D., BARBOSA-MATOS, C., MENDES-FRIAS, A., TORRADO, E., COSTA, S., SILVESTRE, R., CUNHA, C. & CARVALHO, A. 2022. Hypoxia inducible-factor 1 alpha regulates neutrophil recruitment during fungal-elicited granulomatous inflammation. *Front Cell Infect Microbiol,* 12**,** 1005839.

DAHL, R., WALSH, J. C., LANCKI, D., LASLO, P., IYER, S. R., SINGH, H. & SIMON, M. C. 2003. Regulation of macrophage and neutrophil cell fates by the PU.1:C/EBP α ratio and granulocyte colony-stimulating factor. *Nature Immunology,* 4**,** 1029-1036.

DARBY, I. A. & HEWITSON, T. D. 2016. Hypoxia in tissue repair and fibrosis. *Cell Tissue Res,* 365**,** 553-62.

DASGUPTA, S., REDDAM, A., LIU, Z., LIU, J. & VOLZ, D. C. 2020. High-content screening in zebrafish identifies perfluorooctanesulfonamide as a potent developmental toxicant. *Environ Pollut,* 256**,** 113550.

DAVISON, J. M., AKITAKE, C. M., GOLL, M. G., RHEE, J. M., GOSSE, N., BAIER, H., HALPERN, M. E., LEACH, S. D. & PARSONS, M. J. 2007. Transactivation from Gal4-VP16 transgenic insertions for tissue-specific cell labeling and ablation in zebrafish. *Dev Biol,* 304**,** 811-24.

DE OLIVEIRA, S., ROSOWSKI, E. E. & HUTTENLOCHER, A. 2016. Neutrophil migration in infection and wound repair: going forward in reverse. *Nat Rev Immunol,* 16**,** 378-91.

DEE, C. T., NAGARAJU, R. T., ATHANASIADIS, E. I., GRAY, C., FERNANDEZ DEL AMA, L., JOHNSTON, S. A., SECOMBES, C. J., CVEJIC, A. & HURLSTONE, A. F. 2016. CD4-Transgenic Zebrafish Reveal Tissue-Resident Th2- and Regulatory T Cell-like Populations and Diverse Mononuclear Phagocytes. *J Immunol,* 197**,** 3520-3530.

DEKKERS, B. G. J., SAAD, S. I., VAN SPELDE, L. J. & BURGESS, J. K. 2021. Basement membranes in obstructive pulmonary diseases. *Matrix Biol Plus,* 12**,** 100092.

DUPRÉ-CROCHET, S., ERARD, M. & NÜ B E, O. 2013. ROS production in phagocytes: why, when, and where? *Journal of Leukocyte Biology,* 94**,** 657-670.

EL-ZAYAT, S. R., SIBAII, H. & MANNAA, F. A. 2019. Toll-like receptors activation, signaling, and targeting: an overview. *Bulletin of the National Research Centre,* 43.

ELKS, P. M., VAN EEDEN, F. J., DIXON, G., WANG, X., REYES-ALDASORO, C. C., INGHAM, P. W., WHYTE, M. K. B., WALMSLEY, S. R. & RENSHAW, S. A. 2011. Activation of hypoxia-inducible factor-1 α (Hif-1 α) delays inflammation resolution by reducing neutrophil apoptosis and reverse migration in a zebrafish inflammation model. *Blood,* 118**,** 712-722.

ELLETT, F., PASE, L., HAYMAN, J. W., ANDRIANOPOULOS, A. & LIESCHKE, G. J. 2011. mpeg1 promoter transgenes direct macrophage-lineage expression in zebrafish. *Blood,* 117**,** e49-56.

FENG, Y., SANTORIELLO, C., MIONE, M., HURLSTONE, A. & MARTIN, P. 2010. Live Imaging of Innate Immune Cell Sensing of Transformed Cells in Zebrafish Larvae: Parallels between Tumor Initiation and Wound Inflammation. *PLoS Biology,* 8**,** e1000562.

FILIPPI, M. D. 2019. Neutrophil transendothelial migration: updates and new perspectives. *Blood,* 133**,** 2149-2158.

FISHER, K. L., LU, J., RIDDLE, L., KIM, K. J., PRESTA, L. G. & BODARY, S. C. 1997. Identification of the binding site in intercellular adhesion molecule 1 for its receptor, leukocyte function-associated antigen 1. *Molecular Biology of the Cell,* 8**,** 501-515.

FOURNIER, B. 2012. The function of TLR2 during staphylococcal diseases. *Front Cell Infect Microbiol,* 2**,** 167.

FRANK, D. & VINCE, J. E. 2019. Pyroptosis versus necroptosis: similarities, differences, and crosstalk. *Cell Death Differ,* 26**,** 99-114.

FU, J., ZONG, X., JIN, M., MIN, J., WANG, F. & WANG, Y. 2023. Mechanisms and regulation of defensins in host defense. *Signal Transduct Target Ther,* 8**,** 300.

GAGGAR, A., JACKSON, P. L., NOERAGER, B. D., O'REILLY, P. J., MCQUAID, D. B., ROWE, S. M., CLANCY, J. P. & BLALOCK, J. E. 2008. A novel proteolytic cascade generates an extracellular matrix-derived chemoattractant in chronic neutrophilic inflammation. *J Immunol,* 180**,** 5662-9.

GALLI, S. J., BORREGAARD, N. & WYNN, T. A. 2011. Phenotypic and functional plasticity of cells of innate immunity: macrophages, mast cells and neutrophils. *Nature Immunology,* 12**,** 1035-1044.

GARCIA-LOPEZ, J. P., GRIMALDI, A., CHEN, Z., MENESES, C., BRAVO-TELLO, K., BRESCIANI, E., BANDERAS, A., BURGESS, S. M., HERNANDEZ, P. P. & FEIJOO, C. G. 2023. Ontogenetically distinct neutrophils differ in function and transcriptional profile in zebrafish. *Nat Commun,* 14**,** 4942.

GOLENKINA, E. A., VIRYASOVA, G. M., GALKINA, S. I., KONDRATENKO, N. D., GAPONOVA, T. V., ROMANOVA, Y. M., LYAMZAEV, K. G., CHERNYAK, B. V. & SUD'INA, G. F. 2024. Redox processes are major regulators of leukotriene synthesis in neutrophils exposed to bacteria Salmonella typhimurium; the way to manipulate neutrophil swarming. *Front Immunol,* 15**,** 1295150.

GRASSI, L., POURFARZAD, F., ULLRICH, S., MERKEL, A., WERE, F., CARRILLO-DE-SANTA-PAU, E., YI, G., HIEMSTRA, I. H., TOOL, A. T. J., MUL, E., PERNER, J., JANSSEN-MEGENS, E., BERENTSEN, K., KERSTENS, H., HABIBI, E., GUT, M., YASPO, M. L., LINSER, M., LOWY, E., DATTA, A., CLARKE, L., FLICEK, P., VINGRON, M., ROOS, D., VAN DEN BERG, T. K., HEATH, S., RICO, D., FRONTINI, M., KOSTADIMA, M., GUT, I., VALENCIA, A., OUWEHAND, W. H., STUNNENBERG, H. G., MARTENS, J. H. A. & KUIJPERS, T. W. 2018. Dynamics of Transcription Regulation in Human Bone Marrow Myeloid Differentiation to Mature Blood Neutrophils. *Cell Reports,* 24**,** 2784-2794.

GRIGG, J. M., SAVILL, J. S., SARRAF, C., HASLETT, C. & SILVERMAN, M. 1991. Neutrophil apoptosis and clearance from neonatal lungs. *Lancet,* 338**,** 720-2.

GRONLOH, M. L. B., ARTS, J. J. G. & VAN BUUL, J. D. 2021. Neutrophil transendothelial migration hotspots - mechanisms and implications. *J Cell Sci,* 134.

GUAN, Y., OMUETI-AYOADE, K., MUTHA, S. K., HERGENROTHER, P. J. & TAPPING, R. I. 2010. Identification of novel synthetic toll-like receptor 2 agonists by high throughput screening. *J Biol Chem,* 285**,** 23755-62.

GUREVICH, V. V. & GUREVICH, E. V. 2019. GPCR Signaling Regulation: The Role of GRKs and Arrestins. *Front Pharmacol,* 10**,** 125.

HALL, C., FLORES, M. V., STORM, T., CROSIER, K. & CROSIER, P. 2007. The zebrafish lysozyme C promoter drives myeloid-specific expression in transgenic fish. *BMC Dev Biol,* 7**,** 42.

HE, R., CHEN, Y. & CAI, Q. 2020. The role of the LTB4-BLT1 axis in health and disease. *Pharmacol Res,* 158**,** 104857.

HEIT, B., TAVENER, S., RAHARJO, E. & KUBES, P. 2002. An intracellular signaling hierarchy determines direction of migration in opposing chemotactic gradients. *J Cell Biol,* 159**,** 91-102.

HIDALGO, A., CHILVERS, E. R., SUMMERS, C. & KOENDERMAN, L. 2019. The Neutrophil Life Cycle. *Trends Immunol,* 40**,** 584-597.

HIRCHE, T. O., GAUT, J. P., HEINECKE, J. W. & BELAAOUAJ, A. 2005. Myeloperoxidase Plays Critical Roles in KillingKlebsiella pneumoniaeand Inactivating Neutrophil Elastase: Effects on Host Defense. *The Journal of Immunology,* 174**,** 1557-1565.

HOENDERDOS, K. & CONDLIFFE, A. 2013. The Neutrophil in Chronic Obstructive Pulmonary Disease. Too Little, Too Late or Too Much, Too Soon? *American Journal of Respiratory Cell and Molecular Biology,* 48**,** 531-539.

HOENDERDOS, K., LODGE, K. M., HIRST, R. A., CHEN, C., PALAZZO, S. G. C., EMERENCIANA, A., SUMMERS, C., ANGYAL, A., PORTER, L., JUSS, J. K., O'CALLAGHAN, C., CHILVERS, E. R. & CONDLIFFE, A. M. 2016. Hypoxia upregulates neutrophil degranulation and potential for tissue injury. *Thorax,* 71**,** 1030-1038.

HON, W. C., WILSON, M. I., HARLOS, K., CLARIDGE, T. D., SCHOFIELD, C. J., PUGH, C. W., MAXWELL, P. H., RATCLIFFE, P. J., STUART, D. I. & JONES, E. Y. 2002. Structural basis for the recognition of hydroxyproline in HIF-1 alpha by pVHL. *Nature,* 417**,** 975-8.

HOPKE, A., LIN, T., SCHERER, A. K., SHAY, A. E., TIMMER, K. D., WILSON-MIFSUD, B., MANSOUR, M. K., SERHAN, C. N., IRIMIA, D. & HURLEY, B. P. 2022. Transcellular biosynthesis of leukotriene B(4) orchestrates neutrophil swarming to fungi. *iScience,* 25**,** 105226.

HOPKE, A., SCHERER, A., KREUZBURG, S., ABERS, M. S., ZERBE, C. S., DINAUER, M. C., MANSOUR, M. K. & IRIMIA, D. 2020. Neutrophil swarming delays the growth of clusters of pathogenic fungi. *Nature Communications,* 11.

HU, W., VAN STEIJN, L., LI, C., VERBEEK, F. J., CAO, L., MERKS, R. M. H. & SPAINK, H. P. 2021. A Novel Function of TLR2 and MyD88 in the Regulation of Leukocyte Cell Migration Behavior During Wounding in Zebrafish Larvae. *Front Cell Dev Biol,* 9**,** 624571.

HUANG, J., HONG, W., WAN, M. & ZHENG, L. 2022. Molecular mechanisms and therapeutic target of NETosis in diseases. *MedComm (2020),* 3**,** e162.

HUTTENLOCHER, A. & POZNANSKY, M. C. 2008. Reverse leukocyte migration can be attractive or repulsive. *Trends Cell Biol,* 18**,** 298-306.

ISLES, H. M., HERMAN, K. D., ROBERTSON, A. L., LOYNES, C. A., PRINCE, L. R., ELKS, P. M. & RENSHAW, S. A. 2019. The CXCL12/CXCR4 Signaling Axis Retains Neutrophils at Inflammatory Sites in Zebrafish. *Front Immunol,* 10**,** 1784.

ISLES, H. M., LOYNES, C. A., ALASMARI, S., KON, F. C., HENRY, K. M., KADOCHNIKOVA, A., HALES, J., MUIR, C. F., KEIGHTLEY, M. C., KADIRKAMANATHAN, V., HAMILTON, N., LIESCHKE, G. J., RENSHAW, S. A. & ELKS, P. M. 2021. Pioneer neutrophils release chromatin within in vivo swarms. *Elife,* 10.

JACKSON, D. G. 2022. Immune Cell Trafficking in the Lymphatics, Hyaluronan Biology and Tumour Metastasis. *In:* LEONG, S. P., NATHANSON, S. D. & ZAGER, J. S. (eds.) *Cancer Metastasis Through the Lymphovascular System.* Cham: Springer International Publishing.

JACOB, S. W. & HERSCHLER, R. 1986. Pharmacology of DMSO. *Cryobiology,* 23**,** 14-27.

JAQAMAN, K., LOERKE, D., METTLEN, M., KUWATA, H., GRINSTEIN, S., SCHMID, S. L. & DANUSER, G. 2008. Robust single-particle tracking in live-cell time-lapse sequences. *Nat Methods,* 5**,** 695-702.

JITKA, MICHAELI, J., ASSI, S., MISHALIAN, I., KISOS, H., LEVY, L., DAMTI, P., LUMBROSO, D., POLYANSKY, L., RONIT, ARIEL, A., HOVAV, A.-H., HENKE, E., ZVI & GRANOT, Z. 2015. Phenotypic Diversity and Plasticity in Circulating Neutrophil Subpopulations in Cancer. *Cell Reports,* 10**,** 562-573.

JORCH, S. K. & KUBES, P. 2017. An emerging role for neutrophil extracellular traps in noninfectious disease. *Nature Medicine,* 23**,** 279-287.

KAMBAYASHI, T. & LAUFER, T. M. 2014. Atypical MHC class II-expressing antigen-presenting cells: can anything replace a dendritic cell? *Nat Rev Immunol,* 14**,** 719-30.

KAMENYEVA, O., BOULARAN, C., KABAT, J., CHEUNG, G. Y. C., CICALA, C., YEH, A. J., CHAN, J. L., PERIASAMY, S., OTTO, M. & KEHRL, J. H. 2015. Neutrophil Recruitment to Lymph Nodes Limits Local Humoral Response to Staphylococcus aureus. *PLOS Pathogens,* 11**,** e1004827.

KAMUYANGO, A. A. 2017. *STIMULATION OF INNATE IMMUNITY LEADS TO*

CLEARANCE OF C. NEOFORMANS INFECTION IN

ZEBRAFISH. PhD PhD, Unviersity of Sheffield.

KHOYRATTY, T. E., AI, Z., BALLESTEROS, I., EAMES, H. L., MATHIE, S., MARTÍN-SALAMANCA, S., WANG, L., HEMMINGS, A., WILLEMSEN, N., VON WERZ, V., ZEHRER, A., WALZOG, B., VAN GRINSVEN, E., HIDALGO, A. & UDALOVA, I. A. 2021. Distinct transcription factor networks control neutrophil-driven inflammation. *Nature Immunology,* 22**,** 1093-1106.

KIENLE, K., GLASER, K. M., EICKHOFF, S., MIHLAN, M., KNOPPER, K., REATEGUI, E., EPPLE, M. W., GUNZER, M., BAUMEISTER, R., TARRANT, T. K., GERMAIN, R. N., IRIMIA, D., KASTENMULLER, W. & LAMMERMANN, T. 2021. Neutrophils self-limit swarming to contain bacterial growth in vivo. *Science,* 372.

KIENLE, K. & LAMMERMANN, T. 2016. Neutrophil swarming: an essential process of the neutrophil tissue response. *Immunol Rev,* 273**,** 76-93.

KIRCHEIS, R. & PLANZ, O. 2023. The Role of Toll-like Receptors (TLRs) and Their Related Signaling Pathways in Viral Infection and Inflammation. *Int J Mol Sci,* 24.

KOLACZKOWSKA, E. & KUBES, P. 2013. Neutrophil recruitment and function in health and inflammation. *Nature Reviews Immunology,* 13**,** 159-175.

KOSKINEN, K., VAINIO, P. J., SMITH, D. J., PIHLAVISTO, M., YLÄ-HERTTUALA, S., JALKANEN, S. & SALMI, M. 2004. Granulocyte transmigration through the endothelium is regulated by the oxidase activity of vascular adhesion protein-1 (VAP-1). *Blood,* 103**,** 3388-3395.
KRYSKO, D. V., GARG, A. D., KACZMAREK, A., KRYSKO, O., AGOSTINIS, P. & VANDENABEELE, P. 2012. Immunogenic cell death and DAMPs in cancer therapy. *Nature Reviews Cancer,* 12**,** 860-875.
KUBAICHUK, K. & KIETZMANN, T. 2019. Involvement of E3 Ligases and Deubiquitinases in the Control of HIF-alpha Subunit Abundance. *Cells,* 8.
LACY, P. 2006. Mechanisms of Degranulation in Neutrophils. *Allergy, Asthma & Clinical Immunology,* 2**,** 98.
LÄMMERMANN, T. 2016. In the eye of the neutrophil swarm-navigation signals that bring neutrophils together in inflamed and infected tissues. *Journal of Leukocyte Biology,* 100**,** 55-63.
LÄMMERMANN, T., AFONSO, P. V., ANGERMANN, B. R., WANG, J. M., KASTENMÜLLER, W., PARENT, C. A. & GERMAIN, R. N. 2013. Neutrophil swarms require LTB4 and integrins at sites of cell death in vivo. *Nature,* 498**,** 371-375.
LECKBAND, D. E. & DE ROOIJ, J. 2014. Cadherin Adhesion and Mechanotransduction. *Annual Review of Cell and Developmental Biology,* 30**,** 291-315.
LEE, H.-J., WOO, Y., HAHN, T.-W., JUNG, Y. M. & JUNG, Y.-J. 2020. Formation and Maturation of the Phagosome: A Key Mechanism in Innate Immunity against Intracellular Bacterial Infection. *Microorganisms,* 8**,** 1298.
LEE, W. L., HARRISON, R. E. & GRINSTEIN, S. 2003. Phagocytosis by neutrophils. *Microbes Infect,* 5**,** 1299-306.
LI, D. & WU, M. 2021. Pattern recognition receptors in health and diseases. *Signal Transduct Target Ther,* 6**,** 291.
LI, L., JIN, H., XU, J., SHI, Y. & WEN, Z. 2011. Irf8 regulates macrophage versus neutrophil fate during zebrafish primitive myelopoiesis. *Blood,* 117**,** 1359-69.
LI, L., YAN, B., SHI, Y. Q., ZHANG, W. Q. & WEN, Z. L. 2012. Live imaging reveals differing roles of macrophages and neutrophils during zebrafish tail fin regeneration. *J Biol Chem,* 287**,** 25353-60.
LI, P., ZHOU, L., ZHAO, T., LIU, X., ZHANG, P., LIU, Y., ZHENG, X. & LI, Q. 2017. Caspase-9: structure, mechanisms and clinical application. *Oncotarget,* 8**,** 23996-24008.
LIESCHKE, G., GRAIL, D., HODGSON, G., METCALF, D., STANLEY, E., CHEERS, C., FOWLER, K., BASU, S., ZHAN, Y. & DUNN, A. 1994. Mice lacking granulocyte colony-stimulating factor have chronic neutropenia, granulocyte and macrophage progenitor cell deficiency, and impaired neutrophil mobilization. *Blood,* 84**,** 1737-1746.
LIU, Q. 2023. *Real time in vivo investigation of nanoparticle dynamics and immune response during ventilator-assisted nanoparticle inhalation.* Ph.D, Ludwig-Maximilians-Universität zu München.
LIU, Y., FANG, Y., CHEN, X., WANG, Z., LIANG, X., ZHANG, T., LIU, M., ZHOU, N., LV, J., TANG, K., XIE, J., GAO, Y., CHENG, F., ZHOU, Y., ZHANG, Z., HU, Y., ZHANG, X., GAO, Q., ZHANG, Y. & HUANG, B. 2020. Gasdermin E-mediated target cell pyroptosis by CAR T cells triggers cytokine release syndrome. *Sci Immunol,* 5.
LODGE, K. M., COWBURN, A. S., LI, W. & CONDLIFFE, A. M. 2020. The Impact of Hypoxia on Neutrophil Degranulation and Consequences for the Host. *International Journal of Molecular Sciences,* 21**,** 1183.
LOYNES, C. A., LEE, J. A., ROBERTSON, A. L., STEEL, M. J., ELLETT, F., FENG, Y., LEVY, B. D., WHYTE, M. K. B. & RENSHAW, S. A. 2018. PGE(2) production at sites of tissue injury promotes an anti-inflammatory neutrophil phenotype and determines the outcome of inflammation resolution in vivo. *Sci Adv,* 4**,** eaar8320.
LOYNES, C. A., MARTIN, J. S., ROBERTSON, A., TRUSHELL, D. M., INGHAM, P. W., WHYTE, M. K. & RENSHAW, S. A. 2010. Pivotal Advance: Pharmacological manipulation of inflammation

resolution during spontaneously resolving tissue neutrophilia in the zebrafish. *J Leukoc Biol,* 87**,** 203-12.
MALENGIER-DEVLIES, B., METZEMAEKERS, M., WOUTERS, C., PROOST, P. & MATTHYS, P. 2021. Neutrophil Homeostasis and Emergency Granulopoiesis: The Example of Systemic Juvenile Idiopathic Arthritis. *Front Immunol,* 12**,** 766620.
MANZ, M. G. & BOETTCHER, S. 2014. Emergency granulopoiesis. *Nat Rev Immunol,* 14**,** 302-14.
MASSON, N., WILLAM, C., MAXWELL, P. H., PUGH, C. W. & RATCLIFFE, P. J. 2001. Independent function of two destruction domains in hypoxia-inducible factor-alpha chains activated by prolyl hydroxylation. *EMBO J,* 20**,** 5197-206.
MATHIAS, J. R., PERRIN, B. J., LIU, T.-X., KANKI, J., LOOK, A. T. & HUTTENLOCHER, A. 2006. Resolution of inflammation by retrograde chemotaxis of neutrophils in transgenic zebrafish. *Journal of Leukocyte Biology,* 80**,** 1281-1288.
MCCONNELL, S. C., HERNANDEZ, K. M., ANDRADE, J. & DE JONG, J. L. O. 2023. Immune gene variation associated with chromosome-scale differences among individual zebrafish genomes. *Sci Rep,* 13**,** 7777.
MCGOVERN, N. N., COWBURN, A. S., PORTER, L., WALMSLEY, S. R., SUMMERS, C., THOMPSON, A. A. R., ANWAR, S., WILLCOCKS, L. C., WHYTE, M. K. B., CONDLIFFE, A. M. & CHILVERS, E. R. 2011. Hypoxia Selectively Inhibits Respiratory Burst Activity and Killing ofStaphylococcus aureusin Human Neutrophils. *The Journal of Immunology,* 186**,** 453-463.
MCHALE, J. F., HARARI, O. A., MARSHALL, D. & HASKARD, D. O. 1999. TNF-alpha and IL-1 sequentially induce endothelial ICAM-1 and VCAM-1 expression in MRL/lpr lupus-prone mice. *J Immunol,* 163**,** 3993-4000.
MCKENNA, E., WUBBEN, R., ISAZA-CORREA, J. M., MELO, A. M., MHAONAIGH, A. U., CONLON, N., O'DONNELL, J. S., NI CHEALLAIGH, C., HURLEY, T., STEVENSON, N. J., LITTLE, M. A. & MOLLOY, E. J. 2022. Neutrophils in COVID-19: Not Innocent Bystanders. *Front Immunol,* 13**,** 864387.
MEHTA, H. M., MALANDRA, M. & COREY, S. J. 2015. G-CSF and GM-CSF in Neutropenia. *J Immunol,* 195**,** 1341-9.
MEIJER, A. H. 2016. Protection and pathology in TB: learning from the zebrafish model. *Semin Immunopathol,* 38**,** 261-73.
METZEMAEKERS, M., GOUWY, M. & PROOST, P. 2020. Neutrophil chemoattractant receptors in health and disease: double-edged swords. *Cell Mol Immunol,* 17**,** 433-450.
MIAO, K. Z., KIM, G. Y., MEARA, G. K., QIN, X. & FENG, H. 2021. Tipping the Scales With Zebrafish to Understand Adaptive Tumor Immunity. *Front Cell Dev Biol,* 9**,** 660969.
MIFFLIN, L., OFENGEIM, D. & YUAN, J. 2020. Receptor-interacting protein kinase 1 (RIPK1) as a therapeutic target. *Nature Reviews Drug Discovery,* 19**,** 553-571.
MIN, J. H., YANG, H., IVAN, M., GERTLER, F., KAELIN, W. G., JR. & PAVLETICH, N. P. 2002. Structure of an HIF-1alpha -pVHL complex: hydroxyproline recognition in signaling. *Science,* 296**,** 1886-9.
MIRALDA, I., URIARTE, S. M. & MCLEISH, K. R. 2017. Multiple Phenotypic Changes Define Neutrophil Priming. *Front Cell Infect Microbiol,* 7**,** 217.
MOCSAI, A., LIGETI, E., LOWELL, C. A. & BERTON, G. 1999. Adhesion-dependent degranulation of neutrophils requires the Src family kinases Fgr and Hck. *J Immunol,* 162**,** 1120-6.
MORENO, S. G. 2018. Depleting Macrophages In Vivo with Clodronate-Liposomes. *Methods Mol Biol,* 1784**,** 259-262.
MOVAFAGH, S., CROOK, S. & VO, K. 2015. Regulation of hypoxia-inducible factor-1a by reactive oxygen species: new developments in an old debate. *J Cell Biochem,* 116**,** 696-703.
MYERS, C. L., WERTHEIMER, S. J., SCHEMBRI-KING, J., PARKS, T. & WALLACE, R. W. 1992. Induction of ICAM-1 by TNF-alpha, IL-1 beta, and LPS in human endothelial cells after downregulation of PKC. *Am J Physiol,* 263**,** C767-72.

NAEGELEN, I., BEAUME, N., PLANÇON, S., SCHENTEN, V., TSCHIRHART, E. J. & BRÉCHARD, S. 2015. Regulation of Neutrophil Degranulation and Cytokine Secretion: A Novel Model Approach Based on Linear Fitting. *Journal of Immunology Research,* 2015**,** 1-15.

NERLOV, C. & GRAF, T. 1998. PU.1 induces myeloid lineage commitment in multipotent hematopoietic progenitors. *Genes & Development,* 12**,** 2403-2412.

NG, L. G., OSTUNI, R. & HIDALGO, A. 2019. Heterogeneity of neutrophils. *Nat Rev Immunol,* 19**,** 255-265.

NG, L. G., QIN, J. S., ROEDIGER, B., WANG, Y., JAIN, R., CAVANAGH, L. L., SMITH, A. L., JONES, C. A., DE VEER, M., GRIMBALDESTON, M. A., MEEUSEN, E. N. & WENINGER, W. 2011. Visualizing the Neutrophil Response to Sterile Tissue Injury in Mouse Dermis Reveals a Three-Phase Cascade of Events. *Journal of Investigative Dermatology,* 131**,** 2058-2068.

NGUYEN-CHI, M., LAPLACE-BUILHE, B., TRAVNICKOVA, J., LUZ-CRAWFORD, P., TEJEDOR, G., LUTFALLA, G., KISSA, K., JORGENSEN, C. & DJOUAD, F. 2017. TNF signaling and macrophages govern fin regeneration in zebrafish larvae. *Cell Death Dis,* 8**,** e2979.

NGUYEN-CHI, M., LAPLACE-BUILHE, B., TRAVNICKOVA, J., LUZ-CRAWFORD, P., TEJEDOR, G., PHAN, Q. T., DUROUX-RICHARD, I., LEVRAUD, J. P., KISSA, K., LUTFALLA, G., JORGENSEN, C. & DJOUAD, F. 2015. Identification of polarized macrophage subsets in zebrafish. *Elife,* 4**,** e07288.

NIETHAMMER, P., GRABHER, C., LOOK, A. T. & MITCHISON, T. J. 2009. A tissue-scale gradient of hydrogen peroxide mediates rapid wound detection in zebrafish. *Nature,* 459**,** 996-999.

NOURSHARGH, S., RENSHAW, S. A. & IMHOF, B. A. 2016. Reverse Migration of Neutrophils: Where, When, How, and Why? *Trends Immunol,* 37**,** 273-286.

OEHLERS, S. H., CRONAN, M. R., SCOTT, N. R., THOMAS, M. I., OKUDA, K. S., WALTON, E. M., BEERMAN, R. W., CROSIER, P. S. & TOBIN, D. M. 2015. Interception of host angiogenic signalling limits mycobacterial growth. *Nature,* 517**,** 612-5.

OWEN-WOODS, C., JOULIA, R., BARKAWAY, A., ROLAS, L., MA, B., NOTTEBAUM, A. F., ARKILL, K. P., STEIN, M., GIRBL, T., GOLDING, M., BATES, D. O., VESTWEBER, D., VOISIN, M. B. & NOURSHARGH, S. 2020. Local microvascular leakage promotes trafficking of activated neutrophils to remote organs. *J Clin Invest,* 130**,** 2301-2318.

PANDAY, A., SAHOO, M. K., OSORIO, D. & BATRA, S. 2015. NADPH oxidases: an overview from structure to innate immunity-associated pathologies. *Cellular & Molecular Immunology,* 12**,** 5-23.

PAPAYANNOPOULOS, V., METZLER, K. D., HAKKIM, A. & ZYCHLINSKY, A. 2010. Neutrophil elastase and myeloperoxidase regulate the formation of neutrophil extracellular traps. *Journal of Cell Biology,* 191**,** 677-691.

PARRA-IZQUIERDO, I., LAKSHMANAN, H. H. S., MELROSE, A. R., PANG, J., ZHENG, T. J., JORDAN, K. R., REITSMA, S. E., MCCARTY, O. J. T. & ASLAN, J. E. 2021. The Toll-Like Receptor 2 Ligand Pam2CSK4 Activates Platelet Nuclear Factor-kappaB and Bruton's Tyrosine Kinase Signaling to Promote Platelet-Endothelial Cell Interactions. *Front Immunol,* 12**,** 729951.

PATEL, S., FU, S., MASTIO, J., DOMINGUEZ, G. A., PUROHIT, A., KOSSENKOV, A., LIN, C., ALICEA-TORRES, K., SEHGAL, M., NEFEDOVA, Y., ZHOU, J., LANGUINO, L. R., CLENDENIN, C., VONDERHEIDE, R. H., MULLIGAN, C., NAM, B., HOCKSTEIN, N., MASTERS, G., GUARINO, M., SCHUG, Z. T., ALTIERI, D. C. & GABRILOVICH, D. I. 2018. Unique pattern of neutrophil migration and function during tumor progression. *Nat Immunol,* 19**,** 1236-1247.

PETERS-GOLDEN, M. & BROCK, T. G. 2003. 5-lipoxygenase and FLAP. *Prostaglandins Leukot Essent Fatty Acids,* 69**,** 99-109.

PETERS-GOLDEN, M. & HENDERSON, W. R., JR. 2007. Leukotrienes. *N Engl J Med,* 357**,** 1841-54.

PETERS, N. C., EGEN, J. G., SECUNDINO, N., DEBRABANT, A., KIMBLIN, N., KAMHAWI, S., LAWYER, P., FAY, M. P., GERMAIN, R. N. & SACKS, D. 2008. In Vivo Imaging Reveals an Essential Role for Neutrophils in Leishmaniasis Transmitted by Sand Flies. *Science,* 321**,** 970-974.

PETRETTO, A., BRUSCHI, M., PRATESI, F., CROIA, C., CANDIANO, G., GHIGGERI, G. & MIGLIORINI, P. 2019. Neutrophil extracellular traps (NET) induced by different stimuli: A comparative proteomic analysis. *PLOS ONE,* 14**,** e0218946.

PETRI, B., PHILLIPSON, M. & KUBES, P. 2008. The Physiology of Leukocyte Recruitment: An In Vivo Perspective. *The Journal of Immunology,* 180**,** 6439-6446.

PHAN, Q. T., SIPKA, T., GONZALEZ, C., LEVRAUD, J.-P., LUTFALLA, G. & NGUYEN-CHI, M. 2018. Neutrophils use superoxide to control bacterial infection at a distance. *PLOS Pathogens,* 14**,** e1007157.

PHILIPPE, JANKA-JUNTTILA, M., YOUNG, COLIN, CHARLOTTE, KHALED, LOSERT, W., MARCUS & CAROLE 2012. LTB4 Is a Signal-Relay Molecule during Neutrophil Chemotaxis. *Developmental Cell,* 22**,** 1079-1091.

PISHESHA, N., HARMAND, T. J. & PLOEGH, H. L. 2022. A guide to antigen processing and presentation. *Nat Rev Immunol,* 22**,** 751-764.

POLLARD, A. J. & BIJKER, E. M. 2021. A guide to vaccinology: from basic principles to new developments. *Nat Rev Immunol,* 21**,** 83-100.

POPLIMONT, H., GEORGANTZOGLOU, A., BOULCH, M., WALKER, H. A., COOMBS, C., PAPALEONIDOPOULOU, F. & SARRIS, M. 2020. Neutrophil Swarming in Damaged Tissue Is Orchestrated by Connexins and Cooperative Calcium Alarm Signals. *Current Biology,* 30**,** 2761-2776.e7.

PRAJSNAR, T. K., SERBA, J. J., DEKKER, B. M., GIBSON, J. F., MASUD, S., FLEMING, A., JOHNSTON, S. A., RENSHAW, S. A. & MEIJER, A. H. 2021. The autophagic response to Staphylococcus aureus provides an intracellular niche in neutrophils. *Autophagy,* 17**,** 888-902.

PRINCE, L. R., WHYTE, M. K., SABROE, I. & PARKER, L. C. 2011. The role of TLRs in neutrophil activation. *Curr Opin Pharmacol,* 11**,** 397-403.

RABODZEY, A., ALCAIDE, P., LUSCINSKAS, F. W. & LADOUX, B. 2008. Mechanical Forces Induced by the Transendothelial Migration of Human Neutrophils. *Biophysical Journal,* 95**,** 1428-1438.

RASKOV, H., ORHAN, A., CHRISTENSEN, J. P. & GOGENUR, I. 2021. Cytotoxic CD8(+) T cells in cancer and cancer immunotherapy. *Br J Cancer,* 124**,** 359-367.

REÁTEGUI, E., JALALI, F., KHANKHEL, A. H., WONG, E., CHO, H., LEE, J., SERHAN, C. N., DALLI, J., ELLIOTT, H. & IRIMIA, D. 2017. Microscale arrays for the profiling of start and stop signals coordinating human-neutrophil swarming. *Nature Biomedical Engineering,* 1**,** 0094.

REINA-CAMPOS, M., SCHARPING, N. E. & GOLDRATH, A. W. 2021. CD8(+) T cell metabolism in infection and cancer. *Nat Rev Immunol,* 21**,** 718-738.

RENSHAW, S. A., LOYNES, C. A., TRUSHELL, D. M. I., ELWORTHY, S., INGHAM, P. W. & WHYTE, M. K. B. 2006. A transgenic zebrafish model of neutrophilic inflammation. *Blood,* 108**,** 3976-3978.

ROBERTSON, A. L., HOLMES, G. R., BOJARCZUK, A. N., BURGON, J., LOYNES, C. A., CHIMEN, M., SAWTELL, A. K., HAMZA, B., WILLSON, J., WALMSLEY, S. R., ANDERSON, S. R., COLES, M. C., FARROW, S. N., SOLARI, R., JONES, S., PRINCE, L. R., IRIMIA, D., RAINGER, G. E., KADIRKAMANATHAN, V., WHYTE, M. K. & RENSHAW, S. A. 2014. A zebrafish compound screen reveals modulation of neutrophil reverse migration as an anti-inflammatory mechanism. *Sci Transl Med,* 6**,** 225ra29.

RUTHERFORD, H. A., CANDEIAS, D., DUNCAN, C. J. A., RENSHAW, S. A. & HAMILTON, N. 2024. Macrophage transplantation rescues RNASET2-deficient leukodystrophy by replacing deficient microglia in a zebrafish model. *Proc Natl Acad Sci U S A,* 121**,** e2321496121.

SADIK, C. D., KIM, N. D. & LUSTER, A. D. 2011. Neutrophils cascading their way to inflammation. *Trends in Immunology,* 32**,** 452-460.

SAKURADA, S., KATO, T. & OKAMOTO, T. 1996. Induction of cytokines and ICAM-1 by proinflammatory cytokines in primary rheumatoid synovial fibroblasts and inhibition by N-acetyl-L-cysteine and aspirin. *Int Immunol,* 8**,** 1483-93.

SAVILL, J. S., WYLLIE, A. H., HENSON, J. E., WALPORT, M. J., HENSON, P. M. & HASLETT, C. 1989. Macrophage phagocytosis of aging neutrophils in inflammation. Programmed cell death in the neutrophil leads to its recognition by macrophages. *J Clin Invest,* 83**,** 865-75.

SAWA, Y., UEKI, T., HATA, M., IWASAWA, K., TSURUGA, E., KOJIMA, H., ISHIKAWA, H. & YOSHIDA, S. 2008. LPS-induced IL-6, IL-8, VCAM-1, and ICAM-1 Expression in Human Lymphatic Endothelium. *Journal of Histochemistry & Cytochemistry,* 56**,** 97-109.

SCHILD, Y., MOHAMED, A., WOOTTON, E. J., LEWIS, A. & ELKS, P. M. 2020. Hif-1alpha stabilisation is protective against infection in zebrafish comorbid models. *The FEBS Journal,* 287**,** 3925-3943.

SCHINDELIN, J., ARGANDA-CARRERAS, I., FRISE, E., KAYNIG, V., LONGAIR, M., PIETZSCH, T., PREIBISCH, S., RUEDEN, C., SAALFELD, S., SCHMID, B., TINEVEZ, J. Y., WHITE, D. J., HARTENSTEIN, V., ELICEIRI, K., TOMANCAK, P. & CARDONA, A. 2012. Fiji: an open-source platform for biological-image analysis. *Nat Methods,* 9**,** 676-82.

SERHAN, C. N. & SAVILL, J. 2005. Resolution of inflammation: the beginning programs the end. *Nat Immunol,* 6**,** 1191-7.

SHAH, D., ROMERO, F., STAFSTROM, W., DUONG, M. & SUMMER, R. 2014. Extracellular ATP mediates the late phase of neutrophil recruitment to the lung in murine models of acute lung injury. *Am J Physiol Lung Cell Mol Physiol,* 306**,** L152-61.

SHARMA, V. P. 2018. ImageJ plugin HyperStackReg V5.6. Zenodo. Zenodo: Zenodo.

SMOLEN, J. E., PETERSEN, T. K., KOCH, C., O'KEEFE, S. J., HANLON, W. A., SEO, S., PEARSON, D., FOSSETT, M. C. & SIMON, S. I. 2000. L-Selectin Signaling of Neutrophil Adhesion and Degranulation Involves p38 Mitogen-activated Protein Kinase. *Journal of Biological Chemistry,* 275**,** 15876-15884.

SPEIRS, Z. C., LOYNES, C. A., MATHIESSEN, H., ELKS, P. M., RENSHAW, S. A. & JØRGENSEN, L. V. G. 2024. What can we learn about fish neutrophil and macrophage response to immune challenge from studies in zebrafish. *Fish & Shellfish Immunology,* 148**,** 109490.

ST JOHN, A. L. & RATHORE, A. P. S. 2019. Adaptive immune responses to primary and secondary dengue virus infections. *Nat Rev Immunol,* 19**,** 218-230.

STARNES, T. W. & HUTTENLOCHER, A. 2012. Neutrophil reverse migration becomes transparent with zebrafish. *Adv Hematol,* 2012**,** 398640.

STOSIK, M., TOKARZ-DEPTULA, B. & DEPTULA, W. 2022. Haematopoiesis in Zebrafish (Danio Rerio). *Front Immunol,* 13**,** 902941.

STRICKLAND, E., PAN, D., GODFREY, C., KIM, J. S., HOPKE, A., JI, W., DEGRANGE, M., VILLAVICENCIO, B., MANSOUR, M. K., ZERBE, C. S., IRIMIA, D., AMIR, A. & WEINER, O. D. 2024. Self-extinguishing relay waves enable homeostatic control of human neutrophil swarming. *Dev Cell,* 59**,** 2659-2671 e4.

STRINGER, C., WANG, T., MICHAELOS, M. & PACHITARIU, M. 2021. Cellpose: a generalist algorithm for cellular segmentation. *Nat Methods,* 18**,** 100-106.

SUTTON, J. A. F., CARNELL, O. T., LAFAGE, L., GRAY, J., BIBOY, J., GIBSON, J. F., POLLITT, E. J. G., TAZOLL, S. C., TURNBULL, W., HAJDAMOWICZ, N. H., SALAMAGA, B., PIDWILL, G. R., CONDLIFFE, A. M., RENSHAW, S. A., VOLLMER, W. & FOSTER, S. J. 2021. Staphylococcus aureus cell wall structure and dynamics during host-pathogen interaction. *PLoS Pathog,* 17**,** e1009468.

TAMÁS, S. X., ROUX, B. T., VÁMOSI, B., DEHNE, F. G., TÖRÖK, A., FAZEKAS, L. & ENYEDI, B. 2023. A genetically encoded sensor for visualizing leukotriene B4 gradients in vivo. *Nature Communications,* 14.

TAUZIN, S., STARNES, T. W., BECKER, F. B., LAM, P. Y. & HUTTENLOCHER, A. 2014. Redox and Src family kinase signaling control leukocyte wound attraction and neutrophil reverse migration. *J Cell Biol,* 207**,** 589-98.

TAYLOR, C. T. & SCHOLZ, C. C. 2022. The effect of HIF on metabolism and immunity. *Nat Rev Nephrol,* 18**,** 573-587.

THÉRY, C. & AMIGORENA, S. 2001. The cell biology of antigen presentation in dendritic cells. *Current Opinion in Immunology,* 13**,** 45-51.

THOMAS, L. S. V. & GEHRIG, J. 2020. Multi-template matching: a versatile tool for object-localization in microscopy images. *BMC Bioinformatics,* 21.

TINEVEZ, J. Y., PERRY, N., SCHINDELIN, J., HOOPES, G. M., REYNOLDS, G. D., LAPLANTINE, E., BEDNAREK, S. Y., SHORTE, S. L. & ELICEIRI, K. W. 2017. TrackMate: An open and extensible platform for single-particle tracking. *Methods,* 115**,** 80-90.

TUMMERS, B. & GREEN, D. R. 2017. Caspase-8: regulating life and death. *Immunol Rev,* 277**,** 76-89.

TURK, V., STOKA, V., VASILJEVA, O., RENKO, M., SUN, T., TURK, B. & TURK, D. 2012. Cysteine cathepsins: From structure, function and regulation to new frontiers. *Biochimica et Biophysica Acta (BBA) - Proteins and Proteomics,* 1824**,** 68-88.

TURVEY, S. E. & BROIDE, D. H. 2010. Innate immunity. *Journal of Allergy and Clinical Immunology,* 125**,** S24-S32.

UDERHARDT, S., MARTINS, A. J., TSANG, J. S., LAMMERMANN, T. & GERMAIN, R. N. 2019. Resident Macrophages Cloak Tissue Microlesions to Prevent Neutrophil-Driven Inflammatory Damage. *Cell,* 177**,** 541-555 e17.

VAN ACKER, H. & COENYE, T. 2017. The Role of Reactive Oxygen Species in Antibiotic-Mediated Killing of Bacteria. *Trends in Microbiology,* 25**,** 456-466.

VAN DER VAART, M., SPAINK, H. P. & MEIJER, A. H. 2012. Pathogen recognition and activation of the innate immune response in zebrafish. *Adv Hematol,* 2012**,** 159807.

VANDERBEKE, L., VAN MOL, P., VAN HERCK, Y., DE SMET, F., HUMBLET-BARON, S., MARTINOD, K., ANTORANZ, A., ARIJS, I., BOECKX, B., BOSISIO, F. M., CASAER, M., DAUWE, D., DE WEVER, W., DOOMS, C., DREESEN, E., EMMANEEL, A., FILTJENS, J., GOUWY, M., GUNST, J., HERMANS, G., JANSEN, S., LAGROU, K., LISTON, A., LORENT, N., MEERSSEMAN, P., MERCIER, T., NEYTS, J., ODENT, J., PANOVSKA, D., PENTTILA, P. A., POLLET, E., PROOST, P., QIAN, J., QUINTELIER, K., RAES, J., REX, S., SAEYS, Y., SPROOTEN, J., TEJPAR, S., TESTELMANS, D., THEVISSEN, K., VAN BUYTEN, T., VANDENHAUTE, J., VAN GASSEN, S., VELASQUEZ PEREIRA, L. C., VOS, R., WEYNAND, B., WILMER, A., YSERBYT, J., GARG, A. D., MATTHYS, P., WOUTERS, C., LAMBRECHTS, D., WAUTERS, E. & WAUTERS, J. 2021. Monocyte-driven atypical cytokine storm and aberrant neutrophil activation as key mediators of COVID-19 disease severity. *Nat Commun,* 12**,** 4117.

VARELA, M. & MEIJER, A. H. 2022. A fresh look at mycobacterial pathogenicity with the zebrafish host model. *Mol Microbiol,* 117**,** 661-669.

WANG, H., INOUE, A., LEI, Y., WU, H., HONG, L. & CHENG, X. W. 2023. Cathepsins in the extracellular space: Focusing on non-lysosomal proteolytic functions with clinical implications. *Cell Signal,* 103**,** 110531.

WANG, M., ISHIKAWA, T., LAI, Y., NALLAPOTHULA, D. & SINGH, R. R. 2022. Diverse Roles of NETosis in the Pathogenesis of Lupus. *Front Immunol,* 13**,** 895216.

WEATHINGTON, N. M., VAN HOUWELINGEN, A. H., NOERAGER, B. D., JACKSON, P. L., KRANEVELD, A. D., GALIN, F. S., FOLKERTS, G., NIJKAMP, F. P. & BLALOCK, J. E. 2006. A novel peptide CXCR ligand derived from extracellular matrix degradation during airway inflammation. *Nat Med,* 12**,** 317-23.

WILLSON, J. A., ARIENTI, S., SADIKU, P., REYES, L., COELHO, P., MORRISON, T., RINALDI, G., DOCKRELL, D. H., WHYTE, M. K. B. & WALMSLEY, S. R. 2022. Neutrophil HIF-1alpha stabilization is augmented by mitochondrial ROS produced via the glycerol 3-phosphate shuttle. *Blood,* 139**,** 281-286.

WINTERBOURN, C. C., HAMPTON, M. B., LIVESEY, J. H. & KETTLE, A. J. 2006. Modeling the Reactions of Superoxide and Myeloperoxidase in the Neutrophil Phagosome. *Journal of Biological Chemistry,* 281**,** 39860-39869.

WU, X., XIAO, L., SUN, Y., ZHANG, J., MA, T. & HE, L. 2022. A survey of human-in-the-loop for machine learning. *Future Generation Computer Systems,* 135**,** 364-381.

XIA, M., STEGMEYER, R. I., SHIRAKURA, K., BUTZ, S., THIRIOT, A., VON ANDRIAN, U. H. & VESTWEBER, D. 2024. Conditions that promote transcellular neutrophil migration in vivo. *Scientific Reports,* 14**,** 14471.

XIANG, Y., JIN, C., WANG, W., WANG, Z., HUANG, Y., FAN, F., MA, Y., ZHANG, X., XU, W., YIN, Y. & HE, Y. 2017. The critical role of myeloperoxidase in Streptococcus pneumoniae clearance and tissue damage during mouse acute otitis media. *Innate Immunity,* 23**,** 296-306.

YAN, B., HAN, P., PAN, L., LU, W., XIONG, J., ZHANG, M., ZHANG, W., LI, L. & WEN, Z. 2014. IL-1beta and reactive oxygen species differentially regulate neutrophil directional migration and Basal random motility in a zebrafish injury-induced inflammation model. *J Immunol,* 192**,** 5998-6008.

YE, K., CHEN, Z. & XU, Y. 2023. The double-edged functions of necroptosis. *Cell Death Dis,* 14**,** 163.

YIPP, B. G. & KUBES, P. 2013. NETosis: how vital is it? *Blood,* 122**,** 2784-2794.

YIPP, B. G., PETRI, B., SALINA, D., JENNE, C. N., SCOTT, B. N. V., ZBYTNUIK, L. D., PITTMAN, K., ASADUZZAMAN, M., WU, K., MEIJNDERT, H. C., MALAWISTA, S. E., DE BOISFLEURY CHEVANCE, A., ZHANG, K., CONLY, J. & KUBES, P. 2012. Infection-induced NETosis is a dynamic process involving neutrophil multitasking in vivo. *Nature Medicine,* 18**,** 1386-1393.

YOO, S. K., STARNES, T. W., DENG, Q. & HUTTENLOCHER, A. 2011. Lyn is a redox sensor that mediates leukocyte wound attraction in vivo. *Nature,* 480**,** 109-112.

YOUSEFI, S., MIHALACHE, C., KOZLOWSKI, E., SCHMID, I. & SIMON, H. U. 2009. Viable neutrophils release mitochondrial DNA to form neutrophil extracellular traps. *Cell Death & Differentiation,* 16**,** 1438-1444.

YU, P., ZHANG, X., LIU, N., TANG, L., PENG, C. & CHEN, X. 2021. Pyroptosis: mechanisms and diseases. *Signal Transduct Target Ther,* 6**,** 128.

ZARBOCK, A., LEY, K., MCEVER, R. P. & HIDALGO, A. 2011. Leukocyte ligands for endothelial selectins: specialized glycoconjugates that mediate rolling and signaling under flow. *Blood,* 118**,** 6743-6751.

ZHANG, J. H., CHUNG, T. D. & OLDENBURG, K. R. 1999. A Simple Statistical Parameter for Use in Evaluation and Validation of High Throughput Screening Assays. *J Biomol Screen,* 4**,** 67-73.

ZHAO, W., FOGG, D. K. & KAPLAN, M. J. 2015. A novel image-based quantitative method for the characterization of NETosis. *Journal of Immunological Methods,* 423**,** 104-110.

ZHENG, X., NARAYANAN, S., XU, C., ELIASSON ANGELSTIG, S., GRUNLER, J., ZHAO, A., DI TORO, A., BERNARDI, L., MAZZONE, M., CARMELIET, P., DEL SOLE, M., SOLAINI, G., FORSBERG, E. A., ZHANG, A., BRISMAR, K., SCHIFFER, T. A., RAJAMAND EKBERG, N., BOTUSAN, I. R., PALM, F. & CATRINA, S. B. 2022. Repression of hypoxia-inducible factor-1 contributes to increased mitochondrial reactive oxygen species production in diabetes. *Elife,* 11.

ZHU, Y., HUANG, Y., JI, Q., FU, S., GU, J., TAI, N. & WANG, X. 2021. Interplay between Extracellular Matrix and Neutrophils in Diseases. *J Immunol Res,* 2021**,** 8243378.